Gas turbine power cycles for retrofitting and repowering coal plants with post-combustion carbon dioxide capture

Maria Sanchez del Rio Saez

Thesis submitted for the Degree of Doctor of Philosophy in Engineering to the University of Edinburgh

School of Engineering
University of Edinburgh

June 2015

In memory of my grandmother

Dedicated to my parents and brother

Declaration of originality

The work included in this Ph.D. thesis, except when referenced, is the result of the effort of years that has been done by the author alone under the guidance of her supervisors Dr Mathieu Luquieud, Prof. Jon Gibbins and Dr. Hannah Chalmers. The author acknowledges essential contributions by others in the acknowledgment section of this thesis and in further sections of the work where required. This Ph.D. thesis has not been submitted for any other degree or professional qualification in the UK or elsewhere. The author recommends referencing this thesis as follows:

Sanchez del Rio M. (2015), Gas turbine power cycles for retrofitting and repowering coal plants with post-combustion carbon dioxide capture, Ph.D. Thesis, School of Engineering, University of Edinburgh, United Kingdom of Great Britain and Northern Ireland (UK).

MARIA SANCHEZ DEL RIO SAEZ

Edinburgh, June 2015

ABSTRACT

A widely-proposed way to retrofit coal-fired power plants with post-combustion CO_2 capture (PCC) is to supply all the electricity and heat required to operate the capture equipment from the existing steam cycle (an 'integrated retrofit'), at the expense of a reduction in site power output. As an alternative, it is possible to add a gas turbine (GT) plant to maintain, or even increase, the net site power output. The GT can be integrated with the capture plant in various ways to supply all or part of the heat and power required for the capture and compression systems. But there is then the issue of how to capture the CO_2 emissions from the added GT plant. In this study a novel retrofit configuration is proposed. The exhaust gas of the GT replaces part of the secondary air for the coal boiler and a common capture system is used for both coal- and natural gas-derived CO_2. This new 'GT flue gas windbox retrofit' is based on the principles of previous hot windbox repowering proposals, with additional modifications to permit operation without extensive coal boiler modifications. To achieve this, the heat recovery steam generator (HRSG) attached to GT is designed to maintain the main steam turbine flow rates and temperatures, to compensate for a necessary reduction in coal feed rates, and this, with the GT output, maintains the net power output of the site

A techno-economic analysis of coal plants retrofitted with GT power cycles shows that these 'power matched' retrofits can be competitive with integrated retrofits at lower natural gas prices (as is now the case in North America). In particular, the novel GT flue gas windbox retrofit provides a promising alternative for adapting integrated capture retrofits that are initially designed for flexible operation with zero to full (~90%) capture (as at the Boundary Dam 3 unit) for subsequent operation only with full capture. In this case the addition of a GT flue gas windbox retrofit will restore the full power output of the site with full CO_2 capture and using the original capture plant. In general, techno-economic analysis shows that the economic performance of GT retrofit options depends on the site power export capacity. If there is no limit on power export then retrofits may advantageously also include an additional steam cycle, to give a combined cycle with the GT, otherwise retrofits with a single pressure HRSG producing process steam only are preferred.

LIST OF CONTENT

Declaration of originality 3
1.- INTRODUCTION 17
1.1.- Motivation for Carbon Capture and Storage 17
1.2.- CCS power plants: new build and retrofits 19
1.3.- The potential for CCS retrofits 20
1.4.- Post-Combustion Carbon Capture Retrofit 22
1.4.1.- The Aqueous Amine Scrubbing Process 22
1.4.2.- Thermodynamic Integration of the amine process with the power cycle and with CO_2 compression 24
1. 4.3.- An introduction to retrofit options with gas turbine power cycles 26
2.- ACHIEVING HIGH LEVELS OF CO_2 CAPTURE IN PULVERISED COAL PLANT RETROFIT OPTIONS WITH GAS TURBINE POWER CYCLES 30
2.1.-Post-combustion carbon capture retrofit of a coal power plant with the addition of gas turbine power cycle 30
2.2.- Hot windbox repowering of coal power plants for carbon capture retrofit 34
2.3.- Gas Turbine Flue Gas Windbox Retrofit 36
2.4.- Objectives and outline of the thesis 37
3.- ENGINEERING FUNDAMENTALS A GAS TURBINE FLUE GAS WINDBOX CARBON CAPTURE RETROFIT 39
3.1.- Introduction 39
3.1.1.- Description of the pulverised coal power plant 40
3.2.- FUNDAMENTALS OF BOILER HEAT TRANSFER 45
3.2.1.- Fundamentals of heat transfer 45
3.2.2.- Furnace heat transfer 51
3.2.3.- Cavities heat transfer 55
3.2.4.- Boiler banks heat transfer 56
3.3.- FUNDAMENTALS OF BOILER DESIGN 58
3.3.1.- Tube diameter: 58
3.3.2.- Furnace design: 59
3.3.3.- Convection pass design: 60
3.4.- Fundamentals of air heaters 63

3.5.- Fundamentals of feed-water heat exchangers and condenser: ... 64
3.6.- Fundamentals of steam turbines ... 65
3.6.1.- Thermodynamic of the axial turbine stage ... 66
3.6.2.- Degree of reaction of a steam turbine stage ... 69
4.- PERFORMANCE MODELLING OF THE GAS TURBINE FLUE GAS WINDBOX CARBON CAPTURE RETROFIT ... 73
4.1.- Rating process calculations of the pulverised coal power plant ... 73
4.1.1. Boiler modelling ... 73
4.1.2. Air pre-heaters modelling: ... 75
4.1.3. Steam turbines modelling: ... 75
4.1.4. Feed-water heaters modelling: ... 78
4.1.5. Condenser modelling: ... 78
4.2.- Off design process calculations of the pulverised coal power plant ... 79
4.2.1. Boiler modelling ... 79
4.2.2. Air pre-heaters modelling: ... 84
4.2.3. Steam turbines modelling: ... 84
4.2.4. feed-water heaters modelling: ... 86
4.2.5. Condenser modelling: ... 87
4.3.- Process calculation of the gas turbine and heat recovery steam generator ... 87
4.4.- Process calculation of the carbon capture plant ... 89
5.- RESULTS AND TECHNICAL DISCUSSION OF THE GAS TURBINE FLUE GAS WINDBOX CARBON CAPTURE RETROFIT ... 91
5.1.- Results of the simulations ... 91
5.1.1.- Results of the retrofitted pulverised coal power plant ... 91
5.1.3.- Thermodynamic integration of the steam cycle, the HRSG and the reboiler of the carbon capture plant ... 99
5.1.4.- Results of the carbon capture plant ... 102
5.2.- Technical discussion ... 104
5.2.1.- Impact on the existing gas cycle ... 104
5.2.2.- Impact on the existing steam cycle: ... 105
5.2.3.- Benefits of the GT flue gas windbox carbon capture retrofit: ... 106
6.- ALTERNATIVE OPTIONS FOR PULVERISED COAL RETROFITS WITH GAS TURBINE POWER CYCLES ... 107

6.1 Options achieving high levels of CO_2 capture 113
6.2 Options using partial capture to achieve interim emission performance targets..... 114
6.3.- Relevant technical metrics:... 117
7.- TECHNO-ECONOMIC COMPARISON OF CARBON CAPTURE RETROFITS........................ 123
7.1.- Background of the economic analysis 123
7.2.- Economic modelling approach 125
7.2.1.- Capital expenditures and operational expenditures 125
7.2.2.- Finance structure 131
7.2.3.- Financial modelling: total revenue requirement 134
7.3.- Results of the techno-economic analysis 138
7.3.1.- Relevant metrics: 138
7.3.2.- Results for options achieving high levels of CO_2 capture 143
7.3.3.- Results for intermediate capture levels.. 154
7.4.- Sensitivity analysis for power matched retrofits 162
7.4.1.- Sensitivity to CO_2 emission charges 162
7.4.2.- Sensitivity to the additional capital cost component of the existing power cycle 164
7.4.3.- Sensitivity to fuel prices, coal and gas 166
7.4.4.- Sensitivity to Load Factor.. 169
7.4.5.- Sensitivity to CO_2 selling price 170
7.4.6.- Sensitivity to Capital Cost of equipment of the gas turbine power cycle and the post-combustion capture and compression plant... 171
8.- CONCLUSIONS.. 174
8.1.- Thesis overview 174
8.2.- Summary of findings about the feasibility of the flue gas windbox carbon capture retrofit.. 175
8.2.1.- Optimisation of the integration between steam cycle of the coal plant and the heat recovery steam generator: 175
8.2.2.- Optimisation of the integration between the steam cycle of the coal power plant and the HRSG and the carbon capture plant:... 176
8.2.3.- Impact on the subcritical boiler of the coal plant.. 176
8.2.4.- Benefits of the GT flue gas windbox retrofit: 177
8.2.5.- Disadvantages of the GT flue gas windbox retrofit: 178

8. 3.- Summary of findings from the techno-economic comparison of carbon capture retrofits with gas turbine power cycles 178

8.3.1.- Retrofits achieving high levels of CO_2 capture consisting of 90% on both fuel sources 178

8.3.1.- Retrofits for intermediate CO_2 capture levels 179

8. 4.- Summary of findings from the sensitivity analysis for power matched retrofit options 180

8. 5.- Limitations and recommendations for future work 181

APPENDIX I.- DESIGN BASIS.. 193

APPENDIX II.- CARBON CAPTURE PLANT METHODOLOGY 202

APPENDIX III.- FORTRAN AND EXCELL CALCULATOR BLOCKS IMPLEMTEND ON ASPEN PLUS SOFTWARE 211

LIST OF FIGURES

Figure 1.1.- EU GHG emissions towards an 80% domestic reduction (100% - 1990) (European Commission 2011)……20
Figure 1.2.- Total coal-fired power plant capacity globally - age and generation capacity (IEA 2012)……23
Figure 1.3.- Total coal-fired power plant capacity globally - age and performance level (IEA 2012)……23
Figure 1.4.- Process Flow Diagram of the Carbon Capture Plant……25
Figure 1.5.- Process Flow Diagram of the CO2 Compression System……26
Figure 1.6.- Schematic diagram of a fully integrated retrofit……29
Figure 1.7.- Schematic diagram of the power matched retrofit……30
Figure 1.8.- Schematic diagram of the heat matched retrofit……30
Figure 2.1.- Effect of absorber height on reboiler duty and rich loading at 11% v/v CO_2 concentration……35
Figure 2.2.- Effect of absorber height on reboiler duty and rich loading at 13% v/v CO_2 concentration……35
Figure 3.1.- Steam generator of the original coal powerplant……45
Figure 3.2.- Process flow diagram of a gas turbine flue gas windboxretrofit*……46
Figure 3.3.- Process flow diagram of coal original powerplant……47
Figure 3.4.- Basic. Radiation heat transfer coefficient (Kitto & Stultz 2005)……53
Figure 3.5.- Fuel factor(Kitto & Stultz 2005)……53
Figure 3.6.- Dimensional parameters of a boiler heat exchanger……63
Figure 3.7.- Schematic plan arrangement of a boiler heat exchangers ……65
Figure 3.8 Steam velocity triangle diagram and Mollier diagram for a turbine stage (Schobeiri 2012)……72
Figure 3.9.- Stage efficiency of turbines with different degree of reaction for $\alpha 2$ = 80º……74
Figure 3.10.- Effect of degree of reaction on the stage configuration (Schobeiri 2012)……75

Figure 4.1.- Iterative method –Furnace Surface Arrangement……79
Figure 4.2.- Iterative method –Surface Arrangement……80

Figure 4.3.- Iterative method –Performance of retrofitted boiler…………………………......83

Figure 4.4.- Iterative method – Screen exit gas temperature………………………………….…...85

Figure 4.5.- Iterative method – Cavity exit gas temperature………….…………………….…...86

Figure 4.6.- Steam Cycle of the GT flue gas windbox carbon capture retrofit……..……..93

Figure 5.1.- Effect of Coal reduction in the Flue Gas Flow rate of the GT windbox retrofit…………………………………………………………………………………………94

Figure 5.3.- Effect of gas flow rate on the HRSG gas temperature profile….……………….95

Figure 5.3.- Flue gas composition at different GT exhaust gas flow rates….……………..96

Figure 5.4a.- Gas temperature and flame emissivity…………………………………………98

Figure 5.4b.- Gas temperature and Boltzman number………………………………………98

Figure 5.5.- Effect of flame radiation reduction on the total heat absorbed by the banks……………………………………………………………………………..……………...99

Figure 5.6.- Total heat absorbed by reheater banks……………………...……………...100

Figure 5.7.- Power output of the site…………………………………………………..…100

Figure 5.8.- Effect of the exhaust gas temperature on the exit HRSG gas temperature..101

Figure 5.9.- Temperature profile of the HRSG…………………………………………...102

Figure 5.10.- Effect of absorber height on reboiler duty and rich loading………………..105

Figure 5.11.- Reboiler duty and stripper pressure dependence on the Lean Loading…..106

Figure 5.12.- Optimisation of solvent flow rate……………………………………...…107

Figure 6.1.- Carbon Capture Retrofit Options……………………………………...……110

Figure 6.2.- Process flow diagram of the Standard Integrated Retrofit configuration with steam extraction from the main steam cycle providing all of the heat for CO2 capture and power requirements from the main generator………………………...……….112

Figure 6 3a.- Optimum MEA lean loading depending on Reboiler duty and Stripper pressure……………..…………………………………………………………………...116

Figure 6 3b.- Optimum MEA lean loading to maximize power output……………..…….113

Figure 6.4.- Process flow diagram of a heat matched carbon capture retrofit with a combined cycle gas turbine providing all of the heat for CO2 capture and power requirements from the combined cycle gas turbine (Case E1, E2 and E3)………..…123

Figure 6.5.- Process flow diagram of a heat matched carbon capture with a gas turbine and a single pressure heat recovery steam generator providing all of the heat for

CO2 capture from the heat recovery steam generator and power requirements from the gas turbine (Case F1, F2 and F3)…………………………………………………..…124

Figure 6.6.- Process flow diagram of a power matched carbon capture retrofit with a combined cycle gas turbine providing all of the heat for CO2 capture and power requirements from both the combined cycle gas turbine and the main steam cycle (Case B1, B2, B3 and C1)……………………………………………………………….125

Figure 7.1a.- Uniform revenue to cover costs of fully abated power matched retrofits in North America…………………………………………………………………….…151

Figure 7.1b.- Uniform revenue with sales to Enhanced Oil Recovery at $10/tCO2 in North America…………………………………………………………………….……151

Figure 7.2a.- Uniform revenue to cover costs of fully abated power matched retrofits in Europe………………………………………………………………………………...152

Figure 7.2b.- Uniform revenue with sales to Enhanced Oil Recovery at $10/tCO2 in Europe……………………………………………………………………………..….152

Figure 7.3a.- Uniform revenue considering the additional costs of the new CCGT needed to re-store the power output of the site for North American scenarios………………...153

Figure 7.3b.- Uniform revenue considering the additional costs of the new CCGT needed to re-store the power output of the site for European scenarios………………………..153

Figure 7.4a.- Uniform revenue with the additional cost of a new GT and HRSG to re-store the power output of the site……………………………………………………………….156

Figure 7.4b.- Uniform revenue with sales to Enhanced Oil Recovery at $10/tCO2 and with the additional cost of a new GT and HRSG ……………………………………………156

Figure 7.5a.- Uniform revenue to cover costs of power matched retrofits reaching interim capture levels in North America……………………………………….....…………160

Figure 7.5b.- Uniform revenue with sales to Enhanced Oil Recovery at $10/tCO2 of power matched retrofits reaching interim capture levels in North America…………….....161

Figure 7.6a.- Uniform revenue to cover costs of power matched retrofits reaching interim capture levels in Europe……………………………………………………………….161

Figure 7.6b.- Uniform revenue with sales to Enhanced Oil Recovery at $10/tCO2 of power matched retrofits reaching interim capture levels in Europe……………….....………162

Figure 7.7a.- Uniform revenue considering the additional costs of the new CCGT needed to re-store the power output of the site ……………………...…………………………162

Figure 7.7b.- Uniform revenue considering the additional costs of the new CCGT needed to re-store the power output of the site ………………………..…………………………163
Figure 7.8a.- Uniform revenue to cover costs of heat matched retrofits reaching interim capture levels in Europe…………………………………………….……………………163
Figure 7.8b.- Uniform revenue with sales to Enhanced Oil Recovery at $10/tCO2 of heat matched retrofits reaching interim capture levels in Europe …………………..…….164
Figure 7.9a.- Uniform revenue to cover costs of heat matched retrofits reaching interim capture levels in North America…………………………………..…………………..164
Figure 7.9b.- Uniform revenue with sales to Enhanced Oil Recovery at $10/tCO2 of heat matched retrofits reaching interim capture levels in North America……………….165
Figure 7.10a.- Effect of CO2 emissions charges on the LCOE in Europe……………………..166
Figure 7.10b.- Effect of CO2 emissions charges on the LCOE in North America ………..….166
Figure 7.11a.- Effect of additional capital cost component of the existing power cycle on LCOE in Europe…………………………………………………………..……...168
Figure 7.11b.- Effect of additional capital cost component of the existing power cycle on LCOE in North America……………………………………………………………….168
Figure 7.12a.- Effect of coal price on LCOE in Europe. The natural gas price is 34.18 $/MWh_th…….……………………………………………………………………………..169
Figure 7.12b.- Effect of coal price on LCOE in North America. The natural gas price is 14 $/MWh_th…………………………………………………………………………….170
Figure 7.13a.- Effect of natural gas price on LCOE in Europe. The coal price is 12.24 $/MWh_th ……………………………………………………………………………………..171
Figure 7.13b.- Effect of natural gas price on LCOE in North America. The coal price is 8.09$/MWh_th ………………………………………………………..……..………171
Figure 7.14.- Effect of load factor on equivalent LCOE ………………………………………..172
Figure 7.15a.- Effect of CO2 selling price on total revenue requirement in Europe…………173
Figure 7.15b.- Effect of CO2 selling price on total revenue requirement in North America…………………………………………………………………………………………..174
Figure 7.16a.- Effect of variation in CCGT CAPEX on the LCOE in North America………..175
Figure 7.16b.- Effect of variation in CCGT CAPEX on the LCOE in Europe……………...….175
Figure 7.16a.- Effect of variation in PCC plant CAPEX on the LCOE in North America…...176
Figure 7.16b.- Effect of variation in PCC plant CAPEX on the LCOE in Europe …………...176

LIST OF TABLES

Table 2.1.- Flue gas composition of coal plant, GT Plant and flue gas mixture……………………………………………………………………………………….….30

Table 3.1.- Physical arrangement per component………………………………...……..62

Table 5.1.- Boiler coal, combustion air and flue gas mass flow rates…………..………...92
Table 5.2.- Furnace characteristics…………………………………………..…………94

Table 6.1.- Fully abated CO_2 capture retrofit options…………………………….……113
Table 6.2.- Partially abated CO_2 capture retrofit options……………………………..…..115

Table 7.1.- Project and Process Contingencies (DOE/NETL 2013)………………………….…126
Table 7.2.- Owner's Costs……………………………………………………………….…126
Table 7.3.-Illustrative Capital Cost of PCC retrofits…………………………………….…127
Table 7.4.-O&M Costs…………………………………………….……………………..129
Table 7.5.-Fossil Fuel Costs…………………………………….…………………………130
Table 7.6.- Risk profile of the projects (DOE/NETL 2013)……….………………………..132
Table 7.7.- Finance structure. Treatment of capital costs (DOE/NETL 2013)….……………...132
Table 7.8.- Finance structure. Income taxes (DOE/NETL 2013)……………….…………….134
Table 7.9.- Finance structure. Escalation of operating revenues and costs.……..……………134
Table 7.10.- Technical performance results of the retrofits with high levels of capture …....146
Table 7.11.- Economic comparison of PCC retrofits with high level of CO2 capture in North America………………………...…………………………………………………..…152
Table 7.12.- Economic comparison of PCC retrofits with high level of CO2 capture in Europe…………………………...……………………………………………...….152
Table 7.13.- Technical performance results for interim capture levels ………………….…156

NOMENCLATURE

Carbon dioxide	CO_2
Carbon capture and storage	CCS
Capital Expenditures	CAPEX
Cavity	CAV
Combined Cycle Gas Turbine	CCGT
Combined heat and power	CHP
Direct contact cooler	DCC
Economiser	ECO
Electric Power Research Institute	EPRI
Electricity Output Penalty	EOP
Emission Performance Standard	EPS
European Union	EU
Final superheater	FSH
Flue gas desulphurisation	FGD
Gas Turbine	GT
Gas Turbine Combined Cycle	GTCC
Greenhouse gases	GHG
Heat recovery steam generator	HRSG
High Pressure	HP
Intermedium Pressure	IP
International Energy Agency	IEA
IEA Greenhouse Gas R&D Programme	IEAGHG
Integrated Environmental Control Model	IECM
Intergovernmental Panel on Climate Change	IPCC
Levelised Cost of Electricity	LCOE
Low Pressure	LP
Methane	CH_4
Monoethanolamine	MEA
Nitrogen oxides	NO_x
Operating Expenditures	OPEX

Reheater Out Leg	RHOL
Oxygen	O_2
Particulate matter	PM
Platen secondary superheater	PlatSH
Post-combustion carbon capture	PCC
Primary superheater	PSH
Reheater bank	RHB
Research, Development and Demonstration	RD&D
Rich-lean heat exchanger	RLHX
Rotterdam Opslag en Afvang Demonstratie	ROAD
Sulphur dioxide	SO_2
The United States	US
The United Kingdom	UK
Water	H_2O

1.- INTRODUCTION

1.1.- Motivation for Carbon Capture and Storage

Multiple scientific facts show unequivocally that the climate system is warming: atmosphere and ocean warming, melted ice and snow, increase in sea levels and in greenhouse gases (GHG) concentrations. The observed warming has been much faster in recent decades than any time since 1850 and an urgent response is required (IPCC 2013).

The atmospheric concentration of carbon dioxide (CO_2), methane (CH_4), and nitrous oxide (NO_x) have been increased, especially CO_2 from fossil fuel emissions. Continued emissions of these gases will cause further warming and changes in all components of the climate system. Responses to global warming imply considerable emissions reductions.

It is clear that the world needs to considerably mitigate its energy related to CO_2 emissions in the near future, and so, substantial deployment of different clean energy technologies, such as renewable energy, nuclear energy and carbon capture and storage (CCS), is required. In the meantime, the carbon intensity per unit of Gross Domestic Product (GDP) can be reduced by improving the efficiency of power stations and other industrial facilities.

The European Commission adopted a roadmap towards the creation of a competitive low carbon economy by 2050. The roadmap describes the way to reach the EU's objective of reducing GHG emissions by 80% in 2050 compared to 1990 and concludes that GHG emissions must be cut by 40% and 60% below 1990 levels in 2030 and 2040, respectively, in order to meet EU's goal (European Commission 2011).

Figure 1.1 illustrates the analysis of different scenarios moving towards an 80% EU GHG emissions reductions by 2050 and reveals that the cost-effective pathway to reach EU's goal would require a reduction of 25% in GHG emissions by 2020, however, implementing current policies, the EU will only achieve a 20% domestic reduction in 2020 below 1990 levels, and 30% in 2030.

Given the importance of fossil fuels and carbon-intensive industries in our economy, CCS becomes a critical way to reduce GHG emissions. In order to achieve ambitious emission reduction levels at low cost, almost all new-build fossil-fuel power plants must be equipped with CCS and existing fossil-fuel power plants must be retrofitted with CCS equipment in the next decades. CCS Retrofit is expected to play an important role in mitigating CO_2 emissions from fossil-fuel power plants.

The Intergovernmental Panel on Climate Change (IPCC) recently published a synthesis report where they expressed the urgent need of implementing CCS in the coming years **(IPCC 2014)**. This report stated that large-scale changes in energy systems are required to reduce earth warming. In order to maintain warming at below 2ºC the GHG emissions have to be reduced by 40% to 70% and zero- and low-carbon energy supply has to be at least tripled by 2050 relative to 2010 levels. From an economic point of view, the report stated that either a delay in the implementation of mitigation technologies or a restricted availability of a specific technology would reduce costs in the near future but would drastically increase mitigation costs in the medium- to long-term. For example, if CCS is not implemented the total discounted mitigations costs relative to a default technology assumption would increase by 138% for a 2ºC scenario, as defined by the IPCC, and if the implementation of mitigation technologies in general was delayed until 2030 the mitigation costs relative to immediately implementation would increase by 44%.

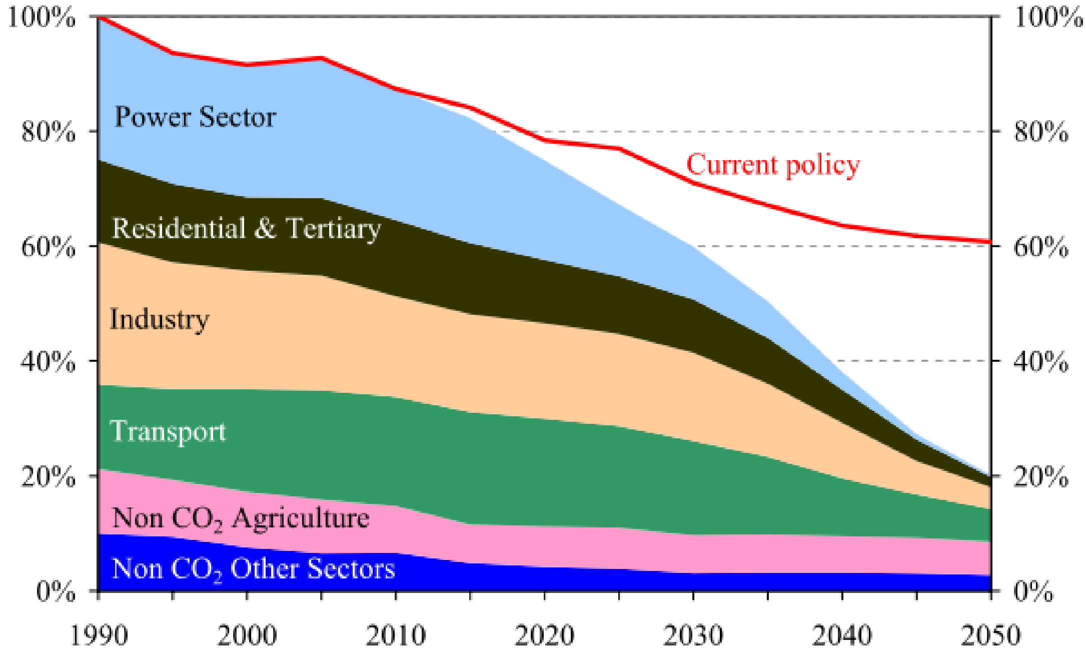

Figure 1.1.- EU GHG emissions towards an 80% domestic reduction (100% - 1990) (European Commission 2011)

The technology required for CCS is generally well understood and, in most cases, industrially mature. Nevertheless, an important largest challenge for CCS is the integration of capture technology into large-scale demonstration projects. A lack of understanding and confidence in capital expenditures (CAPEX) and operating expenditures (OPEX) is likely to undermine demonstration of the technology until CCS power plants come into existence. For this reason large-scale demonstration plants are of vital importance.

Fifty five large-scale CCS projects were identified by the Global CCS Institute around the world (Global CCS Institute 2014a) from which only thirteen are in operation at the time of writing. In the power generation sector three projects are currently focusing on retrofitting post-combustion carbon capture (PCC) to pulverised coal power plants: the Boundary Dam Integrated CCS Demonstration Project in Canada, in operation since October 2014, the NRG Energy Parish CCS Project in the United States, expected to become operational in 2016 and the Rotterdam Opslag en Afvang Demonstratie project (ROAD), one of the most advanced European CCS projects currently under development.

1.2.- CCS power plants: new build and retrofits

Previous studies have shown that carbon capture retrofits might be a cost-effective way to reduce CO_2 emissions as the costs associated with a premature closure of the existing plant can be avoided (i.e., decommissioning costs, capital costs of a new build power plant…). Some of these studies are described below.

Rao and Rubin studied the technical and economic viability of CCS at pulverised coal power plants (Rao & Rubin 2002). In particular, they compared the costs of a new build power plant with CCS to retrofit at an existing plant. Performance and cost models of the post-combustion carbon capture (PCC) and the coal power plants were analysed and integrated with a modelling framework, the Integrated Environmental Control Model (IECM). This modelling framework includes multipollutant control technologies for other regulated emissions. The authors observed that the integration of the carbon capture process with the power cycle of the coal power plant can be more challenging for retrofit systems than for new build plants and, consequently, the energy penalty and the CO_2 avoidance cost for carbon capture retrofit systems is typically higher. However, they pointed out that the levelised cost of electricity (LCOE) for retrofitted plants is lower than for new build plants due to the fact that the LCOE of the retrofitted case comprises only operating and maintenance costs and CO_2 capture plant capital cost.

Chalmers et al stressed the need of retrofitting existing coal power plants with PCC in order to implement rapid reductions in CO_2 emissions. Additionally, they examined different challenges that must be confronted in PCC retrofit due to the fact that most of the existing power plants have not been designed as 'capture ready'. Authors also pointed out that the limited life of some existing plants might not be a drawback for early capture retrofits due to the fact that the rapid improvement in CCS technology makes carbon capture plants become obsolete very fast. In accordance with Rao & Rubin, this work concluded that although abatement cost for new build plants are lower than that for retrofitted plants, the capital cost of the retrofitted plant is minimised and, thus, LCOE for the retrofitted plant is lower. Making maximum use of existing plants seemed to be valuable (Chalmers et al. 2009).

The Electric Power Research Institute (EPRI) identified different areas where a rapid RD&D programme is needed to guarantee the viability of CCS for pulverised coal power plants, and thus, to reach large-scale CO_2 emissions reductions while meeting future U.S. electricity demand requirements (Specker et al. 2009). In 2013 EPRI reported a techno economic analysis of carbon capture retrofits at five different North American sites (Dillon et al. 2013). Assuming that the capital cost of the existing plant is fully paid off and power plant life left is 30 years, they also found out that LCOE of a carbon capture retrofit is lower than that of a new build plant.

A comprehensive technical and economic study undertaken on carbon capture retrofit was commissioned earlier than the EPRI study in 2011 by IEAGHG (IEAGHG 2011). This report assessed a wide range of retrofit options and compared the performances and relative costs to each other and to new build plants with CCS. The authors concluded that CCS retrofit could be a competitive alternative to closing existing plants and replacing them with new capacity with CCS and suggested that all options should be examined objectively.

1.3.- The potential for CCS retrofits

The International Energy Agency (IEA) examined perspectives for energy technologies and forecasted new fossil power plants for 2050. The estimate is for 298 GW of new gas-fired plants with CCS and for 550 GW of new coal-fired power plants with CCS. It is also estimated that 114 GW of coal-fired capacity may be retrofitted with CCS globally over the same period, so a significant amount of capacity compared to the capacity of new fossil-fuel power plants (IEA 2010).

Figure 1.2 and Figure 1.3 show the total coal-fired power plant capacity globally, broken down by age, generation capacity and performance level. In terms of power generating capacity, the vast majority of coal-fired power plants that have been commissioned over the last few years operate under subcritical steam conditions and produce a net power output above 500MW. In terms of retrofit potential, the large amount of 'young' power plants with less than 15 years of operation suggests that high number of opportunities for CCS retrofits exist and will continue to exist in the future (IEA 2012).

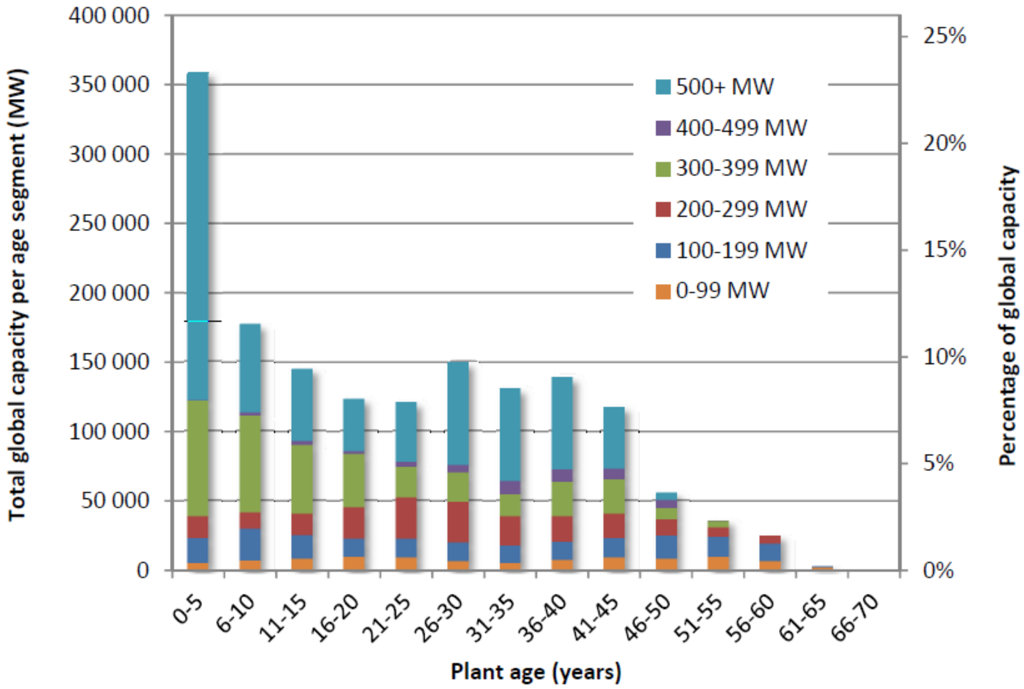

Figure 1.2.- Total coal-fired power plant capacity globally - age and generation capacity (IEA 2012).

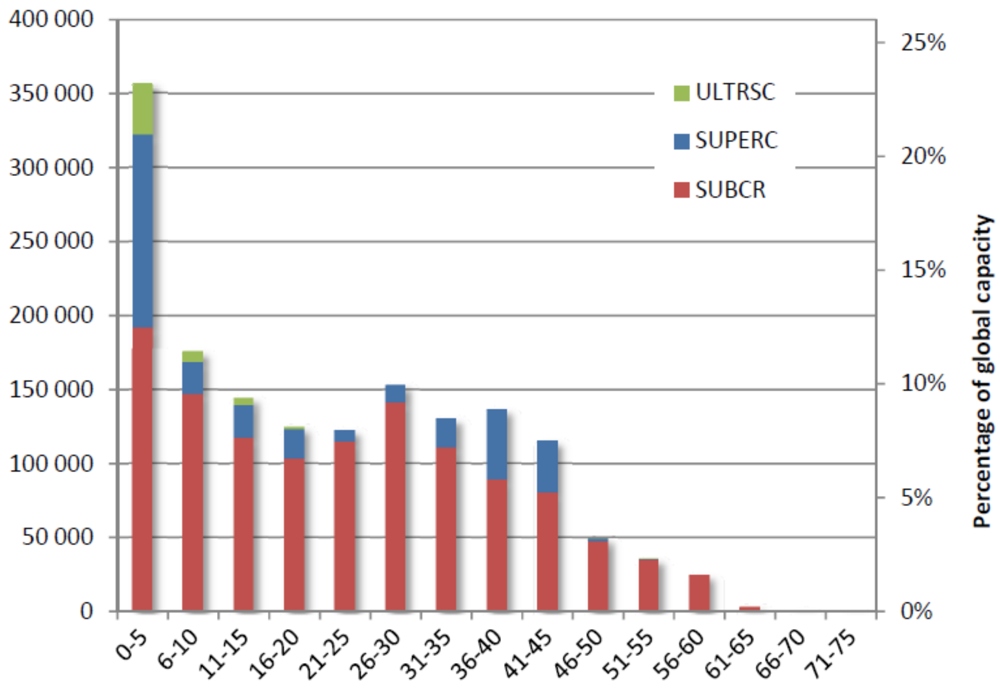

Figure 1.3.- Total coal-fired power plant capacity globally - age and performance level (IEA 2012).

The research work of this thesis address this potential by focusing on gas turbine power cycles for the repowering and retrofitting with post-combustion carbon capture of subcritical pulverised coal power plants. A Caroline-type radiant boiler for pulverised coal firing is selected as the base reference boiler configuration (Kitto & Stultz 2005). The outcome of this research could, however, be extended in the future to other types of supercritical and ultra-supercritical pulverised coal plant.

1.4.- Post-Combustion Carbon Capture Retrofit

Any PCC process requires energy, which can be supplied by the existing plant or by an additional fuel source. The different carbon capture retrofit options evaluated in this thesis can, in principle, be implemented for any PCC process and/or any combination of thermal energy and power requirements. The aqueous amine scrubbing process is used as an example of PCC processes, which needs heat for solvent regeneration and power for CO_2 compression and ancillary equipment.

1.4.1.- The Aqueous Amine Scrubbing Process

The PCC process using an amine-based solvent is located downstream of the conventional pollutant controls for particulate matter (PM), nitrogen oxides (NO_x) and sulphur dioxide (SO_2). The flue gas is conditioned in a direct contact cooler (DCC) prior to contact with the amine solution.

The DCC saturates and cools the incoming flue gas and removes impurities such as acid gas and particles that would otherwise increase solvent degradation. CO_2 lean amine is fed to the top of the absorber and flows downward through the absorber, counter-current to the flue gas, ending up as CO_2 rich amine. Due to the low temperature at the bottom of the absorber high rich loadings can be achieved.

The liquid to gas ratio needs to be carefully controlled in order to achieve the required capture rate at a minimum specific re-boiler duty. The optimum liquid to gas ratio increases the CO_2 partial pressure at the top of the stripper and, subsequently, reduces the water evaporation in the stripper.

In order to minimise amine slip in the absorber a wash section is located above the absorption section, in this manner, alkaline compounds such as amine and ammonia are not sent to the atmosphere. Washing steps also cool down the flue gas leaving the absorber and control the water balance of the CO_2 capture process. Additionally, a demister is located at the top of the absorption column to ensure no carry-over of amine droplets. The flue gas leaves the absorber saturated with water.

Once the aqueous amine solvent has selectively absorbed the CO_2, it is sent to the rich-lean heat exchanger (RLHX) where sensible heat is transferred from the lean to the rich solution. The pre-heated rich solution is pumped to the stripper in which the CO_2 is released by supplying heat in the reboiler. CO_2 stripping heat is provided by condensing low pressure steam, possibly extracted from the power plant steam cycle. The lean amine solution is then recycled to the absorber.

Gas from the stripper overheads, predominantly CO_2 and H_2O, is cooled in a condenser in which a large part of the water is condensed and the remaining gas is routed to the CO_2 compression and conditioning systems. Condensed water is used in different parts of the carbon capture plant, for example, a portion is used to provide a reflux to the stripper.

A typical MEA scrubbing post-combustion capture process with a single absorber, stripper and lean-rich heat exchanger is represented in *Figure 1.4*.

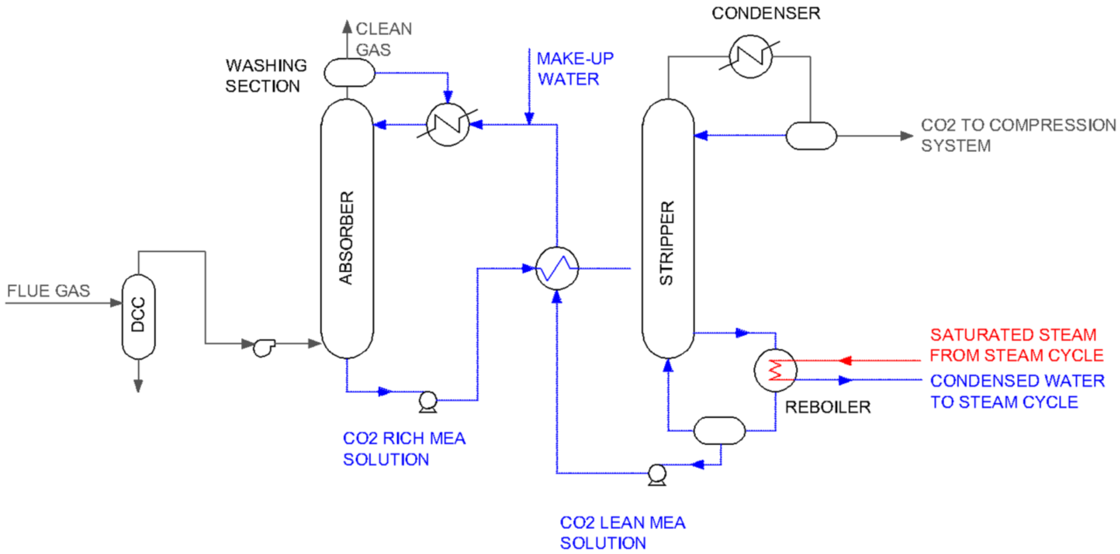

Figure 1.4.- Process Flow Diagram of an Aqueous Amine Based Post-Combustion Carbon Capture Plant

A fraction of the solvent is sent to a thermal reclaiming unit to remove the impurities accumulated from the flue gas and solvent degradation products. NaOH is typically used to neutralise the degradation products which are then heated to boil off water and solvent. Non-volatile impurities and solvent degradation products are accumulated in the Reclaimer System while water and solvent are returned to the stripper column.

CO_2 from the stripper overheads is compressed to 13 bar in a three-stage centrifugal compressor. The inter-coolers are designed to cool the CO_2 down to 50ºC by means of condensate water heating. The number of compression stages depends on the compression ratio. The CO_2 is then liquefied by the use of a propane refrigeration system and pumped to a pressure of 140bar (DOE/NETL 2007).

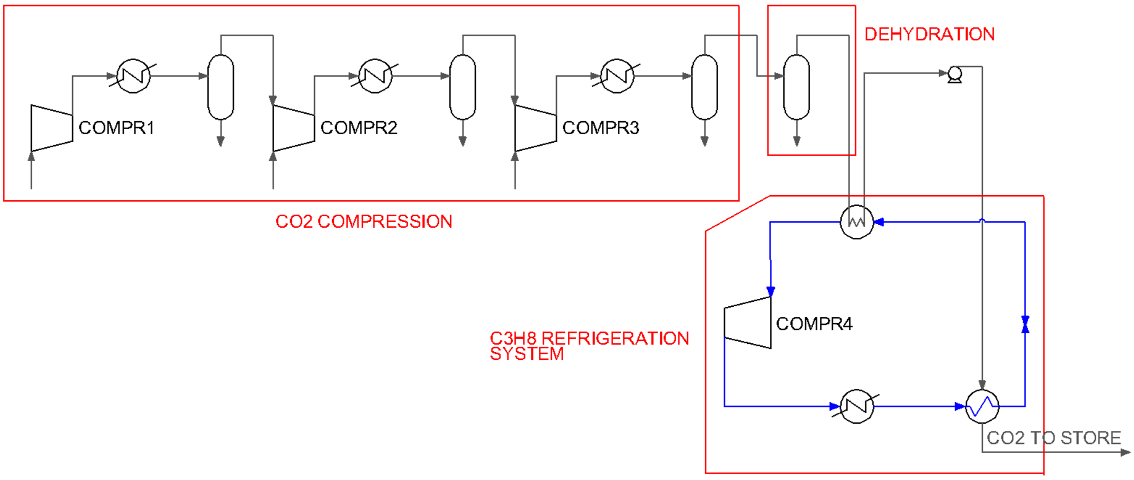

Figure 1.5.- Process Flow Diagram of the CO_2 Compression System

1.4.2.- Thermodynamic Integration of the amine process with the power cycle and with CO_2 compression

The energy requirement for Aqueous Amine Scrubbing post-combustion capture process is a mix of heat supplied to the stripper and electrical energy for CO_2 compression and ancillary equipment, such as circulating pumps and flue gas fans.

The heat provided to a stripper to regenerate the solution is often broken into three separate components (Meldon 2011):

- Sensible heat: heat required to bring the stream of rich amine up to the operating temperature of the reboiler.
- Heat of reaction and of dissolution: heat is necessary to reverse the chemical reactions between the solvent and the CO_2 and to drive out the CO_2 from the liquid
- Heat of water evaporation: heat is required to produce that part of the stripping steam in the reboiler which is being condensed in the overhead condenser.

The recovery of CO_2 from the rich amine stream from the absorber is a highly energy intensive procedure which requires substantial quantities of low/intermediate pressure steam extraction from the power plant turbine cycle.

The power cycle of capture ready plants is designed to accommodate a future retrofit with CO_2 capture, however, this is not the case for most existing plants and the integration of the capture system may incur excessive energy penalties. This section discusses how to achieve an effective thermodynamic integration between the capture and compression plant and the power cycle of a retrofitted unit, and so, how to reduce efficiency penalties close to those of capture ready plants.

One important aspect for the thermodynamic integration is the quality of steam extracted from the power plant steam cycle to provide condensing steam for solvent/sorbent regeneration. The quality of steam is determined by the temperature of the reboiler. The saturation temperature of the steam has to be the temperature of the reboiler plus a reasonable temperature difference. The larger the temperature difference the lower the investment cost of the heat exchanger but the higher the losses in power output.

Solvents tend to be regenerated at the highest sustainable temperature in order to release the CO_2 at the highest possible pressure. For example, MEA is regenerated at around 120ºC to avoid degradation issues. The combination of the Clausius-Clapeyron equation for CO_2 with that for H_2O reveals that the vapour pressure of CO_2 increases with temperature more strongly than the vapour pressure of water (Freguia 2002) The higher the total pressure in the stripper the less the stripping steam required to drive the CO_2 into the gas phase and the lower the reboiler duty required to regenerate the solvent. With a desorber temperature of 120 ºC and a temperature difference of 10 K for the heat exchanger, steam at pressure of 3.05 bar is required.

The optimal steam extraction point was found at the IP/LP crossover due to low energy penalty, low capital cost and good load capability (IEAGHG 2004; Mimura et al. 1997; Desideri & Paolucci 1999; Gibbins et al. 2004). These studies suggested the use of a throttle and a pressure maintaining valve to be able to supply the steam at the required pressure at different operating loads. Other researchers (Lucquiaud & Gibbins 2011a; Lucquiaud & Gibbins 2011c) suggested the use of more appropriate steam turbine solutions.

In the PCC plant there is a significant amount of waste heat that could be integrated into the retrofitted steam cycle, however, most of this heat is available at low temperatures and only heat from the stripper condenser and from the CO_2 compressor intercoolers is used (Mimura et al. 1997; Desideri & Paolucci 1999; Romeo, Espatolero, et al. 2008; Pfaff et al. 2010; Gibbins et al. 2004). Steam extraction for condensate water heating is substituted by heat recovered from the PCC and compression process, so that less steam is extracted from the steam cycle and the power output of the steam cycle is increased, partially offsetting the effect of steam extraction for solvent generation.

1. 4.3.- An introduction to retrofit options with gas turbine power cycles

Since PCC systems are added downstream of the flue gas cleaning process of existing power plants, they do not entail substantial modifications of the base plant. Therefore, the contribution of PCC technology to retrofit existing coal plants can play an important role in the deployment of carbon capture and storage (CCS) for a fast-track emission mitigation strategy (Chalmers et al. 2009).

If pulverised coal power plants were built as capture ready, it is very probable that these plants would be successfully retrofitted in the future. However, this is not the case for most existing plants and many technical and economic factors have an influence on the feasibility of retrofitting capture to an existing pulverised coal power plant.

When retrofitting CO_2 capture to an existing coal plant a large array of technical considerations need to be taken into account. Two issues are considered as show-stoppers:

- A lack of access to a viable geological CO_2 storage site, and
- Space restriction around the existing site. This may include lack of space for the PCC plant, and/or lack of space or access for the equipment associated with the integration of the PCC Plant, e.g. if a flue gas desulphurisation (FGD) unit is required.

These barriers can only be resolved by closing the existing plant, and possibly building a new plant instead.

Other important considerations determine the viability of a scenario where a pulverised coal plant is retrofitted with PCC:

- The additional investment and the associated running costs of the new capacity needed to replace the 'lost' power output of the site and avoid loss of revenue from electricity sales.
- The energy requirement to provide electricity and heat to the PCC plant, and its integration with the power plant.
- Cooling requirements, the availability of water, the return temperature of water to the environment, and whether air-cooling is a viable alternative option.
- Approaches for flexible operation with CCS and strategies for coping with reduced power output from the site.

A common way to retrofit with PCC is to supply all electricity and heat required to operate the capture equipment from the existing steam cycle (a 'standard integrated retrofit). The thermal energy of solvent regeneration is provided by steam extraction from the main power turbine and the electricity output of the site is typically reduced.

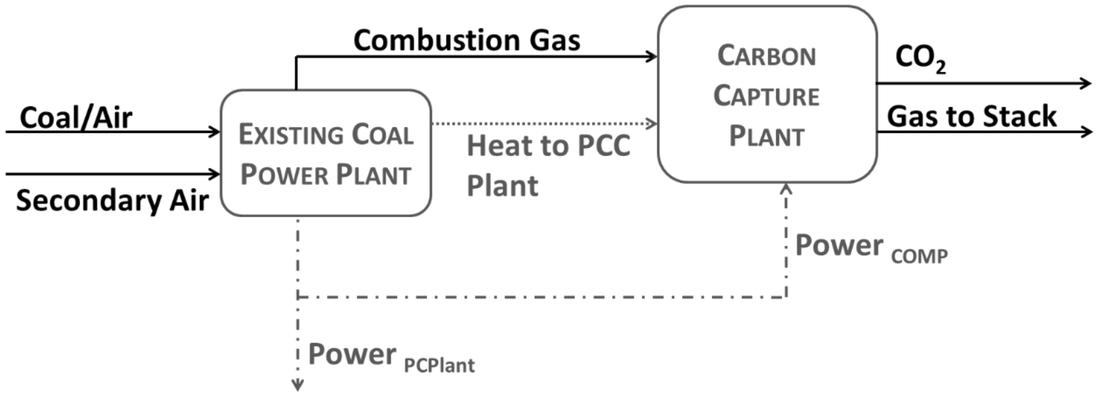

Figure 1.6.- Schematic diagram of a fully integrated retrofit.

The power output penalty associated with CO_2 capture is estimated in Chapter 6 where the performance of a PCC retrofit on a pulverised coal power plant is determined. For a generic 30% wt Monoethanolamine solvent, without advanced process integration, the capture process would require 50 percent of the steam that normally flows through the low-pressure steam turbine. In addition, the auxiliary power requirements for the CO_2 capture and compression process is 50 MWe. Consequently the power output of the site is decreased by approximately 20% (from 600.3 MWe to 473.9 MWe).

As an alternative, it is possible to add a combined heat and power (CHP) plant to maintain, or even increase, the net site power output. The CHP supplies some or all of the heat and power required for the capture system to treat emissions from both, the combined cycle and the retrofitted coal plant.

Different options are considered in this work, based on previous preliminary analysis in (IEAGHG 2011):

Power matched retrofit: a CHP plant provides the electrical power required for the capture process (compression and the ancillary power of capture system) and covers any loss in power output to restore the net power output of the plant to match the net power output of the before capture is added. The remainder of the heat is provided by extraction from the existing steam cycle.

Figure 1.7 shows a schematic diagram of a power matched retrofit.

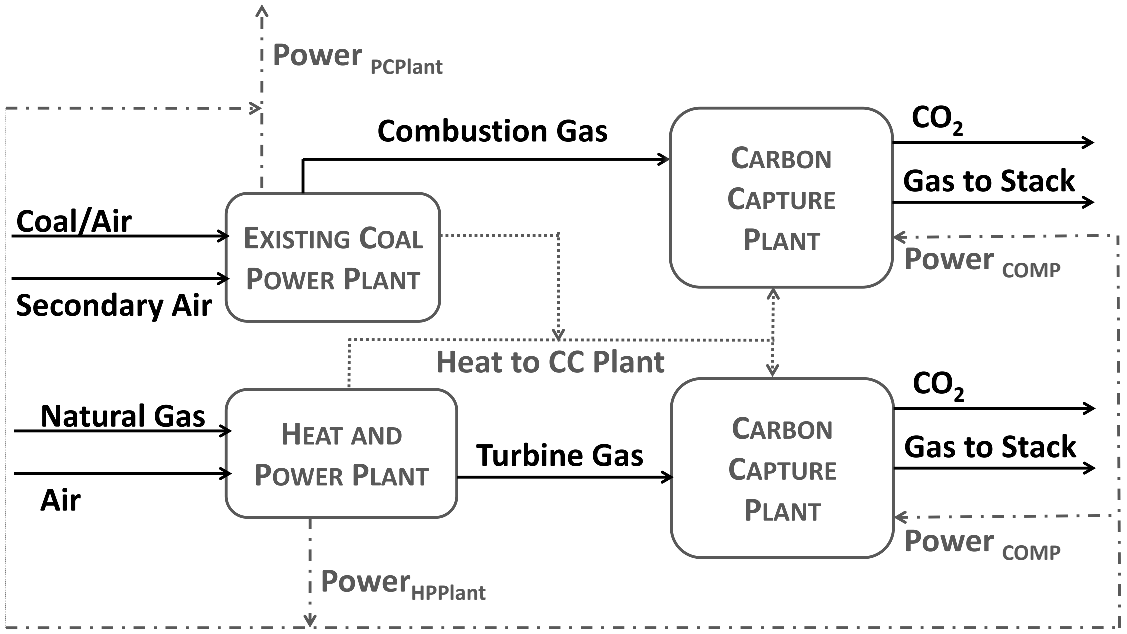

Figure 1.7.- Schematic diagram of the power matched retrofit

Heat matched retrofit: a CHP plant supplies the electrical power and all the heat required for the capture process, matching the thermal energy requirement for solvent regeneration. This option provides additional power increasing the net power output of the site.

Figure 1.8 shows a schematic diagram of a heat matched retrofit

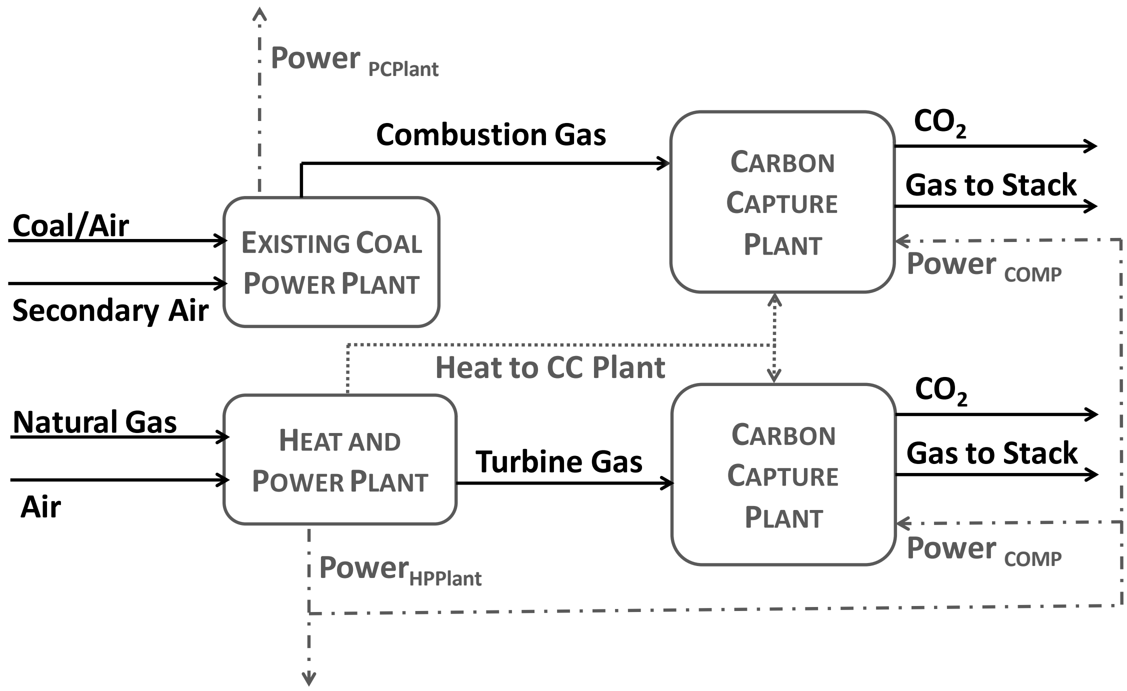

Figure 1.8.- Schematic diagram of the heat matched retrofit.

As one of the rules to optimise the PCC plant performance is ‘to produce as much electricity as possible from any additional fuel used’ (Gibbins et al. 2004)., the combined heat and power plant considered in this thesis consists of a natural gas turbine (GT). Gas turbines supply high power to heat ratio and can be adjusted to provide any mix of heat and power.

An important concern in the context of decarbonisation of fossil fuel use is whether carbon emissions from both the additional fuel source and the retrofitted coal plant are captured, or from the latter only. The thesis examines different options and the associated configuration of PCC retrofit to existing coal plant where the total CO_2 emissions from the plant meet the emission performance standard (EPS) for new UK fossil fuel power station, at 450 gCO_2/kWh (UK Parliament 2013), or where the CO_2 emissions from both fuel sources are captured. The latter is relevant in the context of CCS being deployed as part of a global movement to get deep emission cuts (CCC 2009) so that eventually a large fraction of emissions need to be captured (to achieve <100 gCO_2/kWh).

2.- ACHIEVING HIGH LEVELS OF CO_2 CAPTURE IN PULVERISED COAL PLANT RETROFIT OPTIONS WITH GAS TURBINE POWER CYCLES

2.1.-Post-combustion carbon capture retrofit of a coal power plant with the addition of gas turbine power cycle

In order to largely decarbonise the power generation sector the CO_2 emissions from both fuel sources should be captured and compressed, in the context of the on-site addition of a gas turbine power cycle as part of the retrofit of an existing coal plant.

High levels of CO_2 capture in coal plant retrofits with an additional gas turbine (GT) can possibly be achieved by adding two PCC units downstream of the coal plant and downstream of the GT. or by mixing the flue gas from both fuel sources and treating them in the same PCC Plant.

In some circumstances, efficient mixing of large volumes of gas with different composition and temperature is difficult to achieve and stratification issues might occur. For example, in existing coal power plants some stratification issues can occur when air leaks into the gas stream typical from air-preheaters or when scrubber by-pass gas mixes the flue gas.

Although it is commonly believed that turbulent gas flow minimises the chances of stratification, turbulent eddy diffusion studies reveal that, in order for good mixing to take place with highly stratified gas a duct of at least 100 straight duct diameters in length would be needed (Sherwood & Pigford 1952). In one comprehensive study, in which ten different fossil fuel flue gas ducts were used to take 792 oxygen traverse samples, Luxi found that single point samples generally are nonrepresentative when it comes to large ducts as stratification is usually present (EPA 1974).

Achieving sufficient mixing of the flue gas from a GT and a coal power plant for effective capture in the absorber column of an aqueous amine scrubbing process is likely to be result in similar complications, as flow distributions does not only vary spatially but will also vary over time. Any change in process load would alter the stratification, e.g. at part-load operation of the coal boiler or the gas turbine, or both, or if capture levels in the absorber are intended to be temporarily reduced.

Flue gas mixing is a critical issue as it controls the degree of pollutant dispersion. There is a need to determine if temporal as well as spatial fluctuations affect gas concentration. A single point could be used for samples over the whole sampling period and the data collected would indicate the change in gas concentrations. Traverse data can be difficult to interpret if during the sampling period concentration levels vary at all locations (EPA 1994). For this reason, a complete characterization of pollutant flow distribution is a very complex process and, when possible, stratification issues must be avoided.

Stratification issues could be solved by making use of straightening vanes or baffles, however, these solutions generate large pressure drops with associated consequences for additional power to move the flue gas through the ductwork and, consequently, higher operating costs (EPA 1974).

For the configurations studied in this work corresponding to a pulverised coal plant of 600MW of output and a gas turbine of 140 MW of output, the flue gas composition of the resulting stream is indicated in Table 2.1.

Table 2.1.- Flue gas composition of coal plant, GT Plant and flue gas mixture.

		Coal Plant	GT Plant	Mixing flue gas
O_2	%	3.3%	12.0%	5.6%
CO_2	%	13.6%	4.0%	11.1%
SO_2	%	0.2%	0.0%	0.2%
H_2O	%	8.4%	8.7%	8.5%

The CO_2 concentration at the inlet of the carbon capture plant reaches 11% v/v, in comparison to 13.6 % v/v of the flue gas from the coal plant and 4.0% v/v of the flue gas from the GT plant. At constant capture rate the specific reboiler duty of the PCC plant stripper increases as the CO_2 concentration in the flue gas decreases.

The minimum work required for separating CO_2 from a gas mixture for an isothermal and isobaric process is equal to the negative difference in Gibbs free energy of the separated final state from the mixed initial state. Equation [2.3] indicates the minimum thermodynamic work required to compress the CO_2 from the absorber inlet condition to the stripper outlet conditions (Freguia 2002). The higher the CO_2 concentration at the absorber inlet the lower the thermodynamic work required to desorb it.

$$\frac{W_{min}}{n_{CO2}} = \Delta G_{T,P} = R \cdot T \cdot ln \frac{P_{CO2,out}}{P_{CO2,in}} \qquad [2.1]$$

Where:

$\Delta G_{T,P}$ = Difference in Gibbs free energy for an isothermal and isobaric process

R = Universal gas constant

T = Temperature of the gas at the absorber inlet

$P_{CO2,out}$ = Partial pressure of CO_2 at stripper outlet conditions

$P_{CO2,in}$ = Partial pressure of CO_2 at absorber inlet conditions

However, reaction kinetics and mass transfer also play an important role in the chemical absorption process. Mass transfer rates depend, among other factors, on the available, driving force, which is directly related to the partial pressure of CO_2, and determine the effective loading of the solvent. When mass transfer rates limit the absorption process, the CO_2 loading of the solvent deviates substantially from the equilibrium value, which reduces solvent capacity and has a negative impact on the reboiler duty necessary to regenerate the solvent since more solvent is used to capture the same amount of CO_2. This effect has been taken into account by rigorous modelling of the chemical absorption process using the rate-based model developed by Aspen Plus. Annex 2 briefly describes this rate base approach.

Figure 2.1 and Figure 2.2 illustrate how changes in the absorber packing height influences the reboiler duty and rich solvent loading for the two flue gas CO_2 concentrations discussed earlier. The mass transfer rates in the absorber are relatively slower at lower CO_2 partial pressures. In short columns, the area for mass transfer is also limited resulting in lower CO_2 rich loadings. In these cases, more solvent is circulated in the process to maintain the capture level which leads to higher reboiler duties. This effect is stronger at lower CO_2 partial pressures.

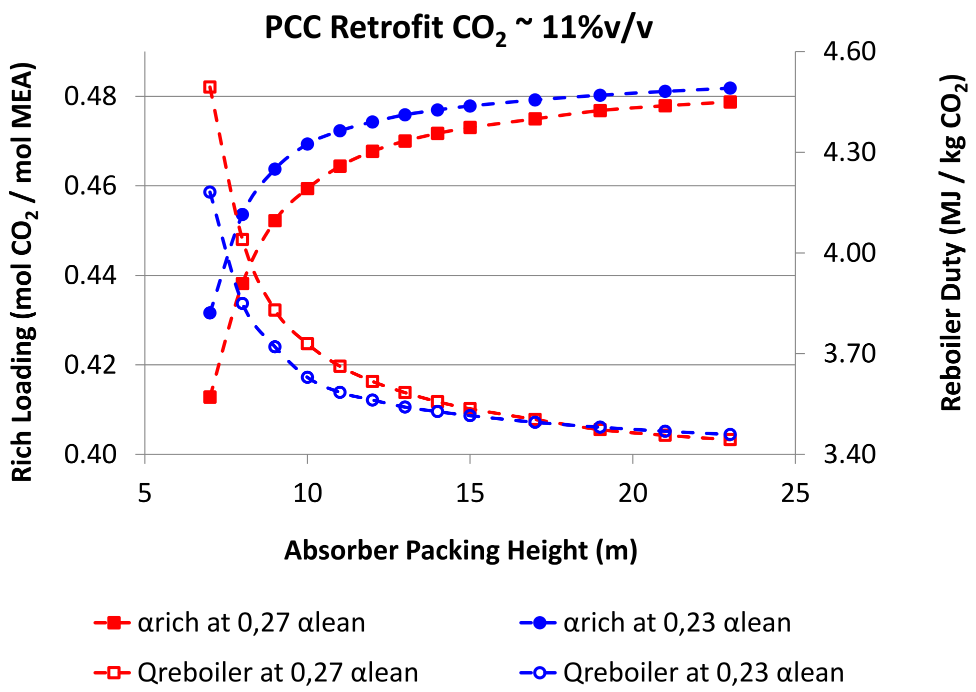

Figure 2.1.- Effect of absorber height on reboiler duty and rich loading at 11% v/v CO_2 concentration

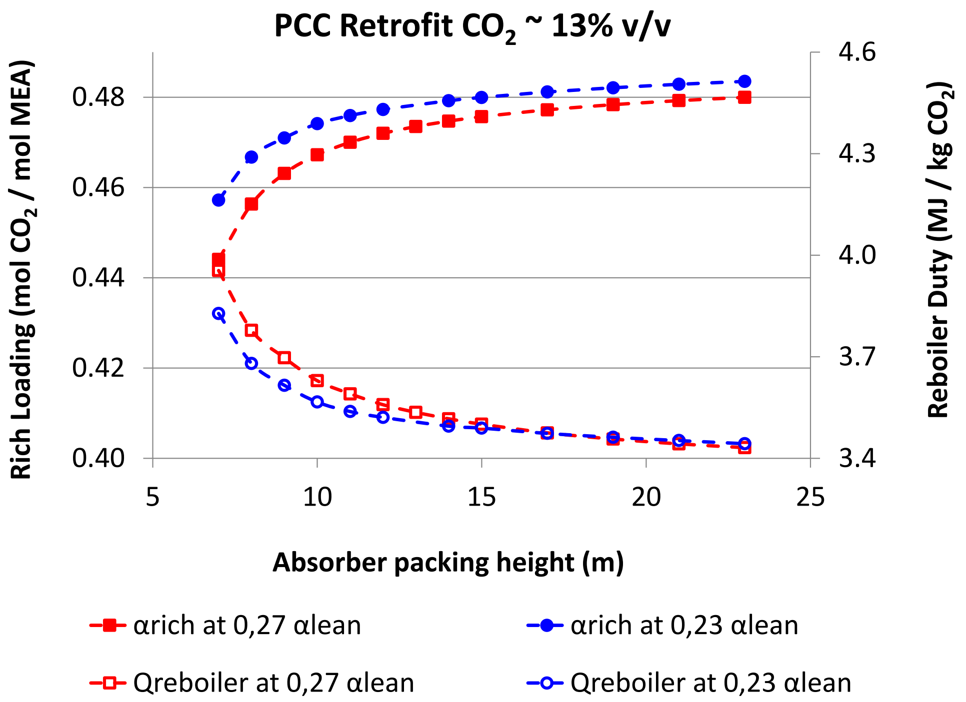

Figure 2.2.- Effect of absorber height on reboiler duty and rich loading at 13% v/v CO_2 concentration

Figure 2.1 shows that at 7m of packing for a CO_2 concentration in flue gas of 11% v/v, the lean and rich solvent are 0.27 mol/mol and 0.44 mol/mol and the reboiler duty is 4.04

MW/kgCO_2. Figure 2.2 shows that at 13% v/v CO_2 concentration in flue gas and the same packing height, the reboiler duty decreases to 3.78 MW/kgCO_2, due to the change in solvent lean and rich laoding of respectively 0.27 mol/mol and 0.46 mol/mol.

The O_2 concentration at the inlet of the carbon capture plant reaches 5.6% v/v, in comparison to 3.2% v/v of the flue gas from the coal plant. This increase in O_2 concentration intensifies MEA degradation and produces oxidized fragments of the solvent such as organic acids and NH_3 (Chi & Rochelle 2002; Goff & Rochelle 2004) . The main reasons for minimising the oxidative degradation are:

- Operating costs.

  The degraded solvent must be replaced so as to maintain the same capacity to remove CO_2. This results in higher operating costs.

  The disposal of the degradation products also represents an operating cost.

- Accelerated corrosion of the carbon capture plant equipment

  Amine degradation products are very corrosive and provoke the corrosion of the carbon capture plant equipment. When amine degradation products are present the protective FeS passivation layer formed on carbon steel is destroyed, carbon steel is then unprotected and can be attacked by the H_2S resulting in an accelerated corrosion rate (Lawson et al. 2003).

Additionally, corrosion failures may occur because of condensation of acid flue gases, when flue gas from both fuel sources are mixed. The temperature of the mixture may drop below the dew point and sulphuric acid may condense as small fog droplets and on the fly ash particles. If a mist is formed, most of the droplets are carried away with the flue gas and provoke steel corrosion (Huijbregts & Leferink 2004).

2.2.- Hot windbox repowering of coal power plants for carbon capture retrofit

Since mixing flue gas streams from two fuel sources can prove to be challenging, a viable method not proposed to date yet is a sequential combustion of gas turbine exhaust gas in the existing coal boiler. It reduces the O_2 concentration in the flue gas entering the capture plant and achieves similar CO_2 concentration to that of the coal power plant. This configuration allows CO_2 capture from both fuels in a single capture plant.

The GT flue gas feeds the boiler and replaces a portion of the combustion air from the original fans. This is based on the same principles used for hot-windbox repowering.

Pulverised coal power plants repowering has been investigated since 1950 to recent years. Repowering involves the addition of a new GT and the utilization of the sensible heat of the GT exhaust gases as an economical method for increasing the power output of an existing PC power plant while improving the plant heat rate and reducing GHG emissions *(GE Power Systems 1994)*.

In the hot-windows repowering, the GT exhausts into the windbox of the boiler and/or the primary air ducts of the coal boiler in place of a portion of the air from the original fans. Since the GT exhaust is hot the secondary and/or the primary air heater are bypassed and additional economizer surface is needed to reduce the temperature of the boiler exit gas. Consequently, duties from the bleeding steam is transferred to the boiler. Because the oxygen content of the GT exhausts is lower than ambient air, the mass flow within the existing boiler must be increased in order to be able to sustain the same combustion.

In 1954 the first boiler repowering took place at the Rio Peces Station, West Texas, and some years later this type of repowering was repeated at the Port Arthur Station, Texas (GE Power Systems 2000a).

In 1987 a screening study was developed to assess the viability of repowering different pulverised coal power plants in Virgina. Two configurations were considered: feedwater heating repowering at Mount Storm Unit and boiler windbox repowering at Bremo 4 Unit and Yorktown 3 Unit (EPRI 1987a). In general, the large amount of plant modifications needed to avoid erosion problems makes the boiler windbox repowering infeasible at Bremo 4 and economically less attractive than a new GTCC at Yorktown 3. Nevertheless, feed heating repowering was technically viable at Mount Storm Unit 3 where the power output of the site and the heat rate were increased.

One year later another screening study made by Florida Power & Light evaluated the feasibility of repowering existing pulverised coal power plants. The configuration assessed consisted of a variant of the boiler windbox repowering where an HRSG was added to cool down the GT exhaust gas and generate extra steam (EPRI 1988). The report concluded that this type of repowering was technically viable and could be taken into account as a possible technique to increase the cycle efficiency and the power output of the site.

However, this form of repowering reaches a significant level of technical complexity and some issues may take place: erosion problems due to high flue gas velocities in the boiler, upgrades in ducts and burners due to the higher temperature and larger volume of air, steam derating due to the lower O_2 and higher CO_2 content in the combustion air which modifies the heat transfer in the boiler and construction of the windbox with steel alloy due to the high temperature GT exhaust gas (GE Power Systems 1994; Stenzel, W., Sopocy, D., Pace 1997).

2.3.- Gas Turbine Flue Gas Windbox Retrofit

Some researchers have recently considered GT repowering as an option to decarbonise power generation because of the lower specific CO_2 emission of Natural Gas compared to Coal. For example, Escosa and Romeo suggested repowering as a short-term technology option to reduce carbon emissions until CCS comes into force (Escosa & Romeo 2009).

Simbeck & McDonald assessed different options to reduce CO_2 emissions from existing PC power plants and classified them in three groups: conversions to lower CO_2 emission technologies without CO_2 recovery, conversions with CO_2 recovery technologies and conversions to technologies with no net CO_2 emissions which include nuclear, 100% biomass and wind energy. The first group relates to the GT repowering options (Simbeck & McDonald 2000; Simbeck 2000).

Romeo et al purposed to use GT repowering to supply power for CO_2 compression (Romeo, Bolea, et al. 2008). Two options were studied:

- Feedwater heater repowering: feedwater heating was supplied by the gas turbine exhaust energy in three stages reducing steam turbine bleedings.
- Heat recovery repowering: the gas turbine exhaust energy was utilised to generate reheat steam in a heat recovery steam generator and supply it to the IP steam turbine.

Furthermore, the authors highlighted some of the drawbacks of using hot-windbox repowering for PCC retrofit. The drawbacks consisted of massive modifications in the air-coal system and steam boiler and erosion problems due to an increased flue gas flow rate.

This work proposes variations of the hot-windbox repowering so that most of drawbacks are avoided and it can be considered as a carbon capture retrofit alternative to largely decarbonise the power generation sector. This novel CO_2 capture retrofit configuration is called a 'Gas Turbinel Flue Gas Windbox Retrofit'.

First of all, in order to reduce the impacts to the boiler coal consumption is reduced so that the flue gas velocities are lowered and erosion problems are diminished. Nevertheless, a reduction in coal consumption leads to lower firing rate and, could lead to a reduction in boiler steam flow rates and steam temperature. This is avoided by adding an HRSG to the GT to cool down the exhaust gas and to generate additional steam that could be used to supply thermal energy to the PCC plant for solvent regeneration or to solve steam derating issues of the coal power plant. Chapter 5 provides the relevant details on the integration.

Another important variation of the hot-windbox repowering is to avoid permanent modifications to the boiler so that the coal power plant can be operated with air if needed. As a result, the secondary and/or the primary air heater are not by-passed, unlike proposed in *(GE Power Systems 1994)*, and the addition of economiser surfaces is not necessary. The flue gas from the HRSG is sent to the air heaters instead of directly to the windbox of the boiler.

Additionally, in order to avoid stratification issues due to mixing flue gas with combustion air, the GT flue gas should replace either all of the secondary air or just the overfire air depending on the amount of the GT flue gas sent to the boiler.

The present thesis examines this novel CO_2 capture retrofit configuration where CO_2 emissions from both fuels are captured in the same capture plant after the sequential combustion of the GT flue gas in the existing coal boiler.

2.4.- Objectives and outline of the thesis

The aim of this thesis are to optimise the integration of gas turbine power cycles with existing pulverised coal power plants and with PCC process and to examine options for carbon capture retrofits to existing coal plants. It presents a novel power matched retrofit configuration with the sequential combustion of gas turbine flue gas in the existing coal boiler while capturing carbon emissions from the combustion of coal and natural gas, the 'Gas Turbine Flue Gas Windbox Retrofit'. A techno-economic comparison of these PCC retrofit options then provides insight into the value of each option and investor owned utility.

The scope of work presented in this thesis is organised as follows:

- Chapter 3 explains the underpinning power plant engineering fundamentals of a pulverised coal power plant, with a focus on boiler heat transfer, boiler design, air preheater and steam turbines. It provides the necessary understanding to assess the off design characteristics of a pulverised coal power plant repowered with a gas turbine power cycle and sequential combustion in the boiler and the addition of post-combustion capture.
- Chapter 4 focuses on the modelling methodology, performance calculations of the boiler when gas turbine flue gas is fed to the windbox of the boiler, the gas turbine, the heat recovery steam generator and the steam cycle, and the process modeling of the carbon capture plant.
- Chapter 5 examines the change in performance when the gas turbine is integrated with the subcritical boiler used as reference in this study, and the thermodynamic integration of the new HRSG, the carbon capture plant and the existing steam cycle.
- Chapter 6 provides the range of relevant discrete heat and power matched retrofit options with partial capture and with higher levels of capture that will be evaluated and compared in Chapter 7.
- Chapter 7 then presents a techno-economic comparison of these PCC retrofit options. The methodology is based on an assessment of total revenue requirements, including electricity sales and CO_2 sales to Enhance Oil Recovery, with a sensitivity analysis of important parameters at the end of the chapter. It assesses trends in energy market and site specific factors that may be more favourable to the deployment of power matched gas turbines flue gas windbox retrofit options.
- Finally, conclusions and recommendations for future work are suggested.

3.- ENGINEERING FUNDAMENTALS A GAS TURBINE FLUE GAS WINDBOX CARBON CAPTURE RETROFIT

3.1.- Introduction

The gas turbine (GT) flue gas windbox carbon capture retrofit is a novel power matched carbon capture retrofit where an additional GT with a heat recovery steam generator (HRSG) supplies steam to the retrofitted coal plant and thermal energy to the stripper of the CO_2 capture plant. Electrical power is supplied to the CO_2 and compression process and then to the existing plant to make up for the loss of output due to steam extraction from the existing cycle and to restore the power output of the site, as closely as practical to the output before capture is added.

The novelty of the process consists of effective integration with the boiler and the steam cycle allowing CO_2 from both fuel sources to be captured in a single CO_2 capture unit by replacing part of the combustion air of the existing coal power plant with flue gas from the GT and delivering it to the secondary air heater. This leads to higher CO_2 concentration and lower O_2 concentration in the flue gas entering the capture unit compared to the concentrations that would be achieved if the flue gas streams of two separate plants were mixed.

The combustion of coal with air and gas turbine flue gas modifies heat transfer in the boiler furnace. As a result, steam production is reduced and steam temperatures decrease to some extent. Steam production levels and superheater and reheater steam temperatures in the boiler can be maintained, for power matched retrofits, with the inclusion of an HRSG attached to the GT supplying steam directly to the steam cycle of the retrofitted plant.

For the power matched retrofits, effective thermodynamic integration between the HRSG and the existing steam cycle is achieved by appropriately sizing an unfired triple pressure HRSG. High pressure (HP) and intermediate pressure (IP) superheated steam generated in the HRSG is then injected at the inlet of the HP and IP steam turbine respectively, and large amounts of low pressure (LP) saturated steam is supplied at the pressure required for optimum regeneration of the solvent in the reboiler of the post-combustion CO_2 capture (PCC) plant. There is no need for either an IP economizer or an IP evaporator as superheated steam taken from the outlet of the HP turbine of the existing steam cycle is injected directly into the HRSG. The existing steam turbines are effectively operated as the combined cycle of the combined cycle gas turbine (CCGT).

The process flow diagram of this novel power matched retrofit is represented in *Figure 3.2*.

The present chapter explains fundamentals of a pulverised coal power plant, with a particular focus on the boiler island, steam turbines and steam cycle. A good understanding of these fundamentals is needed to assess the performance of the coal power plant in the following chapters, where the integration of the GT flue gas windbox retrofit leads to a power matched retrofit with the boiler and the steam turbines operating away from their original design conditions. Chapter 4 then focuses on the methodology used for performance calculations, and chapter 5 presents the thermodynamic integration with a typical subcritical pulverised coal power plant operating in conjunction with an amine based solvent post-combustion capture process. The choice of capture technology is taken as an illustrative example, and it is important to note that the gas turbine flue gas windbox retrofit concept could be applied to other capture technologies. One obvious advantage is that the GT system can be adjusted to provide any mix of heat and power. Another important consideration is to supply a dedicated combined cycle to increase the power output of the site, if matching the power of the existing site is not desirable.

3.1.1.- Description of the pulverised coal power plant

The steam generator of the pulverised coal power plant is a natural circulation balanced draft unit with two parallel paths for gases and subcritical parameters, as schematically illustrated in *Figure 3.1*. The steam generator consists of a water wall furnace, a platen secondary superheater (PlatSH) and a final superheater (FSH) in the upper region of the furnace. It comprises a primary superheater (represented in two parts PSH I and PSH II), a reheater (represented in three parts RHB I, RHB II and RHDL), and economiser (represented in two parts ECO I and ECO II) in the parallel pass convection section. The boiler cavities are represented as CAV I and CAV II.

Feed-water enters the bottom header of the economiser, flows upward through the economiser tubes and then exits to reach the boiler drum. Water from the steam drum passes downward through the downcomer pipes and rises back to the drum after it is heated in the furnace tubes. Steam from the steam drum is provided to the furnace roof and convection walls tubes which connect to the primary superheater. The steam then rises through the different boiler superheaters.

Boiler superheated steam is directed from the FSH to the high pressure (HP) steam turbine where it is partially expanded. Then it is returned to the boiler for reheating in the reheater banks. Reheated steam is routed to the inlet of the IP steam turbine.

After travelling through the steam turbines, partially saturated steam enters the condenser. Condensed water is then pressurized in two stages, and flows through a series of feed water heaters. Just before the second stage of pressurization the condensate flows through a deaerator that removes dissolved oxygen from the water, as illustrated in *Figure 3.2*.

Attemperators located between the Plat SH and the FSH are used to control superheated steam temperature. Additionally, a reheater attemperator is used at transient loads to control reheated steam temperature. There are also control dampers at the end of the parallel pass to regulate the reheated steam temperature by adjusting the proportion of gas flow between the two convection paths.

Secondary Air is driven by a forced draft fan to a regenerative air preheater and then routed to the windbox where it is distributed to the burners. The Primary Air Fan provides air to another regenerative air preheater as schematically illustrated in *Figure 3.3*. A portion of the air is passed unheated around the air preheater to temper the primary air in order to reach the desired pulverized fuel-air mixture outlet temperature of 80ºC. The fuel is ground up and then dried and transported by a flow of primary air to coal classifier sections where fuel particles are carried by the primary air through the coal-air ducts to the burners.

After the coal combustion in the furnace, hot gases pass successively across the Plat SH, FSH and RHDL. The flue gas is then split up into two parallel paths, one gas stream flows over the two reheater banks and ECO I bank and the other stream flows over the two primary superheater banks and the ECO II bank. The flue gas leaving the boiler passes through a SCR system to reduce NOx emissions before the gas travels to the air heaters.

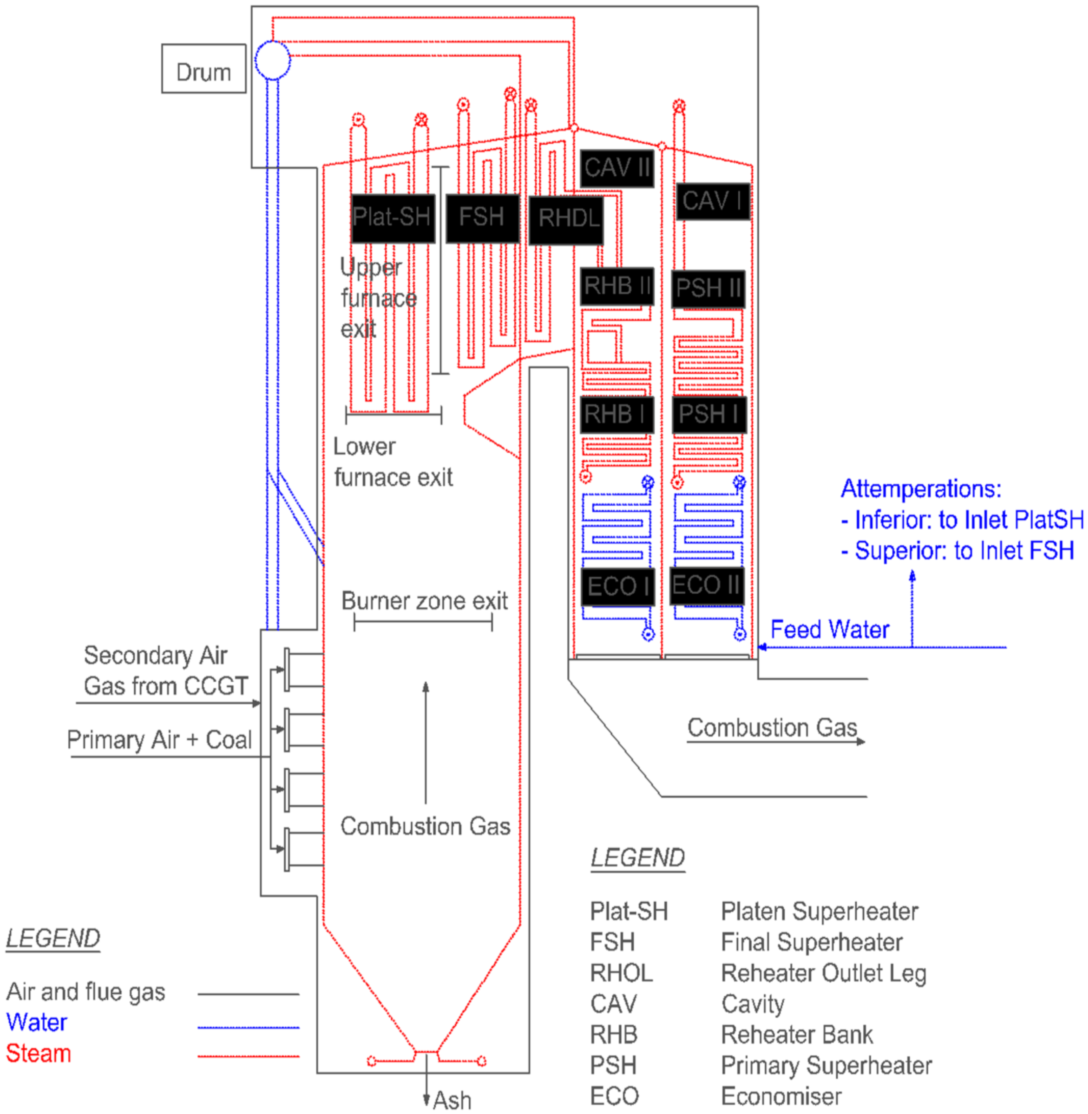

Figure 3.1.- Steam generator of the original coal power plant.

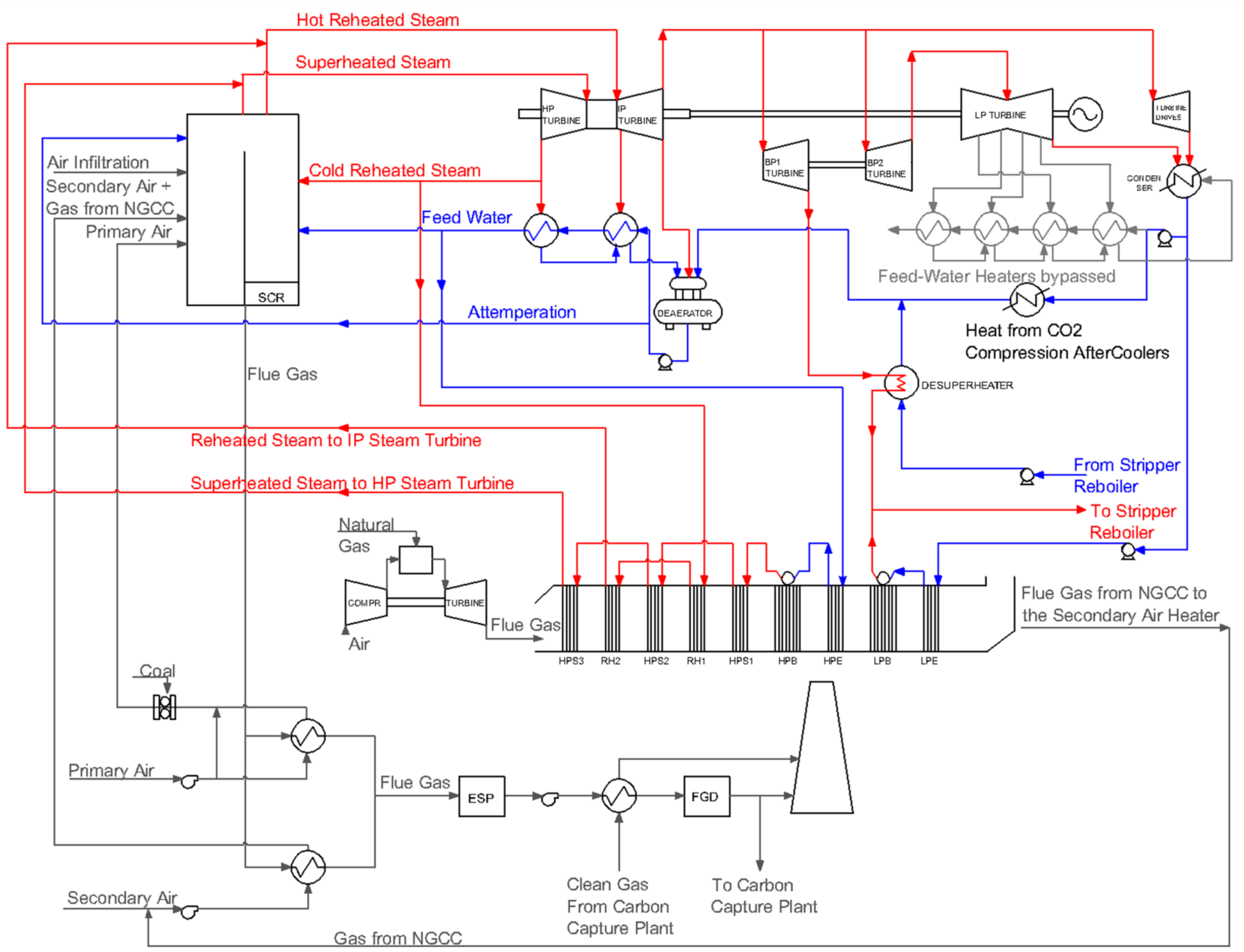

Figure 3.2.- Process flow diagram of a gas turbine flue gas windbox retrofit.*

*The boiler flue gas outlet and all downstream equipment, including the carbon capture plant, are not represented for convenience of presentation)

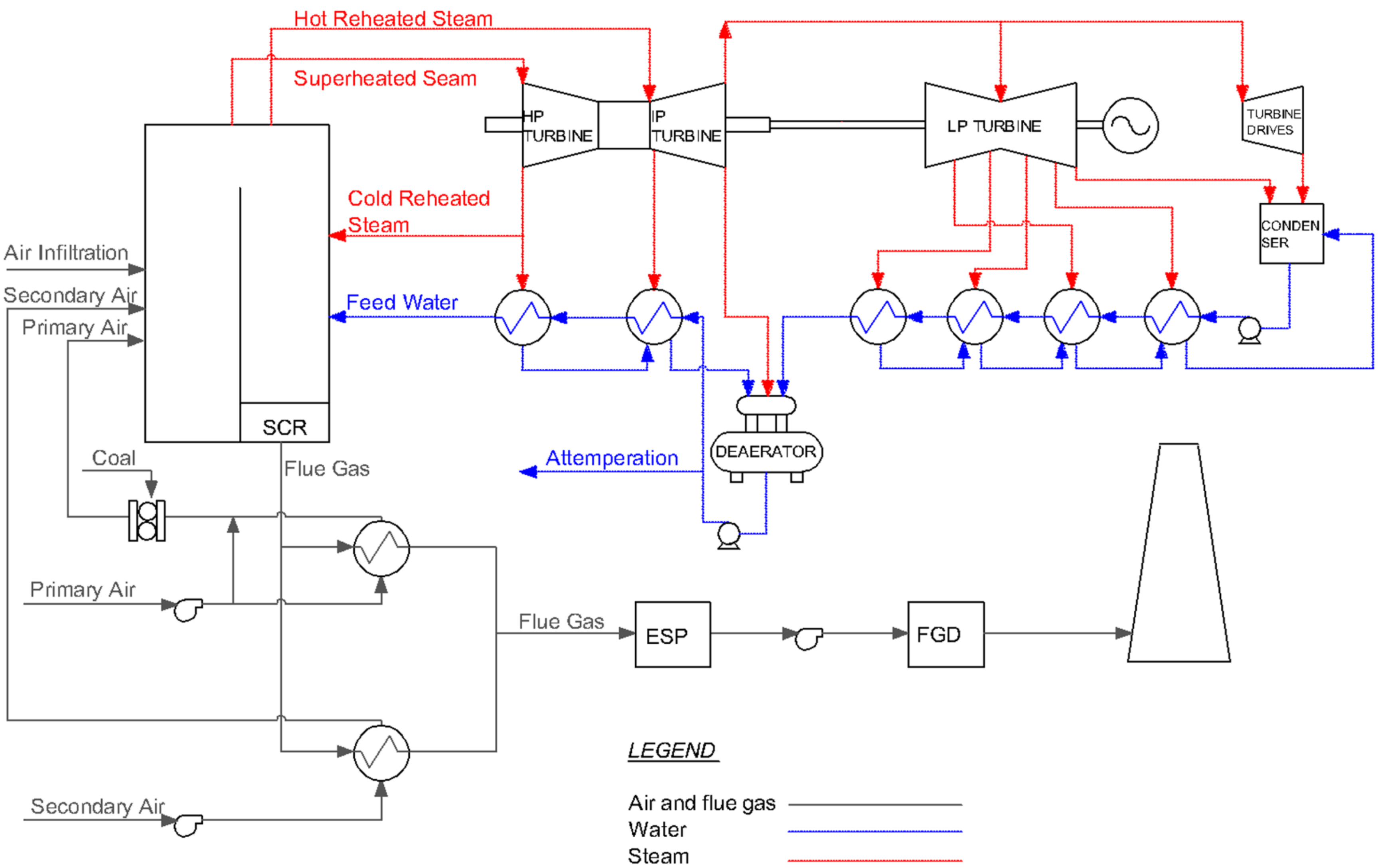

Figure 3.3.- Process flow diagram of coal original power plant

3.2.- FUNDAMENTALS OF BOILER HEAT TRANSFER

This section describes the fundamentals of heat transfer in the boiler required to illustrate the methodology used to assess the overall performance of the GT flue gas windbox retrofit.

3.2.1.- Fundamentals of heat transfer

Previous studies of heat transfer systems have demonstrated that fluid flow and heat transfer data can be correlated by dimensionless numbers. Convective heat transfer coefficient can be characterised by a series of dimensionless numbers.

The Reynolds Number is defined as the ratio of the inertial forces to the viscous forces, as indicated in Equation [3.1].

$$\mathrm{Re} = \frac{\mathrm{G} \cdot \mathrm{L}}{\mu} \qquad [3.1]$$

Where:

Re	=	Reynolds number
G	=	Mass flow per unit area
L	=	Characteristic length of the conduit or channel
μ	=	Dynamic viscosity of the fluid

For internal flows and circular conduits, L corresponds to the inside diameter, while for external flows the outside diameter is used.

The Prandtl Number is the ratio of momentum diffusivity to thermal diffusivity. It also indicates the ratio of the relative thickness of viscous and thermal boundary layers.

$$\mathrm{Pr} = \frac{c_p \cdot \mu}{\mathrm{k}} \qquad [3.2]$$

Where:

Pr	=	Prandtl number
c_p	=	Specific heat of the fluid
k	=	Thermal conductivity of the fluid

The Nussel Numbrer is the ratio of convective to conductive heat transfer across the boundary surface.

$$\mathrm{Nu} = \frac{\mathrm{h} \cdot \mathrm{L}}{\mathrm{k}} \qquad [3.3]$$

Where:

Nu	=	Nussel number
h	=	Convective heat transfer coefficient of the fluid

Turbulent flow inside tubes:

Water and gases in laminar flow inside tubes are not often encountered in pulverised coal boiler applications and will not be examined in this section.

Dittus and Boelter provided a correlation for turbulent heat transfer for fluids with Prandtl number in the approximate range 0.7-160 (McAdams 1954). This range covers all fluids in boiler analysis.

$$\mathrm{Nu} = 0.023 \cdot \mathrm{Re}_f^{0.8} \cdot \mathrm{Pr}_f^{n} \quad [3.4]$$

Here, n = 0.4 if the fluid is being heated and n = 0.3 if the fluid is being cooled. All the physical properties are evaluated at the average bulk temperature of the fluid.

For boiler applications where the flow is fully developed inside tubes, equation [3.4] is re-written in the form of equation [3.5]. A temperature correction factor is added to convert the properties from the bulk to the film temperature.

$$\mathrm{Nu} = 0.023 \cdot \mathrm{Re}_f^{0.8} \cdot \mathrm{Pr}_f^{n} \cdot \left(\frac{T_b}{T_f}\right)^{0.8} \cdot \frac{\mathrm{ID}}{\mathrm{OD}} \quad [3.5]$$

Where:

T_b	=	Bulk temperature of the fluid
T_f	=	Film temperature
ID	=	Inside diameter of the conduit
OD	=	Outside diameter of the conduit

The film temperature is defined as follows:

$$T_f = \frac{T_w + T_b}{2} \quad [3.6]$$

Where:

T_w	=	Wall temperature
T_b	=	Bulk fluid temperature

When one working fluid controls the overall heat transfer coefficient the film temperature can be approached as:

$$T_f = \frac{T_{s\_in} + T_{s\_out}}{2} + \frac{\mathrm{LMTD}}{2} \quad \mathbf{[3.7]}$$

Where:

T_{s_in}	=	Steam temperature entering bank
T_{s_out}	=	Steam temperature leaving bank
LMTD	=	Log mean temperature difference

Turbulent flow around tubes:

Colburn (Colburn 1964) proposed a simple correlation for heat transfer of tubes in cross flow:

$$\mathrm{Nu} = 0.033 \cdot \mathrm{Re}_f^{0.6} \cdot \mathrm{Pr}_f^{1/3} \qquad [3.8]$$

However this correlation can only be applied well for banks with a staggered tubes arrangement and with ten or more rows of tubes in the flow direction.

Huge (Huge 1937) and Pierson (Pierson 1937) reported extensive research on heat transfer during viscous flow across in-line and staggered banks of tubes. Grimison (Grimison 1937) correlated the experimental data of Huge and Pierson for both arrangements and gave a correlation of the form:

$$\mathrm{Nu} = 0.321 \cdot \mathrm{Re}_f^{0.61} \cdot \mathrm{Pr}_f^{0.33} \cdot \mathrm{F_a} \cdot \mathrm{F_d} \qquad [3.9]$$

Where:

F_a	=	Arrangement factor
F_d	=	Depth correction factor

Fa depends on the ratio of tube spacing to diameter and the Reynolds number in the flue gas and Fd takes into account entrance effects for banks of tubes. A depth correction factor, Fd, must be included when a bank of tubes has less than ten rows, otherwise, Fd is equal to unity. Values of Fd and Fa for commercially clean tubes conditions can be found in Chapter 4 of The Steam Book (Kitto & Stultz 2005).

Overall heat transfer rate

Boiler systems basically consist of many heat exchangers where heat from the combustion gas is transferred to the water/steam. The heat transfer rate across a heat exchanger can be evaluated by performing an energy balance on the energy lost by the hot flue gas and the energy gained by the cold fluid and it is usually expressed in the form:

$$q_{0ve\ rall} = \mathrm{U} \cdot \mathrm{A} \cdot \mathrm{LMTD} \qquad [3.10]$$

Where:

$q_{0verall}$	=	Overall heat transfer rate

U	=	Overall heat transfer coefficient
A	=	Total heating surface area

The definition of the log mean temperature difference, LMTD, depends on the heat exchanger configuration.

- For a heat exchanger with the hot and the cold fluids in parallel flow, as for a final superheater

$$\mathrm{LMTD} = \frac{\left(\mathrm{T_{g\_in}} - \mathrm{T_{s\_in}}\right) - \left(\mathrm{T_{g\_out}} - \mathrm{T_{s\_out}}\right)}{\ln\frac{\left(\mathrm{T_{g\_in}} - \mathrm{T_{s\_in}}\right)}{\left(\mathrm{T_{g\_out}} - \mathrm{T_{s\_out}}\right)}} \tag{3.11}$$

- For a heat exchanger with the hot and the cold fluids in counter flow, as for most of the superheaters, reheaters and economisers

$$\mathrm{LMTD} = \frac{\left(\mathrm{T_{g\_in}} - \mathrm{T_{s\_out}}\right) - \left(\mathrm{T_{g\_out}} - \mathrm{T_{s\_in}}\right)}{\ln\frac{\left(\mathrm{T_{g\_in}} - \mathrm{T_{s\_out}}\right)}{\left(\mathrm{T_{g\_out}} - \mathrm{T_{s\_in}}\right)}} \tag{3.12}$$

- For a heat exchanger where the cold fluid is boiling as for Screens

$$\mathrm{LMTD} = \frac{\mathrm{T_{g\_in}} - \mathrm{T_{g\_out}}}{\ln\frac{\left(\mathrm{T_{g\_in}} - \mathrm{T_{sat}}\right)}{\left(\mathrm{T_{g\_out}} - \mathrm{T_{sat}}\right)}} \tag{3.13}$$

Where:

$\mathrm{T_{g\_in}}$	=	Gas temperature entering bank
$\mathrm{T_{g\_out}}$	=	Gas temperature leaving bank
$\mathrm{T_{sat}}$	=	Steam saturation temperature

The overall heat transfer coefficient, U, represents the total resistance to heat transfer from one fluid to another

$$\frac{1}{\mathrm{UA}} = \frac{1}{\mathrm{h_{cs}} \cdot \mathrm{A_i}} + R_w + \frac{1}{\mathrm{h_{cg}} \cdot \mathrm{A_o}} \tag{3.14}$$

Rw	=	Tube wall resistance
$\mathrm{h_{cs}}$	=	Convective heat transfer coefficient of the steam
$\mathrm{h_{cg}}$	=	Convective heat transfer coefficient of the gas
$\mathrm{A_i}$	=	Internal heating surface area (steam side)
$\mathrm{A_o}$	=	External heating surface area (gas side)

The convective heat transfer coefficients can be obtained by combining equation [3.3] with [3.5] for the steam and [3.3] with [3.9] for the flue gas.

Convective heat transfer is in this application the overwhelming driving force for heat transfer. The heat exchanger tube wall resistance, Rw, is usually small compared to the surface resistance and can be neglected.

In boilers, due to the high temperature of the gas flowing around the tubes, a large amount of heat is radiated from the gas to the surface of the tubes. This heat transfer mechanism is called intertube radiation and can be evaluated by means of a radiation heat transfer coefficient.

$$h_{rg} = h_r \cdot K \cdot F_s \qquad [3.15]$$

Where:

h_{rg}	=	Gas side radiation heat transfer coefficient
h_r	=	Basic radiation heat transfer coefficient, equation [3.16]
K	=	Fuel factor, equation [3.17]
F_s	=	Effectiveness factor based on areas

The basic radiation heat transfer coefficient hr can be obtained from *Figure 3.*. This figure shows the basic radiation heat transfer coefficient at different receiving surface temperatures (T_s) and log mean temperature differences (LMTD). The receiving surface temperature is usually taken as the steam temperature at the inlet of the convection bank.

The fuel factor K represents the effect of fuel, partial pressure of CO_2 + H_2O and mean radiating length on the radiation heat transfer coefficient and can be obtained from *Figure 3.*.

Data for the basic radiation heat transfer coefficient and fuel factor from (Kitto & Stultz 2005) are, in this work, correlated numerically with the following equation:

$$h_r\left(\frac{Btu}{hr \cdot ft^2 \cdot F}\right) = 9.8410342 \cdot 10^{-3} \cdot T_s(F) + 5.5432559 \cdot 10^{-3} \cdot LMTD(F) - 3.9736801 \qquad [3.16]$$

$$K = -1.243 \cdot 10^{-5} \cdot HHV \cdot PL - 0.397 * PL^2 + 1.236 \cdot PL + 1.053 - 1.365 \cdot 10^{-4} \cdot HHV + \\ + 5.114 \cdot 10^{-9} \cdot HHV^2 \qquad [3.17]$$

Where:

T_s	=	Receiving surface temperature (F)
HHV	=	High heat value of the coal (Btu/lb)

PL = product of the partial pressure of $CO_2 + H_2O$ by the mean radiating length, (atm · ft)

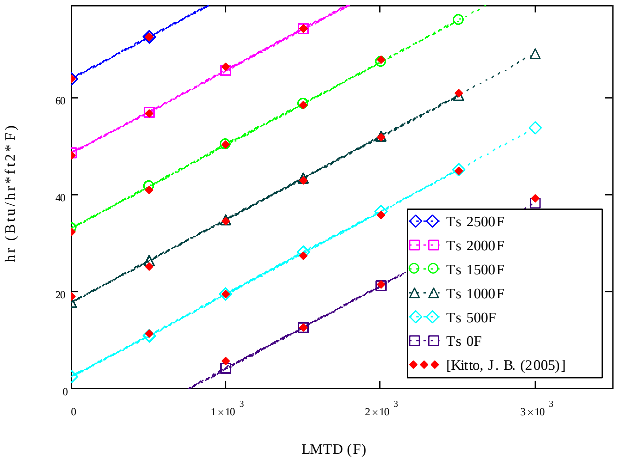

Figure 3.4.- Basic radiation heat transfer coefficient. (Kitto & Stultz 2005)

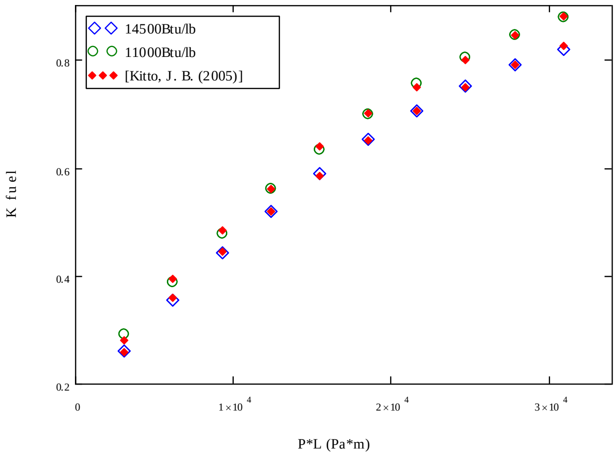

Figure 3.5.- Fuel Factor. (Kitto & Stultz 2005)

Furthermore, an effectiveness factor based on areas is used to eliminate direct radiation from the furnace and cavities. As the intertube radiation is proportional to the total bank heating surface and the direct radiation to the planar area, the effectiveness factor based on area is defined as:

$$F_s = \frac{A - A_{Fp,Bank} \cdot \frac{q_{Rad\_Abs}}{q_{Rad\_Emit}}}{A} \qquad [3.18]$$

Where:

F_s = Effectiveness factor based on areas

$A_{Fp,Bank}$ = Bank flat project area

q_{Rad_Abs} = Total direct radiation absorbed by the bank

q_{Rad_Emit} = Total direct radiation emitted to the bank

Then, the overall heat transfer coefficient for each heat exchanger in the boiler can be evaluated with equation [3.5] and [3.9] for the convective heat transfer coefficient of the steam and gas flows respectively, and the equation [3.15] for the radiative heat transfer coefficient.

- If the steam film inside the tubes is negligible, as in economisers:

$$U = h_{rg} + h_{cg} \quad [3.19]$$

- If steam film is not negligible, as in superheaters and reheaters:

$$U = \frac{h_g \cdot h_s}{h_g + h_s} = \frac{\left(h_{rg} + h_{cg}\right) \cdot h_s}{h_{rg} + h_{cg} + h_s} \quad [3.20]$$

3.2.2.- Furnace heat transfer

The furnace exit gas temperature must be accurately estimated as it affects the design of different components in the boiler. The following heat transfer mechanisms occur in a boiler furnace:

- Nonluminous gas radiation from the products of combustion
- Intersolid radiation between suspended solid particles, tubes and refractory materials
- Convection from the gas to the furnace walls
- Conduction through ash deposits on tubes

However, due to the complexity of the radiation mechanisms and its dependence on the enclosure's geometry, an analytical solution based on theoretical methods alone would not be possible. As an alternative, semi-empirical methods are extensively used in engineering practice to predict local absorption rates in the furnace.

Recently, semi-empirical methods have started to be replaced by numerical methods with increased level of detail and confidence. The most common numerical method is the zone method. By using these methods the radiative heat transfer in an absorbing, emitting, scattering medium can be analysed.

The zone-method consists of dividing the volume and surface of the furnace into zones with uniform temperature and concentration. An energy balance is applied to each zone taking into account the exchange-area coefficients and the emissivity and absorptivity of combustion products as well as the weighted sum of grey gases. In the zone-method analysis a complicated integral equation is replaced by a series of algebraic equations.

Although the use of the zone-method is particularly relevant to analyse the heat transfer in the furnace, the numerical simulation of a pulverised coal boiler with the natural gas flue gas replacing a fraction of the secondary air has not been studied. It would require detailed information of furnace geometry and advanced computational methods relying on the use of a high speed digital computer. It is outside the scope of this study, but could be developed in future work.

As an alternative to the zone model, the semi-empirical method suggested by I. E. Dubovsky (Blokh 1988) is used instead to calculate the heat transfer in the boiler furnace. This method is based on equations of radiative transfer and energy balance in the furnace combined with empirical data and experience of boiler operation.

Since flue gas flows through the furnace at a relatively low velocity the largely dominant force for heat transfer is radiative heat transfer. The convective heat transfer represents only a small fraction of the total heat transferred to the walls and it can be neglected.

Blokh analysed experimental data of heat transfer in furnaces burning different fuels and observed that the dimensionless temperature, $\theta_{exit} = \frac{T_{g,exit}}{T_{th}}$, is a simple function of the furnace parameter, π.

$$\frac{T_{th} - T_{g,exit}}{T_{g,exit}} = \frac{1 - \theta_{exit}}{\theta_{exit}} = \frac{M}{\pi^{0.6}} \qquad [3.21]$$

Where:

θ_{exit}	=	Dimensionless temperature
T_{th}	=	Adiabatic flame temperature
$T_{g,exit}$	=	Furnace exit gas temperature
M	=	Empirical coefficient, equation [3.22]
π	=	Furnace parameter, equation [3.23]

M is an empirical coefficient which value depends on the properties of the fuel and on the location of the burners.

$$M = A - B \cdot \frac{h_{Burner\ \_Center}}{h_{Exit\ \_Center}} \qquad [3.22]$$

Where:

A	=	Coefficients equals to 0.59

B	=	Coefficients equals to 0.5
$h_{Burner\ \_Center}$	=	Height of the mean level of the location of burners
$h_{Exit\ \_Center}$	=	Height of the middle of the furnace exit

The coefficients A and B depend on the type of fuel burnt and on the type of furnace. For pulverised coal furnace and sub-bituminous coal A is equal to 0.59 and B to 0.5 (Basu et al. 2000).

The furnace parameter is defined as:

$$\pi = \frac{1}{\varepsilon_{fu}} \cdot \frac{1}{\psi_w} \cdot Bo \qquad [3.23]$$

Where:

ε_{fu}	=	Furnace emissivity, equation [3.27]
ψ_w	=	Waterwalls thermal efficiency coefficient
Bo	=	Boltzmann number, equation [3.26]

The thermal efficiency of the waterwalls ψ_w characterises the radiative properties of the heating surface taking into account the high thermal resistance of the ash. It is thus defined as the fraction of incident radiation absorbed by the heating surface. Its value depends on the fuel burnt and on the type of waterwall. For pulverised coal furnaces the coefficient can be assumed to be equal to 0.45 (Blokh 1988).

Dubovsky observed that the predicted furnace heat absorption rate depended on the cross-section temperature non-uniformity. Based on the experimental data of the overall heat transfer and flame temperature in the furnaces Dubovsky suggested the following expression:

$$\theta_{exit} = 1 - \frac{0.44}{(\pi^*)^{0.6}} \qquad [3.24]$$

Where:

π^*	=	Furnace parameter

The furnace parameter is defined as

$$\pi^* = 0.1268 \cdot M^{-5/3} \cdot \left(\frac{T_{th}}{1000}\right)^2 \cdot \left(\frac{1}{\varepsilon_{fu}} \cdot \frac{1}{\psi_w} \cdot Bo\right) \qquad [3.25]$$

The Boltzmann number characterises the effect of the furnace loading on heat transfer

$$Bo = \frac{m_{Coal} \cdot \overline{VC_p}}{\sigma \cdot A_w \cdot T_{th}^3} \qquad [3.26]$$

Where:

m_{Coal} = Fuel consumption rate

$\overline{VC_p}$ = Average specific heat in the temperature range from T_{th} to $T_{g,exit}$

A_w = Surface area of the furnace walls

σ = Stefan Boltzman constant equal to $5.678 \cdot 10^{-8}\ W/m^2K^4$

The emissivity, ε_{fu}, characterises the radiative properties of the furnace.

$$\varepsilon_{fu} = \frac{\varepsilon_{fl}}{\varepsilon_{fl} + (1 - \varepsilon_{fl}) \cdot \psi_w} \qquad [3.27]$$

Where:

ε_{fl} = Flame emissivity

The flame emissivity ε_{fl} due to the emission of gases and solid particles of ash and char can be calculated by the following equation:

$$\varepsilon_{fl} = 1 - e^{-k \cdot P \cdot S} \qquad [3.28]$$

Where:

k = Coefficient of radiant absorption in the furnace (1/m·MPa)

P = Pressure of gases in the furnace (MPa)

S = Mean beam length (m)

As flame radiation is absorbed by tri-atomic gases, ash particles and burning char particles the combined coefficient of radiant absorption, k, takes in to account the contribution of these three terms (Basu et al. 2000).

When there is no information of furnace geometry, Holman suggested the following equation to calculate the mean beam length (Holman 1991):

$$S = 3.6 \cdot \left(\frac{V_{fu}}{A_w}\right) \qquad [3.29]$$

Where:

V_{fu} = Furnace chamber volume

A_w = Surface area of the furnace walls

The heat absorbed by the furnace is computed as a fraction of the difference between the total heat available in the furnace and the sensible heat of the flue gas leaving the furnace section. The rest is heat lost due to surface radiation from the furnace exterior.

$$Q_{Furnace} = \emptyset \cdot m_{coal} \cdot \left(Q_{fu} - Q_{exit}\right) = \emptyset \cdot m_g \cdot (h_{th} - h_{exit}) \qquad [3.30]$$

Where:

$Q_{Furnace}$ = heat rate absorbed by furnace

$\emptyset$ = coefficient of heat retention

Q_{fu} = total heat available in furnace

Q_{exit} = sensible heat of flue gas leaving furnace

h_{th} = enthalpy of the flue gas at adiabatic flame temperature

h_{exit} = enthalpy of the flue gas at furnace exit gas temperature

The heat available in the furnace, Q_{fu}, is defined as the energy supplied by the fuel and preheated combustion air, corrected for radiation loss, combustible loss and moisture from the fuel.

3.2.3.- Cavities heat transfer

Cavities refer to the necessary space between tubes banks for sootblowers and to possible surface addition in case heat exchangers need to be upgraded.

Radiation is the only significant mode of heat transfer in the cavity. Heat is transferred from the flue gas volume contained in the cavity to the cooler banks which form its boundaries and the temperature of the gas flowing through the cavity gradually reduces. The respective boundaries of a cavity are defined by the surface of adjacent heat exchangers.

The heat transfer to each boundary can be evaluated by solving the overall heat transfer rate equation, equation [3.10], where the total heating surface corresponds to the flat projected area of the adjacent heat exchanger surface of a given boundary, and the overall heat transfer coefficient to the radiation heat transfer coefficient, equation [3.15].

The effectiveness factor based on areas, F_s, is equal to unity as 100% of the direct radiation of the cavity is absorbed by its boundaries. The mean radiating length of the cavity is determined by solving equation [3.29].

The log mean temperature difference can be estimated by:

$$\mathrm{LMTD_{CAV\_i}} = \frac{\mathrm{T_{g\_in\_CAV}} + \mathrm{T_{g\_out\_CAV}}}{2} - \mathrm{T_{s\_CAV\_i}} \qquad [3.31]$$

Where:

i = number of boundaries, i = 1… 4

$LMTD_{CAV\_i}$ = Cavity log mean temperature difference at boundary i

$T_{g\_in\_CAV}$ = Gas temperature entering cavity

$T_{g\_out\_CAV}$ = Gas temperature leaving cavity

$T_{s\_CAV\_i}$ = Receiving surface temperature at boundary i

The receiving surface temperature is related to the steam temperature at the inlet/outlet of the convection bank located at boundary i, depending on the configuration.

The total overall heat transfer is evaluated as the sum of the rates to each one of the boundaries:

$$q_{Overall\,,CAV} = \sum_{i=1}^{i=N} q_{Overall\,\_i} \qquad [3.32]$$

Where:

$q_{Overall\,,CAV}$ = Total overall heat transfer rate

$q_{Overall\,\_i}$ = Overall heat transfer rate of cavity i

3.2.4.- Boiler banks heat transfer

Three different types of heat exchangers can be classified depending on the heat transfer model involved:

- Radiant banks where direct radiation from the furnace is the only significant mode of heat transfer
- Convection banks where only convection and intertube radiation take place
- Mixed banks where direct radiation takes place in addition to convection and intertube radiation.

The furnace direct radiation absorbed by the radiant heat exchangers and by the exit plane of the furnace can be computed as a fraction of the total heat absorbed in the furnace, equation [3.30]. This fraction consists of the ratio of the effective areas of each surface to the total furnace area. The heat absorbed by the exit plane represents the total furnace direct radiation absorbed by the mixed banks.

Due to the wide spacing between tubes, the heat radiated by the flame to the exit plane reaches the banks of tubes located at the top of the convection pass. An effectiveness factor is used to determine the amount of furnace radiation absorbed by a specific bank based on its configuration; the remainder is then sent to the next bank.

The effectiveness factor used in this work is assumed to be the direct view factor proposed by Hottel for the first row of tubes from an infinite plan (Hottel & Sarofim 1967):

$$F_P = \frac{\left(\frac{Spacing_{\ Tube}}{OD_{Tube}}\right) - \sqrt{\left(\frac{Spacing_{\ Tube}}{OD_{Tube}}\right)^2 - 1} + tan^{-1}\left(\sqrt{\left(\frac{Spacing_{\ Tube}}{OD_{Tube}}\right)^2 - 1}\right)}{\left(\frac{Spacing_{\ Tube}}{OD_{Tube}}\right)} \quad [3.33]$$

On a run by run basis, the radiation from the furnace to the first bank, located directly after the exit plane, is distributed as follows:

- Furnace radiation absorbed by each run:

$$\mathrm{q}_{\mathrm{AbsFurn}\ ,\mathrm{i+1}} = \left(Q_{abs\ \_ExitPlane} - \sum_{i=Run\ 0}^{i=RunN} q_{AbsFurn\ ,i}\right) * F_P \quad [3.34]$$

Where:

$Q_{abs\ \_ExitPlane}$ = heat radiated by the flame to the exit plane

i = number of runs = 0… N and N = total number of runs

$q_{AbsFurn\ ,i}$ = furnace radiation absorbed by run i. The furnace radiation absorbed by run 0 is equal to 0 MJ/hr

$\mathrm{q}_{\mathrm{AbsFurn}\ ,\mathrm{i+1}}$ = furnace radiation absorbed by run I + 1

- The total direct furnace radiation absorbed by the first bank of tubes is:

$$q_{AbsFurn} = \sum_{i=Run\,1}^{i=RunN} q_{AbsFurn\ ,i} \quad [3.35]$$

- The remainder is sent to the next bank:

$$q_{ExitPlane\ ,NextBank} = Q_{abs\ \_ExitPlane} - q_{AbsFurn} \quad [3.36]$$

Then the total direct radiation absorbed by the mixed banks is evaluated by summing the direct radiation from the flame and the radiation from the front and rear cavities.

The heat transferred by direct radiation does not affect the flue gas temperature drop across the mixed bank; however, it represents a fraction of heat absorbed by the steam/water inside the bank tubes. Therefore, the total heat absorbed by the steam takes into account the convection and intertube radiation and the direct radiation from the flame:

$$\mathrm{q}_{\mathrm{Conv\ \_IntertRad}} + \mathrm{q}_{\mathrm{Radiation}} = q_s \quad [3.37]$$

$$q_s = \mathrm{m_s} \cdot \Delta \mathrm{H_s} \quad [3.38]$$

Where:

$\mathrm{q}_{\mathrm{Conv\ \_IntertRad}}$ = heat transfer rate by convection and intertube radiation

$\mathrm{q}_{\mathrm{Radiation}}$ = heat transfer rate by direct radiation

q_s = heat rate absorbed by steam/water

m_s = steam/water mass flow rate

ΔH_s = steam/water enthalpy difference

The gas temperature leaving the bank can be determined by an energy balance:

$$q_{Conv\_IntertRad} = m_g \cdot \Delta H_g \qquad [3.39]$$

Where:

m_g = gas mass flow rate

ΔH_g = gas enthalpy difference

The governing heat transfer equation for convection bank surfaces is defined by equation [3.10]. The overall heat transfer coefficient can be determined by equations [3.19] to [3.20] and the log mean temperature difference by equations [3.11] to [3.13], depending on the heat exchanger configuration.

In practice, the effect of ash or other deposits on the heat transfer surfaces prevents the convection banks from absorbing all the heat transferred and a cleanliness factor needs to be used to account for the associated reduction in heat transfer rate. It can be evaluated by the following expression:

$$F_{Clean} = \frac{q_{Conv\_IntertRad}}{q_{Overall}} \qquad [3.40]$$

Where:

$\boldsymbol{F_{Clean}}$ = cleanliness factor

3.3.- FUNDAMENTALS OF BOILER DESIGN

3.3.1.- Tube diameter:

Heat transfer in most types of heat exchangers is, in general, most effective when tube diameter is minimised. Nevertheless, high steam velocity increases the pressure drop and has an important adverse effect on the steam turbines. Larger diameters also result in thicker-walled tubes. Other factors, such as manufacturing, erection and service limitations, should be taken into account for the selection of an optimum tube diameter.

Tubes of 44.5 to 63.5mm (1.75 to 2.5 in) outside diameter are typical in superheater, reheaters and economisers. Depending on the pressure of the boiler, the tubes are 3-7 mm thick (Kitto

& Stultz 2005). In this project, the tube outside diameter and the wall thickness have been assumed to be 5.08 cm (2 in) and 0.36 cm (0.14 in) respectively.

3.3.2.- Furnace design:

Ash deposition in the furnace reduces furnace heat absorption and increases the furnace exit gas temperature. This would intensify fouling and would cause slagging in the heat exchangers of the convection section of the boiler. Furthermore, in order to be able to reach superheater and reheater steam temperatures the spray flow would have to be increased resulting in a reduction in cycle efficiency. Consequently, furnaces are designed to minimise slagging.

Furnaces should be designed with enough heat transfer surface to cool the flue gas and ash particles to a temperature suitable to minimise the potential for slagging in the convection section. The furnace exit gas temperature (FEGT) is thus below the temperature of ash deformation. Since the initial ash deformation temperature is 1505K in oxidizing atmosphere (DOE/NETL 2012), the maximum value of the furnace exit gas temperature is limited in this work to 1499 K in order to guarantee that ash particles will be in dry solid state and will not stick to heating surfaces.

Platen superheater surfaces are added in the upper zone of the furnace in order to reach the required FEGT. These platen superheaters are designed with wide side spacing to avoid ash particle impaction. The flue gas temperature before the platen superheater should be below 1250 ºC for coal with weak slagging propensity and lower than 1110ºC and 1200ºC for coals with strong and moderate slagging properties respectively (Basu et al. 2000).

Another important parameter to control furnace slagging is the plan area heat release rate at the burners level. For severe slagging coal the limit is around 4.7 MWth / m^2, while for low slagging coals is around 5.7 MWth / m^2.

$$Q_{PlanArea} = \frac{HHV \cdot m_{Coal} \cdot \left(1 - \frac{w_{Ash}}{100} - \frac{UBC}{100}\right)}{Depth_{Furnace} \cdot Width_{Furnace}} = 5.2 \frac{MW_t}{m^2} \qquad [3.41]$$

Where:

$Q_{PlanArea}$	=	Plan area heat release rate
w_{Ash}	=	Ash mass fraction
UBC	=	Unburned coal
$Depth_{Furnace}$	=	Furnace depth

$Width_{Furnace}$ = Furnace width

The classification of slagging potential of the design coal used in this work is medium.

Annex 1 provides the details of the design coal.

The furnace has thus been designed to reach a plan area heat release rate of 5.2 MWth / m^2.

The depth furnace is taken as 13 m (40 ft) and width furnace as 21.3 m (70 ft), based on equation [3.41].

3.3.3.- Convection pass design:

The key for a successful design of convective heating surface consists of minimising the potential for bridging and obstruction of the gas lanes between banks of tubes.

Figure 3. illustrates the geometry of a boiler heat exchanger. The side spacing is defined as the spacing between tubes transverse to gas flow and the back spacing as the spacing between tubes in direction of gas flow.

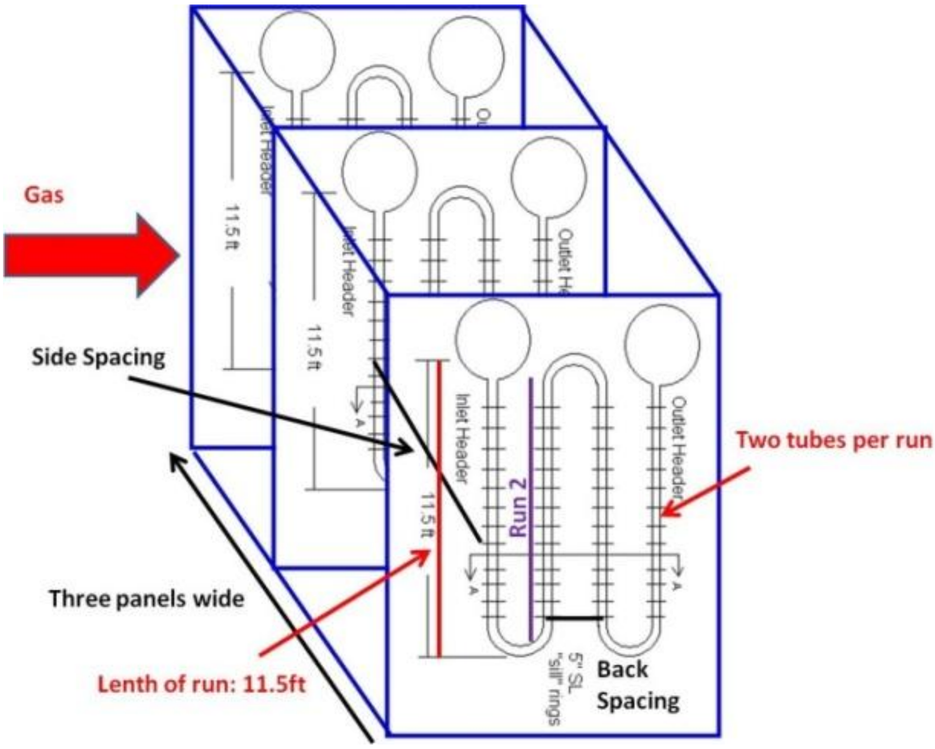

Figure 3.6.- Dimensional parameters of a boiler heat exchanger.

The back spacing between tubes depends on the bend radius of the tubes and has been assumed to be 2.75 in (6.98 cm) for a 2 in OD tube. The side spacing between banks depends on the gas temperature entering the bank and the fouling potential of the design coal. As the Final Superheater and Screen 1 are located just after the furnace exit plane, the gas temperature and the slagging potential are high thus wide side spacing is required. In this study, the final superheaters and the Screen 1 are designed with a side spacing of 60.96 cm (24 in) to minimise the chance of slag bridging across them, based on anecdotal reports on typical values encountered in similar plant configurations (Kitto & Stultz 2005).

As the flue gas is gradually cooled throughout the boiler, the side spacing in following banks is reduced. High gas velocities enhance the heat transfer but lead to high tube erosion problems and fouling type deposits. Even small deposits become troublesome, they restrict gas flow and tend to progress from weak to strongly bonded as their exposure time to the flue gas increases.

Although the fouling potential and the erosion capacity of the design coal is medium, wide enough side spacing is maintained between banks in order to avoid bridging and obstruction of the gas lanes due to ash dislodged from upstream surfaces.

A key design criterion for the convective heat exchangers is the maximum allowable gas velocity. For abrasive high ash coals the typical gas velocity limit is 13.7 m/s and for non-abrasive low ash coals the limit is 19.8 m/s (Kitto & Stultz 2005). In this study the design gas velocity has been assumed to be 10.6 m/s which corresponds to 15.24 cm (6 in) side spacing.

The formation of an insulating slag layer on the tubes of the final superheater might cause slag buildup in the next section of the convection pass, the out leg of the reheater. Consequently, the side spacing of the out leg of the reheater (RHOL) is assumed to be twice the side spacing of its horizontal convective banks, the RHB1 and RHB2, which corresponds to 30.48 cm (12 in).

Figure 3.1 shows the selected plan arrangement of heat exchangers depending on the gas temperature.

Once the side spacing between banks is selected, the number of tubes/width can then be calculated:

$$\text{NºTubes/wide} = \frac{\text{Width}_{\text{Furnace}}}{\text{SideSpacing}_{\text{Tubes}}} \qquad [3.42]$$

Where:

NºTubes/wide	=	Number of tubes/width
$\text{SideSpacing}_{\text{Tubes}}$	=	Side spacing between tubes

Figure 3.7 summarises the physical arrangement of each heat exchanger. Design calculations are performed iteratively to size the total heat transfer surface area of the boiler until the

thermal performance of the model meet the performance of the design basis of Appendix 1. The number of runs and the number of tubes per run is then determined in order to efficiently meet the boiler specifications. Boiler performance specifications are described in the Design Basis, in Appendix 1.

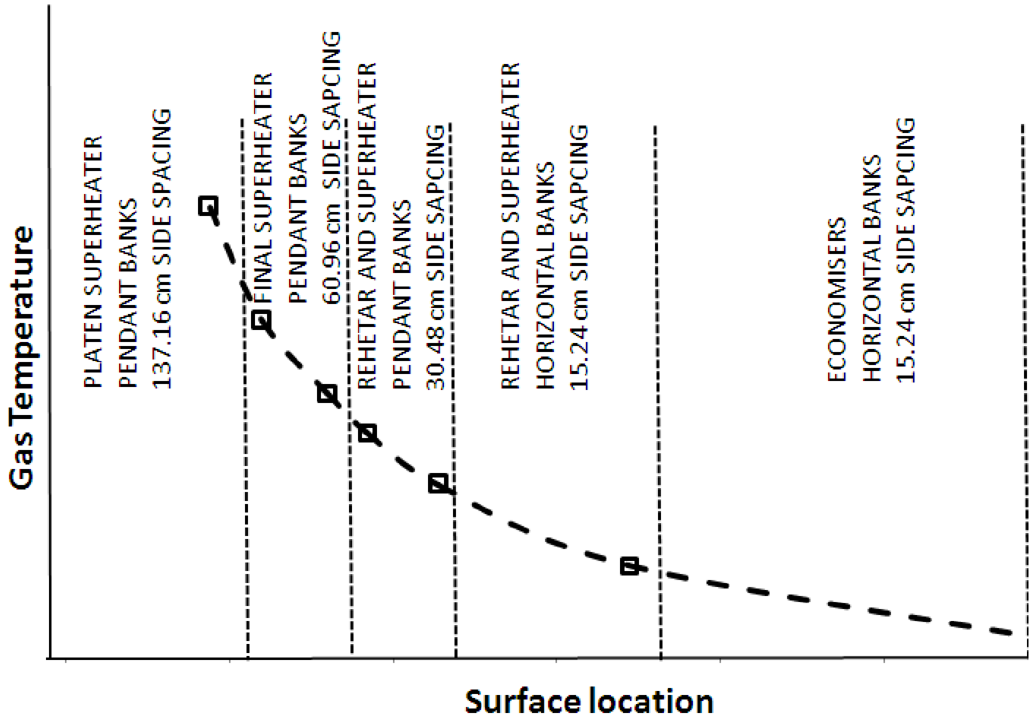

Figure 3.1.- Schematic plan arrangement of boiler heat exchangers

Table 3.1.- Physical arrangement per component.

PHYSICAL ARRANGEMENT – COMPONENTS						
	Tube OD	**Thickness**	**Sidespacing**	**Backspacing**	**Tubes / Wide**	**Length**
	cm	**cm**	**cm**	**cm**	**-**	**cm**
ECO 1	5.08	0.46	15.24	6.98	120,00	609.60
ECO 2	5.08	0.46	15.24	6.98	120,00	609.60
PSH 1	5.08	0.46	15.24	6.98	120,00	609.60
PSH 2	5.08	0.46	30.48	6.98	60,00	609.60
RH 1	5.08	0.46	15.24	6.98	120,00	609.60
RH 2	5.08	0.46	30.48	6.98	60,00	609.60
OUTLEGRH	5.08	0.46	30.48	6.98	60,00	914.40
FSH	5.08	0.46	60.96	6.98	30,00	1128,00
SCR 1	5.08	0.46	60.96	6.98	30,00	914.40
SCR 2	5.08	0.46	30.48	6.98	60,00	914.40

The heat exchanger tubes are arranged in multiple parallel tubes. The total number of tubes is calculated to attain the desired thermal performance of the design basis. The next chapter explains the methodology implemented to compute the heat transfer surface area of the boiler heat exchangers.

3.4.- Fundamentals of air heaters

Combustion air is preheated in air heaters in order to be able to dry the fuel and ensure stable ignition. The most common type of regenerative air heater is the Ljungström type. It consists of several rotating heating surface components and a stationary housing with ducts through which air and gas enter. The hot gas enters the top of the rotor and flows through one half while cold air enters the bottom and flows through the other half. Heat is then transferred indirectly by convection as the rotating heating surfaces are periodically exposed to cold air and hot gas. Due to the rotary operation and the temperature difference between the hot top and cold bottom of the rotor, it expands and deforms, and consequently, a considerable amount of air leaks into the flue gas stream.

As leakage is present the gas temperature measured at the exit of the air preheaters has to be corrected by performing a heat balance. The corrected exit gas temperature is called the undiluted gas temperature.

The air leakage is defined as the weight of air passing from the air side to the gas side and the direction of the leak has been assumed to be from the air inlet to the gas outlet. The leakage flow rates of the primary and secondary air are defined in Appendix 1.

Another important parameter of the air preheaters is the Gas Side Efficiency. It is defined as the ratio of the actual amount of heat released by the combustion gas to the maximum possible amount of heat that could be transferred with an infinite area. It is calculated according to ASME PTC 4-3.

$$\eta_{Preheater} = \frac{T_{g\_in\_Airheater} - T_{g\_out\_UNDIL\_Airheater}}{T_{g\_in\_Airheater} - T_{a\_in\_Airheater}} \quad [3.43]$$

Where:

$\eta_{Preheater}$	=	Gas side efficiency of the air heater
$T_{a\_in\_Airheater}$	=	Air temperature at air heater inlet
$T_{g\_in\_Airheater}$	=	Gas temperature at air heater inlet
$T_{g\_out\_UNDIL\_Airheater}$	=	Undiluted gas temperature

3.5.- Fundamentals of feed-water heat exchangers and condenser:

The feedwater heaters and condenser used in the steam cycle for pulverised coal plants are shell-and-tube exchangers which are generally built of a bundle of round tubes mounted in a cylindrical shell with the tube axis parallel to that of the shell. One fluid flows inside the tubes and the other flows across and along the tubes.

The heat transfer coefficient for the tube-side is evaluated with equation [3.5] and for the shell-side by the Kern equation (Hewitt et al. 2000):

$$Nu = \frac{\mathrm{h_{shell}} \cdot \mathrm{L}}{\mathrm{k}} = 0.36 \cdot Re^{0.55} \cdot Pr^{0.33} \quad [3.44]$$

Where:

h_{shell}	=	Heat transfer coefficient of the shell-side
L	=	Equivalent diameter on the shell-side

All the physical properties are evaluated at the film temperature.

The equivalent diameter for a square pitch is defined as:

$$L = \frac{4 \cdot \left(P^2 - \frac{\pi \cdot d^2}{4}\right)}{\pi \cdot d^2} \quad [3.45]$$

Where:

P	=	pitch size
d	=	outside tube diameter

The denominator corresponds to the wetted perimeter which is the circumference of a circle and the numerator to the free flow area multiplied by four. The free flow area is a square of pitch size minus the area of a circle.

The governing heat transfer equation is determined by equation [3.10], the log mean temperature difference by equation [3.12], and the overall heat transfer coefficient and the total heating surface area as follows:

$$U = \frac{h_{tube} \cdot h_{shell}}{h_{tube} + h_{shell}} \quad [3.46]$$

Where:

h_{shell}	=	Heat transfer coefficient of the shell-side, equation [3.44]
h_{tube}	=	Heat transfer coefficient of the tube-side, equation [3.5]

$$A = N_{tubes} \cdot L \cdot \pi \cdot d = \frac{D_s}{P} \cdot L \cdot \pi \cdot d \quad [3.47]$$

Where:

N_{tubes}	=	Number of tubes at the centreline of the shell
D_s	=	Inner diameter of the shell

Three different zones are distinguished in the feedwater heat exchangers: desuperheating, condensing and drain cooling zone, and only one zone in the condenser, the condensing zone.

In this project, each zone is studied as a separate heat exchanger and heat transfer coefficients are evaluated separately.

In the condensing zone the condensate "wets" the surface and forms a continuous layer over the tube as the drops coalesce. The heat transfer resistance is mainly concentrated in this film. When vapor condenses on the surface of horizontal tubes, the flow is almost always laminar as the flow path is too short for turbulence to develop. In the condensing zone the heat transfer coefficient of equation [3.44] is re-written as (Hewitt et al. 2000):

$$\mathrm{h_{shell}} = 0.725 \cdot \left(\frac{k^3 \cdot \rho \cdot (\rho - \rho_v) \cdot g \cdot \lambda}{\mu \cdot \Delta T \cdot d}\right)^{1/4} \cdot N_{tubes}{}^{1/6} \quad [3.48]$$

Where:

ρ	=	Water density
ρ_v	=	Steam density
μ	=	Water dynamic viscosity
k	=	Water thermal conductivity
λ	=	Latent heat of vaporization
ΔT	=	Driving force for condensation

All the physical properties are evaluated at the film temperature of the condensed liquid.

The driving force for condensation is the temperature difference between the cold wall surface and the saturation temperature. The tube wall temperature is computed as follows:

$$\mathrm{h_{shell}} \cdot A \cdot (\mathrm{T_{sat}} - \mathrm{T_{wall}}) = \mathrm{h_{tube}} \cdot A \cdot (\mathrm{T_{wall}} - \mathrm{T_{FW}}) \quad [3.49]$$

3.6.- Fundamentals of steam turbines

Steam turbines are devices which convert thermal energy from pressurized steam into mechanical work on a rotating output shaft. This rotary motion is used to drive an electrical generator.

The steam turbines of the subcritical reference plant, described in Appendix 1, consist of HP-IP-two LP (double flow) sections enclosed in three casings. Each component includes several stages consisting of a row of stationary blades, often called a stator row and a row of moving blades or buckets, called rotor row.

3.6.1.- Thermodynamic of the axial turbine stage

Steam enters the turbine and passes through the first stator row where it experiences some deflection and acceleration. The potential energy of the steam is partially converted into kinetic energy. Then, steam passes through the first rotor row where part of the total energy of the steam is converted into mechanical energy due to the rotational motion of the rotor. This rotational motion is used to drive an electrical generator and generate power. The same process is repeated in the following stages until the exit conditions are reached.

Applying the principles of conservation of mass and energy across the stator gives:

$$\dot{Q}_{net} + \dot{m} \cdot \left(h_1 + \frac{C_1^{\,2}}{2} + g \cdot z_1 \right) = \dot{W}_{net} + \dot{m} \cdot \left(h_2 + \frac{C_2^{\,2}}{2} + g \cdot z_2 \right) \qquad [3.50]$$

Assuming steady state, stead flow and adiabatic process and neglecting the potential energy in the stator and rotor equation [3.50] is re-written as equation [3.51] for the stator and as equation [3.52] for the rotor.

$$\left(h_1 + \frac{C_1^{\,2}}{2} \right) = \left(h_2 + \frac{C_2^{\,2}}{2} \right) \quad \rightarrow \quad h_{01} = h_{02} \qquad [3.51]$$

Where:

h_1	=	Steam specific enthalpy at stator inlet
C_1	=	Steam velocity at stator inlet
h_2	=	Steam specific enthalpy at stator outlet
C_2	=	Steam velocity at stator outlet
h_{01}	=	Steam stagnation enthalpy at stator inlet
h_{02}	=	Steam stagnation enthalpy at stator outlet

Equation [3.51] reveals that the stagnation enthalpy of the fluid in the stator remains unchanged.

The actual turbine rotor specific work is:

$$\frac{\dot{W}_{net}}{\dot{m}} = \left(h_2 + \frac{C_2^{\,2}}{2} \right) - \left(h_3 + \frac{C_3^{\,2}}{2} \right) = h_{02} - h_{03} \qquad [3.52]$$

Where:

$\frac{\dot{W_{net}}}{\dot{m}}$	=	Actual turbine rotor specific work
h_3	=	Steam specific enthalpy at rotor outlet
C_3	=	Steam velocity at rotor outlet
h_{03}	=	Steam stagnation enthalpy at rotor outlet

Similarly, the ideal turbine rotor specific work is:

$$\frac{\dot{W_{max}}}{\dot{m}} = \left(h_2 + \frac{{C_2}^2}{2}\right) - \left(h_{3\_s} + \frac{{C_{3\_s}}^2}{2}\right) = h_{0\_2} - h_{0\_3\_s} \quad [3.53]$$

Where:

$\frac{\dot{W_{max}}}{\dot{m}}$	=	Ideal turbine rotor specific work
C_{3_s}	=	Steam velocity at rotor outlet for the isentropic process
h_{3_s}	=	Steam specific enthalpy at rotor outlet for the isentropic process
h_{03}	=	Steam stagnation enthalpy at rotor outlet for the isentropic process

The turbine stage adiabatic efficiency, expressed as the ratio of the actual turbine work to the ideal turbine work, can be defined in two different ways depending whether the exit kinetic energy is usefully employed or wasted:

- The exit kinetic energy from one stage of a multistage turbine is used in next stage and the stage adiabatic efficiency is called total-to-total efficiency. It presents the following expression:

  $$\eta_{tt} = \frac{\dot{W_{net}}}{\dot{W_{max}}} = \frac{h_{02} - h_{03}}{h_{02} - h_{03\_s}} \quad [3.54]$$

  Where:

  η_{tt} = Total-to-total efficiency

  If the difference between the inlet and outlet kinetic energies is small, equation [3.54] can be re-written as:

  $$\eta_{tt} = \frac{\dot{W_{net}}}{\dot{W_{max}}} = \frac{h_2 - h_3}{h_2 - h_{3s}} \quad [3.55]$$

- The last stage of the steam turbine exhausts in the condenser of the steam cycle of the plant and the kinetic energy is wasted, in this case, the stage adiabatic efficiency is called total-to-state efficiency and is represented as follows:

$$\eta_{ts} = \frac{\dot{W_{net}}}{\dot{W_{max}}} = \frac{h_{02} - h_{03}}{h_{02} - h_{03s} + \frac{1}{2} \cdot {C_{3\_s}}^2} \quad [3.56]$$

Where:

η_{ts} = Total-to-state efficiency

If the difference between the inlet and outlet kinetic energies is small, equation [3.56] can be re-written as:

$$\eta_{ts} = \frac{\dot{W_{net}}}{\dot{W_{max}}} = \frac{h_2 - h_3}{h_2 - h_{3s} + \frac{1}{2} \cdot {C_2}^2} \quad [3.57]$$

The actual turbine rotor specific work can also be calculated by applying the Euler equation of motion. Thus, for a rotor running at angular velocity Ω, the work done by the fluid on the rotor is:

$$\dot{W} = \dot{m} \cdot (r \cdot \Omega \cdot \dot{C_{2\sigma}} - r \cdot \Omega \cdot C_{3\sigma}) \quad [3.58]$$

$$\frac{\dot{W}}{\dot{m}} = U \cdot C_{2\sigma} \dot{-} U \cdot C_{3\sigma} \quad [3.59]$$

Where:

r = Radius of the flow path

Ω = Rotor angular velocity

U = Blade speed

$C_{2\sigma}$ = Tangential steam velocity at rotor inlet

$C_{3\sigma}$ = Tangential steam velocity at rotor outlet

Equalling equation [3.52] to [3.59]:

$$U \cdot (\dot{C_{2\sigma}} - C_{3\sigma}) = h_{02} - h_{03} = (h_2 - h_3) + \frac{1}{2} \cdot \left({C_2}^2 - {C_3}^2\right) \quad [3.60]$$

From the velocity triangle diagram illustrated in *Figure 3.82*, equation [3.60] can be re-written as equation [3.61], where the relative velocity, w, is obtained by subtracting, vectorially, the blade speed U from the absolute velocity C.

$$h_2 + \frac{1}{2} \cdot {w_2}^2 = h_2 + \frac{1}{2} \cdot {w_3}^2 \quad [3.61]$$

$$h_{02\_rel} = h_{03\_rel} \quad [3.62]$$

Where:

w_2 = Relative velocity at rotor inlet

w_3 = Relative velocity at rotor outlet

h_{02_rel} = Relative stagnation enthalpy at rotor inlet

h_{03_rel} = Relative stagnation enthalpy at rotor outlet

Equation [3.62] reveals that the relative stagnation enthalpy remains unchanged through the rotor.

Now, all the information necessary to represent the turbine stage expansion process at its design point on the h-s diagram is available. *Figure 3.82* shows the Mollier diagram for a turbine stage.

In power generation applications multi-stage axial flow steam turbines are used in order to generate high power output. The stage velocity triangle is to be very similar in all the stages. This is achieved by designing stages with constant axial velocity and mean blade radius throughout the turbine. Additionally, the flow angles at exit from each stage must be equal to those at inlet, $\alpha_1 = \alpha_3$. Stages satisfying these requirements are often referred as normal stages.

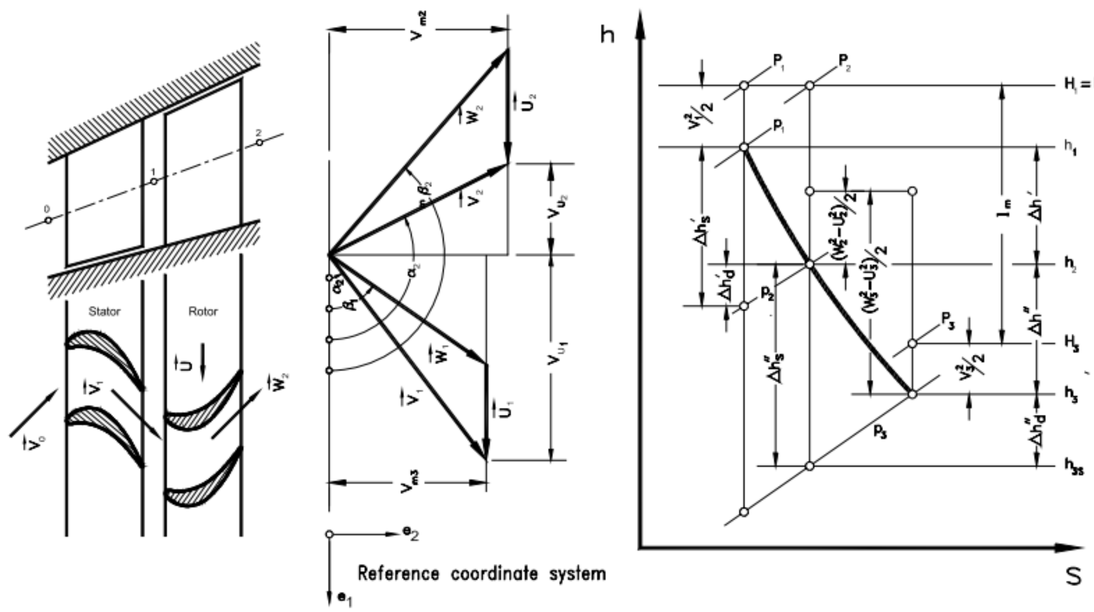

Figure 3.82.- Steam velocity triangle diagram and Mollier diagram for a turbine stage **(Schobeiri 2012)**.

3.6.2.- Degree of reaction of a steam turbine stage

The stage reaction is defined as the ratio of the static enthalpy drop in the rotor to the static enthalpy drop across the stage. It indicates the portion of the total energy of the steam transferred to the rotor.

$$R = \frac{h_2 - h_3}{h_1 - h_3} \tag{3.63}$$

Where:

R = Degree of reaction of a steam turbine stage

The degree of reaction characterises the asymmetry of the velocity triangle and is therefore a statement of blade geometries.

From the turbine stage velocity triangle diagram, equation [3.63] can be re-written as follows:

$$R = \frac{\mathrm{w}_{3\sigma} - \mathrm{w}_{2\sigma}}{2 \cdot U} = \frac{c_x}{2 \cdot U} \cdot (\tan \beta_3 - \tan \beta_2) = \frac{c_x}{2 \cdot U} \cdot (\tan \beta_3 - \tan \alpha_2) + \frac{1}{2} \tag{3.64}$$

Where:

c_x = Axial steam velocity

β_2 = Relative velocity angle at rotor inlet

β_3 = Relative velocity angle at rotor outlet

α_2 = Flow angle at stator exit

$\mathrm{w}_{2\sigma}$ = Tangential relative velocity at rotor inlet

$\mathrm{w}_{3\sigma}$ = Tangential relative velocity at rotor outlet

For turbine blades with 0% reaction of stage the flow is deflected in the rotor blades at constant enthalpy. As a result, the magnitude of the relative velocity remains constant through the rotor.

As $\mathrm{w}_2 = \mathrm{w}_3$ and $\beta_3 = \beta_2$ the Euler equation of work for 0% stage reaction can be re-written as:

$$\frac{\dot{W}}{\dot{m}} = U \cdot 2 \cdot (C_2 \cdot \sin \alpha_2 - U) \tag{3.65}$$

The entire stage static enthalpy drop occurs in the stator, thus, the maximum available work is:

$$\frac{\dot{W}_{max}}{\dot{m}} = \frac{1}{2} \cdot {C_2}^2 \tag{3.66}$$

Then, the efficiency of a turbine stage for a 0% degree of reaction presents the following equation:

$$\eta = 4 \cdot \frac{U}{C_2} \cdot \left(\sin \alpha_2 - \frac{U}{C_2}\right) \tag{3.67}$$

Maximum efficiency will be attained when:

$$\frac{d\eta}{d\frac{U}{C_2}} = 0 \quad \rightarrow \quad \frac{U}{C_2} = \frac{\sin\alpha_2}{2} \tag{3.68}$$

Then, the maximum power produced that can be reached is:

$$\frac{\dot{W}}{\dot{m}} = \frac{1}{2} \cdot U^2 \tag{3.69}$$

For turbine blades with 50% reaction of stage a symmetric velocity triangle is obtained and, so, a symmetric blade configuration is established. The enthalpy drop in the nozzle row equals the enthalpy drop in the rotor.

$$(h_2 - h_3) = \frac{1}{2} \cdot (h_1 - h_3) \quad \rightarrow \quad (h_2 - h_3) = (h_1 - h_2) \tag{3.70}$$

As $w_3 = C_2$ and $\beta_3 = \alpha_2$ the Euler equation of work for 50% stage reaction can be re-written:

$$\frac{\dot{W}}{\dot{m}} == U \cdot (2 \cdot C_2 \cdot \sin\alpha_2 - U) \tag{3.71}$$

The enthalpy drop is identical in the rotor and the stator, thus the maximum work available is:

$$\frac{\dot{W_{max}}}{\dot{m}} = {C_2}^2 \tag{3.72}$$

The stage efficiency for a 50% reaction stage is:

$$\eta = \frac{U}{C_2} \cdot \left(2 \cdot \sin\alpha_2 - \frac{U}{C_2}\right) \tag{3.73}$$

Maximum efficiency will be attained when:

$$\frac{d\eta}{d\frac{U}{C_2}} = 0 \quad \rightarrow \quad \frac{U}{C_2} = \sin\alpha_2 \tag{3.74}$$

Then maximum power produced that can be reached is:

$$\frac{\dot{W}}{\dot{m}} = U^2 \tag{3.75}$$

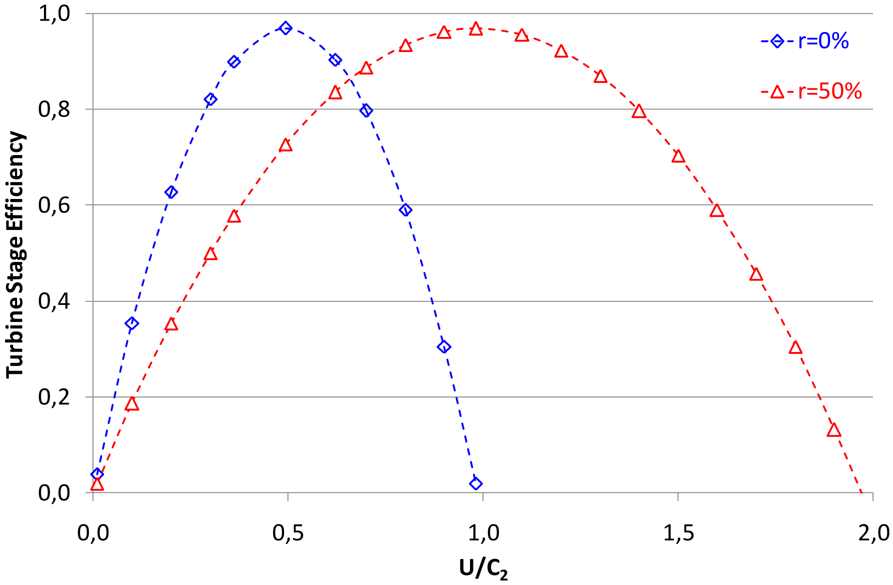

Figure 3.93.- Stage efficiency of turbines with different degree of reaction for $\alpha_2 = 80º$

The comparison of equation [3.69] and equation [3.75] bring the conclusion that 0% reaction stage produces twice as much as power as a 50% reaction stage. Consequently, for a given application a design with 0% reaction stages need twice as less stages. However, blades are exposed to higher stresses.

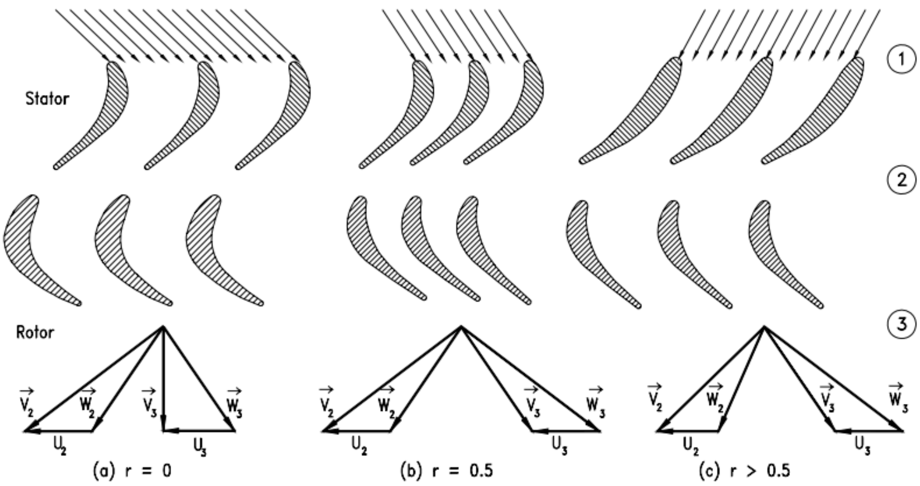

Figure 3.4.- Effect of degree of reaction on the stage configuration (Schobeiri 2012)

4.- PERFORMANCE MODELLING OF THE GAS TURBINE FLUE GAS WINDBOX CARBON CAPTURE RETROFIT

This chapter focuses on the methodology used for the performance calculations of a power matched retrofit of a subcritical coal plant with a gas turbine (GT) flue gas windbox and solvent based post-combustion capture (PCC).

The first stage of performance calculations is the rating process which sizes the geometry of the heat transfer equipment with the aim of reaching the pulverised coal power plant specifications for the design basis with air firing. Combustion calculations, mass and energy balances and heat transfer coefficient are determined.

Once the surface areas of the heat exchangers are known, the off-design performance of the retrofitted pulverised coal power plant can be studied. Retrofit options where gas turbine flue gas is introduced to the boiler to replace a fraction of the combustion air are examined taking into account changes in flame temperature and heat transfer coefficients with the new gas composition, and the associated changes in mass and energy balances to determine steam temperature and flow rates.

4.1.- Rating process calculations of the pulverised coal power plant

During rating process calculation the heat transfer surface area is determined by assuming an initial surface arrangement and then confirming the desired thermal performance of the design basis with air firing.

4.1.1. Boiler modelling

The model of the boiler generally follows the direction of flue gas flow from the furnace to the stack. The equations for heat transfer, mass and energy balances are solved iteratively for all the heat exchangers until they are consistent with the energy and mass balances of the overall boiler unit.

Furnace rating process

The furnace must be designed to be large enough to reduce the furnace exit gas temperature below the ash deformation temperature (see Section 3.3). Thus, in this work, the upper furnace exit gas temperature for air firing is taken as 1499 K.

The furnace exit plane delimits the boundary of the furnace volume and the flat projected furnace enclosure area. It corresponds with the plane above the furnace nose tip.

The furnace is divided into two sections: the lower/bottom furnace is only enclosed by water walls whereas the upper furnace in addition to the water walls also has platen superheater surfaces.

The gas temperature at the lower furnace exit is calculated by applying equation [3.24] to the lower furnace only, whereas this equation has to be applied to the whole furnace in order to calculate the gas temperature at the upper furnace exit.

The furnace wall and platen superheaters effectiveness factor vary with wall cleanliness, but the sensitivity of the overall performance of the plant to the effectiveness factors is low. They have been estimated in order to reach the desired thermal performance.

The heat absorbed by each section of the furnace is computed by solving equation [3.30]. Then the heat absorbed by the water walls, platen superheaters and exit plane is determined based on the ratio of the effective areas of each type of surface to the total furnace area.

The furnace size and the effectiveness factors are adjusted when the gas temperature at the upper furnace exit reaches the design value of 1499K and when the amounts of heat absorbed by the water walls and by the platen superheater are consistent with their energy balances.

Figure 4.1 shows a sketch of the iterative method used to determine the heating surface areas of the furnace and platen superheaters.

<u>Mixed and convection banks rating process:</u>

In this work, mixed banks consist of the final-superheater, located over the nose of the furnace wall, and the outlet leg of the reheater situated at the top of the parallel pass. Convection banks consist of the reheater, the primary superheater, and economisers in the parallel pass as indicated in Figure 3.1.

Due to the wide spacing between tubes, the heat radiated by the flame to the exit plane reaches the final superheater, the screen and the outlet leg of the reheater. The furnace radiation absorbed by these banks of tubes is computed by using equations [3.34] to [3.36].

Then the total direct radiation absorbed by the mixed banks can be evaluated by summing the direct radiation from the flame and the radiation from the front and rear cavities.

The convection and intertube radiation is determined by solving equation [3.37] and the overall heat transfer rate by means of equation [3.10]. Then, the cleanliness factor can be determined with equation [3.40].

The dimensional parameters are re-estimated and calculations have to be repeated until the cleanliness factor value is close to 1.

Figure 4.2 shows a sketch of the iterative method used to determine the surface arrangement (number of runs and number of tubes per run) of the convection banks.

4.1.2. Air pre-heaters modelling:

For the regenerative air heater the heat transfer rate is determined by energy balance.

The gas side efficiency of the air heaters is computed by means of equation [3.43]. The leakage flow rates of the primary and secondary air are defined in Appendix 1.

The measured gas temperature at the exit of the air heaters is corrected by performing a heat balance as leakage is present.

4.1.3. Steam turbines modelling:

All the fundamentals required to predict the turbine performance behaviour at the design point have been reviewed in Chapter 3.

Knowing the temperature and the pressure at the inlet, the enthalpy and entropy can be obtained from the steam stables. Then, angles involved in the velocity diagram need to be determined.

Once all the angles involved in the velocity diagram are determined, the velocities and their components are fully described. The stage turbine efficiency can be computed by solving either equation [3.67] or equation [3.73], the amount of power produced by solving either equation [3.65] or equation [3.71] and the complete expansion process from the energy balance relationships, equation [3.51] and equation [3.52].

Detailed information is, however, necessary to represent the turbine stage expansion process on the h-s diagram, such as, the turbine mass flow, the turbine pressure ratio, the exit blade angles for each individual stage and the degree of reaction. This analysis also requires accurate information about temperature and pressure distribution along the expansion path.

As the only information available is the steam temperature and pressure at the inlet, outlet and extraction points of the steam turbine (see Appendix 1), the turbine component will be arranged in block of stages, n+1 expansion block of stages for a turbine with n extractions.

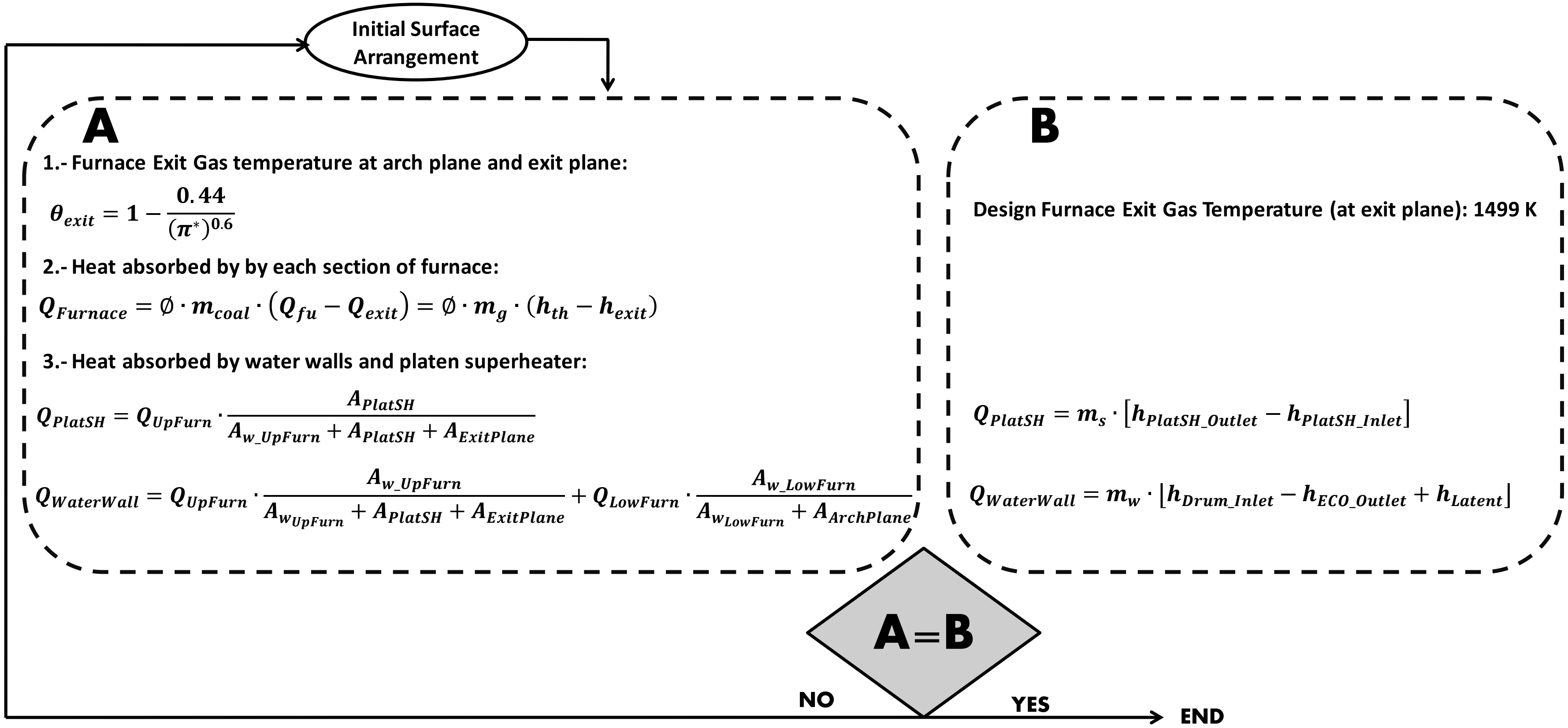

Figure 4.1.- *Iterative method –Furnace Surface Arrangement.*

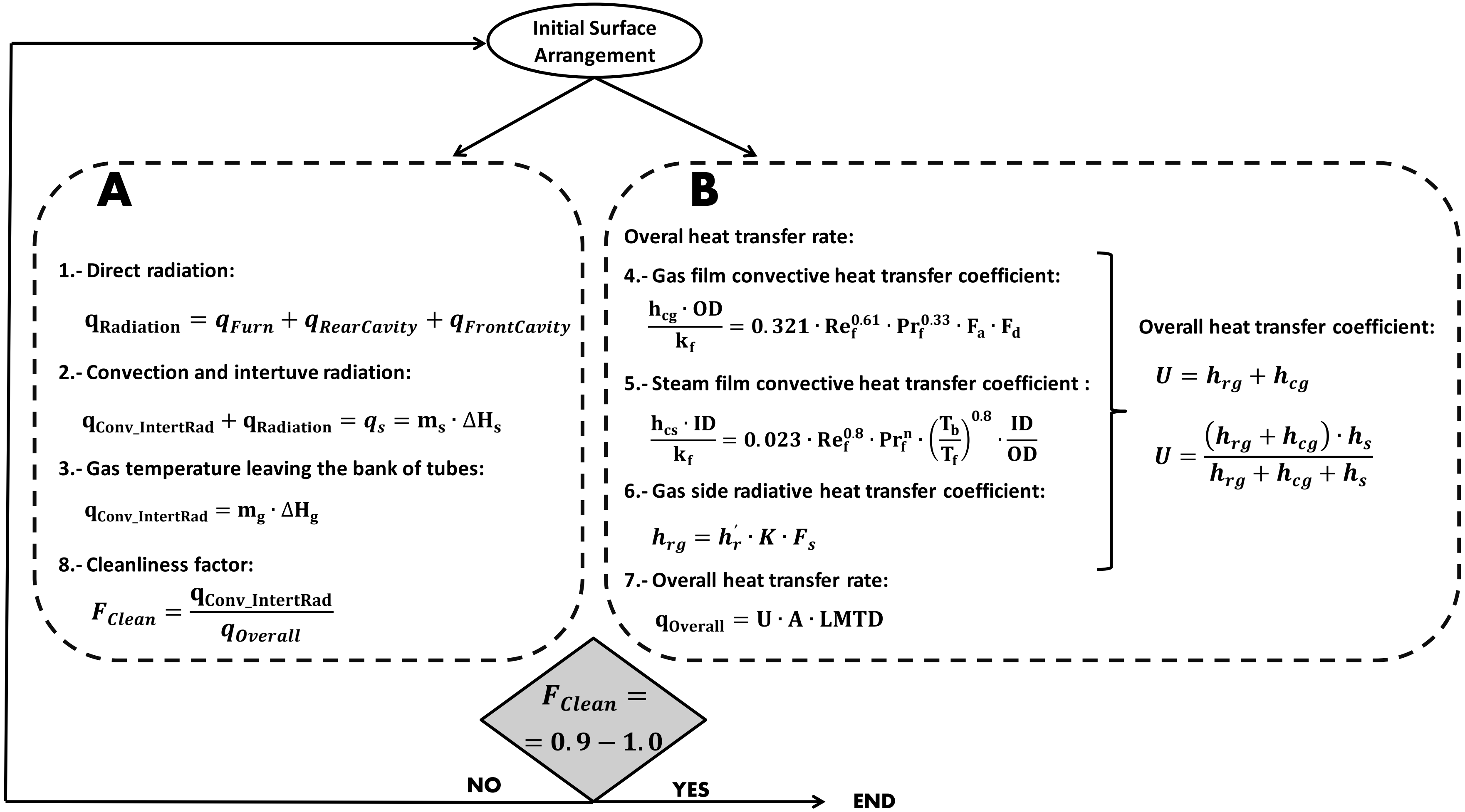

Figure 4.2.- Iterative method –Surface Arrangement.

In that way, assuming that the difference between inlet and outlet kinetic energies is small, the efficiency of every block of stages can be calculated by solving equation [3.55]. For the last block of stages of the LP steam turbine the equation [3.57] will be used instead.

4.1.4. Feed-water heaters modelling:

Similar to the rating process for the boiler convection banks, the heat transfer surface area of the feed-water heat exchangers will be determined by assuming an initial surface arrangement and confirming the desired thermal performance of the design basis with air firing.

Three different zones are distinguished in the feedwater heat exchangers: desuperheating, condensing and drain cooling zone. As the condensing zone is the lowest shell-side thermal resistance, the feedwater heat exchangers are evaluated as two separate heat exchangers, one for the desuperheating and condensing zone and the other for the drain cooling zone.

The overall heat transfer rate is determined by solving equation [3.10] where the overall heat transfer coefficient is defined by equation [3.46], the log mean temperature difference by equation [3.12] and the total heating surface area by equation [3.47].

The overall heat transfer rate has to be consistent with the energy balance of the heat exchanger. If these heat transfer rate calculations do not agree, then dimensional parameters are re-estimated and calculations repeated.

4.1.5. Condenser modelling:

The condenser modelling is very similar to the feed-water heaters with the difference that it only consists of a condensing zone. In this case, the overall heat transfer coefficient is evaluated with equation [3.5] and [3.48] for the convective heat transfer coefficient of the tube- and shell-side respectively.

The iterative procedure required to calculate the wall temperature consists of the following steps:

- Assume a wall temperature, T_w
- Calculate the film temperature as a weighted mean of the wall temperature and the bulk fluid temperature.
- Evaluate the fluid properties at the film temperature

- Calculate the condensing heat transfer coefficient and the tube-side heat transfer coefficient with equations [3.48] and [3.5] respectively.
- Calculate the wall temperature with equation [3.58].
- Compare the calculated wall temperature to that from the initial step. If not equal, re-calculate the film temperature and repeat.

Once the wall temperature is computed, the overall heat transfer rate is determined by solving equation **[3.10].** It has to meet the energy balance of the condenser, otherwise, dimensional parameters have to be re-estimated.

4.2.- Off design process calculations of the pulverised coal power plant

4.2.1. Boiler modelling

Once the surface areas and the cleanliness factors of the heat exchangers are known, the off-design performance of the retrofitted boiler can be evaluated.

When the coal power plant is retrofitted by adding a GT with a supplementary HRSG and the flue gas from the GT replaces part of the combustion air, the radiative properties of the furnace are altered.

Furnace performance calculation procedure

The furnace exit gas temperature is computed by solving equation [3.24] and the amount of heat absorbed by the water walls and by the platen superheater is determined by multiplying the equation [3.30] by the ratio of the effective areas of each type of surface.

Due to the lower coal feed rate the steam production is reduced. The steam mass flow rate and the steam temperature at the platen superheater outlet are computed by solving the energy balance in the water walls and in the platen superheater respectively.

Mixed and Convection banks performance calculation procedure

Calculations start by assuming a steam temperature leaving the convection bank. This is used to establish the thermo-physical properties and to calculate the thermal performance of heat transfer bank. Equation [3.10] will be used to evaluate the overall heat transfer rate. The overall heat transfer rate multiplied by the cleanliness factor has to be the same as the convection and intertube radiation transfer rate (equation [3.37]). If these heat transfer rate calculations do not agree, then the steam outlet temperature must be re-estimated and the calculations repeated until agreement is achieved.

Figure 4.3 shows a sketch of the iterative method used to determine the steam temperature at the exit of the convection banks.

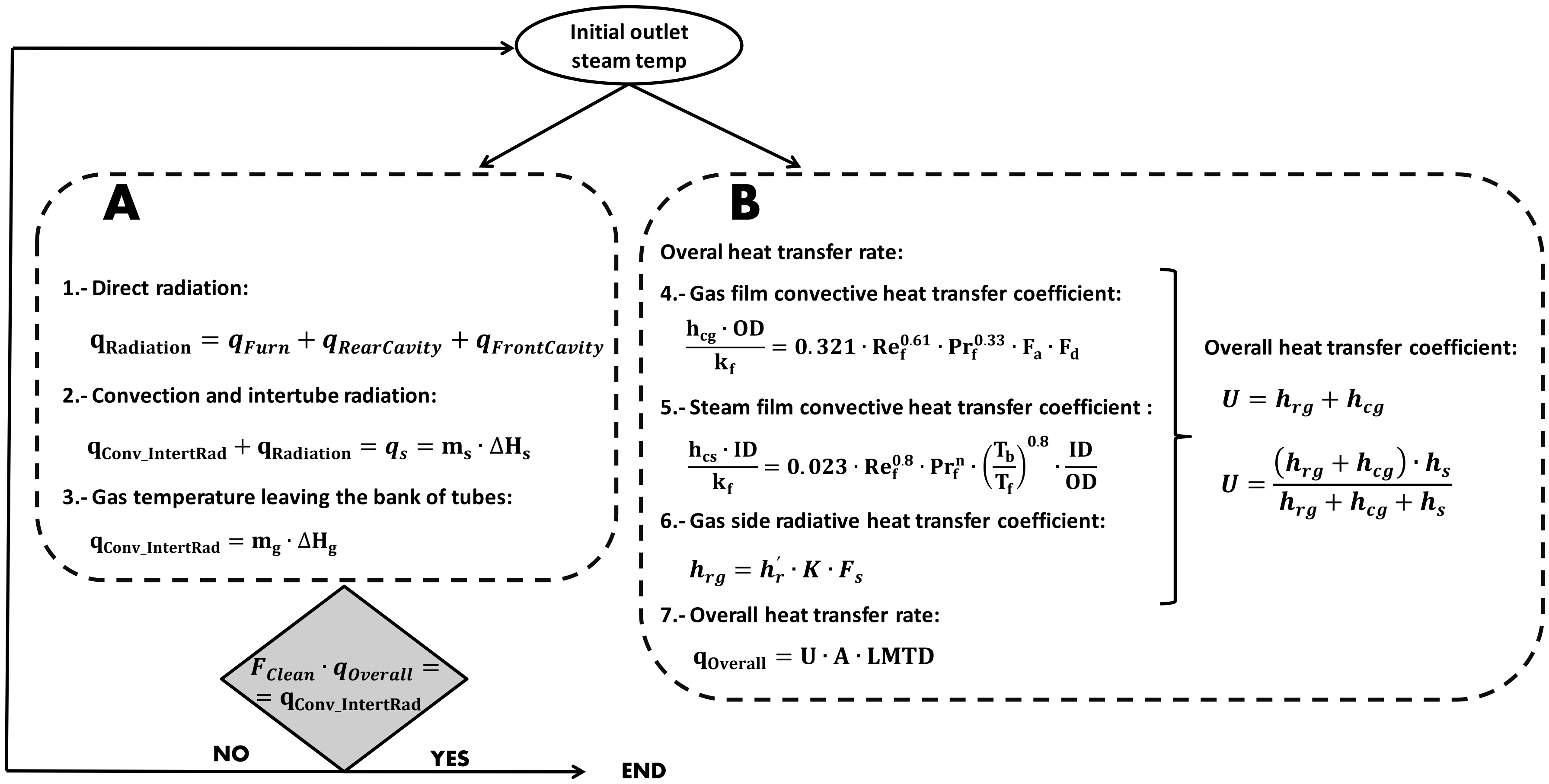

Figure 4.3.- Iterative method –Performance of retrofitted boiler.

Screens performance calculation procedure

In this work the Screens correspond with Screen1 located after the Final Superheater and with Screen2 located after the Cavity 1 as indicated in Figure 3.1.

Calculations start by assuming a gas temperature leaving the screen. This assumption is verified later.

The overall heat transfer rate can be evaluated by solving equation [3.10]. In this case, LMTD corresponds to the log mean temperature difference of equation [3.13] and U to the overall heat transfer coefficient of equation [3.19] as the steam film inside the tubes is negligible.

The gas temperature leaving the screen can be checked by an energy balance. The flue gas exit temperature assumption can then be verified. If this does not agree with the earlier assumption, the exit gas temperature is iterated until agreement is reached.

Figure 4.4 shows a sketch of the iterative method used to determine the screen exit gas temperature.

Cavities performance calculation procedure

The configuration of the subcritical boiler only comprises two cavities. Cavity 1 is located between Final Reheater and Screen 2 and Cavity 2 is located after Screen 2 as shown in Figure 3.1.

The calculation starts with a guessed value for the gas temperature leaving the cavity. The methodology of section 3.2.3 is used to compute heat transferred from the flue gas volume contained in the cavity to the cooler banks which form its boundaries.

The receiving surface temperature is related to the steam temperature at the inlet/outlet of the convection bank located at boundary i, depending on the configuration. For example, for Cavity 1, the receiving surface temperature at each boundary is:

- Boundary 1- Final Reheater, FRH. Inlet steam temperature
- Boundary 2 – Roof. Saturation temperature
- Boundary 3 - Screen 2. Saturation steam temperature
- Boundary 4 – Reheater, RHB2. Outlet steam temperature

The total overall heat transfer is calculated as the sum of the rates to each boundary, equation [3.32]. The gas temperature leaving the cavity is then checked by an energy balance.

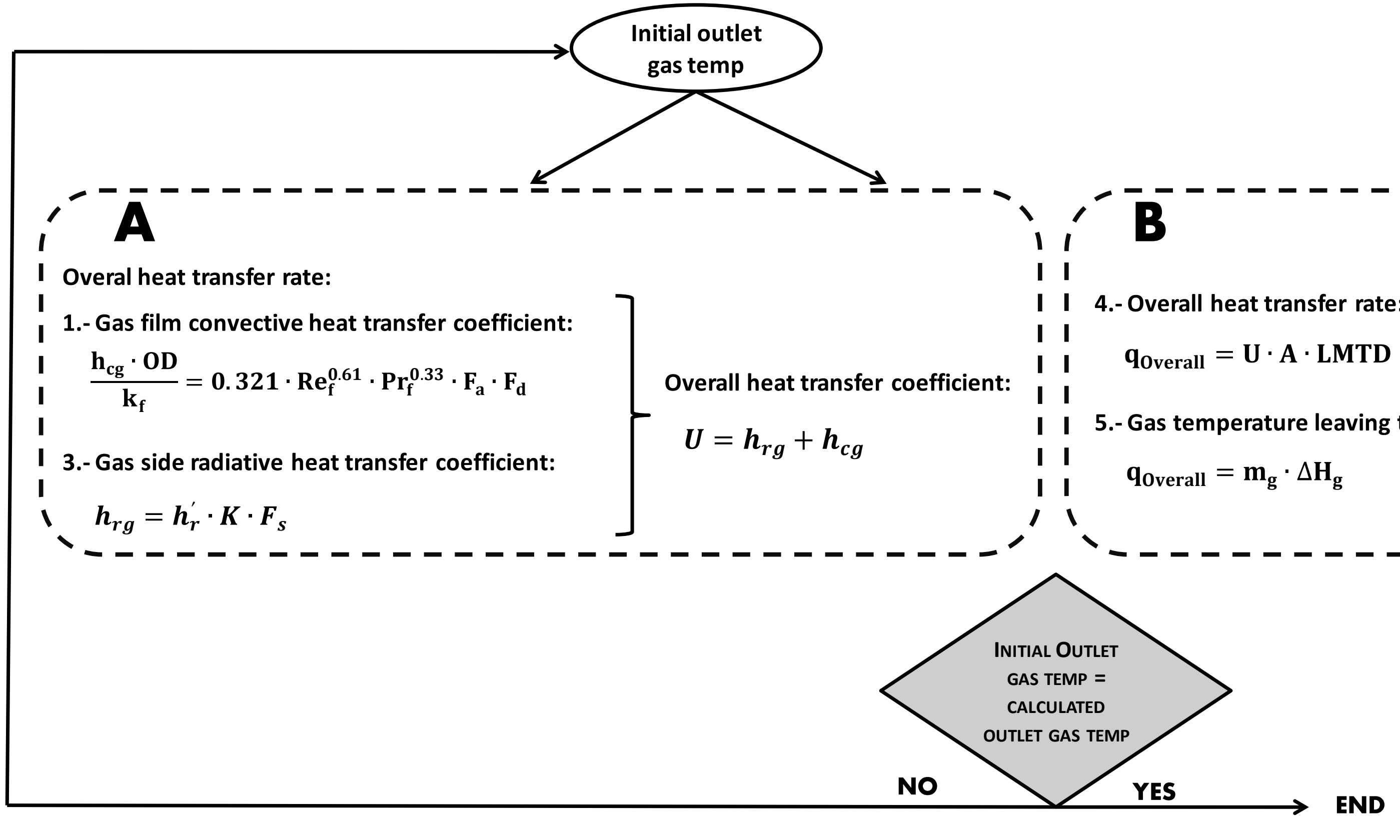

Figure 4.4.- *Iterative method – Screen exit gas temperature.*

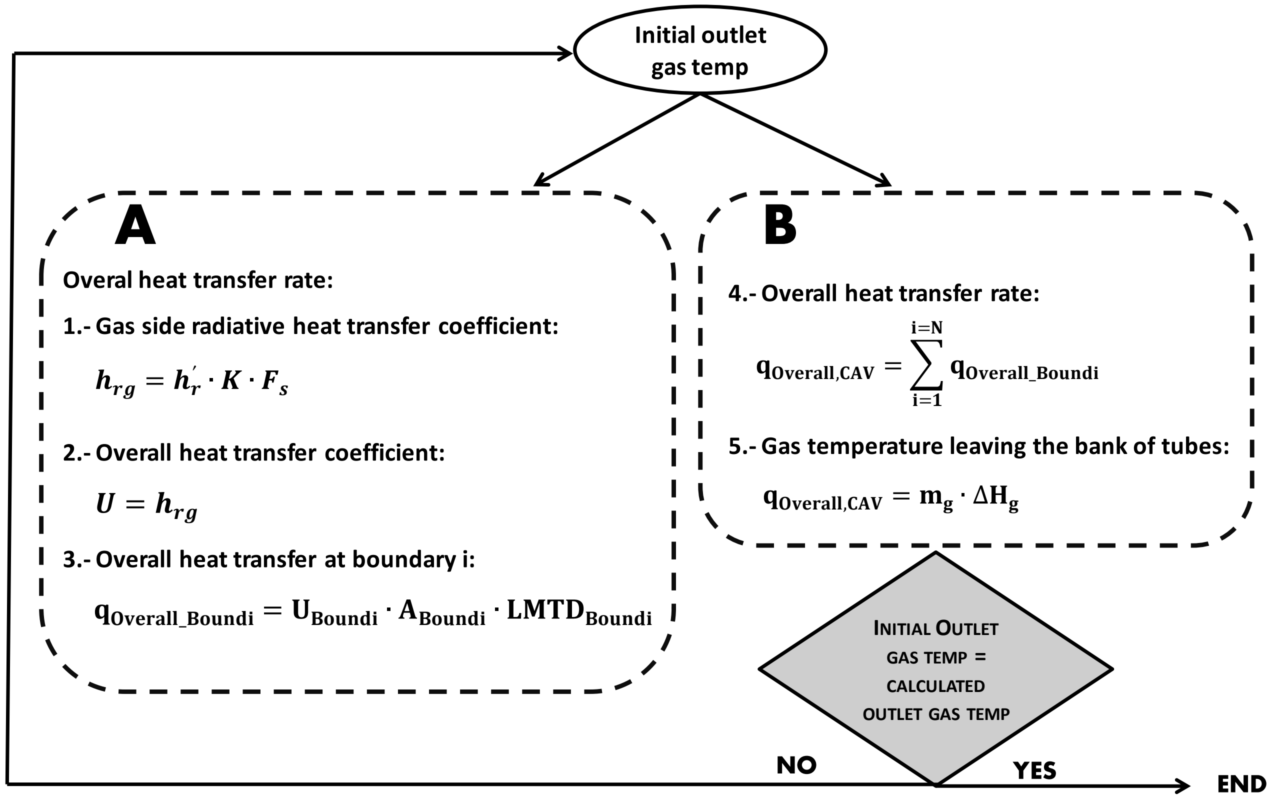

Figure 4.5.- *Iterative method – Cavity exit gas temperature.*

If the assumed value is not the same as this new temperature further iteration is required. The temperature obtained from the energy balance is used as a new starting value and calculations will be repeated.

Figure 4.5 shows a sketch of the iterative method used to determine the cavity exit gas temperature.

4.2.2. Air pre-heaters modelling:

The off-design performance calculations of the PC power plant has been developed assuming that the air preheaters operate with a constant percentage of air leakage and a constant gas side efficiency, since the sensitivity to the overall performance to these parameters is extremely low.

In order to avoid corrosion problems, the flue gas temperature must not reach the acid dew point, otherwise sulphuric acid condensates on metal surfaces causing corrosion problems in air-heaters, electrostatic precipitators (ESP) and fans. The operating gas temperature at the air-heaters outlet is thus typically limited to a minimum of 433.15 K.

4.2.3. Steam turbines modelling:

Off-design polytropic efficiency

Turbine off-design poly-tropic efficiencies are assumed to be the same as the designed value, provided that the given off-design mass flow permits a normal turbine operation.

The polytropic efficiency of the steam turbine mainly depends on the blade speed, steam velocity and flow angle at nozzle exit as indicated in equation [3.67] and [3.73].

In power generation applications the steam turbine rotor is synchronised with the grid frequency and at constant flow path radius the blade speed will remain unchanged.

Additionally, the flow angle at nozzle exit is assumed to be invariable. Although changes in the incidence and deviation angel alter the total flow deflection, HP and IP steam turbines with thick blade profiles are less sensitive to changes of the inlet flow direction, due to their characteristic low subsonic Mach numbers. Thus, the change of incidence will not significantly increase the profile loss and the flow angle at nozzle exit will not be altered. However, the blade profile of the last stages of the LP steam turbines is subjected to a high subsonic, even transonic, inlet flow condition and changes of incidence will affect its profile loss. The error made with this assumption is expected to be small as it only affects the last stages of the LP steam turbine.

Consequently, it is possible to assume that, to a first order approximation, the efficiency of the steam turbine principally depends on the steam velocity, if secondary losses, e.g. vortex and tip leakages, are ignored.

Given that the ratio U/C_2 at off-design conditions largely stay within the 0.36 to 0.62 range for a zero degree of reaction blade design, the polytropic efficiency can be assumed to be the same as the design value (See *Figure 3.93*).

Off-design performance using global turbine characteristics method

An alternative to the row-by-row expansion, the method of Stodola is used to predict the off-design operation of the steam turbines **(Cooke 1983)**. This method treats each block of stages as if it were a single nozzle and this equivalence is known as Stodola's Ellipse which states as follow:

$$\frac{m_{in}}{\sqrt{P_{in}/vol_{in}}} = K \cdot \sqrt{1 - \left(\frac{P_{out}}{P_{in}}\right)^{\frac{n+1}{n}}} \quad [4.1]$$

$$\frac{n-1}{n} = \eta \cdot \left(\frac{k-1}{k}\right) \quad [4.2]$$

Where:

vol_{in}	=	Inlet specific volume to the first stage nozzle of any group
m_{in}	=	Inlet flow to the first stage nozzle of any group
P_{in}	=	Inlet total pressure to the first stage nozzle of any group
P_{out}	=	Exit static pressure from the last stage of any group
n	=	Polytropic exponent
k	=	Isentropic exponent
η	=	Small stage efficiency
K	=	Swallowing capacity

The swallowing capacity, K, is determined for each block of stages at designed conditions. It is then used to predict steam turbines behaviour when mass flow and/or pressure change.

When carbon capture is integrated with the existing steam cycle of the reference plant, part of the steam flow passing through the IP/LP crossover is sent to the reboiler. The retrofit configuration includes a back pressure steam turbine expanding that steam to the required pressure for solvent regeneration. A dedicated generator and alternator generate additional power, compared to the configuration where the steam is throttled through a valve (Figure 4.6). As a result of steam extraction from the crossover, the amount of steam entering the LP steam turbine is reduced and the inlet pressure is recalculated by solving equation [4.1].

This method assumes that the exit static pressure from the last stage of each block is equal to the inlet total pressure of the next block. The change in exhaust losses associated with the kinetic energy of steam exiting the last stage have not been included in the analysis but could be included in future work.

The use of the global turbine characterist method to determine the behaviour of a multi-stage steam turbine under off-design conditions also requires information on the off-design polytropic efficiency, equation [4.2].

4.2.4. feed-water heaters modelling:

The overall heat transfer rate at off-design conditions is predicted by solving equation **[3.10]**. The heat transfer coefficient, however, is estimated by using the power law approximation that computes the heat transfer coefficient as a function of the flow.

By dividing equation [3.4] and [3.51] by its design value, the following expressions are obtained:

$$\frac{h_{tube\_OP}}{h_{tube\_D}} \cdot \frac{k_D}{k_{OP}} = \left(\frac{Re_{f\_OP}}{Re_{f\_D}}\right)^{0.8} \cdot \left(\frac{Pr_{f\_OP}}{Pr_{f\_D}}\right)^{n} \qquad [4.3]$$

$$\frac{h_{shell\_OP}}{h_{shell\_D}} \cdot \frac{k_D}{k_{OP}} = \left(\frac{Re_{f\_OP}}{Re_{f\_D}}\right)^{0.55} \cdot \left(\frac{Pr_{f\_OP}}{Pr_{f\_D}}\right)^{0.33} \qquad [4.4]$$

The Prandtl number, viscosity and conductivity do not vary greatly over the operational range of the carbon capture retrofit. The equation [4.3] and the equation [4.4] can then be simplified so that it is only a function of the ratio of the actual mass flow and the design mass flow:

$$\frac{h_{OP}}{h_D} = \left(\frac{\dot{m}_{OP}}{\dot{m}_D}\right)^{0.8} \qquad [4.76]$$

$$\frac{h_{shell\_OP}}{h_{shell\_D}} = \left(\frac{\dot{m}_{OP}}{\dot{m}_{D}}\right)^{0.55} \quad \textbf{[4.77]}$$

Considering the heat transfer of tube- and shell-side the off-design overall heat transfer coefficient can be expressed as:

$$U_{OP} = \frac{h_{tube\_OP} \cdot h_{shell\_OP}}{h_{tube\_OP} + h_{shell\_OP}} \quad \textbf{[4.6]}$$

As the overall heat transfer rate has to be consistent with the energy balance of the heat exchanger, the feed-water and drain cooling temperature at the exit of each heat exchanger can be computed by a system of two equations:

$$m_s \cdot \Delta H_s = U_{OP} \cdot A \cdot LMTD \quad \textbf{[4.7]}$$

$$m_s \cdot \Delta H_s = m_{FW} \cdot \Delta H_{FW} \quad \textbf{[4.8]}$$

4.2.5. Condenser modelling:

The condenser modelling is very similar to the feed-water heaters with the difference that only the condensing zone is distinguished.

The iterative procedure proposed to calculate the wall temperature in **section 4.1.5** is used to evaluate the fluid properties at the film temperature.

The off-design heat transfer coefficient of the tube-side can be simplified by equation **[4.5]**, however, the off-design heat transfer coefficient of the shell-side needs to be computed by solving equation **[3.48]**.

The overall heat transfer rate is determined by solving equation **[3.10]**. Equaling the overall heat transfer rate to the energy balance of the condenser, the cooling water temperature and mass flow rate can be computed.

4.3.- Process calculation of the gas turbine and heat recovery steam generator

The supplementary gas firing unit consists of a gas turbine and an unfired three pressures level Heat Recovery Steam Generator (HRSG).

The gas turbine is designed to provide the electrical power required for the capture process (compression and the ancillary power for the capture system) and to cover any loss in power output to restore the net power output of the plant. It is assumed that the turbine outlet temperature is 623 ºC, a typical value for the PG 7251 FB General Electric (GE) gas turbine

(GE Power Systems 2000b). High exhaust temperatures improve the heat transfer in the HRSG and help to reduce the gas temperature at the exit of the HRSG. See Chapter 5 for more detailed information. The natural gas flow rate is then calculated to size an assumed GT that will maintain the power output of the site.

The PG 7251 FB gas turbine generates more power at full load (~184 MW) than the amount of power required to restoring the power output of the site (~127 MW). Consequently, this gas turbine could be used to retrofit two different groups of the power station and maintain the power output of the site or to retrofit just one group and increase the power output of the site. The present thesis, however, does no evaluate the off design behaviour of the gas turbine, it just analyses the feasibility of the power matched retrofit concept. Future work could include the off design operation of these components.

Once the pulverised coal power plant is retrofitted by introducing flue gas from the GT into the boiler furnace the firing rate has to be reduced due to the different composition of the GT flue gas compared to the combustion air in order to maintain gas velocity through the boiler at acceptable levels. Consequently, boiler steam production and temperature decreases.

A reduction in the superheated and reheated steam temperature at the HP and the IP turbine inlet lead to a reduction of all pressures in the steam cycle. At constant condenser pressure, the dryness fraction of the LP turbine outlet increases, which lead to a reduction of the work output of the LP turbine and, by extension, the overall cycle.

Effective thermodynamic integration between the HRSG and the existing steam cycle is achieved by appropriately sizing the unfired triple pressure HRSG to supply steam to the existing steam cycle, as shown in Figure 3.1, and to the reboiler of the PCC plant. In this analysis of the feasibility of the concept, as noted earlier the GT is sized, without reference to commercially available sizes, to supply electricity to fully restore the power output of the site.

HP boiler condensate, taken after the last feedwater heater, is fed to the HP economiser of the HRSG and then generates HP superheated steam entering the HP turbine and compensating for the reduction in flow rate of the boiler superheaters. IP steam taken from the cold reheat of the steam cycle is fed to two consecutive reheaters in the HRSG to generate hot reheated steam entering the IP turbine and compensating for the reduction in flow rate of the reheater of the boiler. As a result, the IP economiser and the IP evaporator typically found in a triple pressure HRSG are here redundant.

Water exiting the condenser of the steam cycle is fed to a LP economiser and a LP evaporator to produce LP saturated steam for solvent regeneration.

The existing turbines effectively constitute the combined cycle of the gas plant, which does not have a dedicated combined cycle, as shown in Figure 4.6.

4.4.- Process calculation of the carbon capture plant

A typical MEA scrubbing post-combustion capture process with a single absorber, stripper and lean-rich heat exchanger is taken in this work as an illustrative example of post-combustion capture technologies. It is worth remembering that one obvious advantage is that the GT and HRSG system can be adjusted to provide any mix of heat and power.

The capture plant was validated by Sánchez Fernández (Sanchez Fernandez et al. 2014) based on various data sets from different pilot plants (Razi et al. 2013).

A setup with two absorber trains of 13m diameter and 17m column height (not including the water wash) is used throughout this study. RadFrac columns are selected for both the absorber and the stripper. In the rate-based approach, actual rates of multi-component mass and heat transfer as well as chemical reactions are considered directly. **Appendix 2** describes the methodology of the rate based approach

CO_2 from the stripper overheads is compressed to 13 bar in a three-stage centrifugal compressor. It is then liquefied by the use of a propane refrigeration system and pumped to a pressure of 140 bar **(DOE/NETL 2007).** The compressor inter-coolers are designed to cool the CO_2 down by means of condensate water heating. In order to replace all the condensate heating of the existing steam cycle by recovered heat from the intercoolers the CO_2 temperature at the exit of the CO_2 compressors must reach 135 ºC.

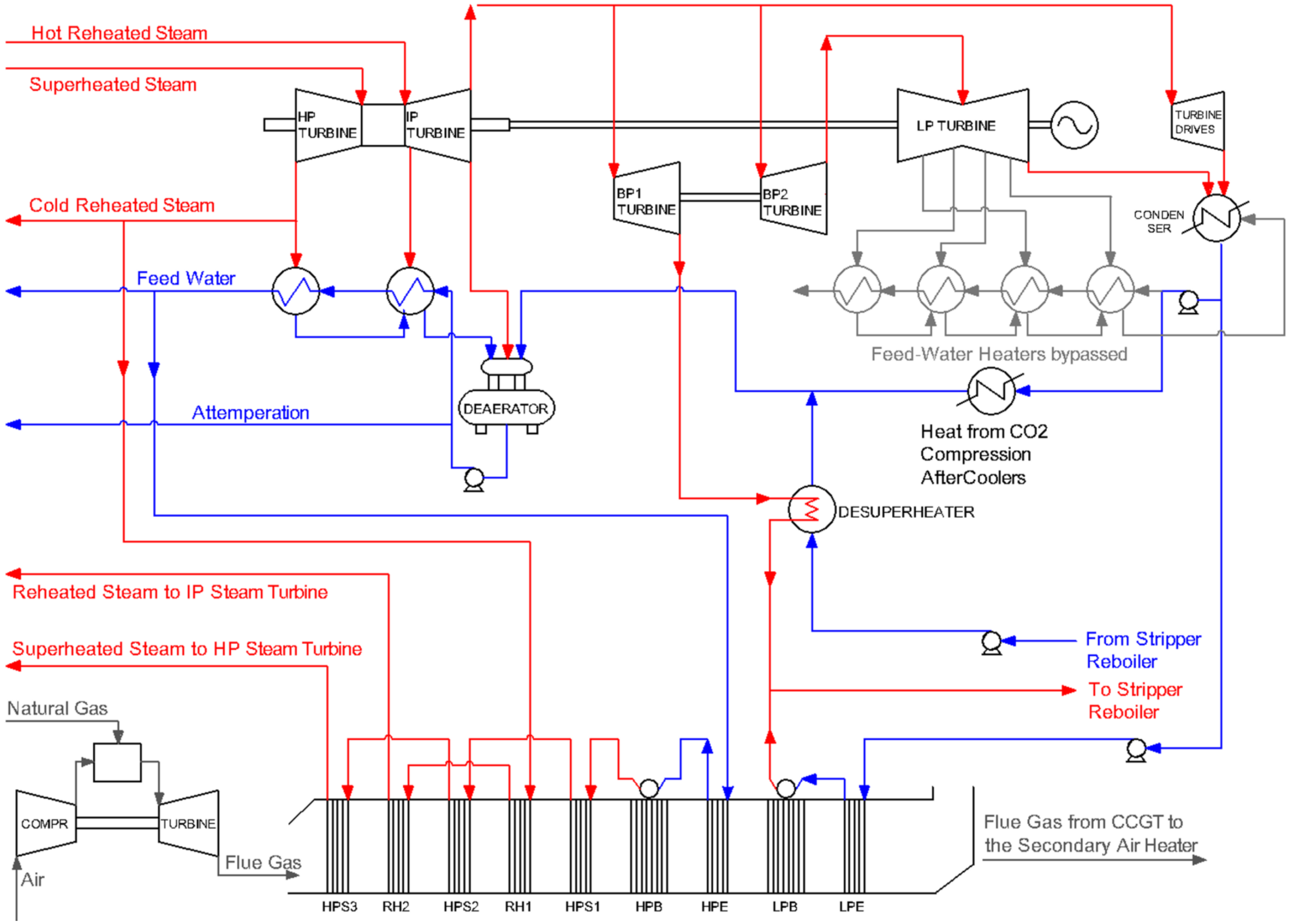

Figure 4.6.- Steam Cycle of the GT flue gas windbox carbon capture retrofit.

5.- RESULTS AND TECHNICAL DISCUSSION OF THE GAS TURBINE FLUE GAS WINDBOX CARBON CAPTURE RETROFIT

This chapter shows the results of the simulations of the GT flue gas windbox carbon capture retrofit for an amine based solvent post-combustion capture process and discusses the characteristics of this novel configuration.

5.1.- Results of the simulations

5.1.1.- Results of the retrofitted pulverised coal power plant

Total Combustion Air and Gas Flow Rate:

Since the oxygen content in the gas turbine exhaust gases (15%) is lower than in air, a higher amount of combustion agent, i.e. the combined mass flow rate of GT flue gas and primary and secondary air, is required per kg of fuel than in the air-firing case in order to maintain the same level of excess oxygen after the combustion of coal in the air/flue gas mixture. Consequently, the flue gas mass flow rate within the existing boiler is also increased if the coal input is unchanged. But in order to avoid this increase in flue gas mass flow rate, the coal consumption can be reduced, as indicated in Figure 5.1.

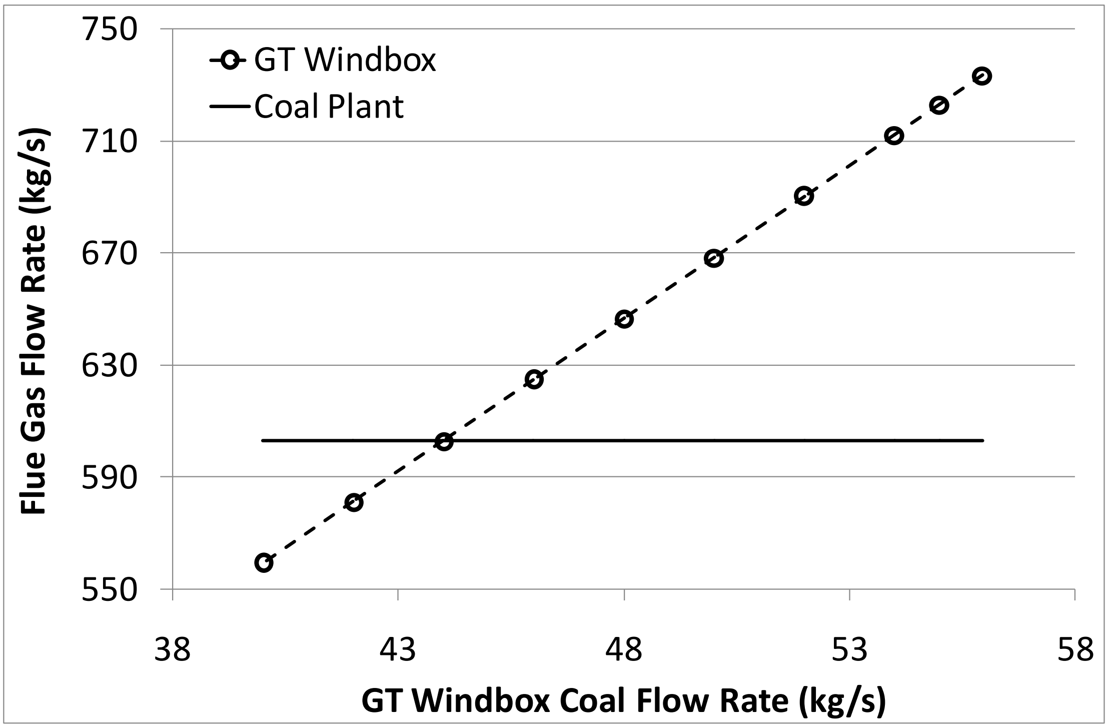

Figure 5.1.- Effect of Coal reduction in the Flue Gas Flow rate of the GT windbox retrofit.

Nevertheless, a reduction in coal consumption leads to lower heat release rate and, consequently, to a reduction in boiler steam flow rates and steam temperature.

In order to maintain steam flow rates and reach adequate steam temperatures in the steam cycle, an unfired triple pressure HRSG is appropriately sized to supply steam directly to the steam turbines and avoid a derating of HP and IP turbines.

With a gas turbine flue gas windbox retrofit purposely designed as a power matched retrofit, the gas turbine is sized to compensate for the reduction of output of the LP turbine caused by steam extraction and for the power requirements of compression and ancillaries. Since the amount of steam generated in the HRSG is then limited by both the exhaust gas flow rate of the gas turbine and the pinch temperature of the HP evaporator, as indicated in Figure 5.2, this determines the new coal flow rate should be reduced by 10%.

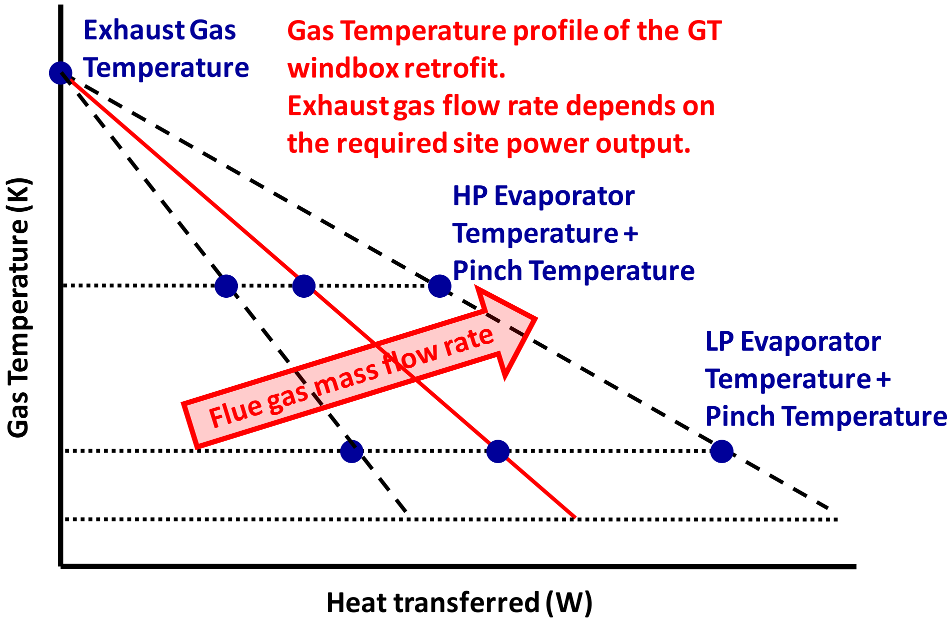

Figure 5.2.- Effect of gas flow rate on the HRSG gas temperature profile

Table 5.1.- Boiler coal, combustion air and flue gas mass flow rates

		Existing PC Plant	GT flue gas windbox CCS Retrofit
Coal Flow Rate	Kg/s	55.9	49.7
Primary Air Flow Rate	Kg/s	127.6	129.2
Secondary Air Flow Rate	Kg/s	415.4	208.2
Infiltration Air Flow Rate	Kg/s	9.6	9.6
GT Flue Gas Rate	Kg/s	0.0	280.7
Flue Gas Flow Rate	Kg/s	607.2	676.2

For power matched retrofits, the coal feed rate is reduced by an amount depending on the existing coal feed rate, the performance of the carbon capture process and the overall capture level.

An alternative solution to power matched retrofits is to size the GT and the HRSG to supply the amount of steam required to maintain the main steam turbine flow rates and the coal boiler flue gas flow rate. Excess power could be exported from the site. The change in coal feed rate would obviously then depend on the desired output after repowering and retrofitting.

Flue gas composition:

The flue gas composition is slightly altered when part of the combustion air of the existing plant is replaced by exhaust gas from the gas turbine.

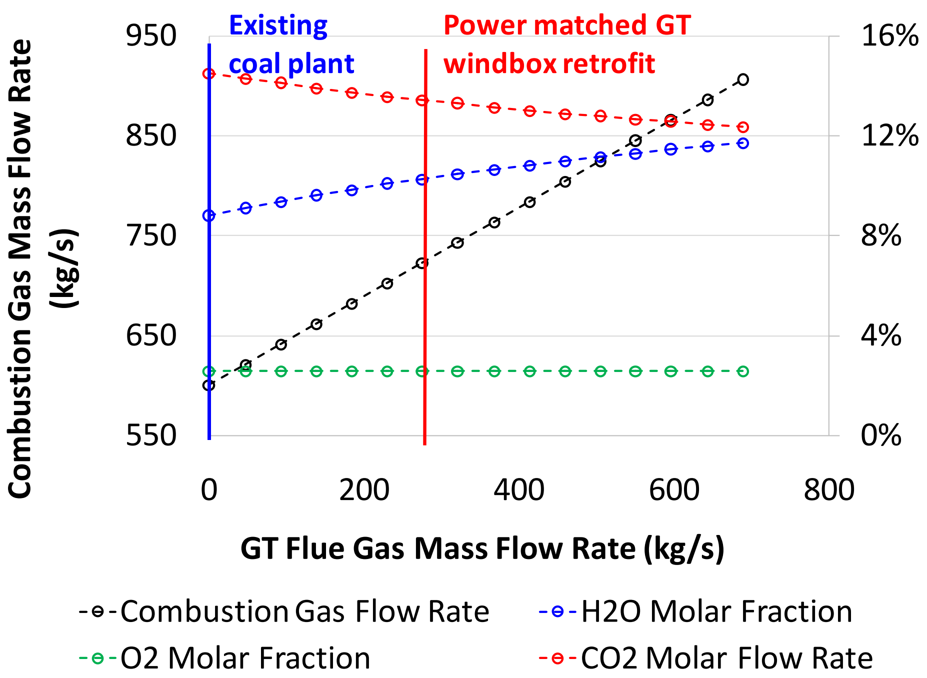

Figure 5.3.- Flue gas composition at different GT exhaust gas flow rates

Figure 5.2 illustrates the change in flue gas composition with the GT exhaust gas flow rate and shows that the higher the GT flue gas flow rate the lower the CO_2 concentration, the higher the H_2O concentration of the coal boiler flue gas. The oxygen concentration is kept constant by design.

Gas temperature:

Water vapour and carbon dioxide absorb significant amount of radiation at every point throughout the furnace. The presence of CO and SO_2 is neglected since they are weakly participating and overlap with the infrared spectrum of H_2O and CO_2.

In addition to the gas radiation from the products of combustion, the presence of suspended ash particles also cause an attenuation of the radiation due to absorption and anisotropic scattering. The equation of the flame emissivity proposed in chapter 3, equation **[3.34]**, is used here to study the influence of CO_2, H_2O and solid particles in the furnace radiation. The combined coefficient of radiation absorption, k, takes into consideration the contribution of these three contributions (Basu et al. 2000). However, radiation scattering by ash particles is not included by Basu et al. The inclusion of this effect is complex and is outside the scope of this study since particle size is difficult to know and the scattering is anisotropic. Future work could include a detailed furnace zone model where absorption and anisotropic scattering are analysed.

Figure 5.3 shows how the adiabatic flame temperature, the furnace exit gas temperature and the flame emissivity change when the GT exhaust gas flow rate is added and so the flue gas composition is modified.

The water concentration of the flue gas rises to 10% v/v, in comparison to 8.8% v/v for the coal plant with air-firing. This 18% relative increase modifies furnace heat transfer characteristics: the flame emissivity is increased and the adiabatic flame temperature and the furnace exit gas temperature are reduced. This also results in a lower flue gas temperature to the superheater

The difference between the adiabatic flame temperature and the furnace exit gas temperature, shown in Figure 5.3 for both cases, reflects the amount of heat absorbed in the furnace.

Table 5.2 shows the temperature profile of the flue gas across the furnace.

Table 5.2.- Furnace characteristics

FURNACE CHARACTERISTICS		Existing Coal Plant	GT flue gas windbox CCS Retrofit
Adiabatic Flame Temperature	K	2121	1876
Burner Zone Exit Gas Temperature	K	1803	1631
Upper Furnace Exit Gas Temperature	K	1499	1398
Heat absorbed by Water Walls	Watt	3,23E+08	2,77E+08
Heat absorbed by Platen Super Heater	Watt	1,55E+08	1,33E+08

The Boltzmann number of equation [3.32] can be used in order to study the influence of the two main heat transfer mechanisms in the furnace, radiation and convection. Boltzmann number increases indicate either an increase in convection or a reduction in radiation, or both effects combined. As expected, the Boltzmann number, shown in Figure 5.4, increases due to the increase in convection and the reduction in radiation.

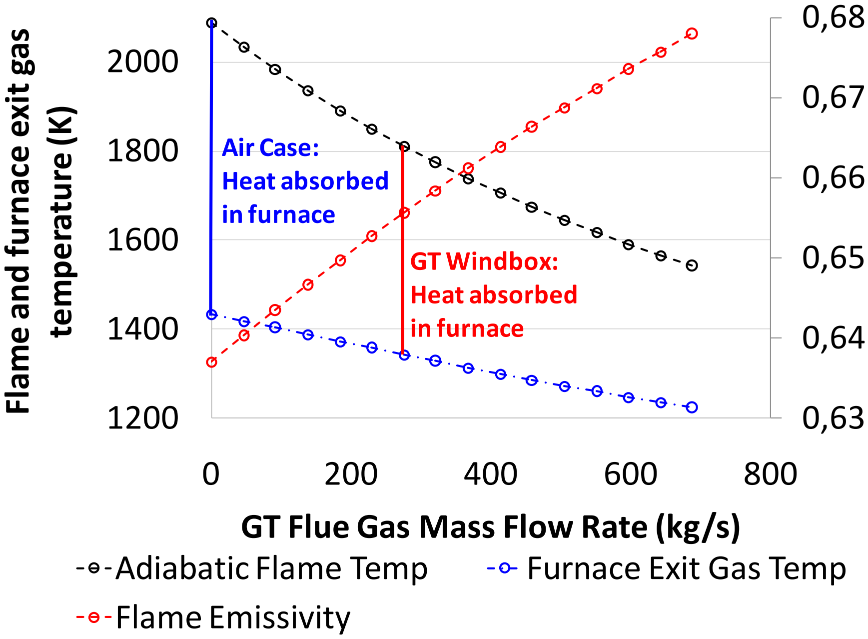

Figure 5.4a.- Gas temperature and flame emissivity

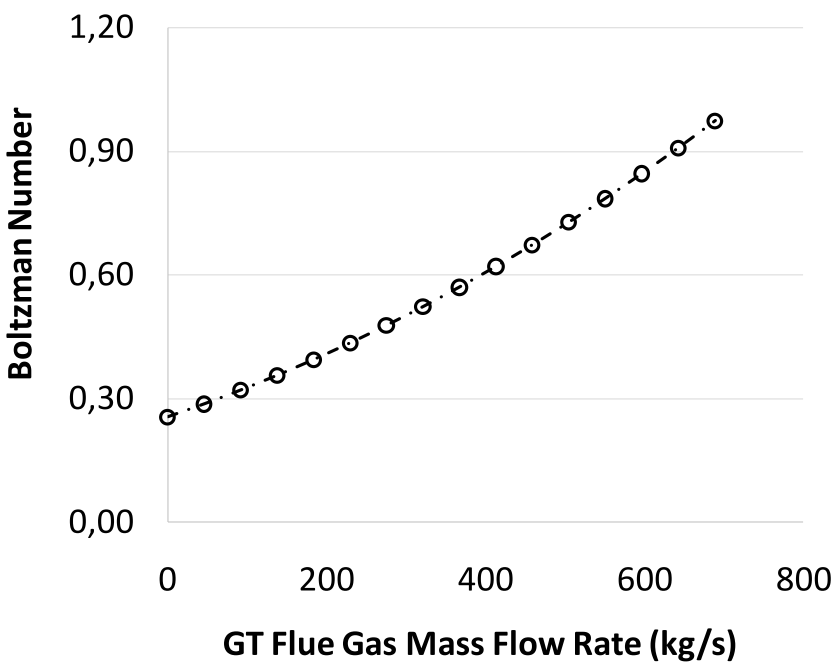

Figure 5.4b.- Gas temperature and Boltzmann number

Steam Temperature:

The lower flue gas temperature to the superheater would cause a reduction in superheated steam temperature if the HRSG were not efficiently integrated to the steam cycle to provide high pressure high temperature steam to the existing steam cycle. Figure 3.1 shows the integration of the HRSG with the steam cycle.

Radiation and convective heat transfer:

The analysis of heat transfer in the boiler banks also reveals a reduction in radiation and an increase in convective heat transfer, for the configuration of the boiler used in this study, shown in Figure 3.2.

The variation in the amount of heat absorbed by the different banks of the reheater, the outlet leg (RHOL) the bank of tubes RHB2, and the bank of tubes RHB1, is plotted in Figure 5.5. A large fraction of the total heat transfer shifts from convective heat transfer in the first bank to radiative heat transfer in the last bank of tubes.

Figure 5.6 shows the variation in overall heat transfer across the flue gas pathway due to the reduction in flame radiation.

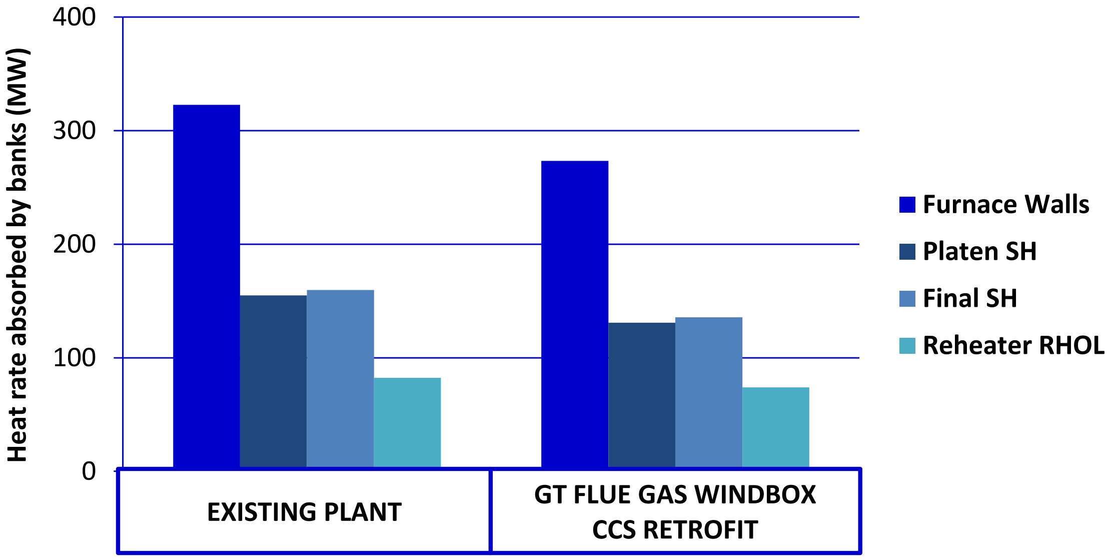

Figure 5.5.- Effect of flame radiation reduction on the total heat absorbed by the banks.

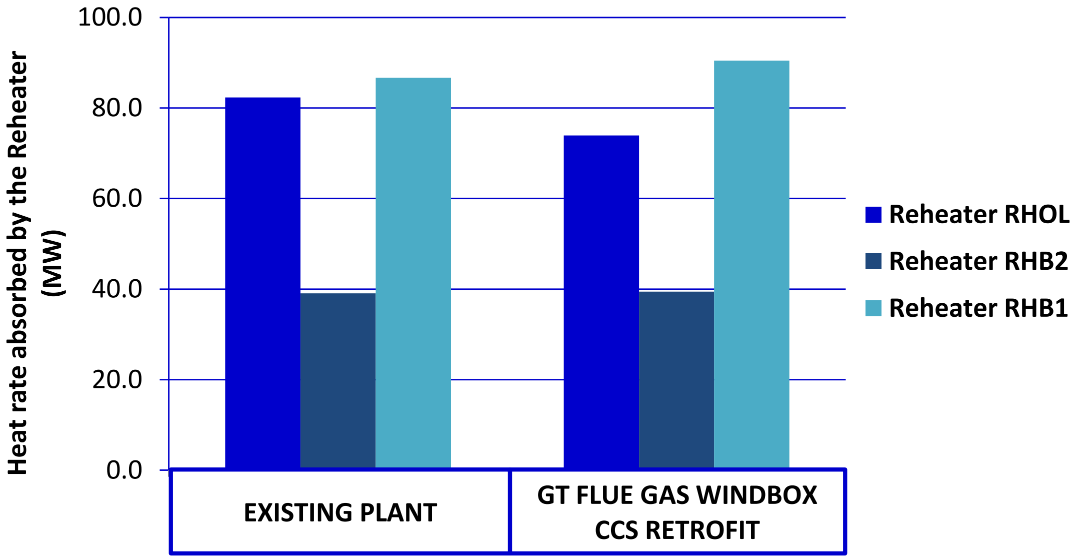

Figure 5.6.- Total heat absorbed by reheater banks.

5.1.2.- Results of the combined cycle gas turbine

The gas turbine is sized to provide the electrical power required to maintain the power output of the site. It will supply the electrical power required for the capture process (compression and the ancillary power of capture system) and it will cover any loss in power output to restore the power output of the plant.

Figure 5.7 indicates the amount of power produced by the CCGT and the coal power plant when the coal power plant is retrofitted as a GT flue gas windbox carbon capture retrofit.

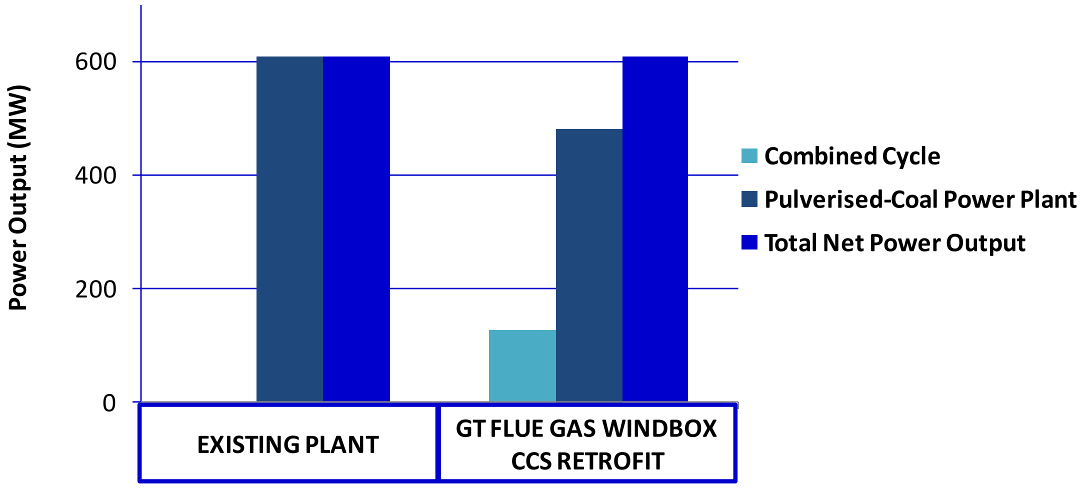

Figure 5.7.- Power output of the site

The heat transfer in the HRSG is determined by the gas turbine exhaust temperature and the pinch point temperature difference of the LP evaporator. These two points fix the slope of the gas temperature profile, as indicated in Figure 5.8. The gas temperature at the exit of the HRSG can only be reduced by either increasing the gas turbine exhaust temperature or reducing the pinch point temperature difference.

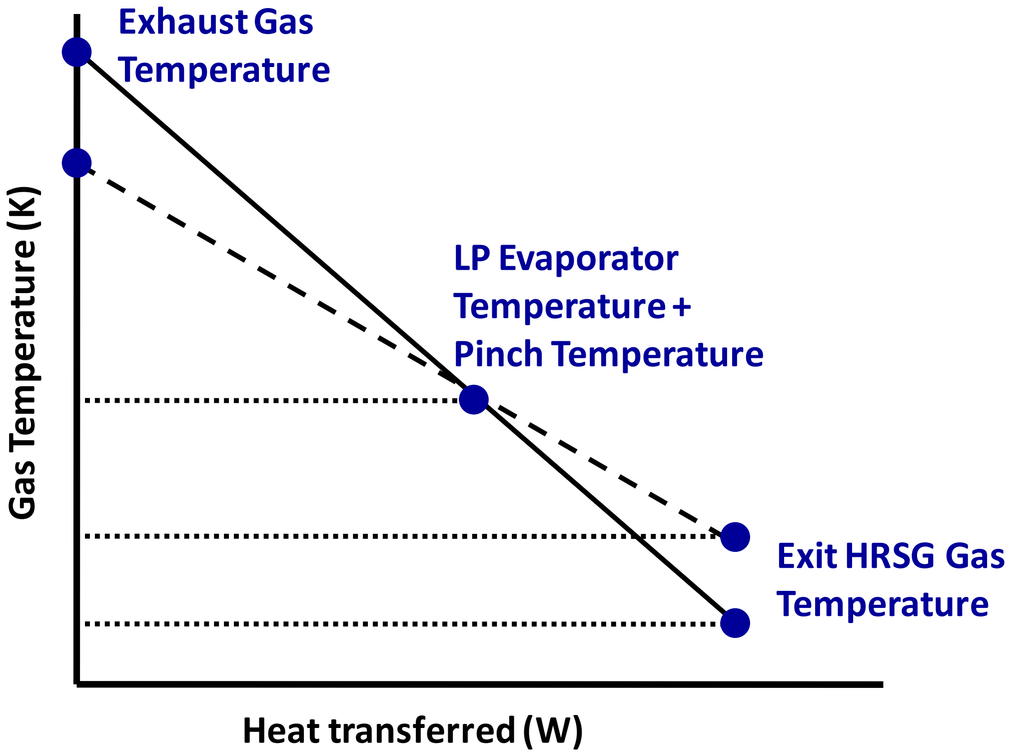

Figure 5.8.- Effect of the exhaust gas temperature on the exit HRSG gas temperature

Decreasing the pinch point temperature difference implies an increase in the LP evaporator heat transfer surface and costs. As a result, the exhaust gas temperature is assumed to be high, about 623 ºC, typical value for the PG 7251 FB General Electric (GE) gas turbine (GE Power Systems 2000b). A reheated gas turbine would also exhaust at a higher temperature but it is outside the scope of this thesis and could be evaluated as possible future work.

The performance of the CCS retrofitted plant is strongly influenced by the integration of the HRSG with the existing steam cycle. As shown in ***Figure*** the HRSG generates HP and IP superheated steam feeds that are sent to the HP and IP steam turbine cylinders respectively and LP saturated steam which, together with steam extracted from the existing steam cycle, is used in the reboiler for solvent regeneration. The HRSG effectively operates the existing steam turbines as the combined cycle of the CCGT. The high CCGT efficiency, 54%, gives an idea of the good integration of the HRSG with the steam cycle.

When the CCS retrofit is combined with an external plant, it is important to examine the best possible use of the calorific value of the additional fuel; hence, the maximum possible useful work for power regeneration is recovered from the additional fuel before supplying heat to the CC process. The metric used is the marginal efficiency of the use of natural gas (See Chapter 6 and 7 for more detailed information).

The high natural gas marginal efficiency, 52%, reveals that an important fraction of the calorific value of the natural gas is recovered as power. The absence of the IP evaporator reduces the irreversibilities of the system and increases the natural gas marginal efficiency. Figure 5.9 illustrates the temperature profile of the HRSG.

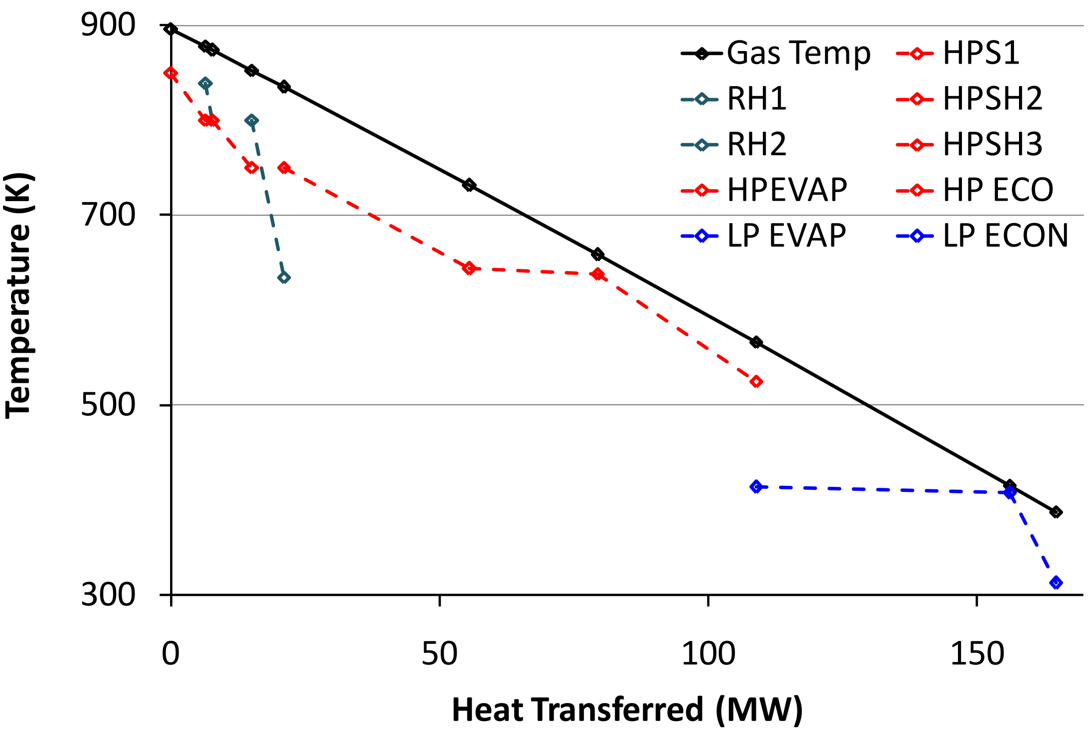

Figure 5.9.- Temperature profile of the HRSG

5.1.3.- Thermodynamic integration of the steam cycle, the HRSG and the reboiler of the carbon capture plant

One important aspect of the thermodynamic integration of the reboiler of the capture process is the quality of the steam extracted from the power plant steam cycle and of the steam generated by the low pressure evaporator of the HRSG in order to provide condensing steam for solvent/sorbent regeneration. The quality of steam is determined by the temperature of the reboiler. The saturation temperature of the steam is effectively the temperature of the reboiler plus a reasonable temperature difference. In this paper the temperature difference is assumed to be 10K. The larger the temperature difference the lower the investment cost of the heat exchanger but the higher the losses in power output.

Solvents tend to be regenerated at the highest sustainable temperature in order to release the CO_2 at the highest possible pressure (Lucquiaud 2010). For example, MEA is regenerated at around 120ºC to largely avoid degradation issues. The higher the total pressure is reached in the stripper the less stripping steam is required to drive the CO_2 into the gas phase and lower the reboiler duty required to regenerate the solvent, as indicated by Oexmann (Oexmann 2011).

With a desorber temperature of 120ºC and a temperature difference of 10 K for the heat exchanger, steam at pressure of 2.7 bar (130ºC saturation temperature) is required to regenerate the solvent.

Numerous researchers looked at different ways to minimise the overall net efficiency loss when MEA plants are integrated into the pulverised coal power plant (Mimura et al. 1995; Mimura et al. 1997; Desideri & Paolucci 1999; Parsons et al. 2002; Gibbins et al. 2004; IEAGHG 2004). They analysed different locations to extract steam for solvent regeneration and found out that the optimal extraction point is the IP/LP crossover. They also suggested the use of a throttle and a pressure maintaining valve to be able to supply the steam at the required pressure at different operating loads.

Lucquiaud and Gibbins examined different steam turbine retrofit options for the effective thermodynamic integration of existing plants with PCC. They highlighted that the electricity output penalty of adding capture could be minimised with the implementation of appropriate steam turbine solutions (Lucquiaud & Gibbins 2011a; Lucquiaud & Gibbins 2011c). They suggested two steam turbine solutions for retrofits with PCC depending on space restrictions; if space is available near the turbine island the power cycle of an existing plant can be retrofitted with two let-down pressure turbines, one in the steam extraction line to the reboiler and the second one between the extraction and the inlet of the LP turbine. This was shown to make it possible to achieve a retrofit electricity output penalty close to that of a new build power cycle designed for capture from the outset.

If space is constrained within the turbine island, Lucquiaud and Gibbins also showed that the addition of a smaller single let-down turbine in the extraction line is most likely worthwhile, and that it is possible to avoid thermodynamic losses occurring when throttling the LP turbine, by allowing as much additional steam expansion in the very last stages of the IP turbine as possible. The latter is similar to operation with uncontrolled extraction and can be implemented within the limits of the existing turbine blade design; the limiting factor being increased bending moments and other mechanical stress on the blades and the increased end thrust on the IP turbine balancing pistons.

A dual back pressure turbine retrofit is implemented in this study because it does not require changes in the operation of the IP turbine and cylinder mechanical stress are not increased. It is worth noting that the addition of a back pressure turbine in the extraction line has been studied in detail previously for retrofit of a subcritical plant (Ramezan et al. 2007), and a retrofitted additional (condensing) turbine taking steam from the IP/LP crossover of the existing turbine island was implemented at the Wilhelmshaven Power Plant in Germany (E.ON Kraftwerke GmbH 2010).

Steam extracted from the IP/LP crossover for solvent regeneration is expanded to 3.3 bar in a back pressure steam turbine. The steam temperature at the exit of the turbine is around 240 ºC and needs to be desuperheated to its dew point, at 134ºC approx, taking into account the pipe and heat exchanger pressure drops (0.3 – 0.6 bar). An optimised solution is to make use of this sensible heat into the steam cycle by using reboiler condensate returning to the steam cycle to desuperheat this steam. Desuperheated steam is then mixed with LP saturated steam coming from the low pressure evaporator of the HRSG.

In the carbon capture plant there is a large amount of low grade heat that can be integrate into the retrofitted steam cycle, however, most of this heat is available at very low temperatures and only heat from the stripper condenser and from the CO_2 compressor intercoolers can be used.

Previous work on the heat integration of the PCC system with the coal power plant focuses on minimising the energy requirements of the PCC process by using energy from either the stripper condenser or the CO_2 compressor for feedwater heating. Some of these studies are described below:

Works done by Gibbins and Crane showed an increase in efficiency up to 1.3 percentage points when all the condensate heating is replaced by recovered heat (Gibbins & Crane 2004). They estimated that the efficiency penalty could be reduced to 8 percentage points, on a lower heating value basis (LHV), by the use of improved thermodynamic integration and lower energy solvent.

Romeo et al examined the integration of the carbon capture process with the existing steam cycle by using the heat available from the CO_2 compressor to heat boiler feedwater (Romeo, Espatolero, et al. 2008). This approach leaded to lower power output and efficiency penalties, which agreed with previous work proposed by Gibbins and Crane (IEAGHG 2004).

In this study, steam extraction for condensate water heating is substituted by heat recovered from the CO_2 compressor intercoolers; so that less steam is extracted from the steam cycle and the efficiency of the existing steam cycle is increased.

5.1.4.- Results of the carbon capture plant

The mass transfer rates in the absorber are slow and an increase in the transfer area would improve the performance significantly, so, the effect of the absorber height on the performance of the carbon capture process should be analysed. Figure 5.10 illustrates how the absorber height affects the reboiler duty and rich loading. The diameter of the absorber is kept constant.

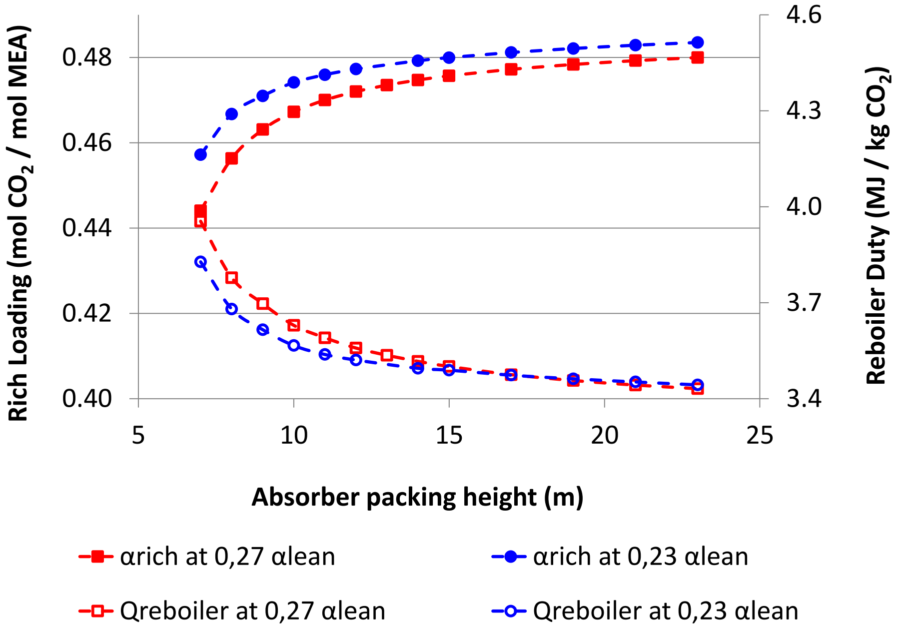

Figure 5.10.- Effect of absorber height on reboiler duty and rich loading

Higher columns imply larger mass transfer area and, consequently, the performance of the process improves when the height of the column increases, the higher the column the lower the reboiler duty. Nevertheless, when the absorber column reaches 17m height, the rich loading is quite close to the equilibrium value and further increases in height do not improve its performance significantly.

A 17m height column is used in the simulation of the absorption process. Higher columns would increase the pressure drop along the column and its capital cost and the reduction in reboiler duty would be insignificant.

Additionally, the carbon capture plant operates with an optimum lean loading to minimise the reboiler duty. The optimum reboiler duty for the GT flue gas windbox carbon capture retrofit was determined by conducting a sensitivity analysis of the effect of the lean loading on the reboiler duty and stripper pressure, the lean loading being varied from 0.20 to 0.27.

At higher lean loadings the solvent capacity is reduced and a higher solvent flow rate is required to maintain the CO_2 removal rate. As a result, additional sensible heat demand arises and the reboiler duty increases. At lower lean loadings, although the solvent capacity is increased the generation of stripping steam is significantly higher and the reboiler duty increases as well.

The minimum reboiler duty (3.49 MW/kgCO_2) was found at 0.25 lean loading which corresponds to a stripper pressure of 1.817 bar as indicated in Figure 5.11 and Figure 5.12.

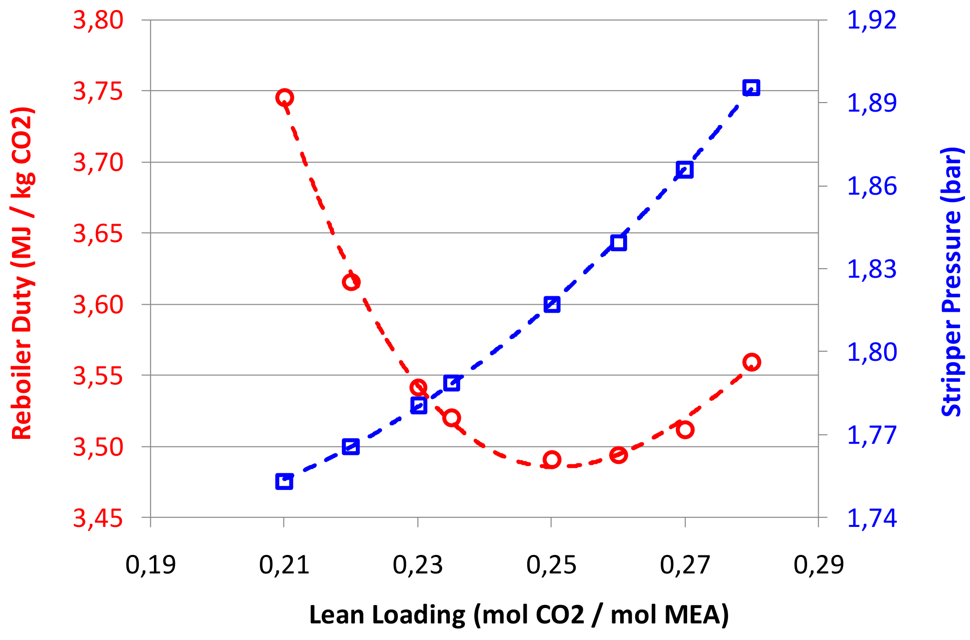

Figure 5.11.- Reboiler duty and stripper pressure dependence on the Lean Loading

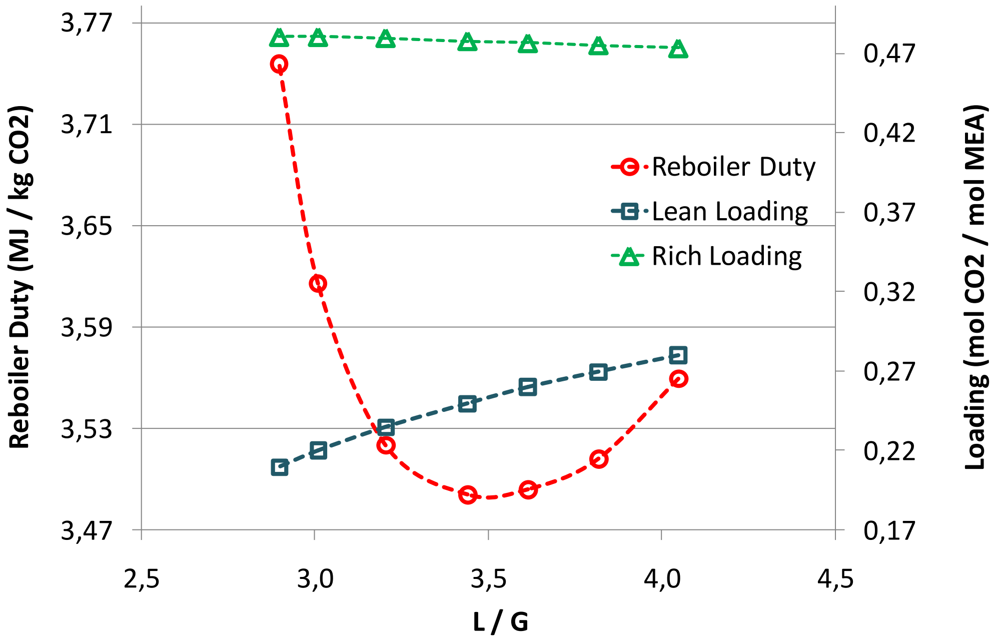

Figure 5.12.- Optimisation of solvent flow rate

The metric used in this project to indicate the overall energy requirement for CO_2 capture is the electricity output penalty (EOP). The EOP for the GT flue gas windbox carbon capture retrofit can be expressed as the power output of the CCGT divided by the amount of compressed CO_2 leaving the boundary of the plant.(see Chapter 6 for more details).

There is a benefit on the reboiler duty since the CO_2 concentration of the flue gas entering the capture plant is high, close to that of a coal plant. The EOP of the GT flue gas windbox retrofit reaches 291 kWh/t CO_2, lower than the EOP of a standard integrated retrofit. Chapter 7 compares and explains the EOP of different power matched retrofits achieving high level of CO_2 capture.

5.2.- Technical discussion

A comparative analysis of the main operating variables allow us to study the effect of this novel carbon capture configuration on the existing PC power plant and to discuss the advantages of this configuration compared to other carbon capture retrofit options.

5.2.1.- Impact on the existing gas cycle

As the combustion gas flow increases and so does the average gas velocity, the existing reheater banks could be eroded if the plant operated with an abrasive highs ash coal. The velocity limits depends on the amount of ash and on the proportions of abrasive constituents in the ash.

The typical limits are 19.8 m/s for relatively non-abrasive low ash coals and 13.7 m/s or less for abrasive high ash coals (Kitto & Stultz 2005). In this work the maximum velocity achieved is limited to an intermediate value of 16.3 m/s.

The increase in the total flow rate of gas is of the order of 10% and results in an increase of the power input required for the fans. For certain plants, the existing fans would need to be replaced to accommodate the additional flow, although this needs to be determined on a site by site basis.

Regarding the geometry of the burners, the Primary Air Velocity is identical to the air firing case. The Secondary Air velocity is, however, higher as a fraction has now been replaced by a larger portion of flue gas with lower oxygen content. In practice, a GT flue gas windbox PCC retrofit is expected to require tuning for all the burner settings, such as cone-damper opening, swirler position, etc. in order to obtain a suitable flame shape of the flame. The GT flue gas could, however, perhaps alternatively be used as over fire air (OFA) so as to reduce the formation of unburned coal and avoid stratification issues due to mixing GT flue gas with combustion air.

Thermal and fuel NOx emissions are expected to be reduced with the lower flame temperature and the reduction in coal flow rate.

5.2.2.- Impact on the existing steam cycle:

It is very important to achieve high enough superheated and reheated steam temperatures in order to avoid an increase in the formation of water droplets in the last stages of the low pressure (LP) steam turbine which would reduce isentropic efficiency and increase blade tip erosion.

Attemperators located between the platen superheater (PlatSH) and the final superheater (FSH) in Figure 3.2 are used to control the superheated steam temperature. A set of dampers installed at the exit of the boiler are used to control steam temperature at the reheater outlet by adjusting the proportion of gas flow between the two convection paths.

An alternative solution would be to increase the surface of the final superheater banks and the capacity of the attemperators, in that way the main steam temperature can be always reached by only adjusting the spray flow rate.

5.2.3.- Benefits of the GT flue gas windbox carbon capture retrofit:

The main benefits of this novel configuration are as follows:

- In the GT flue gas windbox retrofit gases from both fuel sources are treated in the same PCC plant without the need for mixing large gas volumes. Stratification problems are then avoided.
- MEA degradation has been found to increase with both oxygen concentration and temperature (Vevelstad et al. 2014). MEA degradation problems are avoided due to the low O_2 contain in the flue gas. The O_2 concentration at the inlet of the carbon capture plant reaches 3,2% v/v, in comparison to 12.5% v/v at the exhaust gas of the turbine.
- The HRSG is integrated with the steam cycle of the existing coal plant so that the gas CHP plant does not have a dedicated combined cycle. The existing steam turbines are operated as the combined cycle of the CCGT. This also results in significant capital cost savings.
- Thermal and fuel NOx emissions decrease due to a lower flame temperature and a reduced coal flow rate. SOx emissions are expected to decrease as well.
- Most of the hot-windbox repowering issues (Romeo, Bolea, et al. 2008), i.e. erosion problems, are avoided with this novel carbon capture retrofit configuration as the flue gas flow rate does not increase as much as in the hot-windbox case and the HRSG is efficiently integrated with the steam cycle of the coal power plant.
- The total volume of CO_2 to be treated in the carbon capture plant is similar to the air firing integrated retrofit case. This makes the GT flue gas windbox retrofit a promising alternative for adapting integrated capture retrofits that are initially designed for operation with zero to ~90% capture (as at the Boundary Dam 3 unit) for subsequent operation only with full capture. In this case the addition of a GT flue gas windbox retrofit will restore the full power output of the site with full CO_2 capture and using the original capture plant.

In conclusion, GT flue gas windbox carbon capture retrofit seems to be a promising option to capture CO_2 from both fuel sources in a single carbon capture unit However, an economic analysis is needed to compare the performance with other GT retrofit options and this will be to topic for Chapter 7, after some alternative options have been discussed in Chapter 6.

6.- ALTERNATIVE OPTIONS FOR PULVERISED COAL RETROFITS WITH GAS TURBINE POWER CYCLES

Previous chapters demonstrated that sequential combustion with a gas turbine flue gas windbox is practically feasible. This chapter presents a comprehensive comparison of other relevant PCC retrofit options with gas turbine power cycles. The following discrete configurations are selected to cover the main options based on the decision diagram below, but, obviously a continuous range of intermediate variations are possible. For example, other Emission Performance Standard values would yield different values of the metrics although is anticipated that the general integration principles proposed here would stand.

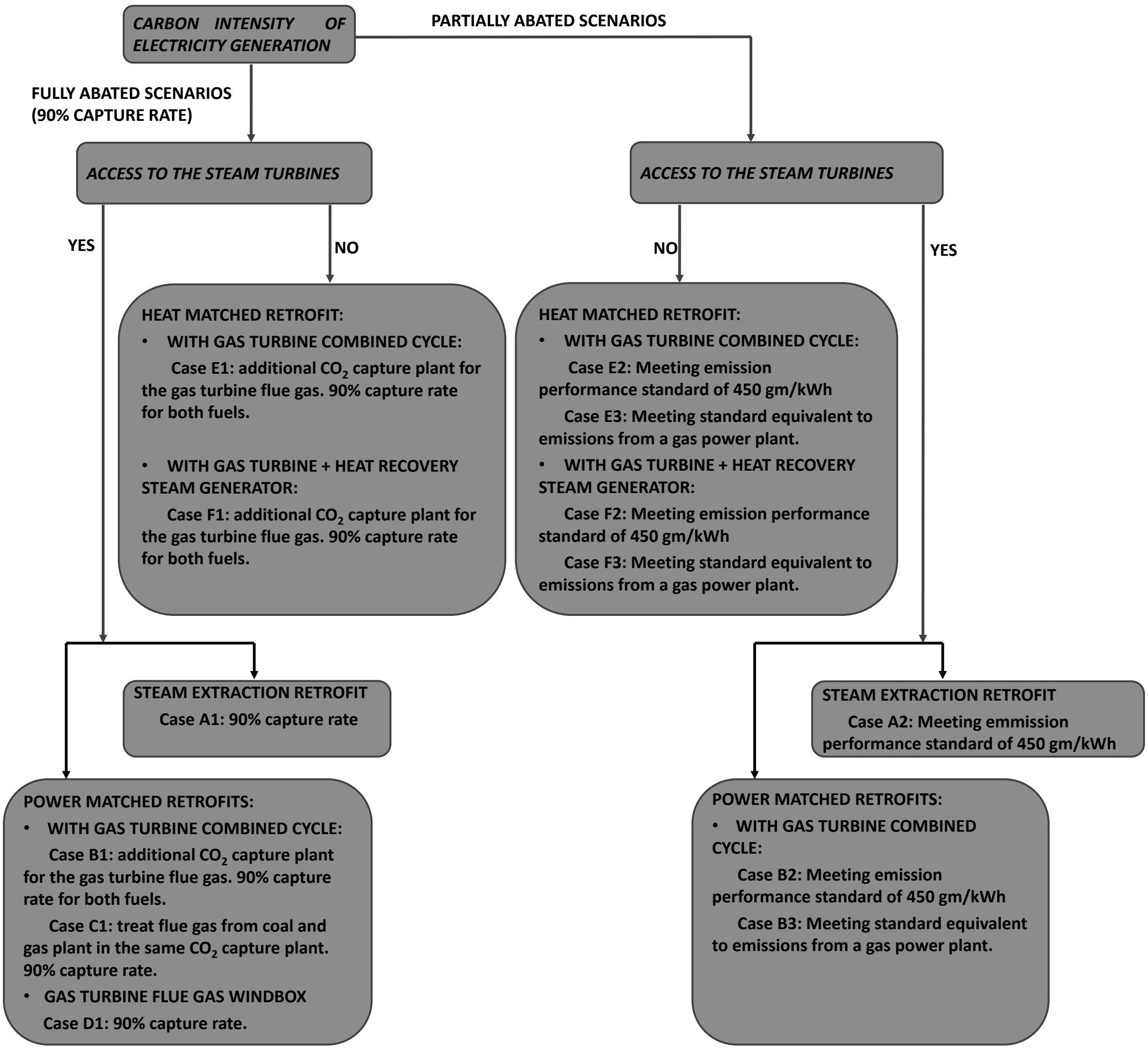

Figure 6.1.- Carbon capture retrofit options considered in this work

It is also important to note that, although it has not been studied in this work, there is an array of possible gas turbine sizes to achieve a power output in between those of heat matched and power matched retrofit or possible lower.

A widely-proposed way to retrofit coal-fired power plants with post-combustion CO_2 capture (PCC) is the 'integrated retrofit with steam extraction, where all the electricity and heat required to operate the capture equipment is supplied from the existing steam cycle, at expense of a reduction in site power output.

For example, ALSTOM Power Inc. evaluated the technical and economic viability of applying CO_2 capture to Conesville power plant Unit 5. The main purpose of this report was to supply useful information to help government, regulators and power plant owners to take decisions and actions concerning GHG emissions reduction. The first study (Bozzuto et al. 2001) discussed two potential retrofit options: PCC and oxyfuel. Regarding the PCC case, an integrated retrofit with steam extractions was evaluated; some modifications in the steam cycle were needed in order to provide the steam at the required quality for solvent reboiler. The steam was extracted from the IP/LP crossover, expanded in a new back pressure steam turbine to 4.5 bar and de-superheated by mixing it with condensate from the reboiler. The authors suggested that further work should be undertaken using improved solvents and steam integration. In the second study (Ramezan et al. 2007), the same US coal-fired power plant was retrofitted by using advanced amine-based capture technology supplied by Fluor. The solvent regeneration duty was reduced by approximately a third. The carbon capture process integration was improved as follows: steam for solvent regeneration was extracted at 3.1 bar instead of 4.5 bar and considerable quantities of heat rejected from the CO_2 capture and compression process were integrated with the steam/water cycle. Consequently, the electricity output penalty was considerably reduced compared to Bozzuto et al's study from 470.90 kWh/tCO_2 to 368.85 kWh/tCO_2.

A configuration with steam extraction from the power cycle supplying all of the thermal energy required for solvent regeneration, the 'Standard Integrated Retrofit', is included in this thesis for a comparative assessment and corresponds to Case A of ***Table 6.1*** and Case A1 of *Table 6.2*. The process flow diagram is illustrated in *Figure 6.2*.

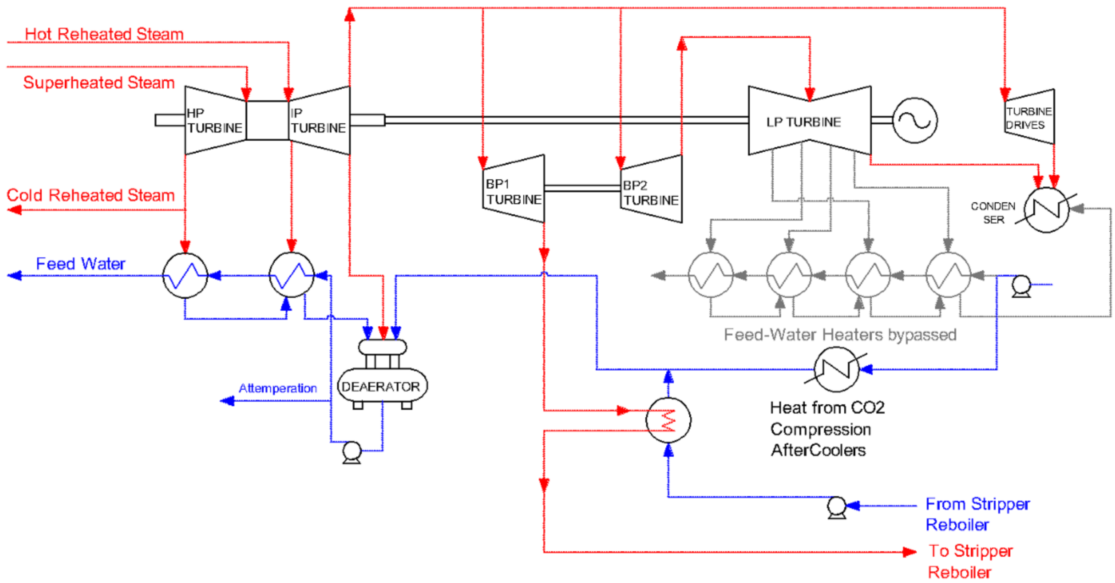

Figure 6.2.- Process flow diagram of the Standard Integrated Retrofit configuration with steam extraction from the main steam cycle providing all of the heat for CO_2 capture and power requirements from the main generator.

In order to minimise energy requirements the PCC plant is closely integrated with the existing steam cycle. A dual back pressure turbine supplies steam for solvent regeneration at the lowest pressure that satisfies the reboiler requirements and avoids the associate thermodynamic losses from throttling the inlet of the LP turbine to maintain the crossover pressure, as proposed in Lucquiaud and Gibbins (2011b) and unlike in Ramezan et al. Additionally, steam extraction for condensate water heating is substituted by heat recovered from the CO_2 compressor intercoolers.

The addition of a turbine connected to the IP/LP crossover as a retrofit to an existing steam cycle, although not a routine operation, is currently in use at Wilhelmshaven power plant power plant in Germany (E.ON Kraftwerke GmbH 2010).

Lucquiaud and Gibbins developed a rigorous model to provide correlations to estimate EOP values for PCC and compression systems that are well-integrated with the power plant (Lucquiaud & Gibbins 2011b). This model showed that the Electricity Output Penalty (EOP) of steam extraction had a strong dependence on solvent thermal stability and hence the maximum temperature available for heat recovery in the steam cycle.

In this thesis, a sensitivity analysis is carried out to find out the optimum lean loading of the solvent that minimises the overall electricity output penalty at solvent regeneration temperature of 120ºC and maximise power output. Results are represented in Figure 6.3. Low reboiler duties imply high power output due to lower steam extraction; however, high stripper pressures reduce the electrical power consumed during CO_2 compression. Both factors need to be examined in conjunction.

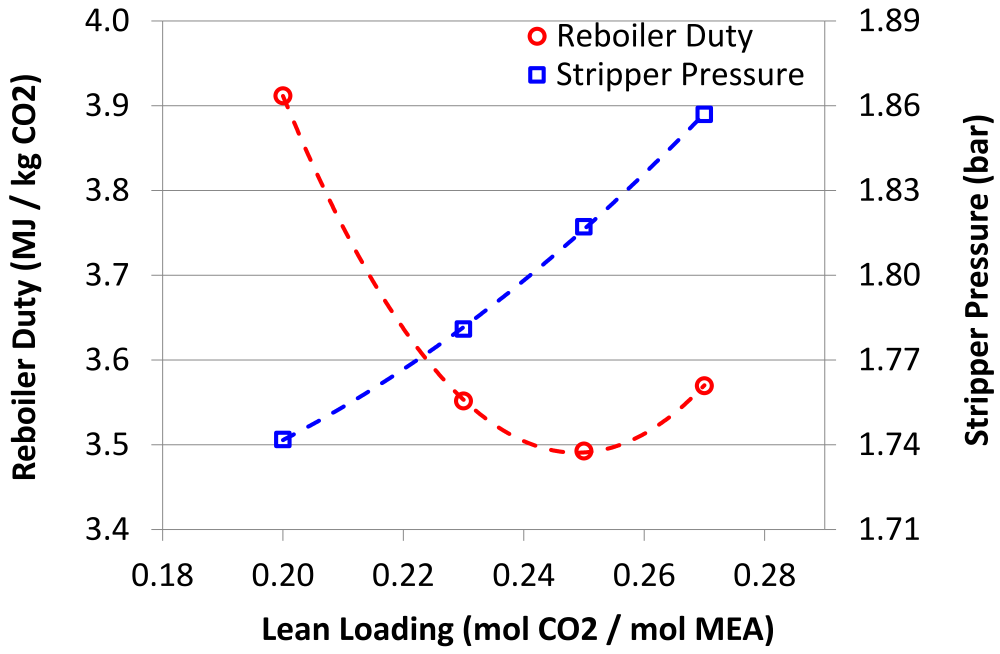

Figure 6.3a.- Optimum MEA lean loading

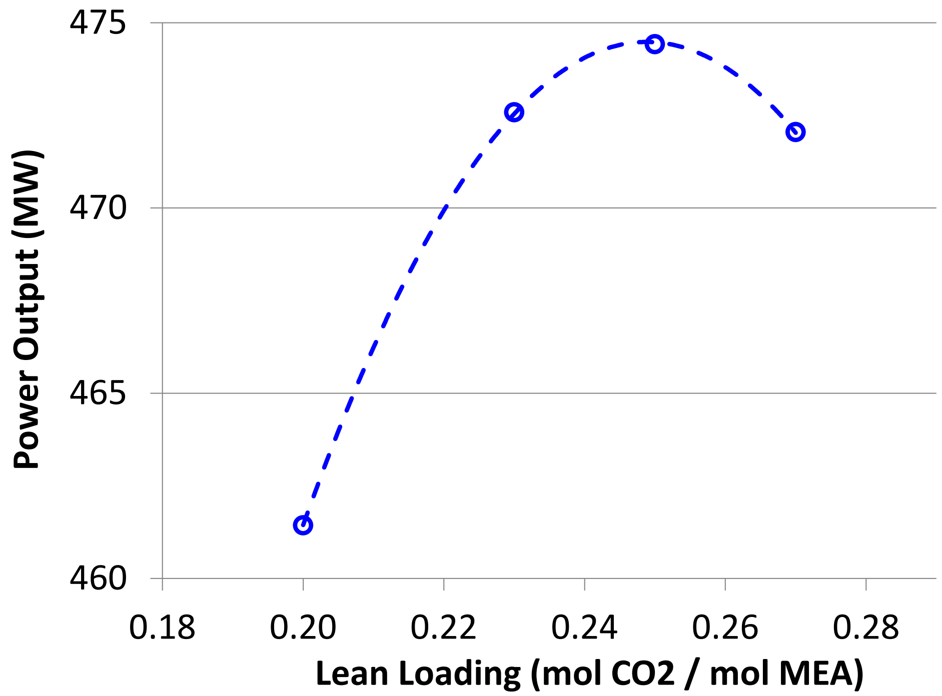

Figure 6.3b. - Optimum MEA lean loading

Considering the influence of the reboiler duty and the stripper pressure on the power output of the site, the maximum power output (474MW) was found at 0.25 lean loading.

As an alternative to the Standard Integrated Retrofit with only steam extraction from the main steam cycle, it is possible to supply all or part of the heat and power required for the capture and compression systems with a combined heat and power (CHP) plant.

Gibbins et al. proposed six rules to optimise the PCC plant thermodynamic and economic performance (Gibbins et al. 2004). These rules were updated by Lucquiaud in 2010 (Lucquiaud 2010). Updated Rule 3 states as follows: "Produce as much electricity as possible from the power cycle (i.e. be prepared to use additional turbines for retrofit projects if commercially justified) and from any additional fuel used, consistent with rejecting heat at the required temperature for solvent regeneration". The application of this rule suggests the use of gas CHP plants with the highest possible power to heat ratio for the fuel and the lowest steam supply temperature to the reboiler for a given regeneration temperature. Consequently, the present thesis considers only gas turbine (GT) based CHP retrofit as follows, and discards gas ancillary boilers retrofits on the basis of low efficiency:

- Power matched retrofit where a gas turbine combined cycle (GTCC) is used to supply a significant fraction of the electrical power required for the capture process. The output of site is maintained with the GTCC plant making up for losses in output from the existing plant due to the steam extraction.
- Heat matched retrofit where either a GT with a heat recovery steam generator (HRSG), or a GTCC, is used to supply all the heat required for the capture process. Any excess power can be exported from the site, if the grid connection allows.

Previous studies supporting this choice are discussed below:

Singh et al made a techno-economic analysis of CO_2 capture from an existing coal power plant with two approaches: MEA scrubbing and oxycombustion (Singh et al. 2003). For the MEA scrubbing approach the authors proposed the addition of a supplemental steam power supply which consisted of a GT with an HRSG and a separate natural gas ancillary boiler. It seems that the GT was added with the purpose of restoring the power output of the site and the HRSG and the ancillary boiler to provide steam for solvent regeneration. Unsurprisingly, the results of the analysis revealed that this approach presented a high cost of abatement. It is obvious that this breaks Rule 3.

Romeo and coworkers (Romeo, Bolea, et al. 2008) studied different ways to supply the energy requirements of the CC process. Their research consists of a techno-economic analysis where only 60-65% of the original emissions were captured. They use either a natural gas auxiliary boiler to generate steam for solvent regeneration or a GT to supply power for CO_2 compression. In concordance with Singh et al, the less efficient and cost-effective option is found to be the heat matched retrofit with a natural gas auxiliary boiler, since even with a back pressure turbine auxiliary natural gas boilers only use a fraction of the calorific value in producingelectricity. The corresponding Carnot ideal efficiency is significantly lower than combustion in a gas turbine and they achieve very low overall efficiencies.

Bashadi examined different carbon capture retrofit options where an auxiliary natural gas power plant was used to supply the thermal energy of the carbon capture process. Capture from the additional fossil fuel source was not considered though (Bashadi 2010). The most attractive option was found to be the CCGT and the least attractive a natural gas boiler plant.

The broadest technical and economic study undertaken on carbon capture retrofit that the author is aware of was commissioned by IEAGHG (IEAGHG 2011). The report assessed at a generic level a wide range of retrofit options and compared the performances and relative costs to each other and to new build plants with CCS. The research presented in this chapter is based on the heat and power matched retrofit options assessed in the (IEAGHG 2011) report, but, instead of using its parametric model spreadsheet detailed retrofit performances are implemented in the process simulator Aspen Plus V8, after validation in Mathcad.

An important concern in the context of decarbonisation of fossil fuel use is whether CO_2 emissions from both the additional natural gas source and the retrofitted coal plant are captured, or from the latter only. The present work examines options depending on the carbon intensity of electricity generation: close to fully abated scenarios where 90 % of the CO_2 emissions from both fuel sources are captured and partially abated scenarios where either the total emissions from the plant meet an emission performance standard (EPS) comparable to that of a new fossil fuel power plant at 450 gCO_2/kWh, or 90% of the coal plant emissions are capture but not the emissions from the ancillary GTCC unit.

The relevance of examining an EPS scenario in the context of gas turbine power cycles comes from the fact that it is likely to be considered as a significant upgrade implying that the plant would then have to meet the EPS, as discussed in more details in Section 6.2.

6.1 Options achieving high levels of CO_2 capture

Table 6.1 summarises the close to fully abated CO_2 capture retrofit options analysed in this thesis.

Table 6.1.- Fully abated CO_2 capture retrofit options

CASE A1	**STANDARD INTEGRATED RETROFIT**	
	POWER MATCHED CARBON CAPTURE RETROFITS	
CASE B1	-	RETROFIT WITH ABATED CCGT (Flue gas from coal and gas treated in different carbon capture plants)
CASE C1	-	RETROFIT WITH ABATED CCGT (Flue gas from coal and gas mixed and treated in the same carbon capture plants)
CASE D1	-	GT FLUE GAS WINDBOX CARBON CAPTURE RETROFIT
	HEAT MATCHED CARBON CAPTURE RETROFIT	
CASE E1	-	RETROFIT WITH ABATED CCGT
CASE F1	-	RETROFIT WITH ABATED GT + HRSG

One option to address carbon emissions from the combustion of natural gas is to add a dedicated PCC plant to the CCGT or, if efficient mixing of large gas volumes can be achieved, to treat the flue gas from the coal and the gas plant in the same PCC plant. The process flow diagram of this type of power matched retrofit is represented in ***Figure 6.4*** and corresponds to Case B1 and C1 of ***Table 6.1.*** It consists of a CCGT where the HRSG is a triple pressure system and the steam cycle comprises a High Pressure (HP) and an Intermediate Pressure (IP) turbine. The outlet of the IP turbine feeds to the solvent reboiler of the PCC plant and the combined cycle operates without a low pressure condensing turbine. Additional steam required for solvent regeneration is withdrawn at the IP/LP crossover of the existing coal plant, and with two back pressure turbines in the extraction line and at the front of the LP turbine respectively.

For many existing sites, access to the power cycle and to appropriate steam extraction pressure tapping points may not be possible anyway without undue modifications and/or unnecessary thermodynamic losses. Due to these reasons two heat matched retrofit options are examined: a lower capital cost option where the GT is combined with an HRSG producing only low pressure saturated stream for the reboiler, illustrated in *Figure 6.5* and corresponding to
Case F1 of Table 6.1, and a higher-efficiency option, where a GT with a combined steam cycle produces additional electricity, illustrated in *Figure 6.6* and corresponding to Case E1 of
Table 6.1.

Similar to the configuration of Figure 6.4, the HRSG of the combined cycle consists of a triple pressure system and the steam cycle comprises a High Pressure (HP) and an Intermediate Pressure (IP) steam turbines. The outlet of the IP turbine feeds to the solvent reboiler of the PCC plant and the combined cycle operates without a low pressure condensing turbine.

In both heat matched retrofit configurations the output of the gas turbine of the CHP plant is sized so that the mass flow of steam leaving the IP turbine and the mass flow leaving the LP evaporator match the heat requirement for solvent regeneration with condensing steam. In these configurations the net power output of the site increases if the fuel input to the coal plant is kept constant. If, however, additional power could not be exported it would, in principle, be possible to maintain the site output with the coal plant operated at a lower load. This last option is not, however, evaluated in this study.

6.2 Options using partial capture to achieve interim emission performance targets

Although partial capture can only be an interim stage in achieving full electricity sector decarbonisation, this is currently of interest because of the level of the prevailing emission performance standards (EPS) targets (e.g. 450gCO_2/kWh) in California, the UK, Canada and possibly the USA. Particular attention is given in this study to the carbon intensity of electricity generation of the retrofitted plant in the context of the UK Energy Act 2013, and recent proposals for the inclusion of CO_2 in Clean Air Act Section 111 (Federalregister.gov

2014b) and for a Clean Power Plan by the Environmental Protection Agency (EPA) in the USA (Federalregister.gov 2014a).

Table 6.2 summarises the partially abated CO_2 capture retrofit options analysed in this thesis. The Standard Integrated Retrofit, Case A1, is modified for partial capture to meet an EPS limit comparable to Case A2.

In this work, the PCC plant configuration to achieve intermediate capture levels consists of 90% of the CO_2 contained in a fraction of flue gas passing through the absorber and the rest of the flue gas sent directly to the stack. This ensures that optimum operation of the capture and compression system is achieved and cost minimised, as shown by Rao and Rubin (Rao & Rubin 2006).

The power matched retrofit and heat matched retrofit options are designed to meet either the current EPS levels or to give 90% capture from the coal plant and no capture from the GT flue gases – the latter might be the case where the main objective is to capture CO_2 for Enhanced Oil Recovery (EOR) rather than emission reductions by targeting the higher CO_2 concentration flue gas streams.

Table 6.2.- Partially abated CO_2 capture retrofit options

CASE A2	**STANDARD INTEGRATED RETROFIT** (450 gCO_2/kWh)	
	POWER MATCHED CARBON CAPTURE RETROFITS	
CASE B2	-	RETROFIT WITH CCGT MEETING EPS (450 gCO_2/kWh)
CASE B3	-	RETROFIT WITH UNABATED CCGT
	HEAT MATCHED CARBON CAPTURE RETROFITS	
CASE E2	-	RETROFIT WITH CCGT MEETING EPS (450 gCO_2/kWh)
CASE E3	-	RETROFIT WITH UNABATED CCGT
CASE F2	-	RETROFIT WITH GT + HRSG MEETING EPS (450 gCO_2/kWh)
CASE F3	-	RETROFIT WITH UNABATED GT + HRSG

Examples of heat matched retrofits proposed by CCS project developers include the following:

The Scottish CCS Consortium proposed a PCC retrofit for Longannet Power Station, the third largest coal-fired power station in Europe. The PCC Plant would have treated 50% of the flue gas from either Unit 2 or Unit 3. The captured and compressed CO_2 would have been transported along new and existing pipelines, injected and stored in the Goldeneye reservoir (DECC 2011). Due to the technical design of the steam turbines of the Longannet Power Station, the power plant could not provide thermal energy directly to the PCC process and an independent steam and power supply (SPS) was proposed to be used instead. This SPS consisted of two GT, two single pressure HRSG with supplementary firing and a back pressure steam turbine. An auxiliary boiler was proposed to be used to supply steam for peak demand and PCC plant start up. CO_2 capture from the SPS was not considered (Scottish PowerCCS Consortium 2011).

Unit 8 of the W.A. Parish Generating Station, a pulverised coal plant located in Thompsons, Texas, is, at the time of writing, being retrofitted with a PCC system (NETL 2013; Global CCS Institute 2014b). Amine stripping technology is used to remove CO_2 from a flue gas slipstream equivalent to 240 MW of the 610 MW PC power plant. The captured CO_2 is expected to be compressed, dried and transported to an operating oil field, the West Ranch oil field located in Jackson County, Texas, where it will be used for EOR operations and finally sequestered. A new 75 MW cogeneration plant comprised of a gas combustion turbine with a heat recovery generator, located on site, has been providing peaking power for the electric grid since June 2013. It is expected to supply the power and some of the thermal energy for the carbon capture and compression process when the capture plant is operational with the remaining power sold to the grid.

A recent study of configurations corresponding to heat matched carbon capture retrofits is reported by Deng et al. in 2014. It assessed a hybrid power plant configuration to simplify integration issues for PCC retrofit. A GT cogeneration unit supplied LP steam for regenerating the solvent. Capture from the additional fossil fuel source was not considered. (Deng et al. 2014). The performance of hybrid retrofit options with different types of GT (aeroderivative, E-class and F-class GT) combined with an HRSG were compared. In addition to the HRSG the F-class GT was also combined with a back pressure steam turbine (BP STG) but it is not clear if the design of the HRSGs included three pressure levels as seen by Bashadi (Bashadi 2010) or just one pressure level. Not surprisingly, the F-class GT + HRSG + BP STG case was reported to have a higher efficiency than the other cases.

In much of the literature on retrofits with gas turbine power cycles, no consideration has been given, so far, to reducing CO_2 emissions from the additional fuel used in the CHP unit.

The equivalent carbon intensity for the electricity produced from the natural gas used is then, at best, of the same order as electricity generation from a CCGT without capture, e.g. around 350 gCO_2/kWh, and considerably higher for ancillary boiler retrofits. These emissions cannot indefinitely be expected to be acceptable if there is a need to largely decarbonise power generation to system levels around 50 gCO_2/kWh, as is, for example, suggested by the UK Committee on Climate Change (CCC 2009).

6.3.- Relevant technical metrics:

In this thesis, two different metrics are used to analyse the technical performance of the different PCC retrofit options described in Chapter 6:

- Electricity output penalty
- Natural gas marginal efficiency.

Electricity output penalty

The Electricity Output Penalty (EOP) of capture and compression is a useful metric to indicate the overall energy requirement for CO_2 capture. For standard integrated retrofits the absolute loss of power output per tonne of CO_2 captured does not depend on the efficiency of the power plant (Lucquiaud & Gibbins 2011a).

For standard integrated retrofits where the fuel input stays the same with capture, it is defined as the sum of the loss of generator power output incurred by steam extraction and the power requirement for CO_2 compression and ancillary equipment divided by the absolute mass flow rate of CO_2 captured and compressed.

$$\mathrm{EOP} = \frac{\mathrm{Power\_Loss_{ST}} + \mathrm{Power_{Comp}} + \mathrm{Power_{Anc}}}{\mathrm{m_{CO\,2}}} \qquad [6.1]$$

Where:

EOP	=	Electricity Output Penalty $\left(\mathrm{kW \cdot hr}/_{\mathrm{tn}}\right)$
$Power\_Loss_{ST}$	=	Loss of power output incurred by steam extraction (kW)
$Power_{Comp}$	=	Loss of power output due to CO_2 compression (kW)
$Power_{Anc}$	=	Loss of power output due to ancillary equipment (kW)
m_{CO2}	=	Mass flow rate of CO_2 captured and compressed $\left(\mathrm{tn}/_{\mathrm{hr}}\right)$

With an additional fuel input to the site, i.e. a heat or power matched retrofit, the EOP of the PCC retrofit then needs to account for the net power generated by combustion of the additional fuel source and for the different levels of integration between the configurations.

The EOP then becomes the difference between the output of a carefully selected counterfactual plant and the total net power output of the retrofitted plant, divided by the amount of compressed CO_2 leaving the boundary of the plant, as in equation [6.2]. The total net power output includes the power generated by the existing steam cycle of the coal boiler, the gas turbines and, when applicable, the combined cycle attached to the gas turbines.

$$EOP = \frac{Power_{Counterfact} - Power_{w\ capture}}{m_{CO2}} \qquad [6.2]$$

Where:

$Power_{Counterfact}$ = Power output of the counterfactual power plant (kW)

$Power_{w\ capture}$ = Net power output of the site with CCS.

In a standard integrated retrofit, the counterfactual power plant is effectively the existing PC power plant before capture is added.

In PCC retrofits with an additional natural gas fuel source, the counterfactual power plant includes the existing pulverised coal power plant before capture is added and an unabated combined heat and power plant burning the same amount of natural gas at the same firing temperature as the gas turbine added to the site during the retrofit. The EOP then becomes:

$$EOP = \frac{Power_{w/o\ capture} + Power_{CHPPlant} - Power_{w\ capture}}{m_{CO2}} \qquad [6.3]$$

Where:

$Power_{w/o\ capture}$ = Net Power output of the site without capture (kW)

$\mathrm{Power}_{\mathrm{CHPPlant}}$ = Net Power output of an unabated combined heat and power plant with the same fuel input, firing temperature and efficiency as the gas turbine cycle added to the side (kW).

For power matched retrofits equation **[6.3]** can then be simplified to equation **[6.4]** since the net power output of the retrofitted plant is identical to the power output of the site.

$$EOP = \frac{Power_{CHPPlant}}{m_{CO2}} \qquad [6.4]$$

In the gas turbine windbox retrofit the expression of the power output of the counterfactual plant needs to consider the fact that the coal feed rate of the existing plant is reduced implies that a fraction of the energy available from the exhaust gas of the turbine is used to restore boiler steam production. Then, the EOP for the GT windbox retrofit becomes:

$$EOP = \frac{Power_{w/o\ capture\ \ reduced\ \ coal\ \ rate} + Power_{CHPPlant} - Power_{w\ capture}}{m_{CO2}} \quad [6.5]$$

Where:

$Power_{w/o\ capture\ \ reduced\ \ coal\ \ rate}$ = Net Power output of the site without capture at the reduced coal feed rate (kW)

Natural Gas Marginal Efficiency

Another important metric examines the maximum possible useful work for power regeneration recovered from the combustion of the additional fuel source, before heat is supplied to the PCC process. The marginal efficiency of the use of natural gas indicates the effectiveness of the additional gas consumption.

The power output generated by the combustion of natural gas is the difference between the power output of the retrofitted plant and the power output of the site if the coal power plant were fully retrofitted with the configuration of a standard integrated retrofit.

The marginal efficiency becomes:

$$Marg\_Eff = \frac{Power_{w\ capture} - Power_{SteamRetrofit}}{Input_{Nat\ Gas}} \quad [6.6]$$

Where:

Marg_Eff = Marginal efficiency of natural gas use (% point LHV)

$Input_{NatGas}$ = Fuel input to the gas turbine on a LHV basis (MWth)

$Power_{SteamRetrofit}$ = Power output of the site for a standard integrated retrofit (kW)

Since the existing steam cycle effectively acts as the combined cycle of the GT in the GT flue gas windbox retrofit, the expression of the marginal efficiency needs to reflect the fact that the power output of the generator of the coal plant is partially derived from the combustion of natural gas. For the GT flue gas windbox retrofit the marginal efficiency of natural gas becomes:

$$Marg\_Eff = \frac{\left(Power_{w\ capture} + Power_{HRSG\_Boiler}\right) - Power_{SteamRetrofit}}{Input_{NatGas}} \quad [6.7]$$

Where:

$Power_{HRSG\_Boiler}$ = Net Power generated by the steam produced in the HRSG and sent to the existing steam cycle (kW)

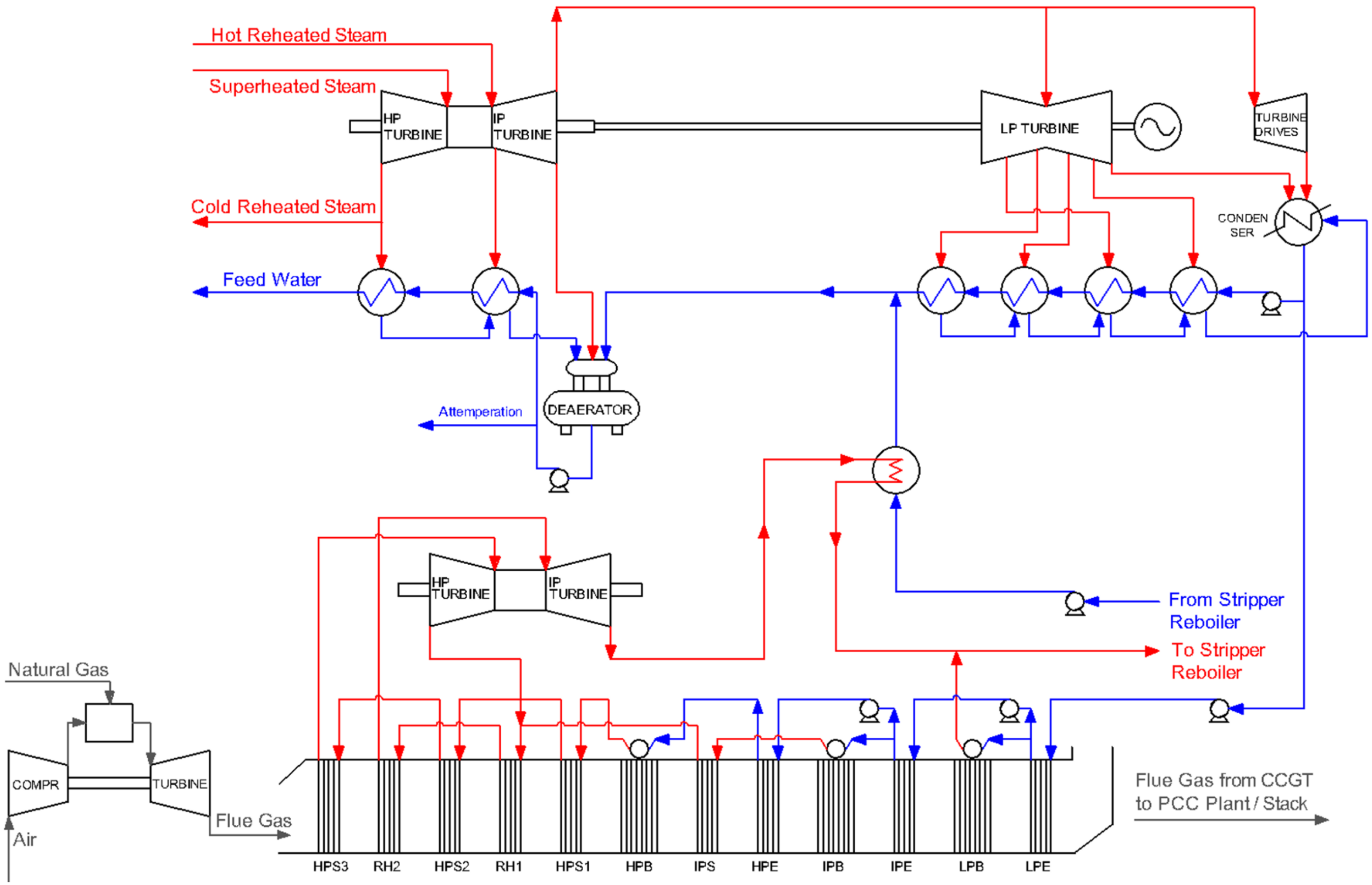

Figure 6.4.- Process flow diagram of a heat matched carbon capture retrofit with a combined cycle gas turbine providing all of the heat for CO_2 capture and power requirements from the combined cycle gas turbine (Case E1, E2 and E3).

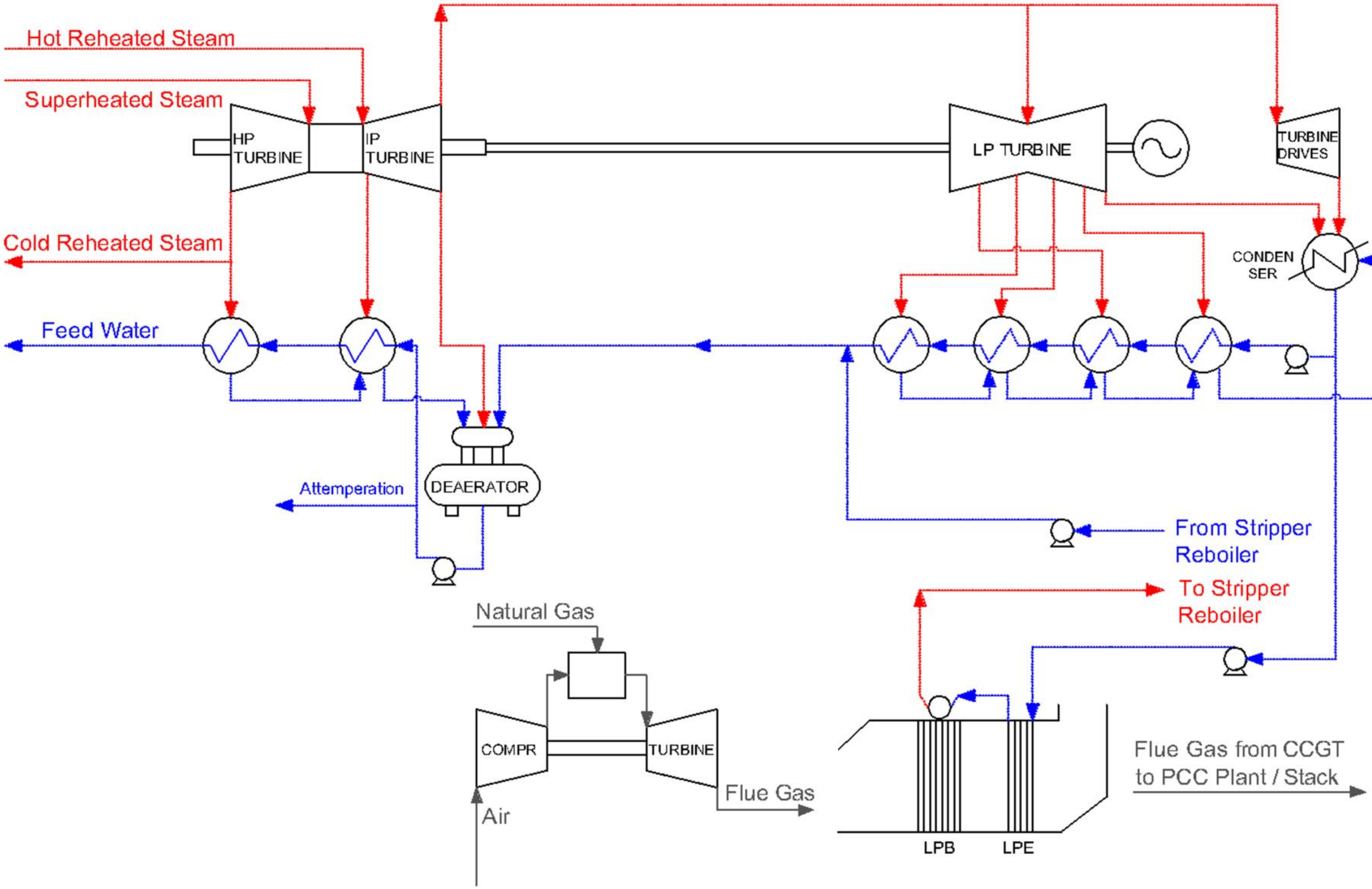

Figure 6.5.- Process flow diagram of a heat matched carbon capture with a gas turbine and a single pressure heat recovery steam generator providing all of the heat for CO_2 capture from the heat recovery steam generator and power requirements from the gas turbine (Case F1, F2 and F3).

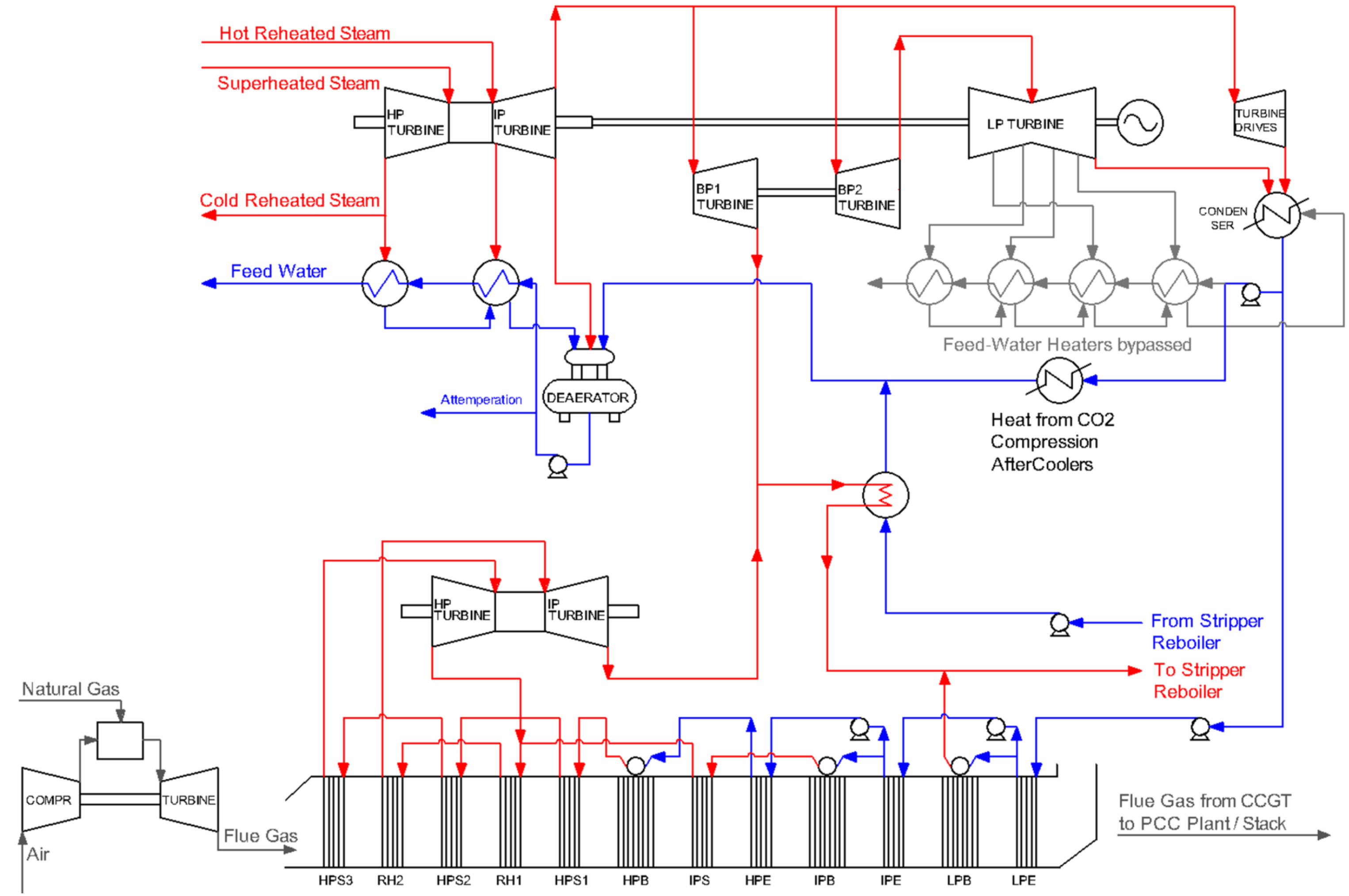

Figure 6.6.- Process flow diagram of a power matched carbon capture retrofit with a combined cycle gas turbine providing all of the heat for CO_2 capture and power requirements from both the combined cycle gas turbine and the main steam cycle (Case B1, B2, B3 and C1)

7.- TECHNO-ECONOMIC COMPARISON OF CARBON CAPTURE RETROFITS

This chapter presents a techno-economic comparison of the different post-combustion carbon capture (PCC) retrofit options discussed in previous chapters.

The primary purpose of this part of the study is to assess which trends in energy market and site-specific factors might be more favourable for the deployment of gas turbine flue gas windbox retrofit options.

As a secondary output a sensitivity analysis is performed on all the GT retrofit options, including with an Emission Performance Standard (EPS) to assess which, if any, have a possible competitive advantage under certain conditions. This takes previous work carried out in an IEAGHG study on retrofits from 2011 (IEAGHG 2011) to a more advanced level. It should be noted, however, that the relative performance of different retrofit options still depends on site-specific factors and should therefore be taken as illustratively representing general trends to provide further insights.

Models of the boiler, the steam cycle and the ancillaries of a pulverised coal plant and of a combined cycle gas turbine (CCGT) were developed in Mathcad and then validated by the process simulator Aspen Plus V8. Models of the CO_2 capture plant and the CO_2 compression system also use the process simulator Aspen Plus V8. The economic model is based on a spreadsheet where the total revenue requirement, defined as the revenue that makes the project break-even, is calculated by annualizing the total capital cost and levelising the total operating and maintenance costs and variable costs. This allows separate assessment of levelised cost of electricity and other revenues, e.g. those generated by the sales of CO_2 for EOR.

7.1.- Background of the economic analysis

In the UK the Energy Act 2013 established an Emissions Performance Standard (EPS) to limit CO_2 emissions from new fossil fuel power station to 450 g/kWh **(UK Parliament 2013)**. Similar approaches have also been proposed or implemented in other jurisdictions (e.g. California), and this is sometimes considered to be a ´natural gas emissions performance standard´ since is generally expected that a natural gas combined cycle power plant can meet this standard without using CCS.

In general, if the plant's annual emissions are below their EPS limit the plant will be compliant with the EPS, otherwise units will have to capture and store enough CO_2 to be compliant.

Although the EPS only applies in the UK to new fossil fuel power plants, the Electricity Market Reform (EMR) White Paper pointed out that existing plants with significant upgrades for life extension should also be subjected to the EPS (HM Government 2007).The repowering and retrofitting of an existing plant with a gas turbine cycle is considered in this study as a significant upgrade and the associated implications are examined in detail in the rest of this chapter.

As previously noted (Chapter 6), the proposed standard for new power plants issued by the US EPA has two compliance options at 1100 lbs CO_2/MWh or between 1000 and 1050 lbs CO_2/MWh, depending on whether CCS is implemented immediately after the power station starts operation or within the first seven years of operation (EPA 2014)

At the time of writing the EPA also proposed to establish state by state targets on the basis of the carbon intensity of electricity generation (lbs/MWh), based on estimates of national CO_2 emissions reductions in 2020 and 2030, which has obvious implications for existing coal plants at state level jurisdictions and the possibility of a retrofit with CCS.

There are different ways to face the problem of CO_2 emissions and meet the EPS in the power generation sector. If penalties for carbon emissions are high and some value can be obtained from the existing power plant, the following two options are recommended:

- Upgrade the power plant to be able to operate with a different fuel. Replace part or all of the existing coal by a lower carbon emissions fuel, like natural gas or biomass.
- Retrofit the power plant with CCS

CCS retrofits are predicted to happen if carbon emission costs rise up to a value close to the long run marginal costs of the retrofitted plant. In that way, the implementation of CCS would reduce some components of the operating costs and would contribute somewhat to paying off the capital costs.

If the existing power plant has reached the end of its operating life the only alternative would be to shut down the power plant. If the available power is still needed in the electricity network an investor has two options:

- Shut down the plant and build a new one that operates with a low carbon emission fuel, such as natural gas or biomass.

- Shut down the plant and build a new one with CCS.

If it were required to comply with a natural gas emissions performance standard the coal power plant could be upgraded to burn biomass or natural gas but if the reduction of CO_2 emission were even stricter than the implementation of CCS would be the best alternative. Furthermore, the options of retrofitting or building a new plant with lower carbon emission fuels highly depend on the alternative fuel price, which can fluctuate considerably.

7.2.- Economic modelling approach

This section describes the methodology implemented to study the economics of the different carbon capture retrofit projects.

It should be noted that the same site is assumed to be used for the different retrofit options so that all the cases take the same advantages of re-using existing grid connections, water supplies and coal or gas delivery facilities (which are all assumed to be available with sufficient capacity for all cases). Furthermore, it has been supposed that there is enough space for additional equipment associated to the integration of the carbon capture plant and adequate access to a viable geological CO_2 storage site.

7.2.1.- Capital expenditures and operational expenditures

7.2.1.1.- Equipment costs

Equipment costs are approximated by 2007 values taken from “Cost and Performance Baseline for Fossil Energy Plants” report (DOE/NETL 2013). Nevertheless, plant construction costs have fluctuated considerably in recent years and this uncertainty is even higher for carbon capture equipment due to lack of experience with large-scale projects. This uncertainty is considered further in the sensitivity analysis in Section 7.4.

The capital cost items are aggregated in five different levels, following the nomenclature of the DOE/NETL (2013) report:

- The Bare Erected Cost (BEC) includes the cost of process equipment, supporting facilities and direct and indirect labour required for its construction and installation.
- The Engineering, Procurement, and Construction Cost (EPCC) comprises the BEC and additional fees for the services provided by the engineering, procurement and construction contractor.
- The Total Plant Cost (TPC) includes the EPCC and the project and process contingencies. The contingencies try to quantify the additional capital costs that will

likely arise as a process design matures into a full-scale commercial plant. Additionally, the project contingencies try to estimate the capital costs that would arise if project needed to be identified in a more detailed design. The following table provides the guidelines for process and project contingency costs (DOE/NETL 2013):

Table 7.1.- Project and Process Contingencies (DOE/NETL 2013)

	Contingencies	
	Project	**Process**
Coal Power Plant	14%	0%
Coal Power Plant with CCS	16%	5%
CCGT	13%	0%
CCGT with CCS	17%	7%

- The Total Overnight Capital (TOC): comprises the TPC plus all other overnight costs, including owner's costs. *Table 7.2* enumerates the owner's costs considered in this project (DOE/NETL 2013).

Table 7.2.- Owner's Costs

Owner's Costs		
Preproduction Costs	**Inventory Capital**	**Others**
- 6 Months All Labour	- 60 day supply of consumables at 100% CF	- Initial Cost for Catalyst and Chemicals
- 1 Month Maintenance Materials	- 0.5% of TPC (spare parts)	- Land
- 1 Month Non-fuel Consumables		- Other Owner's Costs
- 1 Month Waste Disposal		
- 25% of 1 Months Fuel Cost at 100% CF		
- 2% of TPC		

- The Total As-Spent Capital (TASC): consists of the TOC, cost's escalation and the interest on debt incurred during the capital expenditure period.

The capital costs of the carbon capture and compression plant are calculated by subtracting the TOC costs of the power plant without CCS from the TOC costs for the plant with CCS.

It is assumed, in this study, that the existing plant has paid off its original capital investment. The capital cost of the retrofitted coal power plant only involves the costs of the provision of two new back pressure steam turbines added to the existing power cycle to supply the steam at the required conditions for CO_2 capture and reduce the impact of CO_2 capture on power plant efficiency and power output, as shown in Figure 4.6, Figure 6.2 and figure 6.6.

As an example of the capital costs considered in this study, Table 7.3 shows the capital costs of a standard integrated retrofit (Case A1 of Table 6.1) and a power matched retrofit with an abated CCGT (Case B1 of Table 6.1).

7.2.1.2.- Operating and maintenance costs

The operating costs and related maintenance costs belong to the expenses related to the power plant operation and maintenance over its expected life. These costs are classified in two categories, variable O&M costs which depend on the power generation (e.g. consumables, waste disposal, co-products…) and fixed O&M costs which are constant and expressed as a percentage of the TPC (e.g. operating labour, administrative and support labour).

As an example of the fixed and variable O&M costs considered in this study, Table 7.5 shows the O&M costs of a standard integrated retrofit (Case A1 of Table 6.1) and a power matched retrofit with an abated CCGT (Case B1 of Table 6.1).

7.2.1.3.- Fuel costs

Fossil fuel prices have experienced significant variations in the last few years. For example, the U.S. Energy Information Administration (EIA) reports the changes in natural gas spot prices set at Henry Hub natural gas distributor , as indicated in *Figure 7.1* (EIA 2015b).

Table 7.3.-Illustrative Capital Cost of PCC retrofits

		DOE/NETL (2013)	Standard integrated retrofit	Retrofit with CCGT
Total Plant Costs				
Steam turbine costs	$	114 005	16 581.9	16 581.9
Steam turbine size	MW	550.02	80.0	80.0
Costs of PCC Plant added to coal plant	$	492 819	341 896.5	341 896.5
Sieze of PCC Plant added to coal plant	tn CO_2 /hr	596	413.5	413.5
CCGT Cost	$	324 365	0.0	79 078.9
CCGT Size	MW th	1 105.8	0.0	269.6
Costs of PCC Plant added to CCGT	$	24 0335	0.0	58.4
Size of PCC Plant added to CCGT	tn CO_2 /hr	182 170	0.0	44.3
TPC	**$**		**358 478.5**	**437 615.8**
Total Overnight Costs				
Owner's Costs	$	367075	367 075.0	367 075.0
TOC	**$**		**725 553.5**	**804 690.8**
Total As Spent Cost				
Escalation and Interest	Multiplier	1.14	1.14	1.14
TASC	$		**827 131**	**917 347**

Table 7.4.-O&M Costs

		DOE/NETL (2013)	Standard integrated retrofit	Retrofit with CCGT
Fixed O&M Costs				
Fixed Costs of Coal Plant	$	32056744	32056744	32056744
Fixed Costs of PCC Plant added to coal plant	%	4.34%	4.34%	4.34%
Fixed Costs of CCGT	%	3.78%	0.00%	3.78%
Fixed Costs of CCGT added to coal plant	%	3.20%	0.00%	3.20%
Variable O&M Costs				
Power output of the retrofitted site	MW	600	474	600
Variable Costs of Coal Plant	$/MWh	5.15	6.51	5.15
Variable Costs of PCC Plant added to coal plant	$/tn CO_2	1.78	1.78	1.78
Variable Costs of CCGT	$/MWh th	0.66	0.00	0.66
Variable Costs of CCGT added to coal plant	$/tn CO_2	2.66	0.00	2.66

As the results of any economic analysis very much depend on fossil fuel prices two scenarios have been evaluated: a European scenario considering UK fossil fuel prices (Government 2015) and the American one considering a North American one, considering US fossil fuel prices (EIA 2015a).

Table 7.5 shows the economic parameters assumed in this work. These are based on average cost of fuel delivered for electricity generation in 2014 (Government 2015; EIA 2015a).

***Table 7.5.**-Fossil Fuel Costs*

		Fossil Fuel Costs	
		UK	**US**
Coal	$/MWh th	12.24	8.09
Natural Gas	$/MWh th	34.18	16.5

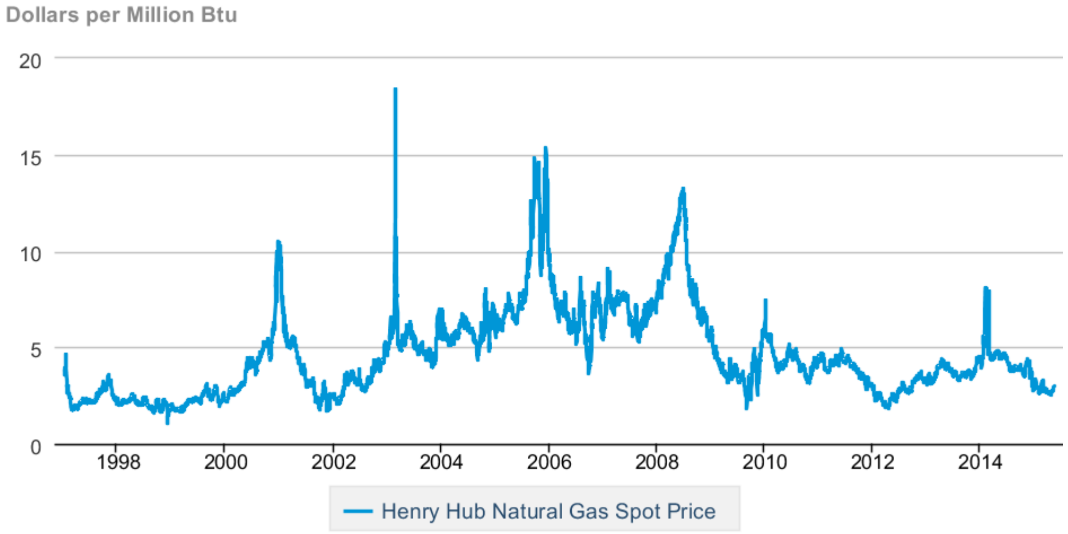

Figure 7.1.- Henry Hub Natural Gas Spot Price (EIA 2015b).

7.2.1.4.- Other variable costs

Other variable costs are related to the operation of the plant and involve carbon charge and CO_2 transport and storage costs.

The carbon price is usually associated with the carbon price support (CPS) rate. The carbon price is not considered in the financial model; the cost of CO_2 avoided is calculated instead and is compared with the current maximum CPS rate.

The CO_2 transport and storage cost are also treated as variable operating costs assuming that other companies will build and operate the transport and storage facilities and will charge the power plant a fee for the service. It has been assumed to be $10/t CO_2 (IEAGHG 2011).

7.2.2.- Finance structure

The finance structure assumption is based on the DOE/NETL (2013) report for comparability of results.

For this study the owner/developer is assumed to be an investor-owned utility (IOU).

The project is financed with a debt/equity finance structure. This type of finance structure involves the sale of bonds/stocks to pay off the total capital of investment. The amount of money that the company must pay back to its investors is called return on debt and equity and is calculated with equation [7.1] and [7.2] respectively.

$$B = (1 + ei) \cdot (1 + B_r) - 1 \qquad [7.1]$$

Where:

B	=	Rate of return for bonds in current dollars (fraction).
ei	=	Inflation rate (fraction)
B_r	=	Rate of return for bonds in constant dollars (fraction).

$$S = (1 + ei) \cdot (1 + S_r) - 1 \qquad [7.2]$$

Where:

S	=	Rate of return for stock in current dollars (fraction).
S_r	=	Rate of return for stock in constant dollars (fraction).

Table 7.6 shows that the rate of return from bonds and stock in current dollars is assumed to be 5.5% and 12% respectively.

The return on investment is then calculated with the weighted average of the return on debt and equity, with the fraction of bonds/stock included in the finance structure also following DOE/NETL 2013 for the illustrative example considered here.

$$r = B \cdot B_f + S \cdot S_f \qquad [7.3]$$

Where:

r	=	Return on investment. It is equal to 9.075 %
B_f	=	Fraction of bonds. It is equal to 45% (from *Table 7.6*)
S_f	=	Fraction of stock. It is equal to 55% (from *Table 7.6*)

Table 7.6.- Risk profile of the projects (DOE/NETL 2013)

Type of security	% of Total	Current (Nominal Dollar Cost	Weighted Current (Nominal) Cost
High Risk			
Debt	45.0%	5.5%	2.475%
Equity	55.0%	12.0%	6.600%
Total			9.075%

Another important concept in the financial structure is booking depreciation. During each accounting period a portion of the cost of the assets is being used and needs to be reported as an annual charge. The method of depreciating assets proposed in this financial study is the straight-line method and is calculated as follows.

$$D_b = \frac{1}{t_{op}} \tag{7.4}$$

Where:

D_b = Book depreciation (fraction).

t_{op} = Operating period (years)

In order to take into account the interest during construction, a 3.6% escalation rate during the capital expenditure period is assumed.

Table 7.7.- Finance structure. Treatment of capital costs (DOE/NETL 2013)

FINANCE STRUCTURE		
ANALYSIS TIME PERIODS		
Capital Expenditure Period	Years	5 years
Operational Period	Years	30 years
TREATMENT OF CAPITAL COSTS		
Capital Cost Escalation During Capital Expenditure Period (nominal annual rate)	%	3.6%
% of Total Overnight Capital that is Depreciated	%	100%

The income tax of the finance structure consists of state and federal taxes. As the state taxes are deductible for federal tax purposes the income tax can be computed as follows.

$$t = t_s + (1 - t_s) \cdot t_f \qquad [7.5]$$

Where:

t	=	Effective income tax rate (fraction).
t_s	=	State tax rate (fraction)
t_f	=	Federal tax rate (fraction).

The finance structure of the project indicates that the state tax rate is 6% and the federal tax rate 34%. The effective income tax rate can then be computed by solving equation **[7.5]**.

In the context of North America where the cost methodology is applied, it is important to distinguish between current income tax and deferred income tax. The current income tax is the amount of income tax payable for the current period based on project's taxable profit (income minus deductible expenses) and the deferred income is the amount of tax payable in the future period as a result of past transactions.

Tax laws allow the company to accelerate the depreciation expenses in order to take more depreciation expenses in the first few years and less in the later years of the asset's life. This saves income tax payments in the first years but results in more taxes in the later years. The accelerated depreciation schedule, $D_{s,n}$, used for tax purpose is a 150% declining balance method over 20 years, as indicated in *Table 7.8*.

The deferred income tax is then computed as the difference between the accelerated depreciation and the book depreciation.

$$t_{d,n} = \left(D_{s,n} - \frac{1}{t_{op}} \right) \cdot t \qquad \textbf{[7.78]}$$

Where:

$t_{d,n}$	=	Deferred income tax per year (fraction).
$D_{s,n}$	=	Depreciation schedule per year for tax purpose (fraction)
n	=	from 1 to t_{op}

Table 7.8.- Finance structure. Income taxes (DOE/NETL 2013)

FINANCE STRUCTURE			
TAXES			
Income Tax Rate	%	38%	
State taxes	%	6%	
Federal taxes	%	34%	
Capital Depreciation	%	150%	20 years, 150% declining balance

In order to take into account the inflation during the operational period, a 3.0% inflation rate is assumed.

Table 7.9.- Finance structure. Escalation of operating revenues and costs (DOE/NETL 2013)

FINANCE STRUCTURE		
ESCALATION OF OPERATING REVENUES AND COSTS		
Escalation of COE (revenue), O&M Costs, Fuel Costs (nominal annual rate)	%	3.0%

7.2.3.- Financial modelling: total revenue requirement

The financial modelling uses an Excel-spreadsheet where the total revenue requirement is calculated by annualising the total capital cost and levelising the total operating and maintenance costs, fuel costs and variable costs. It is based on the methodology presented in the Electric Power Research Institute (EPRI) Technical Assessment Guide (EPRI 1986; EPRI 1987b) and used by Rubin et al in the report 'Modeling of Integrated Environmental Control System s for Coal-Fired Power Plants' (Rubin et al. 1991)

7.2.3.1.- Annualised total capital cost

The annualisation algorithm is used to convert the total required plant investment into a uniform annual payment for each year of the operational period of the project. It consists of three different steps.

<u>First step:</u> the calculation of the total carrying charges related to the capital investment. This consists of book depreciation, deferred taxes, return on investment and income taxes.

The return on debt and equity are based on the remaining balance on the initial investment which is calculated by subtracting the book depreciation and the deferred income tax per year from the initial investment:

$$RB_n = RB_{n-1} - D_b - t_{d,n-1} \qquad [7.7]$$

Where:

RB_n = Remaining balance per year (fraction).

For year 1, the remaining balance would be 1 ($RB_1 = 1$) which multiplied by the capital cost corresponds to the initial investment.

The return on debt is estimated with equation [7.8]:

$$RD_n = RB_n \cdot B \cdot B_f \qquad [7.8]$$

Where:

RD_n = Return on debt per year (fraction).

And the return on equity with equation [7.9]:

$$RE_n = RB_n \cdot S \cdot S_f \qquad [7.9]$$

Where:

RE_n = Return on equity per year (fraction).

The taxes paid per year are estimated as follows:

$$t_{p,n} = \frac{t}{1-t} \cdot \left(D_b - D_{s,n} + t_{d,n} + RE_n\right) \qquad [7.10]$$

Where:

$t_{p,n}$ = Taxes paid per year (fraction).

Then the carrying charges per year are computed as the sum of the book depreciation, deferred taxes, return on debt, return on equity and income taxes paid.

$$CC_n = D_b + t_{d,n} + RD_n + RE_n + t_{p,n} \qquad [7.11]$$

Where:

CC_n = Carry charges per year (fraction).

Second step: calculation of the present value of the future carrying charges. The present value of the future carrying charges for each year is achieved by discounting the future value of each cash flow.

$$CC_{pv} = \sum_{n=1}^{t_{op}} \frac{CC_n}{(1+r)^n} \qquad [7.12]$$

Where:

CC_{pv} = Present value of future carrying charges.

r = Discount rate.

t_{op} = Operational period.

The discount rate used in this study corresponds to a 'before tax discount rate' and is equal to the return of investment of equation [7.3].

Third step: calculation of the annualised carrying charge. This is computed multiplying the capital recovery factor by the present value of the future carrying charges.

The capital recovery factor converts a present value into a stream of equal annual payments over a specified time, at a specified discount rate. The expression of the capital recovery factor is:

$$CRF = \frac{(1+r)^{t_{op}} \cdot r}{(1+r)^{t_{op}} - 1} \qquad [7.13]$$

Where:

CRF = Capital Recovery Factor.

The annualised carrying charge is known as 'fixed charge factor' and is determined with equation [7.14].

$$FCF = CC_l = CC_{pv} \cdot CRF \qquad [7.14]$$

Where:

FCF = Fixed charge factor.

CC_l = Annualised carrying charge.

The fixed charge factor for 30 years of operational period is 0.11

7.2.3.2.- Levelised total variable cost

The total variable costs vary from year to year due to inflation. The levelisation algorithm converts these future expenses into an uniform annual payment for the operational period of the project.

The expenses charges are related to the operation of the plant and consist of operating and maintenance costs, fuel costs and CO_2 transport and storage costs.

The levelisation factor is calculated as follows:

$$L_{t_{op}} = \frac{k \cdot (1-k^{t_{op}})}{(1-k)} \cdot CRF \qquad [7.15]$$

Where:

$L_{t_{op}}$ = Levelisation factor.

And k is calculated using the following expression:

$$k = \frac{1 + ei}{1 + r} \qquad [7.16]$$

Where:

ei = Inflation rate.

Considering an inflation rate of 3.0% and 30 years of operational period, as indicated in Table 7.9, the levelisation factor is 1.36.

7.2.3.3.- Levelised construction costs

The amount of money spent during construction (total cash expended, TCE) is calculated by de-escalating the TOC back in time assuming that expenses were spent uniformly at the middle of each year of the capital expenditure period.

$$TCE = \frac{TOC}{N} \cdot \sum_{j=1}^{j=N} \frac{1}{(1 + e_r)^{j-0.5}} \qquad [7.17]$$

Where:

TCE = Total Cash Expended.

N = Capital expenditure period (years)

e_r = Escalation rate of capital cost during construction (fraction)

TASC takes into account the return on debt incurred during the capital expenditure period and it is estimated at the same the discount rate of equation [7.3]:

$$TASC = \frac{TOC}{t_{ex}} \cdot \sum_{j=1}^{t_{ex}} \frac{(1 + r)^{j-0.5}}{(1 + i)^{j-0.5}} \qquad [7.18]$$

Where:

$TASC$ = Total As Spent Costs

t_{ex} = Expenditure period

The levelisation factor during the expenditure period is found using the following expression:

$$L_{t_{ex}} = \frac{1}{t_{ex}} \cdot \sum_{j=1}^{t_{ex}} \frac{(1 + r)^{j-0.5}}{(1 + i)^{j-0.5}} \qquad [7.19]$$

Considering an escalation rate of 3.6% and 5 years of expenditure period, as indicated in *Table 7.7*, the levelisation factor is 1.14.

7.2.3.4.- Total revenue requirement

Once the fixed charge factor and the levelisation factors are calculated the total revenue requirement can then be analysed.

$$TRR = TOC \cdot FCF \cdot L_{t_{ex}} + (O\&M + Fuel + TSC) \cdot L_{t_{op}} \qquad [7.20]$$

Where:

TRR	=	Total revenue requirement ($)
$O\&M$	=	Operating and Maintenance costs ($).
Fuel	=	Fuel costs ($).
TSC	=	CO_2 transport and Storage costs ($).

7.2.3.5.- Year by year revenue requirement analysis

A year by year revenue requirement analysis is also studied to show the revenue requirement in current dollars over the operating life of the plant.

Total overnight costs:

$$TOC_n = \left(TOC \cdot L_{t_{ex}}\right) \cdot CC_n \qquad [7.21]$$

Total variable costs:

$$TVC_n = (O\&M + Fuel + TSC) \cdot (1 + ei)^n \qquad [7.22]$$

Total revenue requirement:

$$TRR_n = \left(TOC \cdot L_{t_{ex}}\right) \cdot CC_n + (O\&M + Fuel + TSC) \cdot (1 + ei)^n \qquad [7.23]$$

7.3.- Results of the techno-economic analysis

7.3.1.- Relevant metrics:

The economic metrics used to analyse the revenue of the different PCC retrofit options described in Chapter 6 are:

- Equivalent Levelised Cost Of Electricity (LCOE) for the different CCS retrofits.
- Internal Rate of Return (IRR) for the different CCS retrofits.
- Cost of CO_2 avoided relative to the original plant
- Cost of CO_2 captured

7.3.1.1.- Levelised cost of electricity

The LCOE is defined as "the uniform annual cost that produces the same net present value (NPV) as a stream of variable year-to-year costs over a specified plant life" (Rubin 2012). It is related to the amount of uniform revenue that a power plant must generate from the sale of electricity so as to pay off the total capital cost and fully recover the operating costs while earning a specified rate of return over the plant life.

The following expression is used to determine the LCOE when the price of electricity and the rate on return are assumed constant:

$$\sum_t \frac{(P_{site})_t \cdot LCOE}{(1+r)^t} = \sum_t \frac{(TOC)_t}{(1+r)^t} + \sum_t \frac{(O\&M)_t}{(1+r)^t} + \sum_t \frac{(Fuel)_t}{(1+r)^t} + \sum_t \frac{(TSC)_t}{(1+r)^t} \quad [7.24]$$

Where:

LCOE	=	Levelised Cost of Electricity $\left(\$/_{\text{MWhr}}\right)$
P_{site}	=	Power output of the retrofitted site (MWh)
$O\&M$	=	Operating and Maintenance costs ($).
Fuel	=	Fuel costs ($).
TSC	=	CO_2 transport and Storage costs ($).

Section 7.2 described the financial modelling used to calculate the annual cost to operate the plant. This total cost was defined as 'total revenue requirement' (TRR) as it is the revenue that makes the project break-even. The TRR was estimated by levelising the total expenses and annualising the total plant investment. The TRR corresponds to the left hand side of the equation **[7.24]**. Combining equation **[7.24]** with equation **[7.23]** we get the following expression:

$$\sum_t \frac{(P_{site})_t \cdot LCOE}{(1+r)^t} = TOC \cdot FCF \cdot L_{t_{ex}} + (O\&M + Fuel + TSC) \cdot L_{t_{op}} \quad [7.25]$$

Considering the net power output of the retrofitted site constant for the indicative analysis being undertaken in this study, the equation can be re-written as follows:

$$LCOE = \frac{TOC \cdot FCF \cdot L_{t_{ex}} + FOM \cdot L_{t_{op}}}{LF * 365 * 24 \cdot P_{site}} + \left(VOM + FC \cdot \frac{HHV}{P_{site}} + CO_2TS \cdot \frac{F_{CO2Capt}}{P_{site}}\right) \cdot L_{t_{op}} \quad [7.26]$$

Where:

LF	=	Load Factor (%)

FOM = Fixed Operating and Maintenance costs $\left({}^{\$}/_{\mathrm{year}}\right)$.

VOM = Variable Operating and Maintenance costs $\left({}^{\$}/_{\mathrm{MWhr}}\right)$.

FC = Fuel costs $\left({}^{\$}/_{\mathrm{MWth\_hr}}\right)$.

CO_2TS = CO_2 transport and Storage costs ($/t CO_2).

HHV = Fuel high heat value (MWth).

In some studies the LCOE is estimated at constant dollar and the following expression is used instead:

$$LCOE = \frac{TOC \cdot FCF + FOM}{LF * 365 * 24 \cdot P_{site}} + VOM + FC \cdot \frac{HHV}{P_{site}} + CO_2TS \cdot \frac{F_{CO2Capt}}{P_{site}} \qquad [7.27]$$

In this work equation **[7.26]** is used to evaluate the LCOE . Although real power plant output is, of course, variable, the LCOE is used here as a standard form of analysis to inform investment decisions, ignoring the specific characteristics of the generation portfolio of electricity markets.

The results of the LCOE analysis indicates which CCS retrofit option would generate more revenue and can be interpreted as informing decisions for the illustrative investor-owned utility of this study to choose an appropriate way to generate electricity as cost efficiently as possible. It is important to note, however, that electricity generation costs cannot be estimated with 100% certainty, and the estimates given here cannot, for example, reliably predict possible future EMR strike prices.

LCOE is typically calculated using the expression given in equation **[7.26]**. It is important to note, however, that this approach can tend to overestimate the impact of changes in load factor on power plant profitability. A year by year revenue requirement analysis (see section 7.2.3) could incorporate a different load factor per year and could give a better estimation of the revenue requirement per year over the operating life of the plant.

In this work, the impact of load factor change is considered using a method developed in IEAGHG (2011), where appropriate. When the short run marginal cost (SRMC) for generation is higher than the electricity price, retrofitted plants are constrained off the grid. Consequently, a PCC retrofitted plant with a lower SRMC would be able to operate at lower electricity prices and an increased load factor. The revenue associated with these additional operating hours is, however, limited to the difference between the SRMC of the two options that are being compared.

In order to take into account the revenue obtained during this period in the calculation of the LCOE (and particularly the comparison of LCOE for different options), the following procedure was developed in IEAGHG (2011):

The LCOE is computed for the different PCC retrofit cases at the lowest retrofit load factor.

The maximum revenue that can be obtained by the PCC retrofit with the lowest SRMC is calculated by multiplying the SRMC difference by the difference in the number of hours when both plants are operating, equation **[7.28]**.

$$\mathrm{Revenue_{LF}} = (\mathrm{SRMC_A} - \mathrm{SRMC_B}) \cdot \frac{\mathrm{LF_B} - \mathrm{LF_A}}{\mathrm{LF_A}} \qquad [7.28]$$

Where:

$\mathrm{Revenue_{LF}}$	=	Revenue due to a higher load factor $\left(\$/_{\mathrm{MWhr}}\right)$
SRMC	=	Short Run Marginal Cost $\left(\$/_{\mathrm{MWhr}}\right)$

An 'equivalent LCOE' is then calculated for the plant with the higher load factor

$$\mathrm{LCOE_{LF}} = \mathrm{LCOE_0} - \mathrm{Revenue_{LF}} \qquad [7.29]$$

7.3.1.2.- ***Internal rate of return***

The IRR is defined as the discount rate that makes the NPV of all cash flows from a particular project equal to zero.

Considering the net power output exported from the retrofitted site is constant for the indicative analysis being undertaken in this study, the NPV of all cash flows is:

$$NPV = e \cdot \frac{P_{Exported}}{P_{site}} - \mathrm{LCOE} \qquad [7.30]$$

Where:

e	=	Electricity selling price $\left(\$/_{\mathrm{MWhr}}\right)$
P_{Exported}	=	Power exported from the site (MWh)

For illustrative purpose, the cases reported in this thesis assume that the electricity sales revenues meet, at least, the LCOE of the most expensive CCS retrofit project in order to assure that the investment on the most expensive CCS retrofit option reaches its required hurdle rate.

Then the IRR is computed by equalling equation [7.30] to zero. The discount rate of equation [7.30] corresponds now to the IRR.

In order to avoid losses from an investment the IRR must be at least equal to the discount rate of that specific project. Investors may also set a higher 'hurdle rate' that the IRR must be at least equal to for the project to proceed.

7.3.1.3.- Cost of CO_2 avoided

The cost of CO_2 avoided quantifies the average cost of reducing CO_2 emissions. It is calculated by comparing the costs and emissions of the new CHP and retrofitted coal plant with CO_2 capture versus the costs and emissions of the existing plant without CO_2 capture (IEAGHG 2011):

$$CO2AV = \frac{LCOE_{w\ CCS} - LCOE_{w/o\ CCS}}{F_{CO2Emit\_w/o\ CCS} - F_{CO2Emit\_w\ CCS}} \cdot \frac{1}{L_{t_{op}}} \qquad [7.31]$$

Where:

CO2AV = Cost of CO_2 avoided $\left(\$/_{\text{kgCO2}}\right)$

$F_{CO2Emit}$ = Specific emissions of CO_2 $\left(^{\text{kg}}/_{\text{MWhr}}\right)$

The cost of CO_2 avoided represents the carbon tax at which the LCOE of the existing plant equals that of the plant with CCS.

7.3.1.4.- Cost of CO_2 captured

The cost of CO_2 captured quantifies the average costs of capturing CO_2. The costs of CO_2 transport and storage are discounted in this metric.

$$CO2CAP = \frac{\left(LCOE_{w\ CCS} - CO_2TS \cdot F_{CO2Capt}\right) - LCOE_{w/o\ CCS} \cdot L_{t_{op}}}{F_{CO2Capt}} \cdot \frac{1}{L_{t_{op}}} \qquad [7.32]$$

Where:

CO2CAP = Cost of CO2 captured $\left(\$/_{\text{kgCO2}}\right)$

$F_{CO2Capt}$ = Total mass of CO2 captured per MWh for the plant with capture $\left(^{\text{kg}}/_{\text{MWhr}}\right)$.

Additionally, this parameter could also give an idea of the minimum CO_2 selling price if CO_2 could be sold to an enhanced oil recovery (EOR) operator or other user of CO_2 to cover the cost of capture. CO_2 EOR could be particularly useful during early commercialization when cost of capture is still high, but experience in commercial projects is needed to help to reduce costs of capture (Global CCS Institute 2012).

7.3.2.- Results for options achieving high levels of CO_2 capture

7.3.2.1.- Technical analysis of retrofit options with high levels of CO_2 capture:

Table 7.10 shows the results of the different high level CO_2 capture retrofit options discussed in previous chapters.

<u>Standard integrated retrofit (Case A1):</u>

The best possible scenario for thermodynamic integration is considered in this work, with two back pressure turbines added to the existing steam cycle, and, thus, the electricity output of the retro-fitted site is reduced by 20% and the thermal efficiency drops by 8 percentage points. This efficiency penalty is very close to a retrofitted capture ready plant or a new built plant with capture. It is important that this level of integration may not necessarily be always achievable if general access, extraction from the existing turbines or space is a limiting factor.

<u>Gas turbine power matched retrofits:</u>

For existing plants, the amount of gas and the size of the gas turbine combined cycle depend on a range of factors: coal composition, steam cycle configuration, solvent energy of regeneration etc. Although the analysis here is conducted for a single reference plant, with the objective of a power matching, the results would vary from site to site.

The EOP predominantly depends on the reboiler duty and the CO_2 compression power. The reboiler duty is strongly dependent on the CO_2 concentration of the flue gas entering the carbon capture plant, as discussed in Chapter 2. This is one of the main reasons why the EOP of a new CCGT with PCC is always higher than that of a coal power plants with PCC, as indicated in Table 7.9. The other important factor is the ancillary power for flue gas blower, which is proportionally higher per unit of CO2 captured for natural gas flue gas than for coal.

The EOP of the counterfactual CCGT with PPC achieving high levels of CO_2 capture is around 430 kWh / tCO_2 for the post-combustion capture process modelled in this study. The counterfactual CCGT plant with PCC is provided as a reference point to compare the EOP of a new-build NGCC plant with capture. It is important to note that this case does not use the best in class gas turbine available, 60-61% LHV thermal efficiency, but the equivalent CCGT with the off the shelf gas turbine used in this study (PG 7251 FB) with a lower thermal efficiency of 53.6% for the corresponding CCGT, due to its size. It only has a marginal effect on the value of the EOP, since it is largely independent of plant efficiency.

The table shows that for power matched retrofits, the EOP of a coal power plant retrofitted with a CCGT and PCC is consistently lower than that of a CCGT, and within approximately 5% of EOP of the integrated retrofit.

For all gas turbine power cycle retrofits the natural gas calorific value is utilised as effectively as practically possible, as suggested in the rules for thermodynamic integration of the PCC plant with the power cycle (Gibbins et al. 2004; Lucquiaud 2010), to produce power in the gas turbine and high temperature high pressure steam to generate extra power in the steam turbines of the combined cycle.

The high natural gas marginal efficiency indicates a very effective use of the natural gas, an important fraction of the calorific value of the natural gas is recovered as power.

It should be noted that the EOP of heat matched retrofits (e.g. Case E1 reaches 424 kWh / tCO_2) are close to the EOP of the CCGT with PCC due to the large amount of natural gas used to match the thermal heat requirements of the PCC process. The molar concentration of CO_2 at the inlet of the PCC plant is 5% similar to that of a new CCGT (~4%).

For the GT windbox retrofit the CO_2 concentration reaches 12.6% v/v, in comparison to 4.0% v/v at the exhaust gas of the turbine and 13.6%% v/v for the coal plant with air-firing. Consequently, there is a benefit on the reboiler duty since the CO_2 concentration is closer to that of coal plant, as opposed to capturing from two streams at respectively 13.6% v/v and 4.0% v/v. With the reduction in the coal feed rate, the fraction of the energy available from the exhaust gas of the turbine is used to restore boiler steam production, as explained in equation [6.5].

Comparing capture retrofit options where CO_2 from both fuel sources are treated in the same capture plant, Case C1 for a power matched retrofit and Case E1 for a heat matched retrofit, the power matched retrofit reaches a lower EOP due to the lower reboiler duty, and de facto a higher natural gas marginal efficiency.

Comparing the EOP and the natural gas marginal efficiency of the power matched retrofits achieving high levels of CO_2 capture, Case B1, Case C1 and Case D1 from Table 7.9, the GT windbox retrofit (Case D1) reaches the lowest EOP and the highest marginal efficiency due to the following reasons:

- The lower flow rate entering the capture plant results in a lower power consumption of the flue gas blowers.
- The HP and IP steam generated by the HRSG is fed to existing Rankine cycle, with feedwater heating increasing efficiency and the mechanical work extracted per unit of steam, compared to the combined cycle of other GT configurations without feedwater heating.
- The heat addition from the gas turbine flue gas for steam generation is more reversible than in a standard HRSG, since the dedicated HRSG has no IP evaporator. Figure 5.9 shows the pinch diagram of the HRSG.

Table 7.10.- Technical performance results of the retrofits with high levels of CO_2 capture

				POWER MATCHED RETROFIT			HEAT MATCHED RETROFIT	Counterfactual CCGT plant with PCC
		Existing coal plant w/o capture	Standard Integrated Retrofit (90% capture)	GT Windbox Retrofit with capture	90% capture from CCGT. (mixing flue gas streams)	90% capture from CCGT	90% capture from CCGT. (mixing flue gas streams)	90% capture from CCGT
Retrofitted PC Power Plant			*CASE A1*	*CASE D1*	*CASE B1*	*CASE C1*	*CASE E1*	
Coal thermal input	MWth	1517.9	1517.9	1348.6	1517.9	1517.9	1517.9	0.0
Gas thermal input	MWth	0.0	-	358.4	269.6	265.3	4168.5	1290.1
Net Power output	MWe	600.3	473.9	600.3	600.3	600.3	2369.2	600.3
Carbon intensity of electricity generation	g CO_2 / kWh	765.3	96.9	79.5	84.7	84.6	51.5	39.2
Thermal efficiency	% LHV	39.5	31.2	35.2	33.6	33.7	41.7	46.5
Carbon Capture Plant								
Carbon capture rate from coal combustion	w/w	-	0.9	0.9	0.9	0.9	0.9	0.9
Overall carbon capture rate of two fuel sources combined	w/w	-	0.9	0.9	0.9	0.9	0.9	0.9
Total gas flow rate	kg/s	632.8	632.8	697.9	851.0	847.5	4007.0	1044.2
Gas flow rate to CC Plant	kg/s	-	632.8	697.9	632.8	847.5	4007.0	-
Gas flow rate to Gas CC Plant	kg/s	-	-	-	218.2	-	-	1044.2
Flue gas CO_2 concentration from coal combustion	v/v	0.14	0.14	0.13	0.136	0.11	0.05	-
Flue gas CO_2 concentration from gas combustion	v/v	-	-	-	0.04	-	-	0.04
Solvent energy of regeneration – coal	GJ/tonne CO_2	-	3.49	3.49	3.49	3.51	4.00	
solvent energy of regeneration – gas	GJ/tonne CO_2	-	-	-	4.00	-	-	4.10
CO_2 compression power	kWh / tn CO_2	-	111.0	111.0	111.0	111.0	111.01	111.01
Electricity output penalty	kWh / tnCO_2	-	305.8	291.5	315.8	311.3	424.4	431.2
Gas Turbine thermal efficiency, including combined cycle without capture	% LHV	-	-	53.6	53.6	53.6	53.6	53.6
Marginal efficiency of additional gas combustion	% LHV	-	-	53.9	46.9	47.7	45.5	N/A

7.3.2.2.- Economic analysis of retrofit options with high levels of CO_2 capture:

Figure 7.1a and *Figure 7.1b* show the 'total revenue requirement' (TRR) of the fully abated retrofit options in North America broken down by capital expenses, operating costs and CO_2 EOR revenue and *Figure 7.2* and *Figure 7.2b* shows the TRR of the fully abated retrofit options in Europe.

When comparing fully abated retrofit options and considering the default cost data assumed in this work the GT windbox retrofit (Case D1) has a good potential in North America due to its low total revenue requirement of 86.9 $/MWh and 67.4 $/MWh with EOR, compared to other options. The standard integrated retrofit (Case A1) is penalised by the reduced power output and presents the highest TRR, the uniform revenue required to cover the cost of capture, of 90.9 $/MWh. When EOR is taken into account the TRR is reduced to 67.1$/MWh, marginally lower than the GT windbox retrofit.

A different outcome is achieved in Europe, as natural gas is more expensive in the UK than in the USA. Fully abated retrofit options with gas turbine power cycle plant achieve higher TRR than in North America. Consequently, with the default cost data assumed in this work, the standard integrated retrofit (Case A1) achieves a lower TRR than other options with and without sales of CO_2 for EOR. However, it should be noted that this option incur additional costs related to the new capacity needed to re-store the power output of the site. When the additional investment and the associated running costs of the new capacity are considered in the model, the standard integrated retrofit achieves a similar level of revenue than the other options, as indicated in *Figure 7.3*. The costs of the additional capacity are based on the capital expenditures and operational expenditures of Section 7.2.1.

Table 7.11 and Table 7.12 provide more details on the results of the economic analysis for the retrofit options achieving high level of CO_2 capture, including the cost of CO_2 avoided, which is also represented in Figure 7.1 and Figure 7.2.

The cost of CO_2 avoided is equivalent to the value of the carbon tax at which the TRR of the existing plant equals that of the plant with CCS, revealing that a carbon tax could be largely reduced if CO_2 is used for EOR. In accordance with Zhai et al, these results show that the combination of a CO_2 emission trading system with an EOR market would increase the speed of CCS deployment for a fast-track emission mitigation strategy (Zhai et al. 2015).

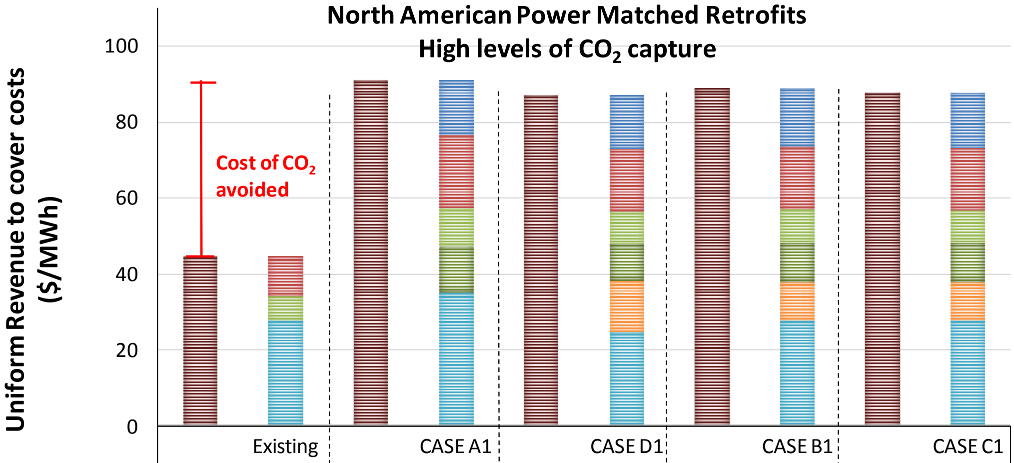

	Existing	CASE A1	CASE D1	CASE B1	CASE C1
Total CAPEX ($/MWh)	0,0	14,4	14,0	15,1	14,3
Fixed Costs ($/MWh)	10,4	19,3	16,3	16,6	16,5
Variable Costs ($/MWh)	6,3	10,0	8,5	8,6	8,5
CO2 T&S Costs ($/MWh)	0,0	11,9	9,8	10,4	10,4
Natural Gas Cost ($/MWh)	0,0	0,0	13,4	10,1	9,9
Coal Cost ($/MWh)	27,9	35,3	24,8	27,9	27,9
EOR Revenue ($/MWh)	0,0	0,0	0,0	0,0	0,0
TRR ($/MWh)	44,5	90,9	86,9	88,7	87,6

Figure 7.1a.- *Uniform revenue to cover costs of fully abated power matched retrofits in North America*

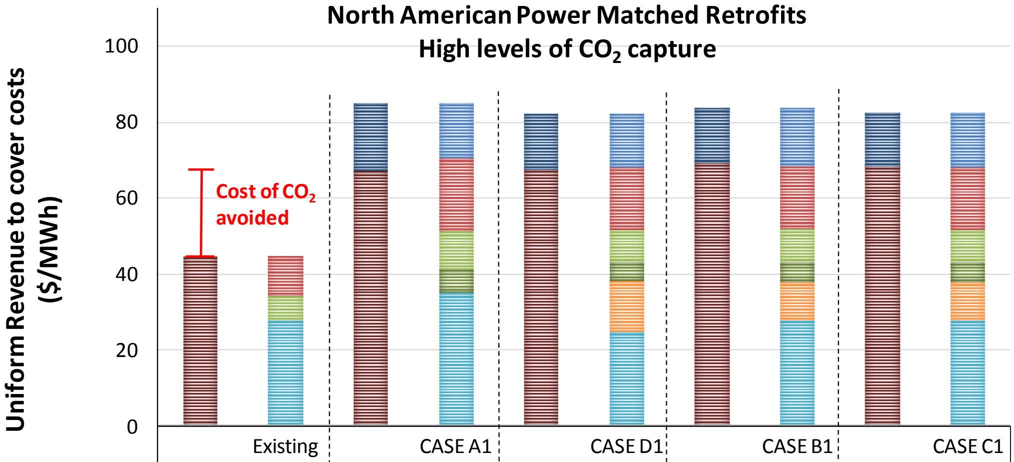

	Existing	CASE A1	CASE D1	CASE B1	CASE C1
Total CAPEX ($/MWh)	0,0	14,4	14,0	15,1	14,3
Fixed Costs ($/MWh)	10,4	19,3	16,3	16,6	16,5
Variable Costs ($/MWh)	6,3	10,0	8,5	8,6	8,5
CO2 T&S Costs ($/MWh)	0,0	5,9	4,9	5,2	5,2
Natural Gas Cost ($/MWh)	0,0	0,0	13,4	10,1	9,9
Coal Cost ($/MWh)	27,9	35,3	24,8	27,9	27,9
EOR Revenue ($/MWh)	0,0	17,8	14,6	14,1	14,1
TRR ($/MWh)	44,5	67,1	67,4	69,4	68,3

Figure 7.1b.- *Uniform revenue with sales to Enhanced Oil Recovery at \$10/tCO_2 in North America*

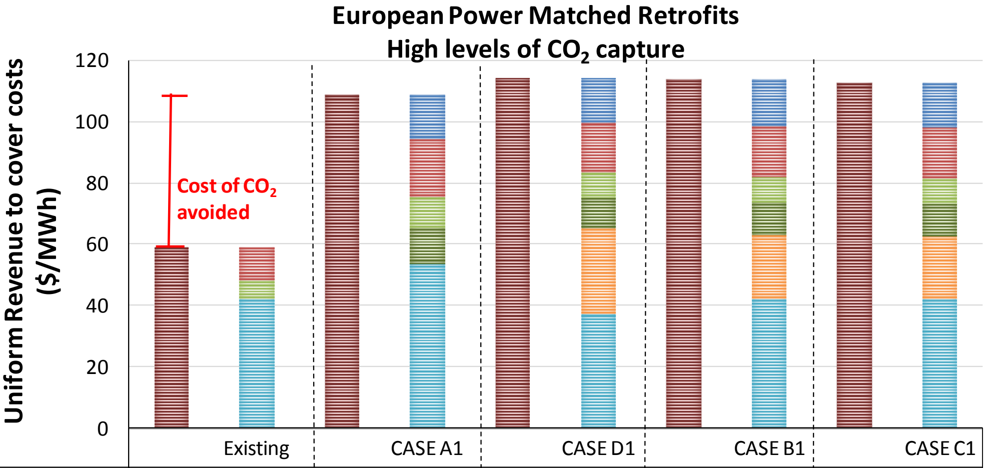

	Existing		CASE A1		CASE D1		CASE B1		CASE C1
Total CAPEX ($/MWh)		0,0		14,4		14,0		15,1	14,3
Fixed Costs ($/MWh)		10,4		19,3		16,3		16,6	16,5
Variable Costs ($/MWh)		6,3		10,0		8,5		8,6	8,5
CO2 T&S Costs ($/MWh)		0,0		11,9		9,8		10,4	10,4
Natural Gas Cost ($/MWh)		0,0		0,0		27,8		20,9	20,6
Coal Cost ($/MWh)		42,2		53,5		37,5		42,2	42,2
EOR Revenue ($/MWh)	0,0		0,0		0,0		0,0	0,0	
TRR ($/MWh)	58,8		109,0		114,0		113,8	112,5	

Figure 7.2a.- Uniform revenue to cover costs of fully abated power matched retrofits in Europe

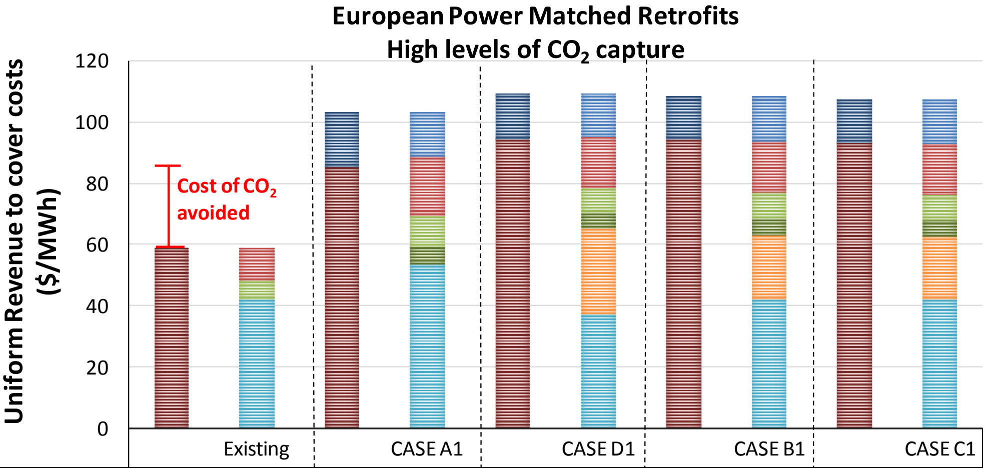

	Existing		CASE A1		CASE D1		CASE B1		CASE C1
Total CAPEX ($/MWh)		0,0		14,4		14,0		15,1	14,3
Fixed Costs ($/MWh)		10,4		19,3		16,3		16,6	16,5
Variable Costs ($/MWh)		6,3		10,0		8,5		8,6	8,5
CO2 T&S Costs ($/MWh)		0,0		5,9		4,9		5,2	5,2
Natural Gas Cost ($/MWh)		0,0		0,0		27,8		20,9	20,6
Coal Cost ($/MWh)		42,2		53,5		37,5		42,2	42,2
EOR Revenue ($/MWh)	0,0		17,8		14,6		14,1	14,1	
TRR ($/MWh)	58,8		85,2		94,5		94,5	93,3	

Figure 7.2b.- Uniform revenue with sales to Enhanced Oil Recovery at $10/tCO₂ in Europe

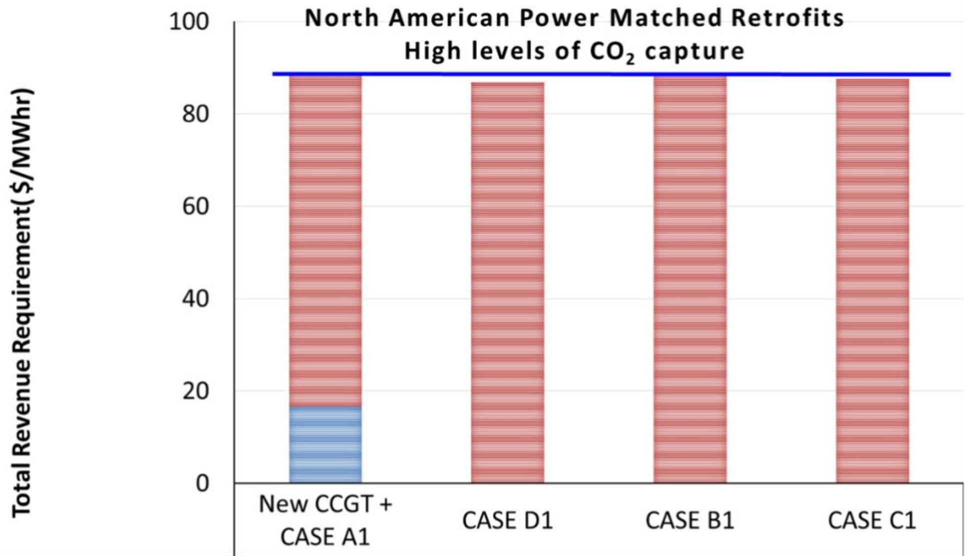

	New CCGT + CASE A1	CASE D1	CASE B1	CASE C1
Retrofit ($/MWh)	71.7	86.9	88.7	87.6
New CGT ($/MWh)	16.6			
Total ($/MWh)	88.3	86.9	88.7	87.6

Figure 7.3a.- *Uniform revenue considering the additional costs of the new CCGT needed to re-store the power output of the site for North American scenarios*

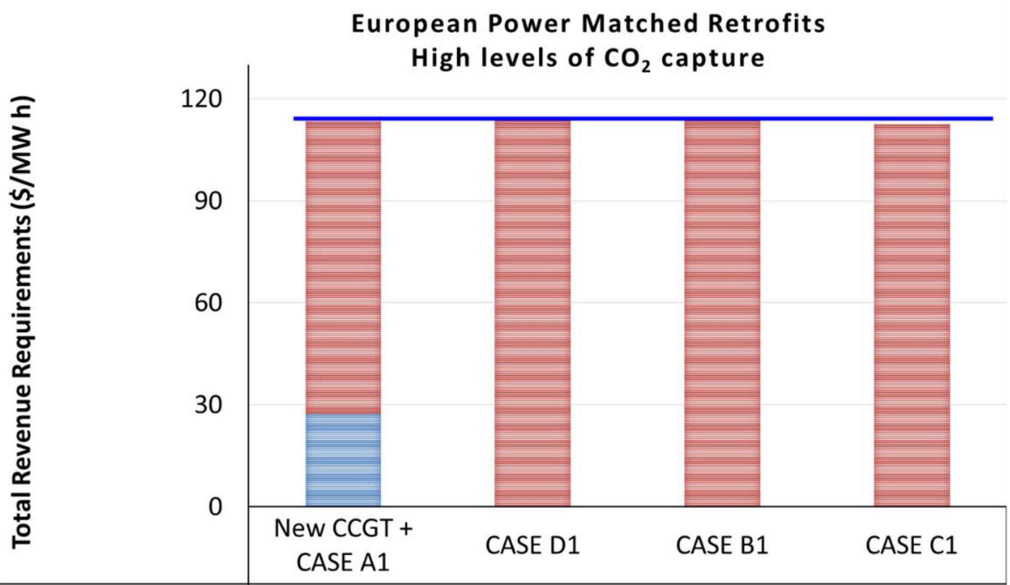

	New CCGT + CASE A1	CASE D1	CASE B1	CASE C1
Retrofit ($/MWh)	86.1	114.0	113.8	112.5
New CGT ($/MWh)	27.4			
Total ($/MWh)	113.5	114.0	113.8	112.5

Figure 7.3b.- *Uniform revenue considering the additional costs of the new CCGT needed to re-store the power output of the site for European scenarios.*

Put in context, the maximum carbon price support (CPS) per tCO_2 that is expected to be implemented from 2016-17 to 2019-2020 in the UK is £18/t CO2 ($28/t CO_2) (HM Revenue & Customs 2014) and the minimum CO_2 avoided cost obtained with the economic model is around $39 / t CO_2 in Europe and $27/t CO_2 in North America.

The values of the LCOE, IRR and CO_2 avoided costs from Table 7.11 indicates that the GT windbox could have potential in North America which is consistent with the results of the total revenue requirement. The IRR is considerably higher than other options, with the exception of the option with the flue gas streams are mixed in one capture plant. Nevertheless, this configuration could involve higher operating costs that could not be considered in the current model, costs related to stratification issues, amine degradation and corrosion of the carbon capture equipment. Chapter 2 discusses the possible operating problems related to this type of retrofit.

It should be noted that CO_2 avoided costs and IRR depend on relatively small differences between much larger LCOE estimates and as a result, even small variations in the LCOE values can have large implications for the previously mentioned metrics.

With the default cost data assumed in this work capturing CO_2 from the coal plant and CCGT in the same capture unit, the retrofit option with flue gas mixing, Case C1 of Table 7.12, reaches the lowest LCOE, CO_2 avoided costs and CO_2 capture costs in Europe, and, importantly, the higher Internal Rate of Return (IRR). If the issues associated with flue gas mixing cannot be avoided cost effectively, then standard integrated retrofits present the highest IRR, with the underlying assumption that effective thermodynamics integration can be achieved.

Additionally, as the CO_2 mass flow rate of the resulting flue gas of the GT flue gas windbox retrofit is close to that of the existing coal plant, as indicated in Table 7.10, a GT windbox configuration provides a promising alternative for repowering standard integrated capture retrofits, without additional emissions by using the existing capture plant without major modifications. If an integrated retrofit is initially designed for operation with zero to ~90% capture (as at the Boundary Dam 3 unit), then subsequent operation with full capture can be achieved. In this case the addition of a GT flue gas windbox retrofit restores the full power output of the site with full CO_2 capture and would use optimally the asset consisting of the original capture plant.

Table 7.11.- Economic comparison of PCC retrofits with high level of CO_2 capture in North America

RETROFITS WITH HIGH LEVEL OF CO_2 CAPTURE IN NORTH AMERICA						
		CASE A1	**CASE A1 + New CCGT**	**CASE D1**	**CASE B1**	**CASE C1**
LCOE	$/MWh	90.9	88.3	86.9	88.7	87.6
Cost of CO_2 Avoided	$/t CO_2 emit.	50.9	47.2	45.3	47.6	46.4
Cost of CO_2 Captured	$/t CO_2 capt.	29.0	32.2	33.4	32.5	31.5
Selling electricity Price	$/MWh	114.0	114.0	114.0	114.0	114.0
IRR	%	32.5%	33.8%	36.6%	33.5%	35.5%
CO_2 selling Price	$/t CO_2 capt.	15.0	15.0	15.0	15.0	15.0
Revenue from EOR	$/MWh	13.1	11.4	10.7	10.3	10.3
Cost of CO_2 Avoided	$/t CO_2 emit.	27.6	27.2	26.7	28.8	27.6

Table 7.12.- Economic comparison of PCC retrofits with high level of CO_2 capture in Europe

RETROFITS WITH HIGH LEVEL OF CO_2 CAPTURE IN EUROPE						
		CASE A1	**CASE A1 + New CCGT**	**CASE D1**	**CASE B1**	**CASE C1**
LCOE	$/MWh	109.0	113.4	114.0	113.8	112.6
Cost of CO_2 Avoided	$/t CO_2 emit.	55.1	58.8	59.0	59.2	57.9
Cost of CO_2 Captured	$/t CO_2 capt.	32.2	42.5	46.5	42.9	41.7
Selling electricity Price	$/MWh	114.0	114.0	114.0	114.0	114.0
IRR	%	16.6%	12.6%	12.1%	12.2%	13.4%
CO_2 selling Price	$/t CO_2 capt.	15.0	15.0	15.0	15.0	15.0
Revenue from EOR	$/MWh	13.1	11.4	10.7	10.3	10.3
Cost of CO_2 Avoided	$/t CO_2 emit.	43.4	38.9	40.4	40.5	39.1

Figure 7.4 illustrates the TRR of the GT windbox retrofit options adapting full CO_2 capture to existing partially abated CCS plants broken down by capital expenses, operating costs and CO_2 EOR revenue.

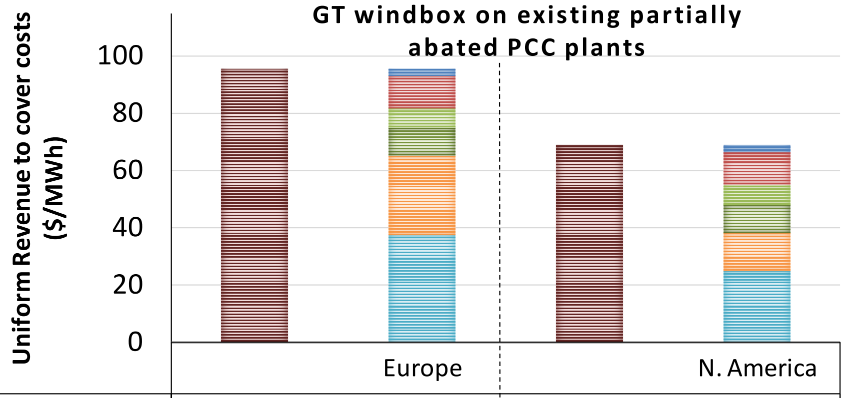

	Europe		N. America	
Total CAPEX ($/MWh)		2,31		2,31
Fixed Costs ($/MWh)		11,34		11,34
Variable Costs ($/MWh)		6,79		7,04
CO2 T&S Costs ($/MWh)		9,76		9,76
Natural Gas Cost ($/MWh)		27,83		13,43
Coal Cost ($/MWh)		37,50		24,77
EOR Revenue ($/MWh)	0,00		0,00	
TRR ($/MWh)	95,52		68,65	

Figure 7.4a.- Uniform revenue with the additional cost of a new GT and HRSG to re-store the power output of the site

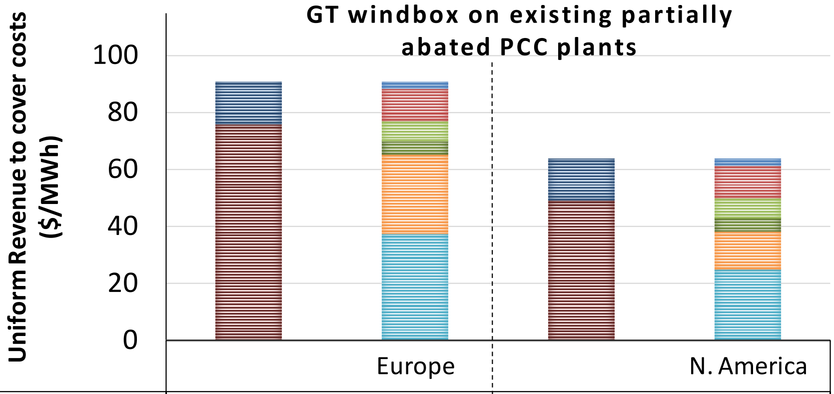

	Europe		N. America	
Total CAPEX ($/MWh)		2,31		2,31
Fixed Costs ($/MWh)		11,34		11,34
Variable Costs ($/MWh)		6,79		7,04
CO2 T&S Costs ($/MWh)		4,88		4,88
Natural Gas Cost ($/MWh)		27,83		13,43
Coal Cost ($/MWh)		37,50		24,77
EOR Revenue ($/MWh)	14,64		14,64	
TRR ($/MWh)	76,00		49,13	

Figure 7.4b.- Uniform revenue with sales to Enhanced Oil Recovery at $10/tCO_2$ and with the additional cost of a new GT and HRSG to re-store the power output of the site

In conclusion to this section, it is important to note that TRR values for all cases are dominated by fuel costs. As a result, the power matched retrofit options in this study are more likely to be deployed in areas with relatively low fuel prices, although they remain a competitive option to continue to use existing assets connected to existing plants, gird capacity, transmission and provision of network services, in countries/markets aiming for rapid electrification and decarbonisation at the same time. The sensitivity analysis of *Section 7.4* studies the influence of this parameter on the net revenue in more details.

7.3.3.- Results for intermediate capture levels

The carbon intensity of electricity generation plays an important role in the techno-economic analysis and this section examines options meeting an EPS of 450 gCO_2/kWh for existing plants undergoing a significant upgrade and compares to standard integrated retrofit with steam extraction.

7.3.3.1.- Technical performance analysis of intermediate capture levels:

Table 7.13 shows the results of the different intermediate capture levels retrofit options discussed in previous chapters. In all these cases the CO_2 concentration of the flue gas entering the capture plant remains constant, ~ 13% v/v, as gas from the natural gas plant is not being treated. Consequently, the reboiler duty is always the same. The EOP for options capturing the same amount of CO_2 will predominantly depend on the integration of the PCC plant with the steam cycle of the HRSG and the coal plant.

The numerator of the EOP expression, equation [6.2], shown below for convenience, represents the difference between the output of the counterfactual plant and the total net power output of the retrofitted plant.

$$EOP = \frac{Power_{Counterfact} \; - Power_{w\ capture}}{m_{CO2}} \qquad [7.33]$$

In PCC retrofits with an additional natural gas fuel source, the counterfactual power plant includes the existing coal power plant before capture is added and an unabated combined heat and power plant burning the same amount of natural gas at the same firing temperature as the gas turbine added to the site during the retrofit. The difference between the output of the counterfactual plant and the total net power output of the retrofitted plant is larger for heat matched retrofits than for power matched retrofits, simply, due to the fact that all the thermal energy for solvent regeneration is provided by the HRSG of the gas turbine power cycle.

The absence of a low pressure steam turbine in the combined cycle affects negatively the marginal efficiency of additional natural gas combustion of the heat matched retrofit options, compared to power matched retrofits a large fraction of steam generated in the HRSG is fully expanded down to the pressure of the condenser of the existing steam cycle.

Table 7.13 also shows that the marginal efficiency of the power matched retrofits are higher than the thermal efficiency of the CCGT efficiency w/o capture. The benefits of integration are similar to those discussed at the end of section 7.33, namely a lower power consumption of the flue gas blower, higher amount of mechanical work extracted from the existing Rankine cycle with feedwater heating and more reversible steam generation in the HRSG. The LP steam generated in the HRSG is sent for solvent regeneration and reduces steam extraction from the IP/LP crossover of the coal power plant. The additional power in the existing steam cycle is accounted in the marginal efficiency of the additional gas combustion. This additional power corresponds to the power that would have been generated in the LP steam turbine of the CCGT if CO_2 were not captured.

Retrofits with a GT and an HRSG achieve the lowest marginal efficiency as the steam generated in the HRSG does not produce any power, and only supplies thermal energy to the carbon capture plant. The natural gas marginal efficiency is about 17 percentage points lower than the configurations comprising GT with a combined cycle. Unsurprisingly, heat matched retrofit with an additional CCGT reaches better technical performance, on the basis of the EOP and the marginal efficiency of natural gas, than gas turbine power cycles with an HRSG only supplying low grade heat, at additional capital cost.

Table 7.13.- Technical performance results for interim capture levels

				HEAT MATCHED RETROFIT				POWER MATCHED RETROFIT	
				GT with HRSG		GTCC		GTCC	
		Standard Integrated Retrofit (90% capture)	Standard Integrated Retrofit (EPS)	90% capture on coal flue gas only	EPS	90% capture on coal flue gas only	EPS	90% capture on coal flue gas only	EPS
Retrofitted PC Power Plant		***CASE A1***	***CASE A2***	***CASE F3***	***CASE F2***	***CASE E3***	***CASE E2***	***CASE B3***	***CASE B2***
Coal thermal input	MWth	1517.9	1517.9	1517.9	1517.9	1517.9	1517.9	1517.9	1517.9
Gas thermal input	MWth	-	-	979.9	521.5	1367.7	622.0	233.9	88.6
Net Power output	MWe	473.9	549.9	890.3	747.3	1167.8	849.9	600.3	600.3
Carbon intensity of electricity generation	g CO_2 / kWh	96.9	450.1	252.5	447.6	253.1	452.8	147.6	450.1
Thermal efficiency	% LHV	31.2	36.2	35.6	36.6	40.5	39.7	34.3	37.4
Carbon Capture Plant									
Carbon capture rate from coal combustion	w/w	0.90	0.90	0.90	0.90	0.90	0.90	0.90	0.90
Overall carbon capture rate of two fuel sources combined	w/w	0.90	0.46	0.65	0.40	0.58	0.33	0.82	0.43
Total gas flow rate	kg/s	632.8	632.8	1426.0	1054.9	1739.8	1136.2	822.1	704.5
Gas flow rate to CC Plant	kg/s	632.8	324.3	632.8	336.8	632.8	287.8	632.8	314.3
Flue gas CO_2 concentration from coal combustion	v/v	0.14	0.14	0.14	0.14	0.14	0.14	0.14	0.14
Solvent energy of regeneration	GJ/tonne CO_2	3.49	3.49	3.49	3.49	3.49	3.49	3.49	3.49
CO_2 compression power	kWh / tn CO_2	111.0	111.0	111.0	111.0	111.0	111.0	111.0	111.0
Electricity output penalti – 90% capture on coal	kWh / tnCO_2	305.8	-	569.4	-	401.1	-	303.3	-
Electricity output penalti for EPS	kWh / tnCO_2		237.9	-	602.6	-	446.1	-	231.4
Gas Turbine thermal efficiency, including combined cycle without capture	% LHV	-	-	53.6	53.6	53.6	53.6	53.6	53.6
Marginal efficiency of additional gas combustion	% LHV	-	-	42.5	38.4	50.7	46.8	54.1	54.1

7.3.3.2.- Economic analysis of intermediate capture levels:

The carbon intensity of electricity generation plays an important role in the techno-economic analysis and options meeting the EPS of 450 gCO_2/kWh are compered in this study.

A comparative example of a standard integrated retrofit and a power matched retrofit meeting the EPS is shown in Figure 7.5 and Figure 7.6 (Case A2 and Case B2). The uniform revenue required to cover costs of power matched retrofit options at that level of carbon intensity of electricity generation is very similar to that of a standard integrated retrofit.

As mentioned before, the standard integrated retrofit (Case A2) for interim capture levels seems to achieve a good economic performance but when the new capacity is added the project becomes more expensive and other options might be preferred. This is illustrated in Figure 7.7.

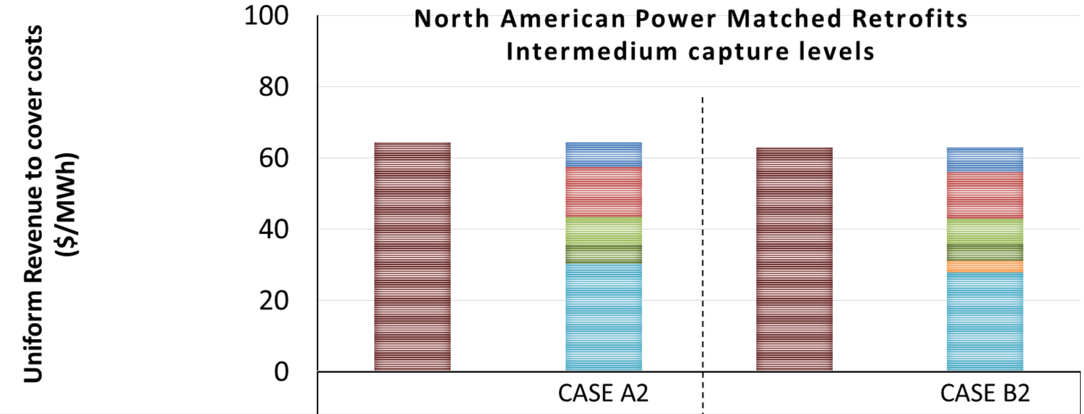

	CASE A2		CASE B2	
Total CAPEX ($/MWh)		7.0		6.8
Fixed Costs ($/MWh)		14.0		13.0
Variable Costs ($/MWh)		7.8		7.2
CO2 T&S Costs ($/MWh)		5.3		4.7
Natural Gas Cost ($/MWh)		0.0		3.3
Coal Cost ($/MWh)		30.4		27.9
EOR Revenue ($/MWh)	0.0		0.0	
TRR ($/MWh)	64.5		63.0	

Figure 7.5a.- Uniform revenue to cover costs of power matched retrofits reaching interim capture levels in North America

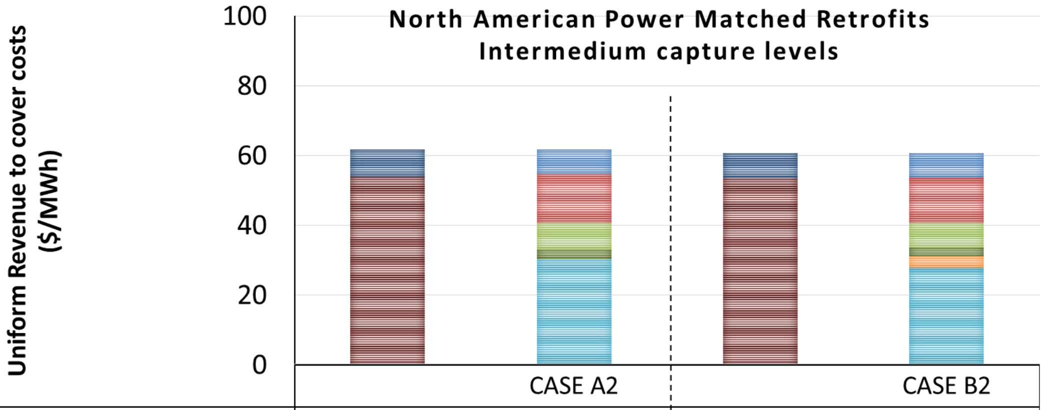

		CASE A2		CASE B2
Total CAPEX ($/MWh)		7.0		6.8
Fixed Costs ($/MWh)		14.0		13.0
Variable Costs ($/MWh)		7.8		7.2
CO2 T&S Costs ($/MWh)		2.6		2.3
Natural Gas Cost ($/MWh)		0.0		3.3
Coal Cost ($/MWh)		30.4		27.9
EOR Revenue ($/MWh)	7.9		7.0	
TRR ($/MWh)	53.9		53.6	

Figure 7.5b.- Uniform revenue with sales to Enhanced Oil Recovery at $10/tCO_2$ of power matched retrofits reaching interim capture levels in North America

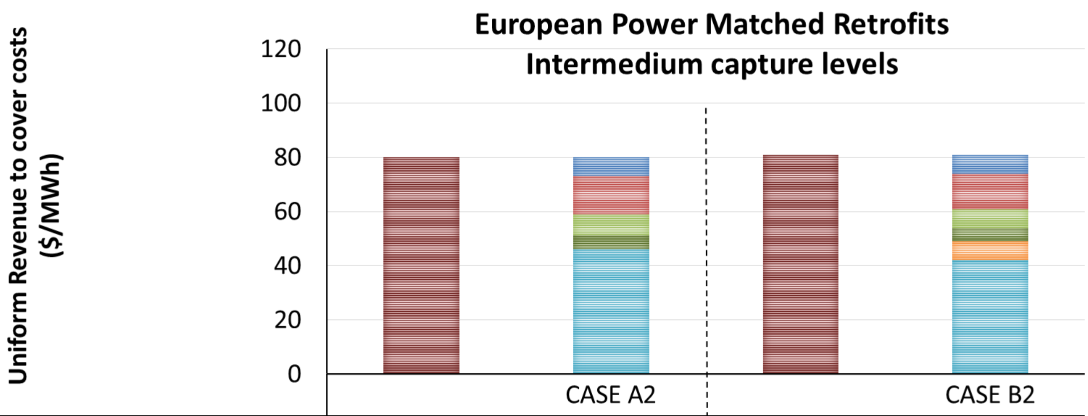

		CASE A2		CASE B2
Total CAPEX ($/MWh)		7.0		6.8
Fixed Costs ($/MWh)		14.0		13.0
Variable Costs ($/MWh)		7.8		7.2
CO2 T&S Costs ($/MWh)		5.3		4.7
Natural Gas Cost ($/MWh)		0.0		6.9
Coal Cost ($/MWh)		46.1		42.2
EOR Revenue ($/MWh)	0.0		0.0	
TRR ($/MWh)	80.1		80.8	

Figure 7.6a.- Uniform revenue to cover costs of power matched retrofits reaching interim capture levels in Europe

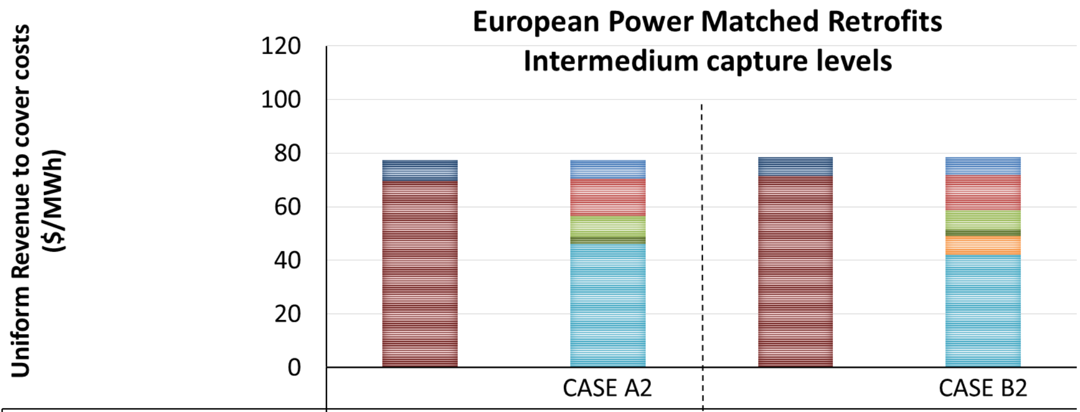

	CASE A2		CASE B2	
Total CAPEX ($/MWh)		7.0		6.8
Fixed Costs ($/MWh)		14.0		13.0
Variable Costs ($/MWh)		7.8		7.2
CO2 T&S Costs ($/MWh)		2.6		2.3
Natural Gas Cost ($/MWh)		0.0		6.9
Coal Cost ($/MWh)		46.1		42.2
EOR Revenue ($/MWh)	7.9		7.0	
TRR ($/MWh)	69.6		71.5	

Figure 7.6b.- Uniform revenue with sales to Enhanced Oil Recovery at $10/tCO_2$ of power matched retrofits reaching interim capture levels in Europe

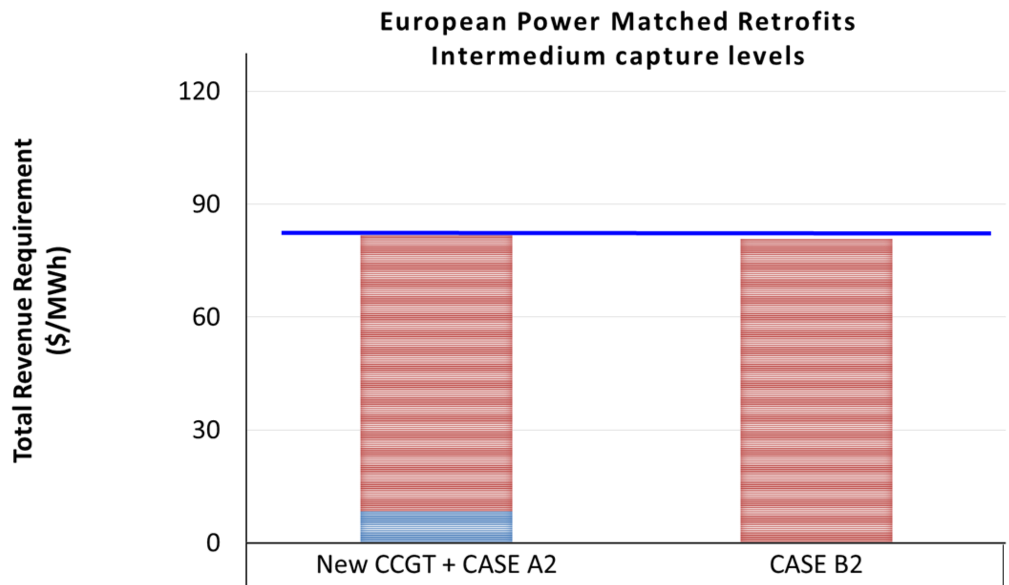

	New CCGT + CASE A2	CASE B2
Retrofit ($/MWh)	73.4	80.8
New CGT ($/MWh)	8.3	
Total ($/MWh)	81.7	80.8

Figure 7.7a.- Uniform revenue considering the additional costs of the new CCGT needed to re-store the power output of the site

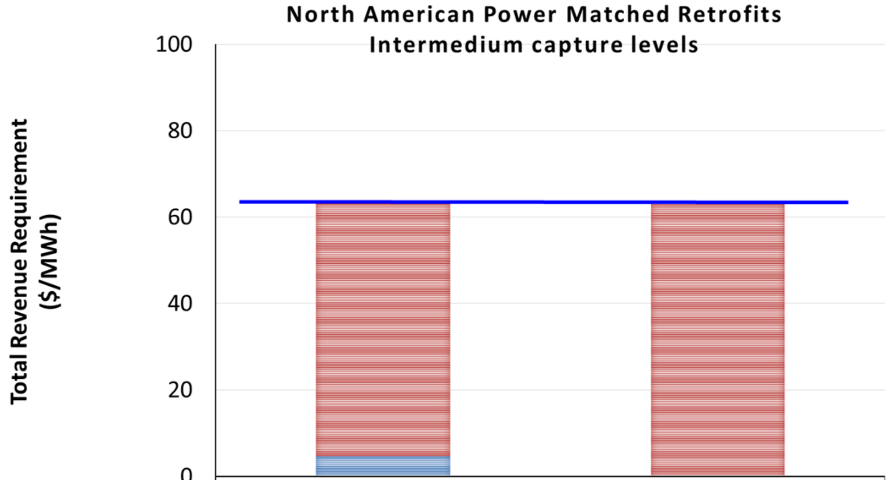

	New CCGT + CASE A2	CASE B2
Retrofit ($/MWh)	59.0	63.0
New CGT ($/MWh)	4.6	
Total ($/MWh)	63.6	63.0

Figure 7.7b.- Uniform revenue considering the additional costs of the new CCGT needed to re-store the power output of the site

Figure 7.8 and Figure 7.9 indicate the TRR for the heat matched retrofit options meeting the EPS and shown that heat matched retrofit with an additional CCGT reaches lower TRR than HRSG boiler options, with and without the additional revenues generated by EOR sales.

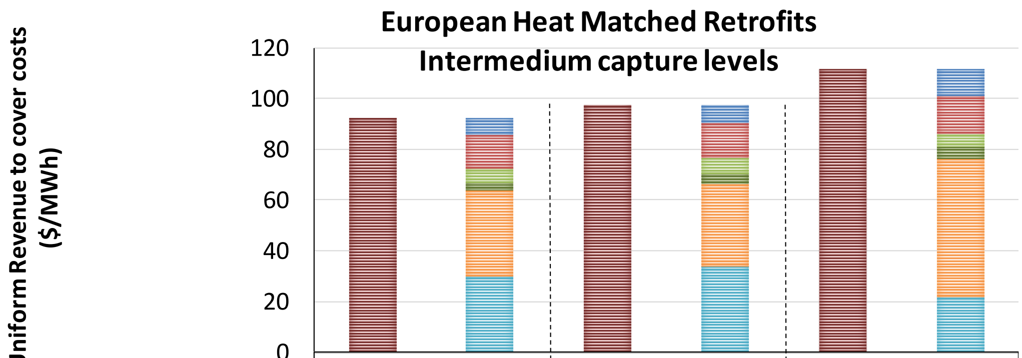

		CASE E2		CASE F2		CASE E3
Total CAPEX ($/MWh)		6,5		7,0		10,4
Fixed Costs ($/MWh)		13,3		13,6		15,0
Variable Costs ($/MWh)		5,6		6,4		5,1
CO2 T&S Costs ($/MWh)		3,0		4,0		4,8
Natural Gas Cost ($/MWh)		34,1		32,5		54,6
Coal Cost ($/MWh)		29,8		33,9		21,7
EOR Revenue ($/MWh)	0,0		0,0		0,0	
TRR ($/MWh)	92,3		97,4		111,6	

Figure 7.8a.- Uniform revenue to cover costs of heat matched retrofits reaching interim capture levels in Europe

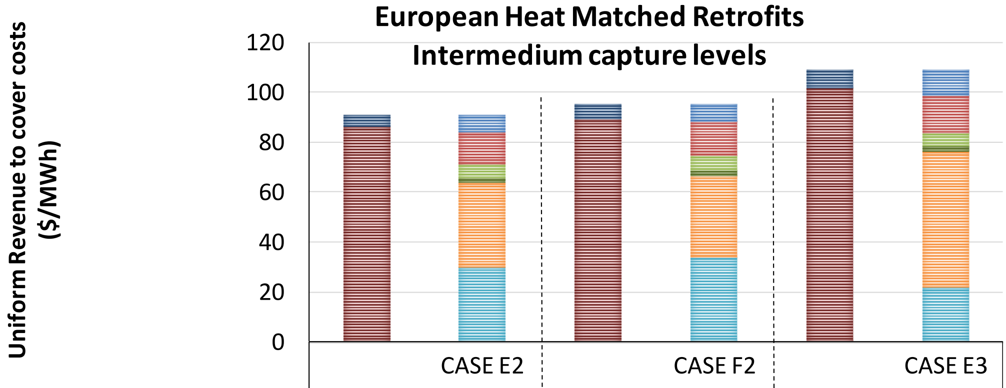

	CASE E2		CASE F2		CASE E3	
Total CAPEX ($/MWh)		6,5		7,0		10,4
Fixed Costs ($/MWh)		13,3		13,6		15,0
Variable Costs ($/MWh)		5,6		6,4		5,1
CO2 T&S Costs ($/MWh)		1,5		2,0		2,4
Natural Gas Cost ($/MWh)		34,1		32,5		54,6
Coal Cost ($/MWh)		29,8		33,9		21,7
EOR Revenue ($/MWh)	4,5		6,0		7,2	
TRR ($/MWh)	86,3		89,4		101,9	

Figure 7.8b.- Uniform revenue with sales to Enhanced Oil Recovery at $10/tCO_2$ of heat matched retrofits reaching interim capture levels in Europe wit

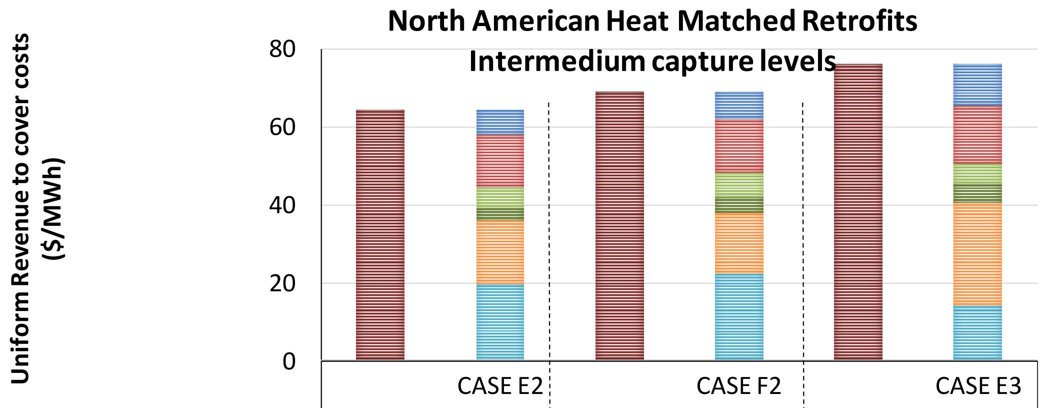

	CASE E2		CASE F2		CASE E3	
Total CAPEX ($/MWh)		6,5		7,0		10,4
Fixed Costs ($/MWh)		13,3		13,6		15,0
Variable Costs ($/MWh)		5,6		6,4		5,1
CO2 T&S Costs ($/MWh)		3,0		4,0		4,8
Natural Gas Cost ($/MWh)		16,5		15,7		26,4
Coal Cost ($/MWh)		19,7		22,4		14,3
EOR Revenue ($/MWh)	0,0		0,0		0,0	
TRR ($/MWh)	64,5		69,1		76,0	

Figure 7.9a.- Uniform revenue to cover costs of heat matched retrofits reaching interim capture levels in North America

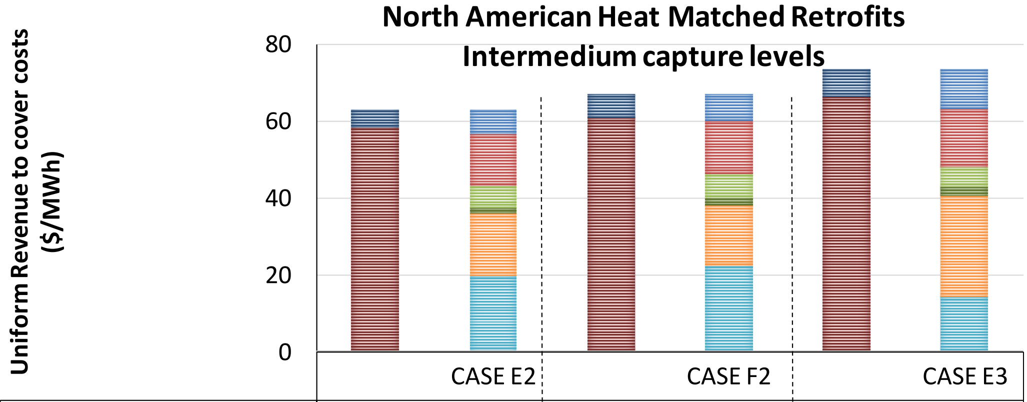

	CASE E2		CASE F2		CASE E3	
Total CAPEX ($/MWh)		6,5		7,0		10,4
Fixed Costs ($/MWh)		13,3		13,6		15,0
Variable Costs ($/MWh)		5,6		6,4		5,1
CO2 T&S Costs ($/MWh)		1,5		2,0		2,4
Natural Gas Cost ($/MWh)		16,5		15,7		26,4
Coal Cost ($/MWh)		19,7		22,4		14,3
EOR Revenue ($/MWh)	4,5		6,0		7,2	
TRR ($/MWh)	58,5		61,1		66,3	

Figure 7.9b.- Uniform revenue with sales to Enhanced Oil Recovery at \$10/tCO_2 of heat matched retrofits reaching interim capture levels in North America

7.4.- Sensitivity analysis for power matched retrofits

This section presents the economic performance of power matched retrofit options when selected parameters are varied. The primary purpose of this is to assess which trends in energy market and site-specific factors might be more favourable for the deployment of gas turbine flue gas windbox retrofit options.

7.4.1.- Sensitivity to CO_2 emission charges

Figure 7.10a and Figure 7.10b show the effect of CO_2 emission charges on LCOE in Europe and North America. As would be expected LCOE values increase with CO_2 emission price. Power matched retrofits with an unabated CCGT are promising at very low CO_2 emission charges, but as this parameter increases the implementation of CCS to the flue gas of both fuel sources rises in importance.

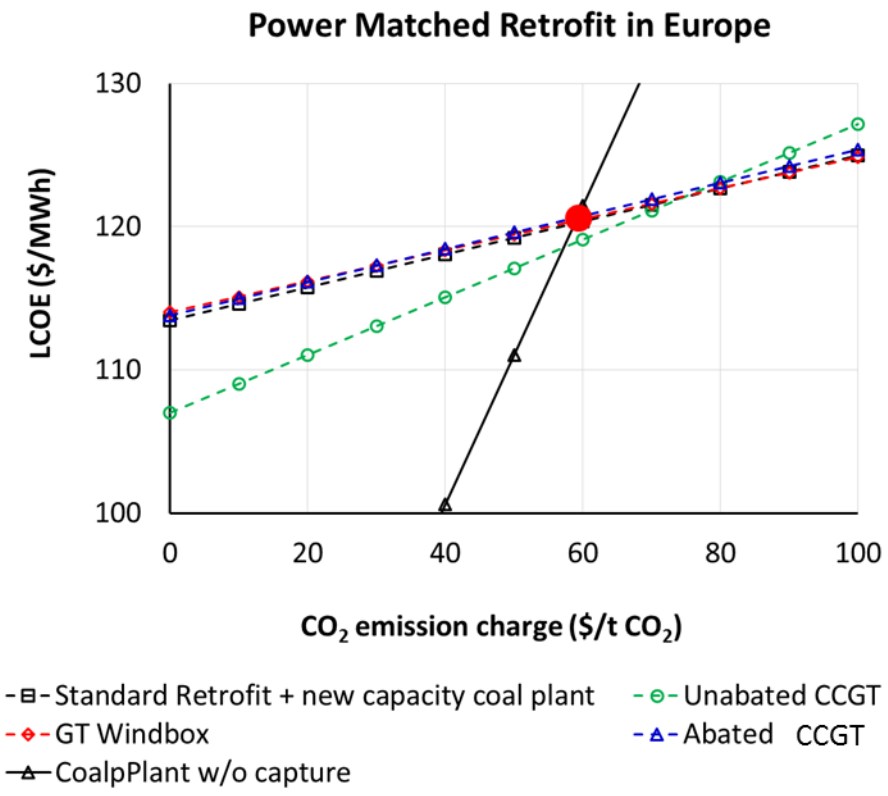

Figure 7.10a.- Effect of CO_2 emissions charges on the LCOE in Europe

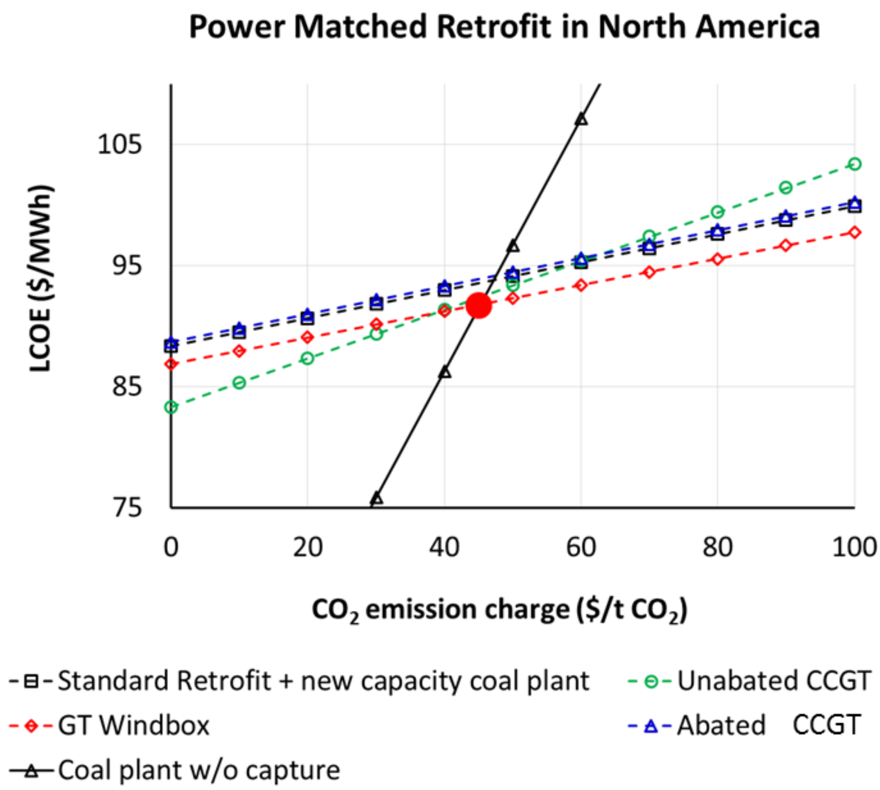

Figure 7.10b.- Effect of CO_2 emissions charges on the LCOE in North America

The red dot indicates the value of the carbon tax at which the LCOE of the coal plant without capture equals that of the GT flue gas windbox retrofit, it corresponds to the cost of CO_2 avoided, which is 59$/t CO_2 in Europe and 45$/t CO_2 in North America. At that point the GT flue gas windbox retrofit reaches the lowest LCOE in North America. If CO_2 is used for EOR the CO_2 charges that make the project break-even would be $40/t CO_2 in Europe and $27/t CO_2 in North America.

It is also interesting to note that the power matched retrofit with an abated CCGT and the GT windbox options have very similar economic performance in Europe for the range of CO_2 charges considered here and the default cost data assumed.

7.4.2.- Sensitivity to the additional capital cost component of the existing power cycle

In this work, it is assumed that the existing plant has paid off its original capital investment. Since the focus is on retrofitting subcritical coal plants For steam extraction retrofits, the additional capital cost within the island of the existing power cycle only involves the cost of the two new back pressure steam turbines to supply the steam at the required conditions for CO_2 capture and reduce the impact of steam extraction on power plant efficiency and power output.

In the GT flue gas windbox retrofit the flue gas mass flow rate within the existing boiler is increased by 10% and some coal power plant upgrades might be required. Consequently, this type of retrofit might present a higher retrofitted capital cost than the other cases considered here.

Figure 7.11a and Figure 7.11b show the sensitivity of the LCOE of the GT flue gas windbox retrofit to the cost implication discussed above. In North America the GT windbox retrofit always reaches a lower LCOE than the power matched retrofit with an abated CCGT retrofit despite the extra retrofitted capital cost, unlike in Europe. Unsurprisingly, the GT windbox retrofit becomes less attractive if significant upgrades are required.

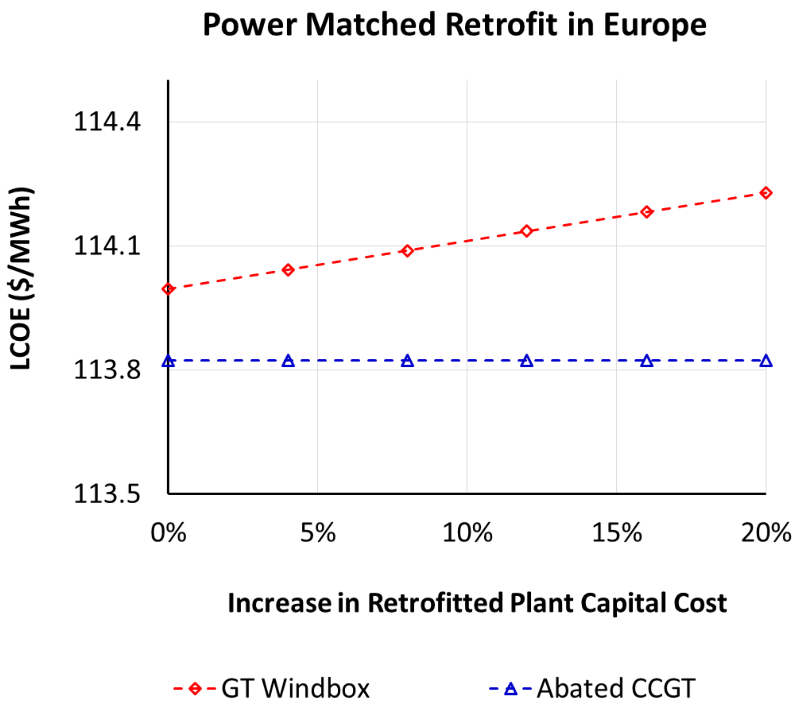

Figure 7.11a.- Effect of *additional capital cost component of the existing power cycle on LCOE in Europe*

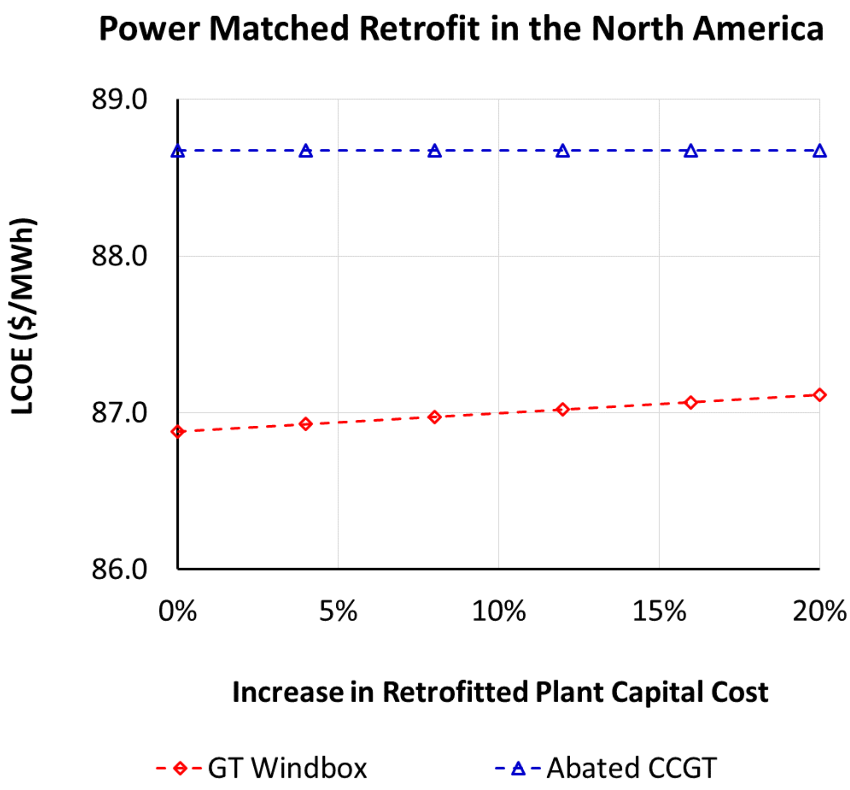

Figure 7.11b.- Effect of *additional capital cost component of the existing power cycle on LCOE in North America*

7.4.3.- Sensitivity to fuel prices, coal and gas

Figure 7.12a and Figure 7.12b indicate the variation of the LCOE with coal price assuming a natural gas price of 34.18 $/MWh_th for Europe and 14 $/MWh_th for North America.

For the default cost values considered in this study, the LCOE differences for power matched retrofitted plants nearly remain unaltered by changes in the coal cost in Europe. Nevertheless, in North America the GT flue gas windbox retrofit becomes more cost-efficient at high coal prices. This is because of the reduced coal consumption typical from this type of retrofit.

Figure 7.13a and Figure 7.13b show the variation of the LCOE with the natural gas price assuming a coal price of 12.24 $/MWh_th for Europe and 8.09 $/MWh_th for the USA. The

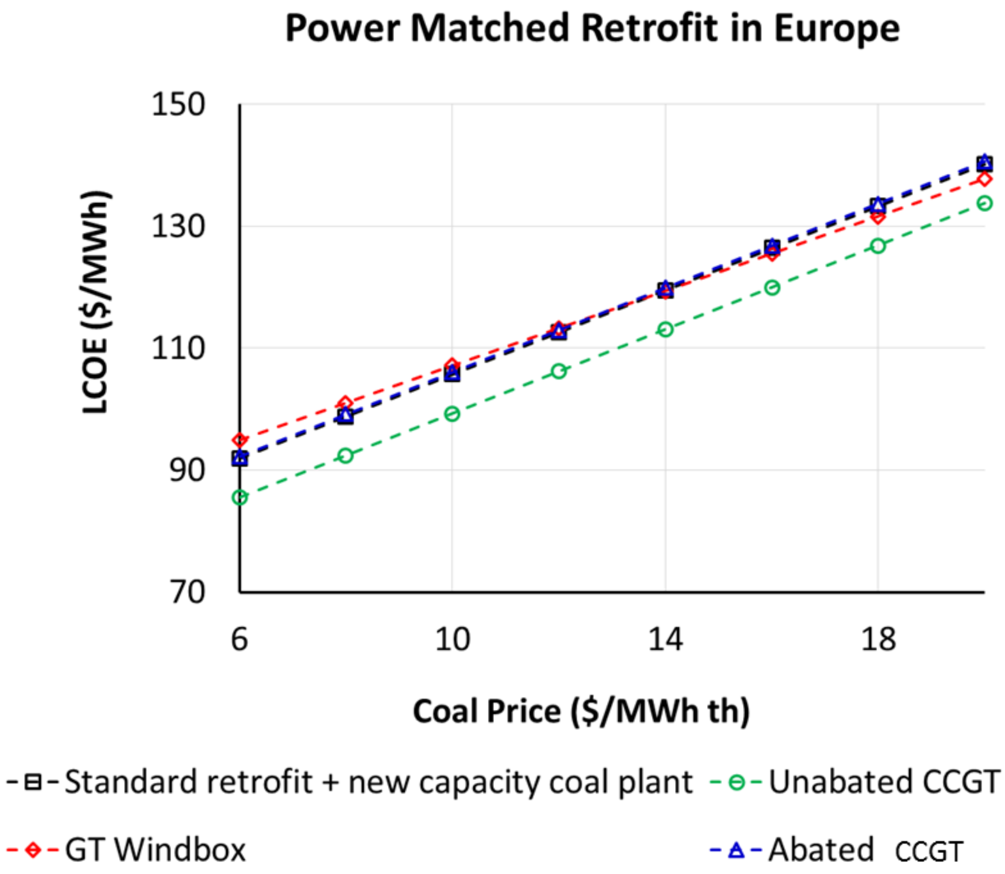

Figure 7.12a.- Effect of coal price on LCOE in Europe. The natural gas price is 34.18 $/MWh_th

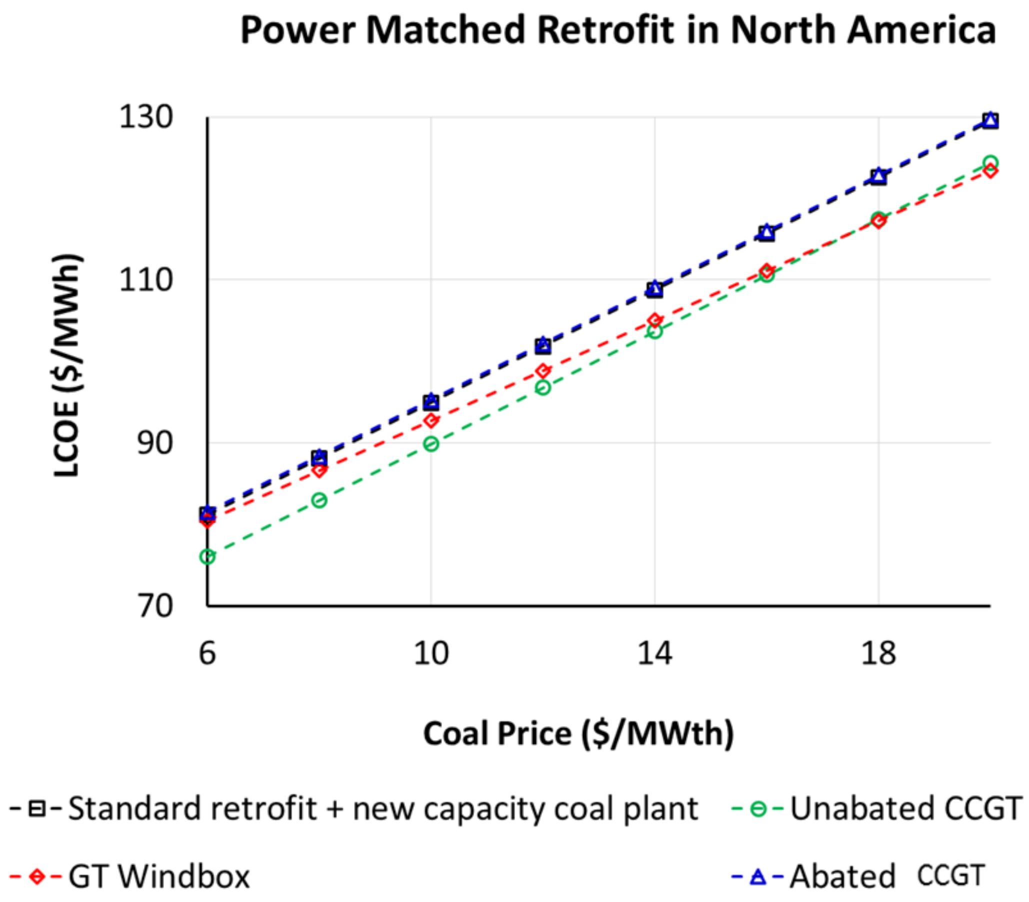

Figure 7.12b.- Effect of coal price on LCOE in North America. The natural gas price is 14 $/MWh_th

LCOE values also increase with natural gas price, nonetheless, the rate of increase is lower than with coal price due to the higher efficiency of the CCGT.

Due to the low natural gas price in North America the GT flue gas windbox retrofit reaches a lower LCOE than other fully abated power matched retrofit options. On the other hand, the natural gas price in Europe would need to reduce to more than 32$/MWh_th to become more cost-efficient given the other assumptions (including coal price) made in this analysis. In general, the lower the natural gas price the better the economic performance of the GT flue gas windbox retrofit.

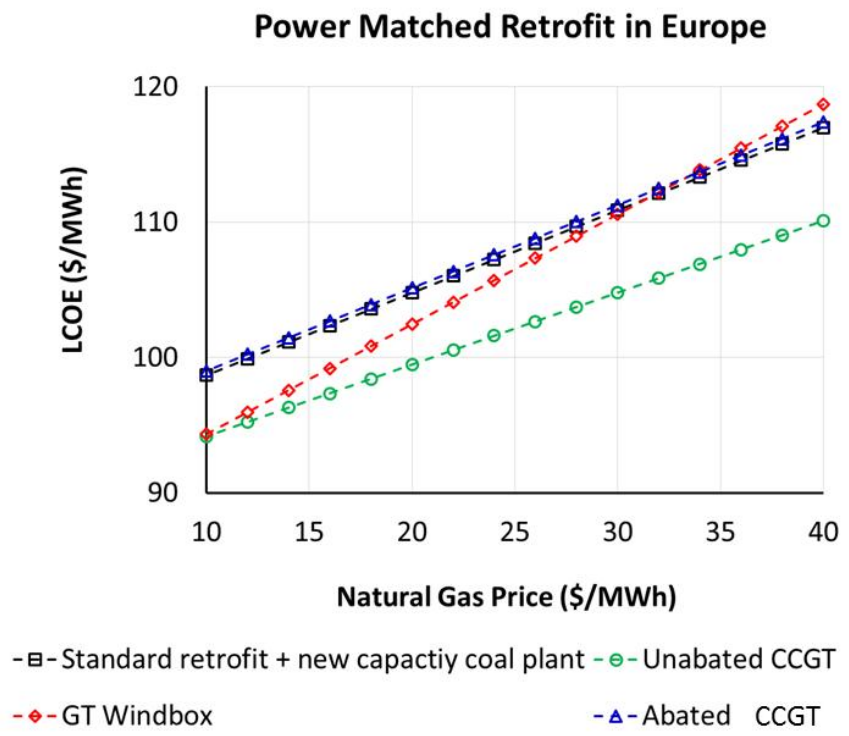

Figure 7.13a.- Effect of natural gas price on LCOE in Europe. The coal price is 12.24 $/MWh_th

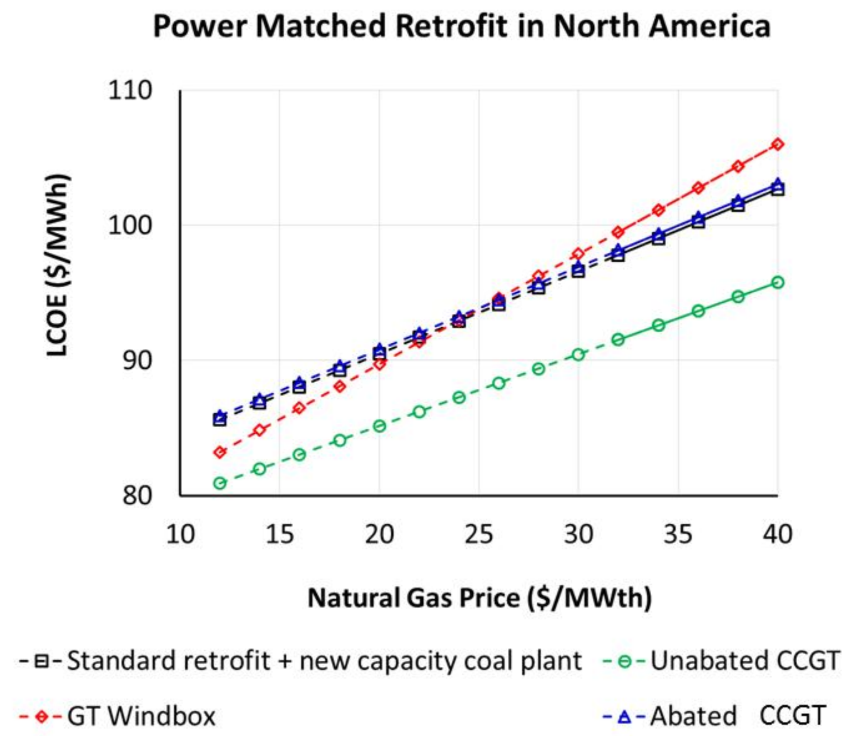

Figure 7.13b.- Effect of natural gas price on LCOE in North America. The coal price is 8.09$/MWh_th

7.4.4.- Sensitivity to Load Factor

Figure 7.14 indicate the effect of the load factor on the 'equivalent LCOE' for the GT flue gas windbox retrofit based North America.

The 'equivalent LCOE' of equation **[7.29]** is used in this section to consider the maximum additional revenue due to a higher load factor. In North America, a GT flue gas retrofit is the retrofit option with higher load factor (constant 80%) than the other retrofitted plants achieving high levels of CO_2 capture, namely 'Standard retrofit with a new capacity coal plant' (Case A1 + CCGT) and 'Abated CCGT' (Case B1), due to a lower SRMC, it therefore gains additional revenues during periods when other plants are not operating. Nevertheless, as the difference in SRMC is marginal, the revenue obtained during this period does not make a big contribution to the equivalent LCOE reduction, as shown in equation [7.40].

$$Revenue_{LF} = (SRMC_A - SRMC_B) \cdot \frac{LF_B - LF_A}{LF_A} = (56.99 - 56.71)\frac{\$}{MWhr} \cdot \frac{0.8 - LF_A}{LF_A} \quad \textbf{[7.40]}$$

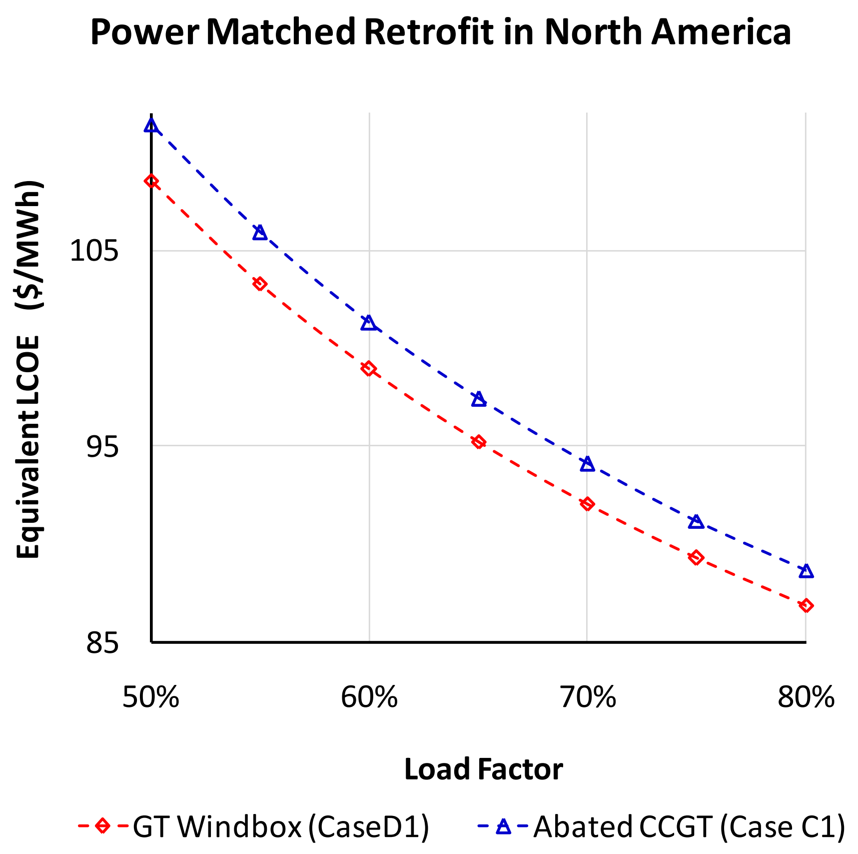

Figure 7.14.- Effect of load factor on equivalent LCOE

7.4.5.- Sensitivity to CO_2 selling price

Figure 7.15a and Figure 7.15b show the effect of the CO_2 selling price on the total revenue requirement. Evidently, the higher the CO_2 selling price the higher the EOR revenue and consequently the lower the total revenue required to cover costs and make the project break-even.

The red dot indicates the minimum value of the CO_2 selling price, if CO_2 could be sold to an enhanced oil recovery (EOR) operator, at which the LCOE of the coal power plant without capture equals that of the GT flue gas windbox retrofit. This value would correspond to the cost of CO_2 captured if CO_2 transport costs for EOR were assumed zero.

The CO_2 selling price that would cover the costs of capture is 51$/t CO_2 captured in Europe and 38$/t CO_2 captured in North America.

The LCOE differences for retrofitted plants remain constant at different selling CO_2 prices in Europe. There is, however, a little reduction in LCOE differences in North America, making the GT flue gas windbox retrofit slightly more cost-effective.

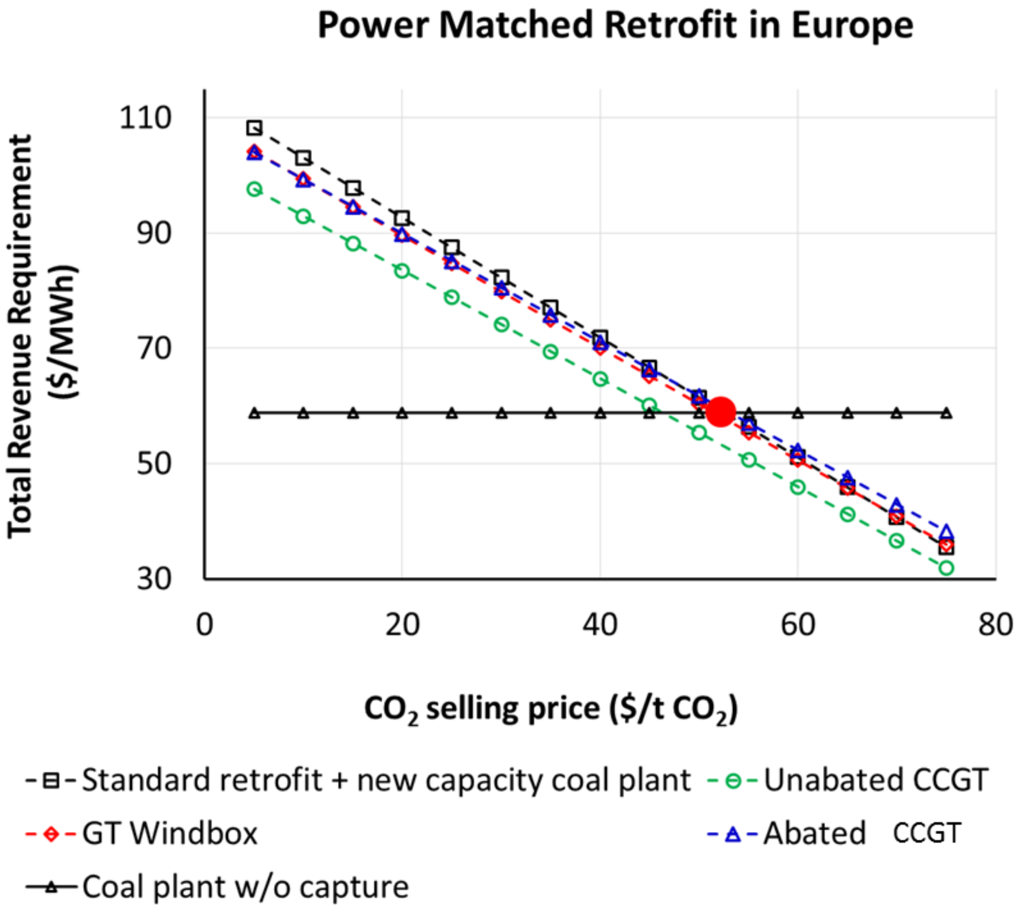

Figure 7.15a.- Effect of CO_2 selling price on total revenue requirement in Europe

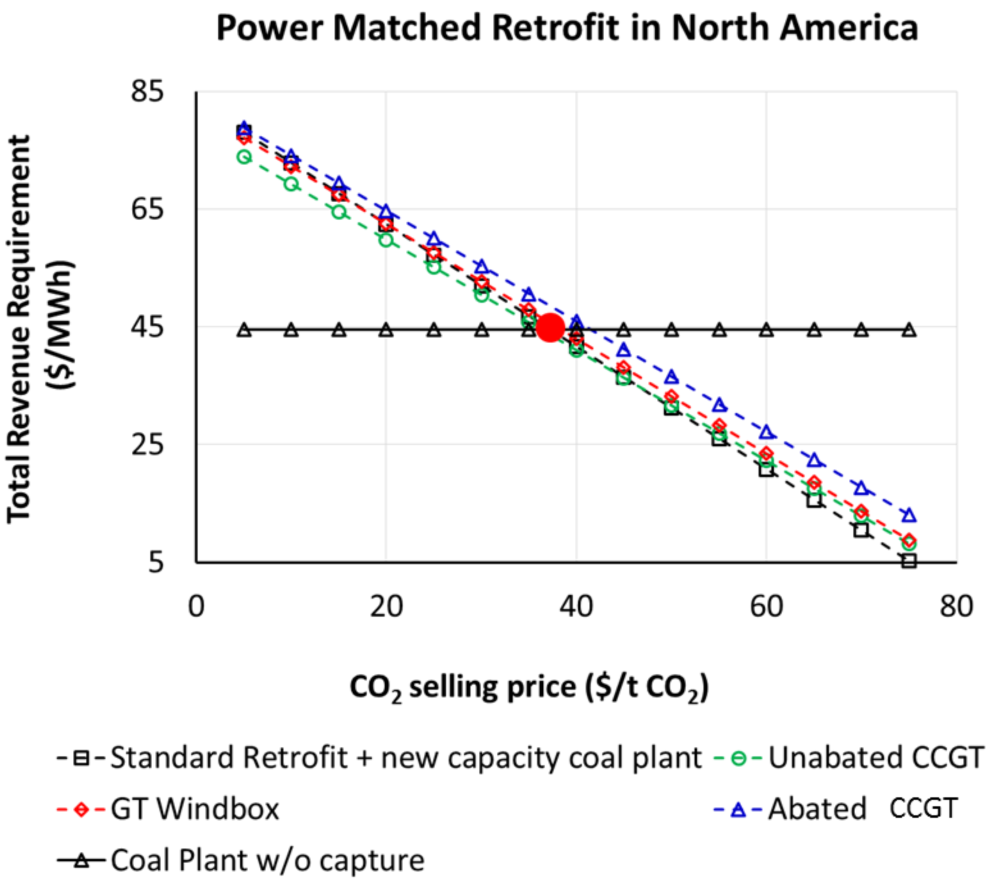

Figure 7.15b.- Effect of CO_2 selling price on total revenue requirement in North America

7.4.6.- Sensitivity to Capital Cost of equipment of the gas turbine power cycle and the post-combustion capture and compression plant

The sensitivity analysis to the capital cost of the CCGT and to the capital cost of the capture and compression plant applies nearly equally to all retrofit options, as indicated in Figure 7.16a to Figure 7.17b. The results show that the sensitivity to the former is small and that the capital costs of capture and compression plant have a larger effect with the LCOE varying from 83 $/MWh to 91 $/MWh in North America and from 111 $/MWh to 118 $/MWh in Europe for +/- 20% in capital costs.

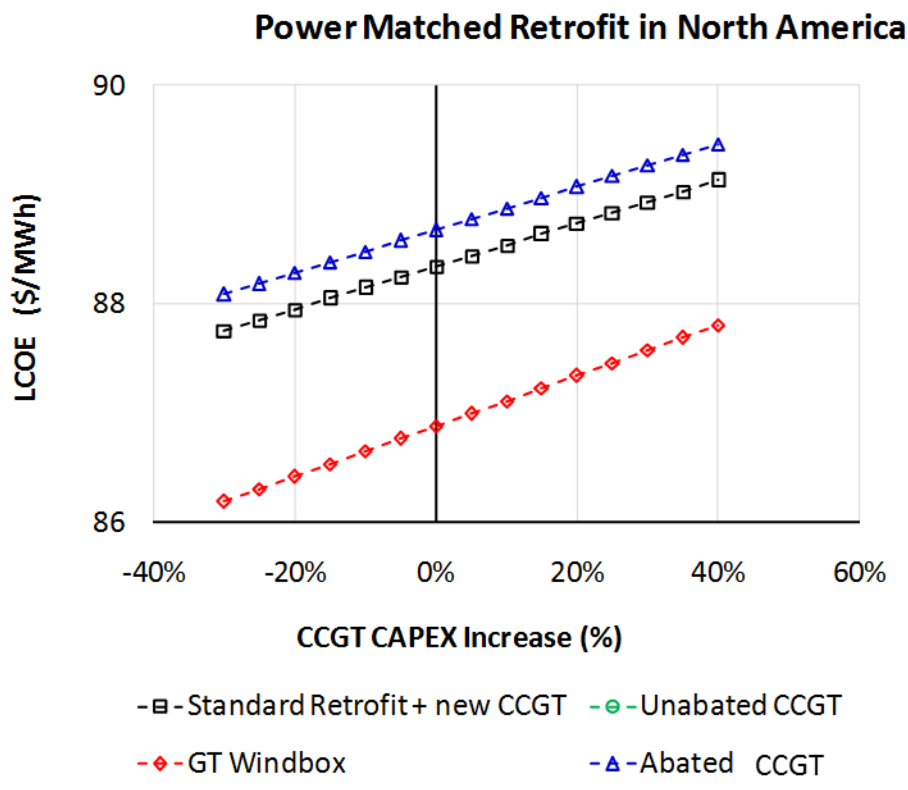

Figure 7.16a.- *Effect of variation in CCGT CAPEX on the LCOE in North America*

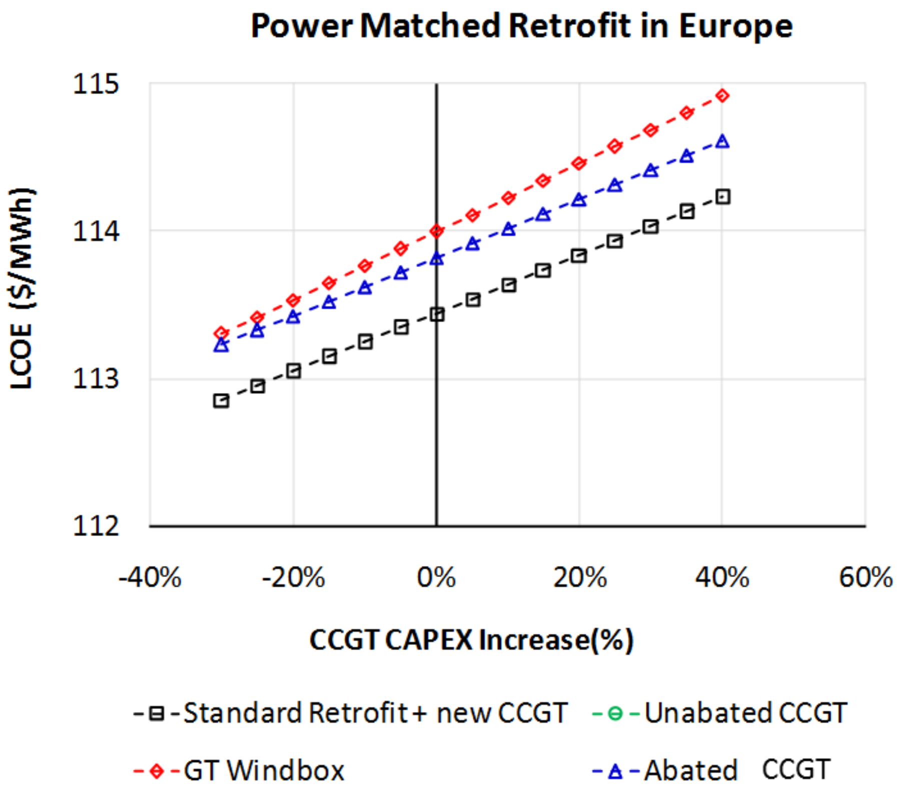

Figure 7.16b.- *Effect of variation in CCGT CAPEX on the LCOE in Europe*

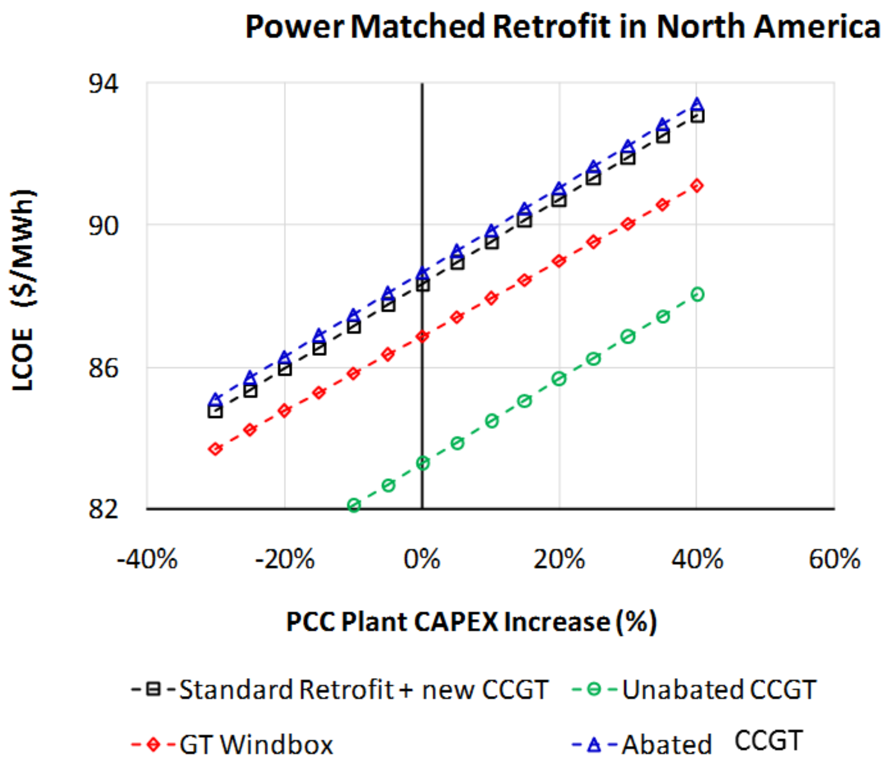

Figure 7.16a.- *Effect of variation in PCC plant CAPEX on the LCOE in North America*

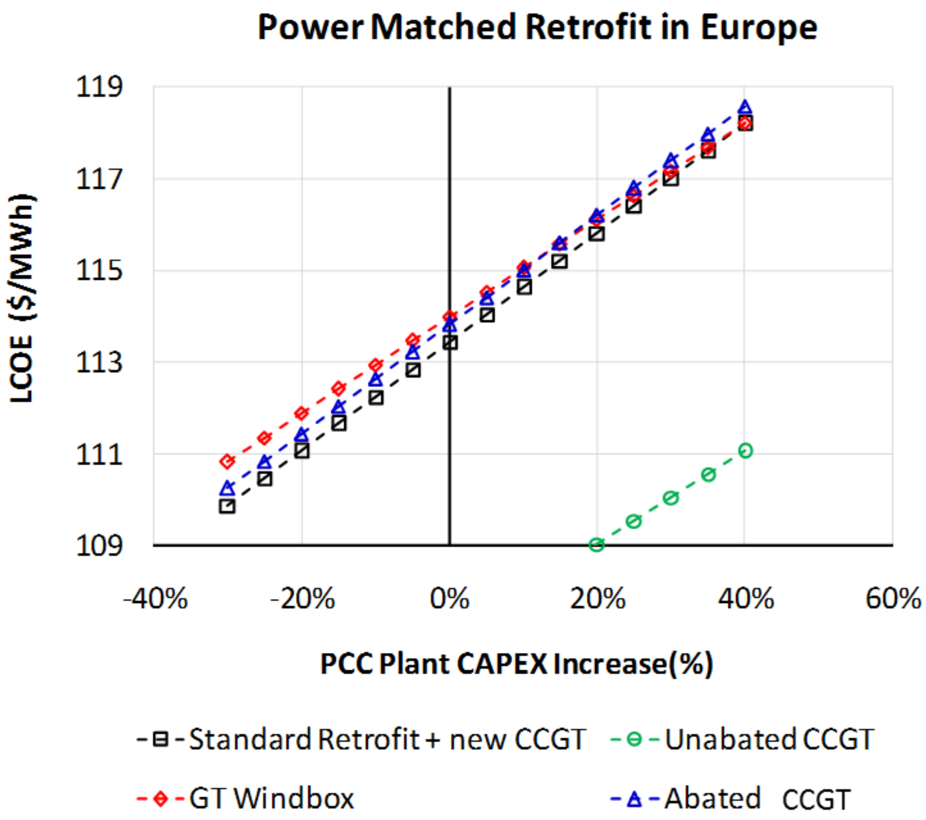

Figure 7.16b.- *Effect of variation in PCC plant CAPEX on the LCOE in Europe*

8.- CONCLUSIONS

8.1.- Thesis overview

Providing the importance of fossil fuels and carbon-intensive industries in our economy carbon capture and storage (CCS) becomes a critical way to reduce green house gas (GHG) emissions.

As previously noted (Chapter 1), *since post-combustion carbon capture (PCC) retrofit systems are added downstream of the flue gas cleaning process of existing power plants, they do not entail substantial modifications of the base plant. Therefore, the contribution of PCC technology to retrofit existing coal plants can play an important role in the deployment of CCS for a fast-track emission mitigation strategy (Chalmers et al. 2009). Previous studies have shown that carbon capture retrofits might be a cost-effective way to reduce CO_2 emissions as the costs associated with a premature closure of the existing plant can be avoided (i.e., decommissioning costs, capital costs of a new built power plant…).*

A common way to retrofit with PCC is to supply all electricity and heat required to operate the capture equipment from the existing steam cycle (a 'standard integrated retrofit). The thermal energy of solvent regeneration is provided by steam extraction from the power cycle and the electricity output of the site is typically reduced. It is, however, possible to avoid a reduction in output with the addition of combined heat and power (CHP) plant to maintain, or even increase, the net site power output. The CHP supplies some or all of the heat and power required for the capture system to treat emissions from both, the combined cycle and the retrofitted coal plant.

The research work of this thesis addresses this potential by focusing on gas turbine power cycles for the repowering and retrofitting with post-combustion carbon capture of subcritical pulverised coal power plants. A radiant type boiler for pulverised coal firing is examined as the base reference boiler configuration.

In order to largely decarbonise the power generation sector the CO_2 emissions from both fuel sources should be captured and compressed. High levels of CO_2 capture in coal boiler retrofits with additional gas turbine (GT) can be achieved by either adding a dedicated PCC plant to the GT plant or by mixing flue gas from both fuel sources and treating them in the same PCC plant, or with a novel CO_2 capture retrofit configuration: a power matched retrofit with the sequential combustion of gas turbine flue gas in the existing coal boiler while capturing carbon emissions from the combustion of coal and natural gas, in other words 'a gas turbine flue gas windbox' retrofit.

A techno-economic comparison of relevant discrete heat and power matched retrofit options with gas turbine power cycles uses a methodology based on an assessment of total revenue requirements from electricity sales and CO2 sales to Enhance Oil Recovery, and includes CO2 emission charges, CO2 selling price for EOR, fuel price, load factor and capital cost. It shows that gas turbine power cycles for repowering and retrofitting with post-combustion capture existing subcritical coal plants can be an attractive option with a higher internal rate of return for an investor-owned utility at natural gas prices currently encountered in North America. At natural gas prices encountered in Europe, they are an attractive option to continue to use existing assets connected to existing plants, gird capacity, transmission and provision of network services, in countries/markets aiming for rapid electrification and decarbonisation at the same time. Gas turbine flue gas windbox retrofit options compare favourably in both markets, especially if the challenges of mixing effectively flue gas from both fuel sources cannot be overcome

8.2.- Summary of findings about the feasibility of the flue gas windbox carbon capture retrofit

This section shows the summary of findings which confirm that sequential combustion in the boiler of an existing subcritical power plant with a gas turbine flue gas windbox is practically feasible.

8.2.1.- Optimisation of the integration between steam cycle of the coal plant and the heat recovery steam generator:

Effective thermodynamic integration between the HRSG and the existing steam cycle is achieved by appropriately sizing an unfired triple pressure HRSG. High pressure (HP) and intermediate pressure (IP) superheated steam generated in the HRSG is injected at the inlet of the HP and IP steam turbine respectively, and large amounts of low pressure (LP) saturated steam is supplied at the pressure required for optimum regeneration of the solvent in the reboiler of the PCC plant. There is no need of either an IP economizer or an IP evaporator as superheated steam taken from the outlet of the HP turbine of the existing steam cycle is injected directly into the HRSG. The absence of the IP evaporator reduces the irreversibilities of the system and increases the natural gas marginal efficiency. The HRSG effectively operates the existing steam turbines as the combined cycle of the CCGT.

8.2.2.- Optimisation of the integration between the steam cycle of the coal power plant and the HRSG and the carbon capture plant:

A dual back pressure turbine retrofit is implemented in this study because it does not require changes in the operation of the IP turbine and cylinder mechanical stress are not increased. It is worth noting that the addition of a back pressure turbine in the extraction line has been studied in detail previously for retrofit of a subcritical plant (Ramezan et al. 2007), and that the addition of a back pressure turbine within the turbine island was implemented (E.ON Kraftwerke GmbH 2010).

Steam extraction for condensate water heating is substituted by heat recovered from the CO_2 compressor intercoolers; so that less steam is extracted from the steam cycle.

8.2.3.- Impact on the subcritical boiler of the coal plant

Because the oxygen content of the gas turbine exhausts is reduced compared to ambient air, the mass flow within the existing boiler is increased in order to be able to sustain the same level of excess air after the combustion of coal in the air/flue gas mixture. Consequently, the average flue gas velocities are increased and erosion problems may take place if retrofitted plants are operated with abrasive high ash coals. In order to reduce the long term impacts to the boiler the coal consumption is reduced so that the flue gas velocities are lowered and erosion problems are diminished.

However, this lowering coal feed rate would cause a reduction in the heat rate absorbed by the furnace, and consequently, a reduction in the steam production, if unmitigated. An unfired triple pressure HRSG is appropriately sized to supply steam directly to the steam turbines and avoid a derating of the HP and IP turbines. Since the amount of steam generated in the HRSG is limited by both the exhaust gas flow rate of the gas turbine and the pinch temperature of the HP evaporator, the coal flow rate is only reduced by 10%. The resultant flue gas flow rate then only increases by 10%.

It should be noted that for certain plants, the existing fans would need to be replaced to accommodate the additional flow, although this needs to be determined on a site by site basis.

The H_2O concentration of the coal boiler flue gas increases when part of the combustion air of the existing plant is replaced by exhaust gas from the gas turbine. The opposite happens to the CO_2 concentration. This change in flue gas composition modifies furnace heat transfer characteristics as follows:

- The adiabatic flame temperature and the furnace exit gas temperature are reduced
- The flue gas temperature to the superheater is reduced
- The amount of heat absorbed in the furnace is reduced

The analysis of heat transfer in the boiler banks also reveals a reduction in radiation and an increase in convective heat transfer.

Despite lower flue gas temperature to the supeheater the steam temperature at the inlet of the HP and IP steam turbines are maintained due to the efficient integration of the HRSG with the steam cycle, attemperators located between the platen superheater (PlatSH) and the final superheater (FSH) and a set of dampers installed at the exit of the boiler.

8.2.4.- Benefits of the GT flue gas windbox retrofit:

Some of the benefits of the GT flue gas windbox retrofit compared to other GT power cycle retrofit options where 90 % of the CO_2 emissions from both coal and gas sources are captured are listed below:

- Lower electricity output and higher marginal efficiency of the combustion of additional natural gas, compared to other gas turbine power cycle retrofit options, and to integrated steam extraction retrofits. This is explained in 8.2.1 and 8.2.2.
- Lower energy requirements of the PCC process

  The CO_2 concentration at the inlet of the carbon capture plant is similar to that of the coal power plant and the total volume of CO_2 to be treated in the carbon capture plant is similar to the air firing case.
- Significant capital cost savings including
  - The gas CHP plant does not have a dedicated combined cycle, the existing steam turbines are operated as the combined cycle of the GT flue gas windbox retrofit.
  - The total volume of CO_2 to be treated in the carbon capture plant is lower and results in capital cost savings of the carbon capture plant.

- Thermal and fuel NOx emissions are expected to reduce due to the lower flame temperature and the reduction in coal flow rate. SOx emissions are expected to decrease as well.
- MEA degradation issues are diminished

  The O_2 concentration at the inlet of the carbon capture plant is the same as that of the coal power plant.

8.2.5.- Disadvantages of the GT flue gas windbox retrofit:

- Significant natural gas consumption

  The retrofitted power plant consumes proportionally a larger amount of natural gas per unit of low carbon electricity compared to other gas turbine power cycle retrofit options. The combustion of natural gas generates more steam than these other options to maintain steam flow rates of the steam turbines. This would may result in higher fuel costs. Although coal consumption is reduced natural gas is, in some places, more expensive than coal.
- Stratification issues:

  If the exhaust gas of the GT only replaces a part of the secondary air of the coal power plant, it needs to be mixed with the rest of the secondary air and stratification issues may occur. However, if the GT flue gas replaces either all of the secondary air or all of the overfire air, this problem would be avoided.

8. 3.- Summary of findings from the techno-economic comparison of carbon capture retrofits with gas turbine power cycles

8.3.1.- Retrofits achieving high levels of CO_2 capture consisting of 90% on both fuel sources

In power matched retrofits, where a coal power plant is retrofitted with a CCGT to maintain the power output of the site while capturing CO_2 from both fuel sources, the EOP is always lower than the EOP of a new CCGT with PCC, except for the GT windbox retrofit.

With regard to the marginal efficiency of the use of natural gas, in the power matched retrofits the efficient integration of the carbon capture plant with the steam cycle of the HRSG and the coal power plant allows a very efficient use of the natural gas and the marginal efficiency reaches high values. On the contrary, in the heat matched retrofits, as there is no heat integration of the carbon capture plant with the steam cycle of the coal power plant the marginal efficiency of the natural gas is low.

The GT windbox retrofit reaches the highest marginal efficiency and the lowest EOP of the power matched retrofits studied in this thesis, as explained in detail in section 8.2.

The economic analysis of the retrofit options with high levels of CO_2 capture indicates that the GT windbox retrofit could have a good potential in North America due to its low total revenue requirement compared to other options. The results of the levelised cost of electricity, internal rate of return and CO_2 avoided costs corroborate this outcome.

A different outcome is achieved in Europe as natural gas is more expensive in the UK than in the USA.

An important outcome of this work is that the GT windbox retrofit seems to be a promising alternative for repowering standard integrated capture retrofits without additional emissions by using the existing capture plant without major modifications. This could be the case, for example of Boundary Dam 3 unit, where a standard integrated retrofit is designed for operation with zero to ~90% capture. The addition of a GT flue gas windbox retrofit would allow full CO_2 capture using the original capture plant and restoring the power output of the site.

8.3.1.- Retrofits for intermediate CO_2 capture levels

Although partial capture can only be an interim stage in achieving full electricity sector decarbonisation, this is currently of interest because of the level of the prevailing emission performance standards (EPS) targets (e.g. 450gCO_2/kWh) in California, the UK, Canada and possibly the USA.

The EOP for options capturing the same amount of CO_2 predominantly depends on the integration of the PCC plant with the steam cycle of the HRSG and the coal plant. Power matched and heat matched retrofits cannot be directly compared since they respond to a different set of requirements with respect to the output of the plant after repowering and retrofitting.

As the best possible scenario for effective integration of steam extraction is considered in this work, with the addition of two back pressure turbines to the existing steam cycle, the marginal efficiency of the natural gas is close to the efficiency of the CCGT for power matched retrofits. On the contrary, heat matched retrofits with a GT and an HRSG supplying thermal energy for solvent regeneration only achieve low marginal efficiency as the steam generated in the HRSG does not produce any power.

The economic analysis of the retrofit options with intermediate levels of CO_2 capture indicates that options meeting the EPS for new fossil fuel power stations achieve the lowest total revenue requirement. Consequently, in order to largely decarbonise the power generation sector carbon emission costs should rise up so that fully CO_2 abated retrofit options become more competitive than unabated options.

8. 4.- Summary of findings from the sensitivity analysis for power matched retrofit options

The sensitivity analysis informs about the specific factors that favour the deployment of GT flue windbox retrofit. With the default cost data assumed in this work the main specific factors are described below:

- Carbon tax:

  The carbon tax at which the LCOE of the coal plant without capture equals that of the GT flue gas windbox retrofit is 59$/t CO_2 in Europe and 45$/t CO_2 in North America. If CO_2 is used for EOR the CO_2 charges are reduced to $40/t CO_2 in Europe and $27/t CO_2 in North America. Carbon tax could be largely reduced if CO_2 is used for EOR, this would increase the speed of CCS deployment for a fast-track emission mitigation strategy.

- CO_2 selling price for EOR:

  If CO_2 could be sold for EOR, the CO_2 selling price at which the LCOE of the coal plant without capture equals to that of the GT flue gas windbox retrofit is 51$/t CO_2 in Europe and 38$/t CO_2 in North America.

- Capital cost of coal power plant upgrades:

  The GT flue gas windbox retrofit might require some upgrades of the coal power plant to cope with the increased flue gas flow rate. Nevertheless, in North America, the LCOE of the GT flue gas windbox retrofit is always lower than power matched retrofits with an abated CCGT despite the extra capital cost. In Europe the economic performance shows that the power matched retrofit with an abated CCGT with flue gas from both fuel sources treated in the same capture plant reaches a lower LCOE than the GT flue gas windbox retrofit. It should be noted that this configuration could lead to higher operating costs due to stratification issues, amine degradation and corrosion of the carbon capture equipment. These operating costs were not considered in the financial model.

- Coal price:

  In North America the GT flue gas windbox retrofit becomes more cost-efficient at high coal prices because of the reduced coal consumption typical from this type of retrofit. In Europe coal price does not have a large influence on the LCOE.

- Natural gas price:

  Natural gas price has a big influence on the economic performance of the GT flue gas windbox retrofit. The low natural gas price in North America increases the potential of the GT flue as windbox retrofit in this country, however, the natural gas price would need to reduce to at least 32$/MWh_th to make the GT flue gas windbox retrofit economically viable in Europe.

8. 5.- Limitations and recommendations for future work

Time was not available within the scope of this study to address all the issues of gas turbine power cycles for retrofitting and repowering coal plants with PCC that have been raised. The following discusses some of the limitations of the work presented here and possible future programmes of work to address them.

a) The research work of this thesis addresses the potential of the GT flue gas windbox retrofit in subcritical coal power plants. The outcome of this research could be extended to:

- Examine repowering and retrofitting with post-combustion capture existing coal plants with supercritical and ultra-supercritical pulverised coal plants.
- Examine repowering existing PCC coal power plants, with either subcritical or supercritical boilers.
- Examine repowering in the context of industrial CCS for steel and iron making processes, refineries and cement plants.

b) The GT flue gas windbox retrofit proposed in this thesis consists of a power matched retrofit that supplies the electrical power required for the capture process and cover any loss in power output to restore the power output of the site. It is important to note that there is an array of possible gas turbine sizes to achieve a power output in between those of heat matched and power matched retrofit or possible lower. The present thesis, however, does no evaluate the off design behaviour of the gas turbine, it just analyses the feasibility of the power matched retrofit concept. It would be of interest to examine the real world implication of natural gas turbine selection.

c) Site specific factors need to be considered to gain a better understanding of project-specific costs under varying geographic and market conditions. For example on the subject of post-combustion carbon capture concerns have been raised about best performing commercially available solvents with advanced process configuration.

d) The aqueous amine scrubbing process is used here as an example of PCC processes, which needs heat for solvent regeneration and power for CO_2 compression and ancillary equipment. The different carbon capture retrofit options evaluated in this thesis can, in principle, be implemented for any PCC process and/or any combination of thermal energy and power requirements.

e) The semi-empirical method suggested by I. E. Dubovsky (Blokh 1988) is used in this thesis to calculate the heat transfer in the boiler furnace. This method is based on equations of radiative transfer and energy balance in the furnace combined with empirical data and experience of boiler operation. The coefficient of radiant absorption used to compute the flame emissivity takes in to account the contribution of the tri-atomic gases, ash particles and burning char particles (Basu et al. 2000). However, radiation scattering by ash particles is not included. The inclusion of this effect is complex and is outside the scope of this study since particle size is difficult to know and the scattering is anisotropic. Future work could include a detailed furnace zone model where absorption and anisotropic scattering are analysed. Recently, semi-empirical methods have started to be replaced by numerical methods with increased level of detail and confidence. The most common numerical method is the zone method. By using these methods the radiative heat transfer in an absorbing, emitting, scattering medium can be analysed.

f) Since the oxygen content in the gas turbine exhaust gases (15%) is lower than in air, the mass flow within the existing boiler is increased in order to maintain the same level of excess oxygen. In order to avoid this increase in flue gas mass flow rate, the coal consumption is reduced. Nevertheless, a reduction in coal consumption leads to lower heat release rate and, consequently, to a reduction in boiler steam flow rates and steam temperature. As an alternative, the oxygen concentration of the flue gas could be increased by an air separation equipment, e.g. air separation membranes, air separation units. Oxygen with high purity level would not be required the air separation membranes might be preferred.

BIBLIOGRAPHY

Austgen, D.M. et al., 1989. Model of Vapor-Liquid Equilibria for Aqueous Acid Gas-Alkanolamine Systems Using the Electrolyte-NRTL Equation? *Ind. Eng. Chem. Res.*, (1967), pp.1060–1073.

Bashadi, S., 2010. Using Auxiliary Gas Power for CCS Energy Needs in Retrofitted Coal Power Plants.

Basu, P., Kefa, C. & Jestin, L., 2000. *Boilers and Burners. Design and theory*, New York: Springer-Verlag.

Bates, R.G. & Pinching, G.D., 1951. Acidic Dissociation Constant and Related Thermodynamic Quantities for Monoethanolammonium Ion in Water From 00 to 500 C. *Journal of Research of the National Bureau of Standards*, 46(5).

Blokh, A.G., 1988. *Heat Transfer In Steam Boiler Furnaces*, New York: Hemisphere Publishing Corporation.

Bozzuto, C.R. et al., 2001. *Engineering feasibility and economics of CO2 capture on an existing coal-fired power plant*, Ohio department of development, Ohio coal development office, US Department of Energy (DOE), National Energy Technology Laboratory (NETL). Report Number PPL-01-CT-09, June, 2001.

CCC, 2009. *Meeting Carbon Budgets – The Need for a Step Change*, Committee on Climate Change; Progress Report to Parliament, October, 2009.

Chalmers, H., Gibbins, J. & Lucquiaud, M., 2009. Retrofitting CO2 capture to existing power plants as a fast track mitigation strategy. In *the 3rd International Conference of Energy Sustainability*. San Francisco, CA, USA, 19-23 July.

Chen, C.-C. & Evans, L.B., 1986. A local composition model for the excess Gibbs energy of aqueous electrolyte systems. *AIChE Journal*, 32(3), pp.444–454. Available at: http://doi.wiley.com/10.1002/aic.690320311.

Chi, S. & Rochelle, G., 2002. Oxidative degradation of monoethanolamine. *Industrial & engineering chemistry research*, 41(17), pp.4178–4186. Available at: http://pubs.acs.org/doi/abs/10.1021/ie010697c.

Colburn, A.P., 1964. A method of correlating forced convection heat-transfer data and a comparison with fluid friction. *International Journal of Heat and Mass Transfer*, 7(12), pp.1359–1384.

Cooke, D.H., 1983. Modeling of off-design multistage turbine pressures by Stodola’s ellipse. In *Energy Incorporated Pepse User’s Group Meeting*. Richmond, Virginia, November, 1983.

DECC, 2011. *Front End Engineering Design study for the UK Carbon Capture and Storage Demonstration Competition*, Available at: http://webarchive.nationalarchives.gov.uk/20121217150422/http://decc.gov.uk/en/content/cms/emissions/ccs/ukccscomm_prog/feed/scottish_power/scottish_power.aspx.

Deng, S., Hynes, R. & Drover, B., 2014. Hybrid Power Generation Plant for CO 2 Capture. *Journal of Engineering for Gas Turbines and Power*, 136(5), p.052001. Available at: http://gasturbinespower.asmedigitalcollection.asme.org/article.aspx?doi=10.1115/1.4026116 [Accessed November 7, 2014].

Desideri, U. & Paolucci, A., 1999. Performance modelling of a carbon dioxide removal system for power plants. *Energy Conversion and Management*, 40(18), pp.1899–1915. Available at: http://linkinghub.elsevier.com/retrieve/pii/S0196890499000746.

Dillon, D. et al., 2013. A Summary of EPRI's Engineering and Economic Studies of Post Combustion Capture Retrofit Applied at Various North American Host Sites. *Energy Procedia*, 37, pp.2349–2358. Available at: http://linkinghub.elsevier.com/retrieve/pii/S1876610213003597 [Accessed November 7, 2014].

DOE/NETL, 2007. *Carbon Dioxide Capture from Existing Coal-Fired Power Plants*, US Deparment of Energy (DOE), National Energy Technology Laboratory (NETL). Report Number 401/110907, November, 2007.

DOE/NETL, 2012. *Coal Specifications for Quality Guidelines*, US Deparment of Energy (DOE), National Energy Technology Laboratory (NETL). Report Number 401/012111, January, 2012.

DOE/NETL, 2013. *Cost and Performance Baseline for Fossil Energy Plants Volume 1: Bituminous Coal and Natural Gas to Electricity*, US Deparment of Energy (DOE), National Energy Technology Laboratory (NETL). Report Number 2010/1397, Revision 2a, September, 2013.

E.ON Kraftwerke GmbH, 2010. Wilhelmshaven power plant. Available at: http://apps.eon.com/documents/Broschuere_Wilhelmshaven_Internet_engl.pdf.

Edwards, T.J. et al., 1978. Vapor-liquid equilibria in multicomponent aqueous solutions of volatile weak electrolytes. *AIChE Journal*, 24(6), pp.966–976. Available at: http://doi.wiley.com/10.1002/aic.690240605.

EIA, 2015a. Average costs for fossil fuel for electricity generation. Available at: http://www.eia.gov/electricity/data.cfm#avgcost.

EIA, 2015b. Henry Hub Natural Gas Spot Price. Available at: http://www.eia.gov/dnav/ng/hist/rngwhhdD.htm.

EPA, 1994. *An Operator ' s Guide To Eliminating Bias In CEM Systems*, EPA/430/R-94-016, November, 1994.

EPA, 1974. *Procedures for measurement in stratified gases. Volume I*, EPA-650/2-74-086-a, September, 1974.

EPA, 2014. *Regulatory Impact Analysis for the Proposed Carbon Pollution Guidelines for Existing Power Plants and Emission Standards for Modified and Reconstructed Power Plants*, Available at: http://www2.epa.gov/sites/production/files/2014-06/documents/20140602ria-clean-power-plan.pdf.

EPRI, 1988. *Repowering Options Study*, Report number AP-5611, Jnauary, 1988.

EPRI, 1987a. *Repowering Reheat Units With Gas Turbines*, Report number AP-5216, May, 1987.

EPRI, 1986. *TAG - Technical Assessment Guide: Electricity Supply*, Palo Alto, CA, 1986.

EPRI, 1987b. *TAG - Technical Assessment Guide: Fundamentals and Methods Supply*, Palo Alto, CA, 1987.

Escosa, J.M. & Romeo, L.M., 2009. Optimizing CO2 avoided cost by means of repowering. *Applied Energy*, 86, pp.2351–2358. Available at: http://dx.doi.org/10.1016/j.apenergy.2009.02.015.

European Commission, 2011. *Roadmap for moving to a competitive low carbon economy in 2050*, Report number COM 2011/112, March, 2011.

Federalregister.gov, 2014a. Carbon Pollution Emission Guidelines for Existing Stationary Sources: Electric Utility Generating Units. Available at: https://www.federalregister.gov/articles/2014/06/18/2014-13726/carbon-pollution-emission-guidelines-for-existing-stationary-sources-electric-utility-generating.

Federalregister.gov, 2014b. Standards of Performance for Greenhouse Gas Emissions From New Stationary Sources: Electric Utility Generating Units. Available at: https://www.federalregister.gov/articles/2014/01/08/2013-28668/standards-of-performance-for-greenhouse-gas-emissions-from-new-stationary-sources-electric-utility.

Freguia, S., 2002. *Modeling of CO2 removal from flue gases with monoethanolamine*. Master Thesis, University of Texas, Austin. Available at: http://www.che.utexas.edu/rochelle_group/Pubs/FreguiaPubThesis.pdf.

GE Power Systems, 2000a. *Combined-Cycle Development, Evolution and Future*, Report number GER-4206, October, 2000. Available at: http://physics.oregonstate.edu/~hetheriw/energy/topics/doc/elec/natgas/cc/combined cycle development evolution and future GER4206.pdf.

GE Power Systems, 2000b. *GE Gas Turbine Performance Characteristics*, Report Number GER 3567H, Schenectady, NY, October, 2000.

GE Power Systems, 1994. *Performance and economic considerations of repowering steam power plants*, Report Number GER-3644D, 1994.

Gibbins, J. & Crane, R., 2004. Scope for reductions in the cost of CO2 capture using flue gas scrubbing with amine solvents. *Proceedings of the Institution of Mechanical Engineers, Part A: Journal of Power and Energy*, 218(4), pp.231–239. Available at: http://pia.sagepub.com/lookup/doi/10.1243/0957650041200678 [Accessed November 8, 2014].

Gibbins, J., Crane, R. & Lambropoulos, D., 2004. Maximising the effectiveness of post-combustion CO2 capture systems. In *7th International Conference on Greenhouse Gas Control Technologies*. 5-9 September 2004, Vancouver, Canada.

Global CCS Institute, 2014a. Large Scale CCS Projects. Available at: http://www.globalccsinstitute.com/projects/large-scale-ccs-projects.

Global CCS Institute, 2014b. Petra Nova Carbon Capture Project (formerly NRG Energy Parish CCS Project). Available at: http://www.globalccsinstitute.com/project/petra-nova-carbon-capture-project.

Global CCS Institute, 2012. Selling CO2 for enhanced oil recovery key for initial commercialisation of CCS. Available at: http://www.globalccsinstitute.com/insights/authors/davidhanly/2012/10/29/selling-co2-enhanced-oil-recovery-key-initial.

Goff, G.S. & Rochelle, G.T., 2004. Monoethanolamine degradation: O_2 mass transfer effects under CO_2 capture conditions. *Industrial & Engineering Chemistry Research*, 43(20), pp.6400–6408. Available at: WOS:000224074200016.

Government, 2015. Quarterly Energy Prices. Available at: https://www.gov.uk/government/collections/quarterly-energy-prices.

Grimison, E.D., 1937. Correlation and Utilization of New Data of Flow Resistance and Heat Transfer for Crossflow of Gases over Tube Banks. *Journal Heat Transfer*, 59, pp.583–594.

Hewitt, G.F., Shires, G.L. & Bott, T.R., 2000. *Process Heat Transfer*, Behel House. Available at: http://books.google.co.uk/books/about/Process_Heat_Transfer.html?id=OztADyim4XcC&pgis=1 [Accessed March 16, 2015].

HM Government, 2007. *Meeting the Energy Challenge A White Paper on Energy*, London: Stationery Office.

HM Revenue & Customs, 2014. *Carbon price floor : reform and other technical amendments Operative date*, Available at: https://www.gov.uk/government/publications/carbon-price-floor-reform.

Holman, J.P., 1991. *Heat Transfer*, New York: McGraw Hill.

Hottel, H.C. & Sarofim, A.F., 1967. *Radiative Transfer* Edition 3., New York: McGraw-Hill Book Company Inc.

Huge, E.C., 1937. "Experimental Investigation of Effects of Equipment Size on Convection Heat Transfer and Flow Resistance in Cross Flow of Gases Over Tube Banks. *Journal of Dynamic Systems, Measurement and Control*, 59(Series G), pp.573–581.

Huijbregts, W.M.M. & Leferink, R.G.I., 2004. Latest advances in the understanding of acid dewpoint corrosion: corrosion and stress corrosion cracking in combustion gas condensates. *Anti-Corrosion Methods and Materials*, 51(3), pp.173–188.

IEA, 2012. *CCS Retrofit: Analysis of the Global Installed Power Plant Fleet*, OECD/IEA 2012, Paris.

IEA, 2010. *Energy Technology Perspectives 2010*, OECD/IEA 2010, Paris.

IEAGHG, 2004. *Improvement in power generation with post-combustion capture of CO2*, Report Number PH4/33, November, 2004.

IEAGHG, 2011. *"Retrofitting CO2 Capture to Existing Power Plants,"* Report Number 2011/02, May, 2011.

IPCC, 2013. *Climate Change 2013: The Physical Science Basis. Contribution of Working Group I to the Fifth Assessment Report of the Intergovern- mental Panel on Climate Change [Stocker, T.F., D. Qin, G.-K. Plattner, M. Tignor, S.K. Allen, J. Boschung, A. Nauels, Y. Xi*, Cambridge University Press, Cambridge, United Kingdom and New York, NY, USA.

IPCC, 2014. *IPCC Climate Change 2014 Synthesis Report*,

Kitto, J.B. & Stultz, S.C., 2005. *Steam, Its Generation and Use* 41st ed., Barberton, Ohio: Babcock & Wilcox Co.

Lawson, G.L., Cummings, A.L. & Mecum, S., 2003. Amine plant corrosion reduced by removal of bicine. In *Gas Processors Association*. San Antonio, Texas, USA, March, 2003, pp. 1–7.

Lucquiaud, M., 2010. STEAM CYCLE OPTIONS FOR CAPTURE - READY POWER PLANTS , RETROFITS AND FLEXIBLE OPERATION WITH POST - COMBUSTION CO 2 CAPTURE. , (July 2010).

Lucquiaud, M. & Gibbins, J., 2011a. Effective retrofitting of post-combustion CO2 capture to coal-fired power plants and insensitivity of CO2 abatement costs to base plant efficiency. *International Journal of Greenhouse Gas Control*, 5(3), pp.427–438.

Lucquiaud, M. & Gibbins, J., 2011b. On the integration of CO2 capture with coal-fired power plants: A methodology to assess and optimise solvent-based post-combustion capture systems. *Chemical Engineering Research and Design*, 89(9), pp.1553–1571.

Lucquiaud, M. & Gibbins, J., 2011c. Steam cycle options for the retrofit of coal and gas power plants with postcombustion capture. *Energy Procedia*, 4, pp.1812–1819.

Ma'mun, S. et al., 2005. Solubility of Carbon Dioxide in 30 mass % Monoethanolamine and 50 mass % Methyldiethanolamine Solutions. *Journal of Chemical & Engineering Data*, 50(2), pp.630–634. Available at: http://pubs.acs.org/doi/abs/10.1021/je0496490.

McAdams, W.H., 1954. *Heat Transmission* 3rd editio., New York: McGraw-Hill Inc.

Meldon, J.H., 2011. Amine screening for flue gas CO 2 capture at coal-fired power plants: Should the heat of desorption be high, low or in between? *Current Opinion in Chemical Engineering*, 1(1), pp.55–63. Available at: http://dx.doi.org/10.1016/j.coche.2011.08.006.

Mimura, T. et al., 1997. Development of energy saving technology for flue gas carbon dioxide recovery in power plant by chemical absorption method and steam system. *Energy Conversion and Management*, 38(96), pp.S57–S62. Available at: http://linkinghub.elsevier.com/retrieve/pii/S0196890496002464.

Mimura, T. et al., 1995. Research and development on energy saving technology for flue gas carbon dioxide recovery and steam system in power plant. *Energy Conversion and Management*, 36(6-9), pp.397–400.

Mock, B., Evans, L.B. & Chen, C.-C., 1986. Thermodynamic representation of phase equilibria of mixed-solvent electrolyte systems. *AIChE Journal*, 32(10), pp.1655–1664. Available at: http://doi.wiley.com/10.1002/aic.690321009.

NETL, 2013. *NRG Energy : W . A . Parish Post-Combustion CO2 Capture and Sequestration Project*, Project Number FE0003311, September, 2013.

Oexmann, J., 2011. *Post Combustion CO 2 Capture : Energetic Evaluation of Chemical Absorption Processes in Coal Fired Steam Power Plants*. PhD Thesis, University of Hamburg - Harburg, Bremen, January 2011.

Parsons, E., Shelton, W. & Lyons, J., 2002. Advanced fossil power systems comparison study. *National Energy Technology …*. Available at: http://netl.doe.gov/publications/others/techrpts/AdvFossilPowerSysCompStudy.pdf.

Pellegrini, L. a., Moioli, S. & Gamba, S., 2011. Energy saving in a CO2 capture plant by MEA scrubbing. *Chemical Engineering Research and Design*, 89(9), pp.1676–1683. Available at:

http://linkinghub.elsevier.com/retrieve/pii/S0263876210002959 [Accessed November 8, 2014].

Pfaff, I., Oexmann, J. & Kather, A., 2010. Optimised integration of post-combustion CO2 capture process in greenfield power plants. *Energy*, 35(10), pp.4030–4041.

Pierson, O.L., 1937. Experimental Investigation of the Influence of Tube Arrangement on Convection Heat Transfer and Flow Resistance in Cross Flow of Gases Over Tube Banks. *Journal of Dynamic Systems, Measurement and Control*, 59(Series G), pp.563–572.

Ramezan, M. et al., 2007. *Carbon Dioxide Capture from Existing Coal-Fired Power Plants.*, US Deparment of Energy (DOE), National Energy Technology Laboratory (NETL). Report Number DOE/NETL-401/110907, November, 2007.

Rao, A.B. & Rubin, E.S., 2002. A Technical, Economic, and Environmental Assessment of Amine-Based CO 2 Capture Technology for Power Plant Greenhouse Gas Control. *Environmental Science & Technology*, 36(412), pp.4467–4475. Available at: http://dx.doi.org/10.1021/es0158861.

Rao, A.B. & Rubin, E.S., 2006. Identifying cost-effective CO 2 control levels for amine-based CO 2 capture systems. *Industrial and Engineering Chemistry Research*, 45(8), pp.2421–2429.

Razi, N., Svendsen, H.F. & Bolland, O., 2013. Validation of mass transfer correlations for CO2 absorption with MEA using pilot data. *International Journal of Greenhouse Gas Control*, 19, pp.478–491. Available at: http://dx.doi.org/10.1016/j.ijggc.2013.10.006.

Romeo, L.M., Bolea, I. & Escosa, J.M., 2008. Integration of power plant and amine scrubbing to reduce CO2 capture costs. *Applied Thermal Engineering*, 28(8-9), pp.1039–1046. Available at: http://linkinghub.elsevier.com/retrieve/pii/S1359431107002189 [Accessed November 21, 2014].

Romeo, L.M., Espatolero, S. & Bolea, I., 2008. Designing a supercritical steam cycle to integrate the energy requirements of CO2 amine scrubbing. *International Journal of Greenhouse Gas Control*, 2(4), pp.563–570. Available at: http://linkinghub.elsevier.com/retrieve/pii/S1750583608000261 [Accessed November 28, 2014].

Rubin, E.S. et al., 1991. *Modeling of Integrated Environmental Control Systems for Coal-Fired Power Plants*, Final Report prepared by Camegie Mellon University for U.S.; Department of Energy Pittsburgh Energy Technology Center: Pittsburgh, PA, May 1991.

Rubin, E.S., 2012. Understanding the pitfalls of CCS cost estimates. *International Journal of Greenhouse Gas Control*, 10, pp.181–190.

Sanchez Fernandez, E. et al., 2014. Thermodynamic assessment of amine based CO2 capture technologies in power plants based on European Benchmarking Task Force methodology. *Fuel*, 129, pp.318–329. Available at: http://dx.doi.org/10.1016/j.fuel.2014.03.042.

Schobeiri, M.T., 2012. *Turbomachinery Flow Physics and Dynamic Performance* Second and., Springer Berlin Heidelberg.

Scottish PowerCCS Consortium, 2011. Front End Engineering Design study for the UK Carbon Capture and Storage Competition. Available at: http://www.decc.gov.uk/en/content/cms/emissions/ccs/ukccscomm_prog/feed/scottish_power/scottish_power.aspx.

Sherwood, T.K. & Pigford, R.L., 1952. *Absorption and Extraction* McGraw-Hill, ed., New York-London. Available at: http://www.sciencemag.org/content/116/3006/156.1.citation [Accessed June 23, 2015].

Simbeck, D., 2000. Update of New Power Plant CO2 Control Options Analysis. In *5th International Conference on Greenhouse Gas Control Technologies*. Cairns, Australia, 12-15 Aug.

Simbeck, D. & McDonald, M., 2000. Existing coal power plant retrofit CO2 control options analysis. In *5th International Conference on Greenhouse Gas Control Technologies*. Cairns, Australia, 12-15 Aug.

Singh, D. et al., 2003. Techno-economic study of CO2 capture from an existing coal-fired power plant: MEA scrubbing vs. O2/CO2 recycle combustion. *Energy Conversion and Management*, 44(19), pp.3073–3091. Available at: http://linkinghub.elsevier.com/retrieve/pii/S0196890403000402 [Accessed December 4, 2014].

Specker, S., Phillips, J. & Dillon, D., 2009. The potential growing role of post-combustion CO2 capture retrofits in early commercial applications of CCS to coal-fired power plants. In *MIT Coal Retrofit Symposium*. Bostom, USA. Available at: https://mitei.mit.edu/system/files/specker-retrofits.pdf [Accessed November 7, 2014].

Stenzel, W., Sopocy, D., Pace, S., 1997. *Repowering Existing Fossil Steam Plants*, SEPRIL Generating Power Solutions.

UK Parliament, 2013. *Energy Act 2013*, Available at: http://www.iea.org/policiesandmeasures/pams/switzerland/name.

Vevelstad, S.J. et al., 2014. Oxygen and Temperature Effect on Formation of Degradation Compounds from MEA. *Energy Procedia*, 63(1876), pp.957–975. Available at: http://linkinghub.elsevier.com/retrieve/pii/S1876610214019201.

WorleyParsons, 2005. *Steam Conditions for PC Plant Designs Market Based Advanced Coal Power Systems Comparison Study*,

Zhai, H., Ou, Y. & Rubin, E.S., 2015. Opportunities for Decarbonizing Existing U.S. Coal-fired Power Plants via CO2 Capture, Utilization and Storage. *Environmental Science & Technology*, p.150529131040006. Available at: http://pubs.acs.org/doi/abs/10.1021/acs.est.5b01120.

APPENDIX I.- DESIGN BASIS

This section gives an overview of the basic engineering data used for the study basis.

Boiler performance specifications were based on the report "Cost and Performance Baseline for Fossil Energy Plants" published by NETL **(DOE/NETL 2013)**. They were selected based on a survey of boiler and steam turbine original equipment manufacturers for commercial projects in the US with subcritical units **(WorleyParsons 2005).**

The final boiler design will have to efficiently meet the specifications with a minimum of surface, materials and flow losses.

A1.1.- Coal Specifications

The design fuel consists of a high volatile bituminous coal, Illinois No. 6, which specifications are presented in the report titled "Coal Specifications for Quality Guidelines" **(DOE/NETL 2012)** and has been reported previously in other studies dating back to 1996. Table A1.1 shows the Proximate and Ultimate Analysis results of the Design Coal, Illinois No. 6:

Table A-1.- Design Coal Analysis (DOE/NETL 2012).

Rank		Bituminous
Seam		Illinois No.6 (Herrin)
Source		Old Ben Mine
Proximate Analysis (as received) (Note A)		
Moisture	weight %	11,12
Ash	weight %	9,70
Volatile Matter	weight %	34,99
Fixed Carbon	weight %	44,19
Total	weight %	100,00
HHV	kJ/kg	27,11
HHV	Btu/lb	11,67
LHV	kJ/kg	26,15
LHV	Btu/lb	11,25
Ultimate Analysis (weight %)		
Moisture	weight %	11,12
Carbon	weight %	63,75
Hydrogen	weight %	4,50
Nitrogen	weight %	1,25
Chlorine	weight %	0,29
Sulfur	weight %	2,51
Ash	weight %	9,70
Oxygen (Note B)	weight %	6,88
Total	weight %	100,00
NOTES:		
A. The proximate analysis assumes sulfur as volatile		
B. By difference		

As coal loss in ignition is not specified in **(DOE/NETL 2012)**, a value of 4% has been selected from other studies where the subciritical coal-fired power plants were also burning Illinois No. 6 coal (Sargent & Lundy (2009)). A loss in ignition of 4% will produce an unburned carbon energy loss of 0.5%.

Figure A1.1 illustrates the Van Krevelen diagram which reveals that Illinois No. 6 is a high volatile bituminous coal.

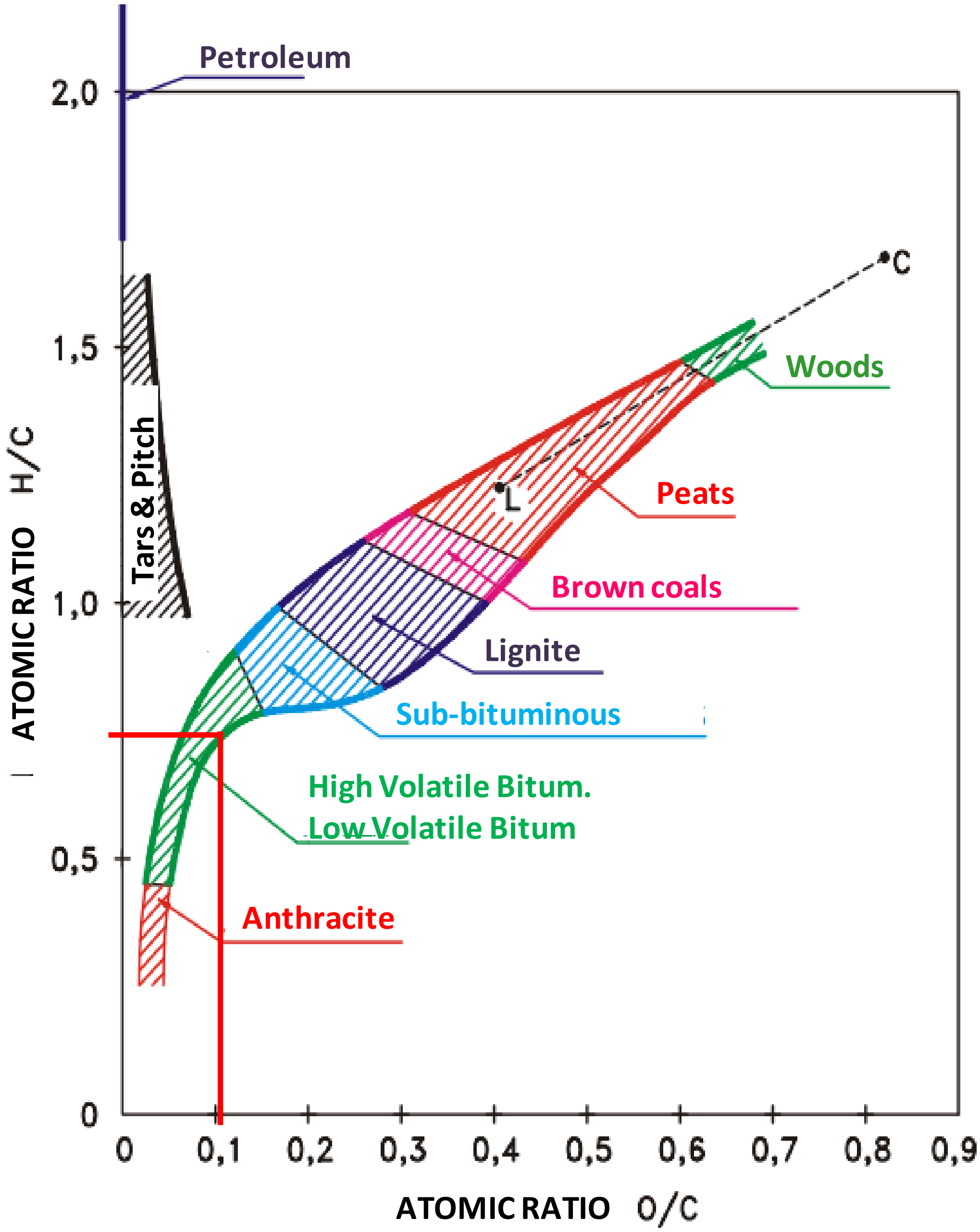

Figure A1.1- *Fuel Classification according to Van Krevelen diagram.*

Table A1.2 shows the ash mineral analysis of the Design Coal.

Table A1.2.- Ash Mineral Analysis (DOE/NETL 2012).

Typical Ash Mineral Analysis		
Silica (SiO_2)	weight %	45,0
Aluminum Oxide (Al_2O_3)	weight %	18,0
Titanium Dioxide (TiO_2)	weight %	1,0
Iron Oxide (Fe_2O_3)	weight %	20,0
Calcium Oxide (CaO)	weight %	7,0
Magnesium Oxide (MgO)	weight %	1,0
Sodium Oxide (Na_2O)	weight %	0,6
Potassium Oxide (K2O)	weight %	1,9
Phosphorus Pentoxide (P_2O_5)	weight %	0,2
Surfur Trioxide (SO_3)	weight %	3,5
Undetermined	weight %	1,8
Typical Ash Fusion Temperature		
Reducing		
Initial - Limted deformation	K	1474
Softening	K	1511
Hemispherical	K	1558
Fluid	K	1597
Oxidizing		
Initial - Limted deformation	K	1505
Softening	K	1533
Hemispherical	K	1605
Fluid	K	1616

Based on ash chemical composition coal ash can be classified as:

- Lignitic ash: when the sum of CaO and MgO is higher than Fe_2O_3.
- Bituminous ash: when there is more Fe_2O_3 than the sum of CaO and MgO.

Due to the high Fe_2O_3 concentration in ash the design coal ash is classified as bituminous.

Coal ash can also be classified as either acidic or basic depending on its components. Acidic components are aluminium, titanium and silicon and Basic components are iron, calcium, magnesium, sodium and potassium. Then, the expression for the base to acid ratio is as follows:

$$\frac{Base}{Acid} = \frac{Fe_2O_3 + CaO + MgO + Na_2O + K_2O}{SiO_2 + Al_2O_3 + TiO_2} = \frac{30.5}{64} = 0.48 \qquad [A1.1]$$

The base to acid ratio reflects the tendency of the ash to form compounds with low melting temperatures. This parameter allows us to determine the slagging and fouling indexes.

Slagging index – bituminous ash (Rs):

The slagging index indicates the likelihood of formation of molten, partially fused or resolidified deposits on furnace walls and other surfaces exposed to radiant heat. It depends on two parameters, the weight percent, on a dry basis, of the sulphur content in coal and the base to acid ratio.

$$R_s = \frac{Base}{Acid} \cdot S \qquad [A1.2]$$

Classification of slagging potential:

- Rs < 0.6 = low
- **0.6 < Rs < 2.0 = medium**
- 2.0 < Rs < 2.6 = high
- 2.6 < Rs = severe

The slagging index of the design coal is 1.34, therefore, the level of slagging potential is medium.

Fouling index – bituminous ash (Rf)

The fouling index indicates the likelihood of formation of high temperature bonded deposits on convection heat absorbing surfaces not exposed to radiant heat. It depends on two parameters, the weight percent of sodium content in the coal ash and the base to acid ratio.

$$R_f = \frac{Base}{Acid} \cdot Na_2O \qquad [A1.3]$$

Classification of fouling potential:

- Rf < 0.2 = low
- **0.2 < Rf < 0.5 = medium**
- 0.5 < Rf < 1.0 = high
- 1.0 < Rf = severe

The fouling index of the design coal is 0.28, therefore, the level of fouling potential is medium.

A1.2.- Natural Gas Specifications

Natural Gas is utilised as the main fuel in the turbine gas of the carbon capture retrofit and its composition is shown in Table A1.3 **(DOE/NETL 2013).**

Table A1.3.- Design Natural Gas Analysis (DOE/NETL 2013)

Natural Gas Composition		
Methane	volume %	93,1
Ethane	volume %	3,2
Propane	volume %	0,7
n-Butane	volume %	0,4
Carbon Dioxide	volume %	1,0
Nitrogen	volume %	1,6
Total	volume %	100,0
LHV	kJ/kg	47,5
LHV	Btu/lb	20,4
HHV	kJ/kg	52,6
HHV	Btu/lb	22,6
NOTE Fuel composition is normalized and heating values were calculated		

A1.3.- Air Specifications

Performance calculations are based on ambient conditions of 10 C, 60% relative humidity and 1.013 bar. Table A1.4 indicates the composition of dry and wet air.

Table A1.4.- Air composition.

DRY AIR COMPOSITION		
Oxygen	volume %	20.90
Argon	volume %	0.90
Carbon Dioxide	volume %	0.03
Nitrogen	volume %	78.17
Molecular Weight	g/mol	28.96
WET AIR COMPOSITION		
Moisture	volume %	1.01
Oxygen	volume %	20.69
Argon	volume %	0.89
Carbon Dioxide	volume %	0.03
Nitrogen	volume %	77.38
Molecular Weight	g/mol	28.85

A1.4.- Performance data – Existing pulverised coal power plant

The following tables indicate the main operating data of air-gas cycle and water-steam cycle **(DOE/NETL 2013)**.

Table A1.5.- Combustion data and mills and air-preheaters operating data (DOE/NETL 2013).

COMBUSTION DATA		
Combustion Primary Air Flow Rate	kg/s	127.60
Combustion Secondary Air Flow Rate	kg/s	415.30
Infiltration Air Flow Rate	kg/s	9.60
MILLS DATA		
Primary Air + Coal Temperature - Mill Outlet *	K	353.15
Coal Temperature - Mill Inlet	k	288.15
AIR-PREHEATERS DATA		
Primary Air leaks	kg/s	17.60
Primary Air Temperature - PAP Inlet	K	299.00
Primary Air Pressure - PAP Inlet	bar	1.11
Secondary Air leaks	kg/s	12.30
Secondary Air Temperature - SAP Inlet	K	292.00
Secondary Air Pressure - SAP Inlet	bar	1.05
Dilutted Gas Temperature - Preheaters outlet	K	443.00
Gas Pressure - Preheaters outlet	psia	0.99
PA FAN		
Primary Air Temperature - PA Fan Inlet	K	288.15
Primary Air Pressure - PA Fan Inlet	bar	1.01
Primary Air Temperature - PA Fan Outlet	K	299.00
Primary Air Pressure - PA Fan Outlet	bar	1.11
SA FAN		
Secondary Air Temperature - SA Fan Inlet	K	288.00
Secondary Air Pressure - SA Fan Inlet	bar	1.01
Secondary Air Temperature - SA Fan Outlet	K	292.00
Secondary Air Pressure - SA Fan Outlet	bar	1.05
ESP		
Gas Temperature Outlet	K	442.59
Gas Pressure Outlet	bara	0.98
INDUCED FAN		
Gas Temperature Outlet	K	453.93
Gas Pressure Outlet	bara	1.05
FGD		
Gas Temperature Outlet	K	330.37
Gas Pressure Outlet	bara	1.02

NOTE*: Assumptions. Information not specified in **(DOE/NETL 2013)**

Table A1.6.- Boiler operating data (DOE/NETL 2013).

BOILER DATA		
ECONOMISER		
Water Pressure Inlet	bara	213.80
Water Temperature Inlet	K	524.50
Water Pressure Outlet *	bara	211.00
Water Temperature Outlet *	K	598.40
DRUM		
Temperature *	K	643.40
Pressure *	bara	211.00
PRIMARY SUPERHEATER		
Steam Temperature Inlet *	K	649.40
Steam Pressure Inlet *	bara	199.90
Steam Temperature Outlet *	K	679.60
Steam Pressure Outlet *	bara	188.70
PLATEN SUPERHEATER		
Steam Temperature Inlet *	K	670.00
Steam Pressure Inlet *	bara	188.70
Steam Temperature Outlet *	K	743.00
Steam Pressure Outlet *	bara	177.60
FINAL SUPERHEATER		
Steam Temperature Inlet *	K	731.40
Steam Pressure Inlet *	bara	177.60
Steam Temperature Outlet	K	838.70
Steam Pressure Outlet	bara	166.50
REHEATER		
Steam Temperature Inlet	K	42.80
Steam Pressure Inlet	bara	636.50
Steam Temperature Outlet	K	40.00
Steam Pressure Outlet	bara	838.70
ATTEMPERATION		
Temperature	K	452.00
Pressure	bara	214.00
Inferior Attemperation Flow Rate *	kg/s	11.60
Superior Attemperation Flow Rate *	kg/s	7.80

NOTE*: Assumptions. Information not specified in **(DOE/NETL 2013)**

Table A1.7.- Feed water heaters train operating data, Part I (DOE/NETL 2013).

FEED WATER HEATERS TRAIN DATA		
HIGH PRESSURE FEED WATER HEATERS		
Steam Extraction Pressure - HP Steam Turbine	bara	42.78
Steam Extraction Pressure - Feed Water Heater 7 Inlet	bara	40.66
Steam Extraction Temperature - HP Steam Turbine / Feed Water Heater 7 Inlet	K	634.59
Drainage Temperature - Feed Water Heater 7 Outlet	K	497.70
Drainage Pressure - Feed Water Heater 7 Outlet	bara	25.28
Water Pressure - Feed Water Heater 7 Inlet	bara	214.12
Water Temperature - Feed Water Heater 7 Inlet	K	492.15
INTERMEDIATE PRESSURE FEED WATER HEATERS		
Steam Extraction Pressure - IP Steam Turbine	bara	24.17
Steam Extraction Pressure - Feed Water Heater 6 Inlet	bara	22.27
Steam Extraction Temperature - IP Steam Turbine / Feed Water Heater 6 Inlet	K	764.20
Drainage Temperature - Feed Water Heater 6 Outlet	K	457.93
Drainage Pressure - Feed Water Heater 6 Outlet	bara	22.27
Water Pressure - Feed Water Heater 6 Inlet	bara	214.46
Water Temperature - Feed Water Heater 6 Inlet	K	452.37
DEAERATOR		
Steam Extraction Pressure - IP Steam Turbine	bara	11.33
Steam Extraction Pressure - Deaerator Inlet	bara	8.96
Steam Extraction Temperature - IP Steam Turbine / Deaerator Inlet	K	659.87
Water Temperature - Deaerator Inlet / Feed Water Heater 4 Outlet	K	413.54
Water Pressure - Deaerator Inlet / Feed Water Heater 4 Outlet	bara	15.17
Water Flow - Deaerator Inlet / Feed Water Heater 4 Outlet	kg/s	389.00
Water Temperature - Deaerator Outlet (before pump)	K	448.32
Water Pressure - Deaerator Outlet (before pump)	bara	8.96

Table A1.8.- Feed water heaters train operating data, Part II (DOE/NETL 2013).

FEED WATER HEATERS TRAIN DATA		
LOW PRESSURE FEEDWATER HEATERS		
Steam Extraction Pressure - LP Steam Turbine	bara	4.43
Steam Extraction Pressure - Feed Water Heater 4 Inlet	bara	3.95
Steam Extraction Temperature - LP Steam Turbine / Feed Water Heater 4 Inlet	K	546.93
Drainage Temperature - Feed Water Heater 4 Outlet	K	404.09
Drainage Pressure - Feed Water Heater 4 Outlet	bara	2.78
Water Pressure - Feed Water Heater 4 Inlet	bara	15.86
Water Temperature - Feed Water Heater 4 Inlet	K	398.54
Steam Extraction Pressure - LP Steam Turbine	bara	2.87
Steam Extraction Pressure - Feed Water Heater 3 Inlet	bara	2.56
Steam Extraction Temperature - LP Steam Turbine / Feed Water Heater 3 Inlet	K	499.37
Drainage Temperature - Feed Water Heater 3 Outlet	K	366.76
Drainage Pressure - Feed Water Heater 3 Outlet	bara	0.81
Water Pressure - Feed Water Heater 3 Inlet	bara	16.20
Water Temperature - Feed Water Heater 3 Inlet	K	361.21
Steam Extraction Pressure - LP Steam Turbine	bara	0.81
Steam Extraction Pressure - Feed Water Heater 2 Inlet	bara	0.72
Steam Extraction Temperature - LP Steam Turbine / Feed Water Heater 2 Inlet	K	382.37
Drainage Temperature - Feed Water Heater 2 Outlet	K	345.82
Drainage Pressure - Feed Water Heater 2 Outlet	bara	0.35
Water Pressure - Feed Water Heater 2 Inlet	bara	16.55
Water Temperature - Feed Water Heater 2 Inlet	K	340.26
Steam Extraction Pressure - LP Steam Turbine	bara	0.34
Steam Extraction Pressure - Feed Water Heater 1 Inlet	bara	0.31
Steam Extraction Temperature - LP Steam Turbine / Feed Water Heater 1 Inlet	K	343.04
Drainage Temperature - Feed Water Heater 1 Outlet	K	317.87
Drainage Pressure - Feed Water Heater 1 Outlet	bara	0.10
Water Pressure - Feed Water Heater 1 Inlet	bara	16.89
Water Temperature - Feed Water Heater 1 Inlet	K	312.32
Steam Extraction Pressure - LP Steam Turbine / Condenser Inlet	bara	0.07
Steam Extraction Temperature - LP Steam Turbine / Condenser Inlet	K	311.54
Water Pressure - Condenser Outlet	bara	0.07
Water Temperature - Condenser Outlet	K	311.54

APPENDIX II.- CARBON CAPTURE PLANT METHODOLOGY

The capture plant of Figure A2.1 was validated by Sánchez Fernández (Sanchez Fernandez et al. 2014) based on various data sets from different pilot plants (Razi et al. 2013).

A2.1.- Post-combustion carbon capture process

Models of the Carbon Capture Plant and the CO_2 compression system use the process simulator Aspen Plus V8. A typical MEA scrubbing post-combustion capture process with a single absorber, stripper and lean-rich heat exchanger is considered in this work.

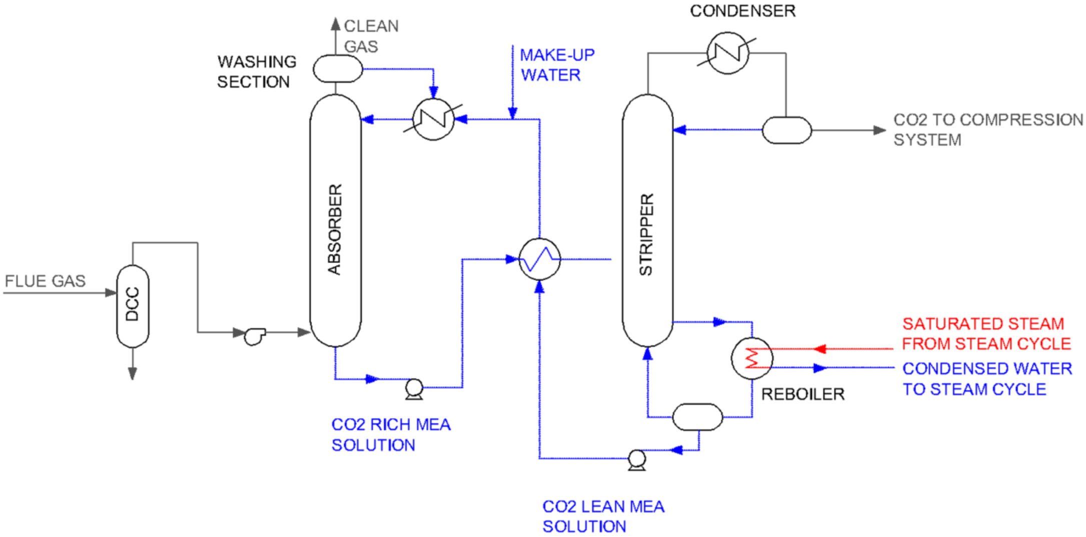

Figure A2.1- Process Flow Diagram of the Carbon Capture Plant

A setup with two absorber trains with a 12.9m diameter and 17m of column height (not including the water wash) is used throughout of the study. RadFrac columns are selected for both the absorber and the stripper.

The boundary conditions of the CO_2 capture process are given in ***Table A2.1***.

Table A2.1- Boundary conditions for CO_2 Capture Plant Model.

Boundary conditions of CO2 capture plant model		
MEA Concentration in solution	%	30
Absorber stages	-	20
Desorber stages	-	20
Desorber pressure (1st stage)	bar	1,8
Rich-lean heat exchanger temperature difference	C	8
Absorber solvent inlet temperature	C	40
Reboiler temperature difference	C	15
Pump efficiency	%	75
Blower isentropic efficiency	%	90

CO_2 from the stripper overheads is compressed to 13 bar in a three-stage centrifugal compressor. The inter-coolers are designed to cool the CO_2 down to 50C by means of condensate water heating. In order to replace all the condensate heating of the existing steam cycle by recovered heat from the intercoolers the CO_2 temperature at the exit of the CO_2 compressors must reach **135C.** Three compression stages with a compression rate of **2.6** are required to compress the CO_2 to 13 bar. The CO_2 is then liquefied by the use of a propane refrigeration system and pumped to a pressure of 140bar **(DOE/NETL 2007)**.

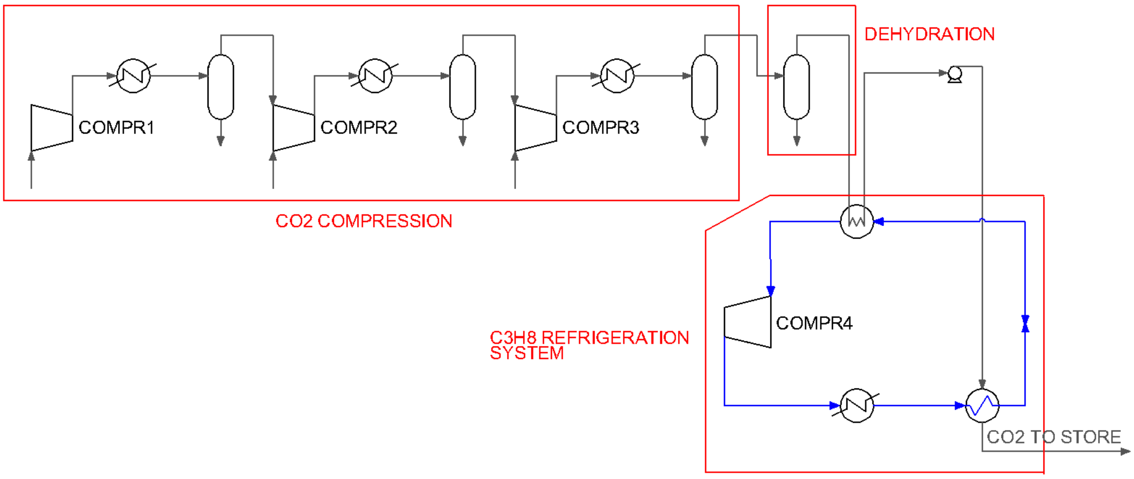

Figure A2.2.- Process Flow Diagram of the CO_2 Compression System

A typical heat exchanger approach temperature of 6 C and a minimum subcooling of 8 C to avoid pump cavitation have been assumed in the refrigeration cycle evaporator. The compressor adiabatic stage efficiency for both CO_2 and Propane compressors has been assumed equal to 75% and the cryogenic pump hydraulic efficiency 75%.

An economizer is added to cool down the propane by the cold cryogenic pump discharge. An approach temperature of 6 C was selected for the economizer.

Figure A2.3 illustrates a sketch of the refrigeration propane system and **Figure A2.4** shows the four steps of the CO_2 compression system.

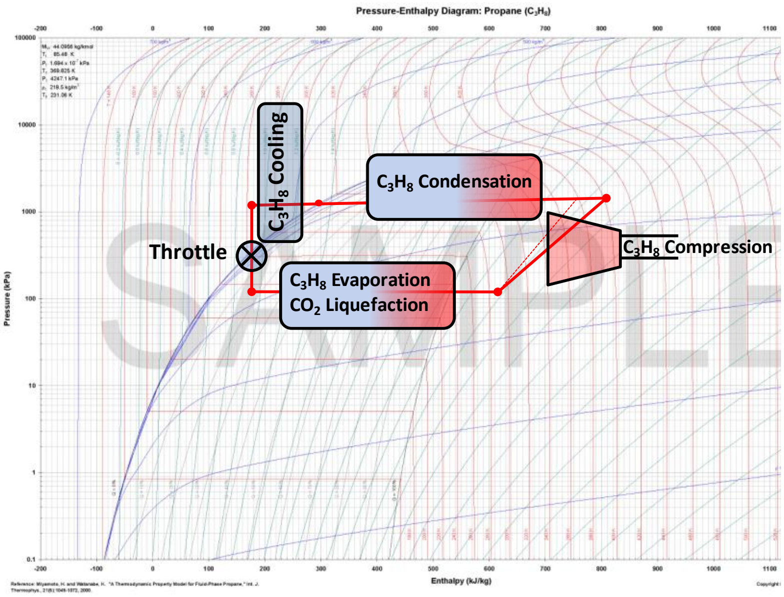

Figure A2.3.- Propane refrigeration system

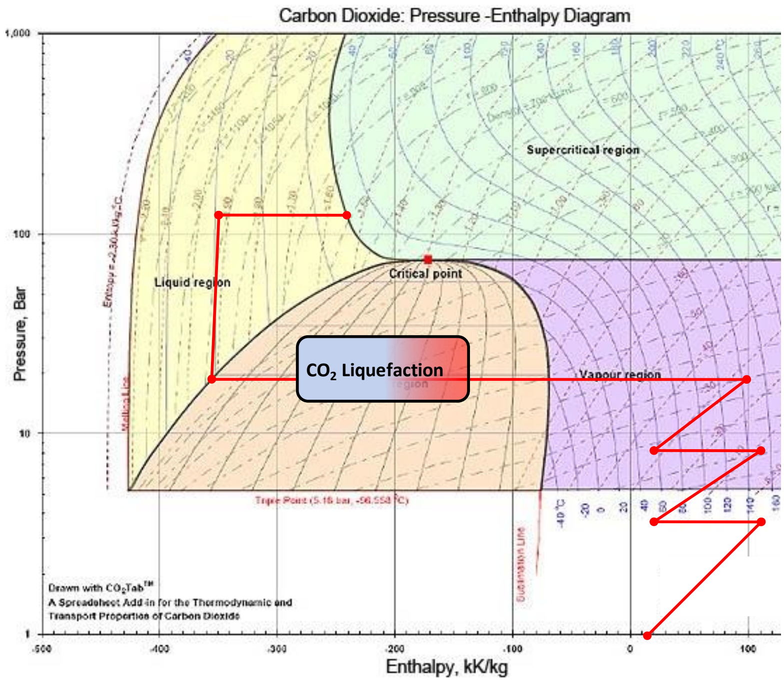

Figure A2.4.- CO_2 compression system

A2.2.- Property method

Acid gases and amine are weak electrolytes. They are partially dissociated in the aqueous phase to form a complex mixture of molecular and ionic species. The equilibrium constants were taken from Austgen **(Austgen et al. 1989)** who reported values from literature resource **like (Bates & Pinching 1951; Edwards et al. 1978).**

(Aspen Plus User Guide) was used to select the property method of this work. Figure A2.5 shows a sketch of Aspen Plus guidelines.

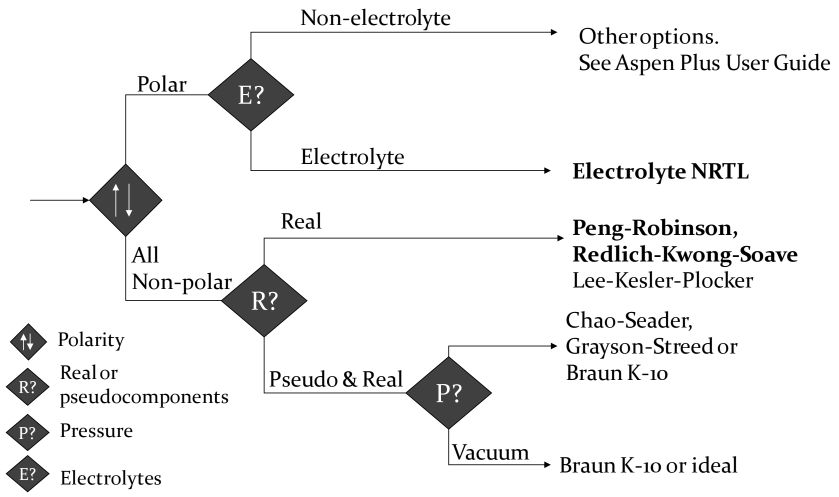

Figure A2.5.- Guideline for choosing a property method (Aspen Plus User Guide)

The mixture of CO_2, MEA and water is highly non-ideal in the liquid phase. The presence of ions and polar molecules creates significant thermal effects in solution. In order to predict equilibrium correctly, a good activity coefficient model is necessary. The electrolyte-NRTL was chosen as the most appropriate model for the system CO_2-amine-water.

The considered system has a large number of binary interaction parameters, such as molecule-molecule, molecule-ion pair and ion pair – ion pair. These binary interaction parameters were taken from (Pellegrini et al. 2011) who derived them from (Chen & Evans 1986; Mock et al. 1986; Ma'mun et al. 2005).

The Soave-Redlich-Kwong (SRK) and the Peng Robinson equations of state (PR) have been selected as the property method for the CO_2 and C_3H_8 respectively

A2.3.- Rate base approach methodology

The rate base approach is based on the two-film model. This model divides liquid and gas phases into two regions, the bulk and the film. It assumes that all the mass transfer resistance is concentrated in the films, and that the only mass transfer mechanism is steady state molecular diffusion. In the bulk region there is no concentration gradient due to the high level of mixing.

The mathematical model behind the rate-based calculations in Aspen Rate-Based consists of material balances, energy balances, mass transfer, energy transfer, phase equilibrium, and summation equations. The model is based on a stage as shown in the Figure A2.6.

In Aspen Rate-Based, the full set of equations is solved using Newton's method, using the solution from the equilibrium-based model as the initial guess.

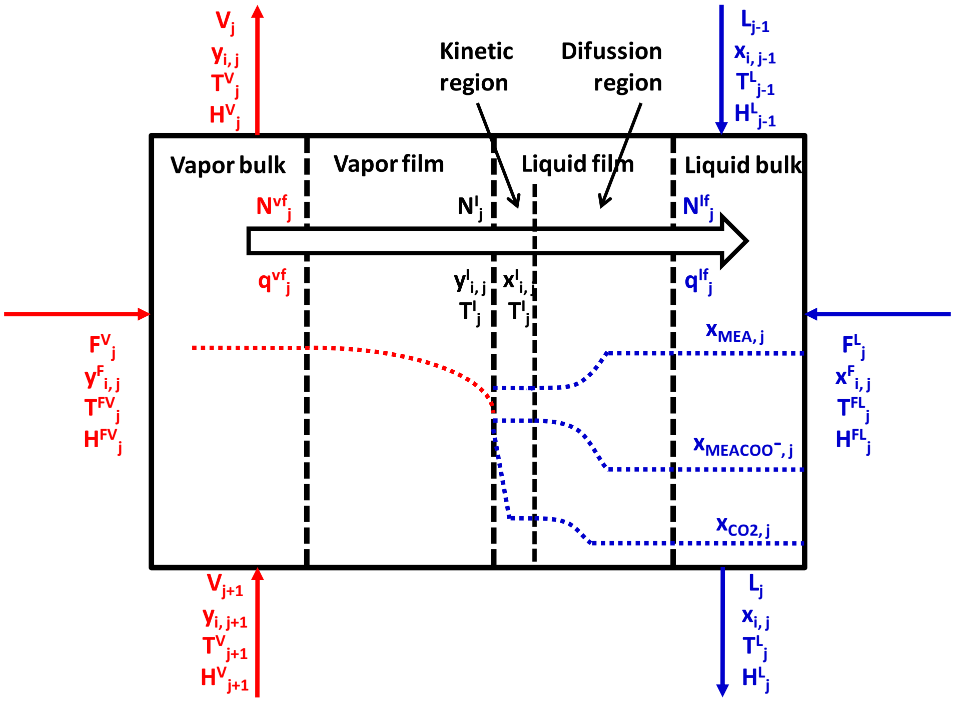

Figure A2.6.- One stage of the rate base process

The equations related to the stage j are:

Material balance for bulk liquid:

$$F_j^L \cdot x_{i,j}^F + L_{j-1} \cdot x_{i,j-1} + N_{i,j}^{lf} - L_j \cdot x_{i,j} = 0 \qquad \text{[A2.1]}$$

Where:

F_j^L	=	molar flow rate of lean amine feed stream, kmol/s (at the top of the absorber)
$x_{i,j}^F$	=	molar fraction of component i of the lean amine feed stream, kmol/kmol
L_{j-1}	=	molar flow rate of liquid at the inlet of stage j, kmol/s
$x_{i,j-1}$	=	molar fraction of component i of liquid at the inlet of stage j, kmol/kmol
L_j	=	molar flow rate of liquid at the outlet of stage j, kmol/s
$x_{i,j}$	=	molar fraction of component i of liquid at the outlet of stage j, kmol/kmol
$N_{i,j}^{lf}$	=	molar flow rate of component i transferred from the interface to the liquid phase, kmol/s

Energy balance for bulk liquid:

$$F_j^L \cdot H_j^{FL} + L_{j-1} \cdot H_{j-1}^L + q_j^{lf} - L_j \cdot H_j^L = 0 \qquad \text{[A2.2]}$$

Where:

H_j^{FL} = enthalpy of lean amine feed stream, kJ/kmol

H_{j-1}^{L} = enthalpy of liquid at the inlet of stage j, kJ/kmol

H_j^{L} = enthalpy of liquid at the outlet of stage j, kJ/kmol

q_j^{lf} = heat rate transferred from the interface to the liquid phase, kJ/s

Material balance for bulk vapor:

$$F_j^V \cdot y_{i,j}^F + V_{j+1} \cdot y_{i,j+1} - N_{i,j}^{vf} - V_j \cdot y_{i,j} = 0 \qquad \text{[A2.3]}$$

Where:

F_j^V = molar flow rate of flue gas feed stream, kmol/s (at the bottom of the absorber)

$y_{i,j}^F$ = molar fraction of component i of the flue gas feed stream, kmol/kmol

V_{j+1} = molar flow rate of vapor at the inlet of stage j, kmol/s

$y_{i,j+1}$ = molar fraction of component i of vapor at the inlet of stage j, kmol/kmol

V_j = molar flow rate of vapor at the outlet of stage j, kmol/s

$y_{i,j}$ = molar fraction of component i of vapor at the outlet of stage j, kmol/kmol

$N_{i,j}^{vf}$ = molar flow rate of component i transferred from the vapor phase to the interfase, kmol/s

Energy balance for bulk vapor:

$$F_j^V \cdot H_j^{FV} + V_{j+1} \cdot H_{j+1}^V - q_j^{vf} - V_j \cdot H_j^V = 0 \qquad \text{[A2.4]}$$

Where:

H_j^{FV} = enthalpy of the flue gas feed stream, kJ/kmol

H_{j+1}^{V} = enthalpy of vapor at the inlet of stage j, kJ/kmol

H_j^{V} = enthalpy of vapor at the outlet of stage j, kJ/kmol

q_j^{vf} = heat rate transferred from the vapor phase to the interface, kJ/s

The bulk phase balances are supplemented by the summation equations for the liquid and gas bulk mole fractions:

$$\sum_{i=1}^{m} x_i = 1; \qquad \sum_{i=1}^{m} y_i = 1 \qquad \text{[A2.5]}$$

The film is considered as an additional balance region, in which reaction and mass transfer occur simultaneously.

The differential component mass balances for the liquid and vapor film regions are

$$\nabla n^{lf} - R^{lf} = 0; \qquad \nabla n^{vf} = 0 \qquad \text{[A2.6]}$$

Where:

R^{lf} = kinetic rate, mol/s/m3

n^{lf} = molar flux of component i in the liquid phase, mol/s/m2

R^{lf} contains all the kinetic (non equilibrium) reactions that CO_2 undergoes in the liquid phase. These include R1 and R2 and their reverse:

$$CO_2 + MEA + H_2O \rightarrow MEACOO^- + H_3O^+ \quad [R1]$$

$$CO_2 + OH^- \rightarrow HCO_3^- \quad [R2]$$

The second reaction is far slower than the first one due to the low concentration of OH- in the solution. In fact, R2 reaction would be taken into account only when the CO_2 concentration in the solution is quite high, at very rich loading. The kinetic constants used in this work are those reported by Hikita et al (1977) and Pinsent et al (1956).

The mass transfer equations the liquid and vapor film regions are:

$$n^{lf} = -\left(D_i^{lf} + \frac{x^2}{t_L}\right) \cdot \nabla[i]^{lf} \quad [A2.7]$$

$$n^{vf} = -\left(D_i^{vf}\right) \cdot \nabla[i]^{vf} \quad [A2.8]$$

Where:

D_i^{lf} = Diffusivity of component i in the liquid film (m2/s)

t_L = Residence time for the liquid, s

D_i^{vf} = Diffusivity of component i in the vapor film (m2/s)

$[i]^{lf}$ = Concentration of component i in the liquid film (mol/m3)

$[i]^{vf}$ = Concentration of component i in the vapor film (mol/m3)

In this work, the Bravo et al (1985) correlation was selected to calculate the mass transfer coefficients. It predicts mass transfer coefficients and interfacial area for structured packing.

The binary mass transfer coefficient for the liquid and the vapor phase are (Bravo, 1985):

$$k_i^{lf} = 2 \cdot \sqrt{\frac{D_i^{lf}}{\pi \cdot t_L}} \quad [A2.9]$$

$$k_i^{vf} = 0.338 \cdot \frac{D_i^{vf}}{d_{eq}} \cdot Re_{vf}^{0.8} \cdot Sc_{vf,i}^{0.333} \quad [A2.10]$$

And the interfacial area for structured packing [Bravo, 1985]:

$$a^I = a_p \cdot A_l \cdot h_p \quad [A2.11]$$

Where:

k_i^{lf} = the binary mass transfer coefficient for the liquid (m/s

k_i^{vf}	=	the binary mass transfer coefficient for the vapor (m/s).
a^I	=	total interfacial area for mass transfer (m^2)
d_{eq}	=	Equivalent diameter (m)
Re_{vf}	=	Reynolds number for the vapor
Sc_{vf}	=	Schmidt number for the vapor
a_p	=	Specific area of the packing (m2/m3)
A_l	=	Cross-sectional area of the columns (m2)
h_p	=	height of the packed section (m)

Aspen Plus uses the Chilton and Colburn method (Taylor and Krishna, 1993) to calculate heat transfer coefficients from the binary mass transfer coefficients.

$$h^{\mathrm{lf}} = k^{lf} \cdot \rho^{lf} \cdot Cp^{lf} \cdot \left(\frac{\lambda^{lf}}{\rho^{lf} \cdot Cp^{lf} \cdot D^{lf}}\right)^{2/3} \quad [A2.12]$$

$$\mathrm{h^{Vf}} = \mathrm{k^{Vf}} \cdot \varrho^{\mathrm{Vf}} \cdot \mathrm{Cp^{Vf}} \cdot \left(\frac{\lambda^{\mathrm{Vf}}}{\varrho^{\mathrm{Vf}} \cdot \mathrm{Cp^{Vf}} \cdot \mathrm{D^{Vf}}}\right)^{2/3} \quad [A2.13]$$

Where:

$h^{\mathrm{lf}}, h^{\mathrm{vf}}$	=	heat transfer coefficient in the liquid and vapor film, W / m2 / K
k^{lf}, k^{vf}	=	average mass transfer coefficient in the liquid and vapor film, m/s
$\rho^{lf}, \varrho^{\mathrm{Vf}}$	=	molar density in the liquid and vapor film, kmol /m3
$Cp^{lf}, \mathrm{Cp^{Vf}}$	=	specific molar heat capacity in the liquid and vapor film, J / kmol / K
$\lambda^{lf}, \lambda^{Vf}$	=	thermal conductivity in the liquid and vapor film, W / m / K
D^{lf}, D^{Vf}	=	average diffusivity in the liquid and vapor film, m2/s

These equations must be complemented by the boundary conditions relevant to the film model:

- $[i]^{lf}\,(\mathrm{x}=0) = [i]^{i}$. Phase equilibrium at the interface
- $[i]^{lf}\,(\mathrm{x}=1) = [i]^{\mathrm{L}}$.

At equilibrium, the fugacities of each volatile component are equal in the vapor and liquid phase. The vapor-liquid equilibria for the system are given by equation 14:

$$\phi_i^v \cdot y_i \cdot p = x_i \cdot \gamma_i^* \cdot H_i \quad [A2.14]$$

Where:

ϕ_i^v	=	fugacity coefficient of component i
y_i	=	molar fraction of component i in the vapor phase
P	=	total pressure

x_i = molar fraction of component i in the liquid phase

γ_i^* = activity coefficient of component i

H_i = Henry constant of component i

The fugacity coefficient in the vapor phase is obtained from the Redlick-Kwan-Soave equation of state and the activity coefficient of the species in the liquid phase by the electrolyte NRTL model.

The system of equations described above is very large and rather difficult to solve because of the complex chemical system. In order to reduce the complexity of this system, some approximations can be assumed (Freguia 2002). The approximation suggested by Freguia consists of dividing the liquid film into two sub-layers: the kinetic region and the diffusion region. All the kinetic reactions occur in a very small fraction of the film, identified as kinetic region in Figure A2.6. In the kinetic region the concentration of all the species, except CO_2, are constant at their interface value, while in the diffusion region they change because of the mass transfer mechanism. The CO_2 concentration reaches an asymptote in the kinetic region due to the fast reaction and changes smoothly in the diffusion region.

Aspen Plus performs liquid holdup calculations for both random and structured packings. In this study the Sulzer packing was selected. Aspen Plus provides the parameters for the Stizhlmair correlation (Stichlmair, 1989) in the built-in packing databank.

$$h_L = h_t \cdot h_P \cdot A_t \qquad [A2.15]$$

$$h_t = 0.555 \cdot Fr_L^{1/3} \cdot (1 + 20 \cdot \Delta P^2) \qquad [A2.16]$$

Where:

h_L = Volumetric liquid holdup

h_t = Fractional holdup

Fr_L = Froude number for the liquid

ΔP = Pressure drop

h_P = Height of the packed section

A_t = Cross sectional area of the column

APPENDIX III.- FORTRAN AND EXCELL CALCULATOR BLOCKS IMPLEMTEND ON ASPEN PLUS SOFTWARE

Models of the boiler, the steam cycle and the ancillaries of a pulverised coal plant and of a CCGT have been developed in Mathcad and validated by the process simulator Aspen Plus V8.

Models of the Carbon Capture Plant and the CO_2 compression system use the process simulator Aspen Plus V8.

This section shows the different calculator blocks implemented on Aspen Plus software in order to study the carbon capture retrofit performance.

A3.1.- Design Specifications

Process design specifications were based on the report "Cost and Performance Baseline for Fossil Energy Plants" published by NETL **(DOE/NETL 2013)**. See **Annex I** for more details of the basic engineering data.

In order to meet process design requirements Aspen Plus provide the Design Specifications tool. This tool allows us to set the value of a calculated variable to a specific value by manipulating an input variable.

In the define tab of the Aspen Plus Design Specifications tool we identify the design variables and in the Spec tab we specify the value of the design variable and its tolerance. The manipulated variable and its range of operation are set in Vary tab. Good estimation of the manipulated variable range will help to meet the design specifications with fewer iterations.

Table A3.1 and Table A3.2 indicate the different design specifications implemented in the model in order to meet the process design requirements:

A3.2.- Calculator block:

Calculator blocks are used to insert equations in FORTRAN code into the Aspen Plus simulation units. These calculator blocks have been mainly used to set input data based on upstream calculated values and to express an equation in terms of flowsheet variables to calculate heat transfer coefficient, for example.

In the define tab we identify all the variables that will be used in the Calculator. These variables need to be defined either as import variable, if they are read from the simulation or as export variable, if they are written to the simulation. In the Calculate tab we enter the equations in FORTRAN code and in the Sequence tab we select the import/export variables as sequence of simulation.

The following calculator blocks have been examined in the existing PC Power plant:

<u>Air preheaters calculator block</u>

It evaluates two parameters, the Air Leakage, as the weight of air passing from the air inlet side to the gas outlet side, and the Gas Side Efficiency by means of equation **[3.43]**. The Gas Side Efficiency is used to predict the undiluted exit gas temperature when the PC Power Plant is retrofitted as GT flue gas windbox carbon capture retrofit.

Table A3.1.- Design Specifications of the coal power plant model

FEED WATER HEATERS TRAIN		
Design variable	**Target**	**Manipulated variable**
Boiler feed water temperature	524.5 K	Steam mass flow rate of HP steam turbine extraction
HP feed water heater inlet temperature	489.5 K	Steam mass flow rate of IP steam turbine first extraction
Deaerator subcooling degrees	0.001 K	Steam mass flow rate of IP steam turbine second extraction
Deaerator inlet LP feed water temperature	413.5 K	Steam mass flow rate of LP steam turbine first extraction
LP feed water heater1 inlet temperature	398.5 K	Steam mass flow rate of LP steam turbine second extraction
LP feed water heater2 inlet temperature	361.2 K	Steam mass flow rate of LP steam turbine third extraction
LP feed water heater3 inlet temperature	340.3 K	Steam mass flow rate of LP steam turbine fourth extraction
COAL PULVERISERS		
Design variable	**Target**	**Manipulated variable**
Pulveriser outlet air & coal temperature	353.1 K	Primary airheater outlet air temperature

Table A3.2.- Design Specifications of the GT flue gas windbox carbon capture retrofit

FEED WATER HEATERS TRAIN		
Design variable	**Target**	**Manipulated variable**
Boiler feed water temperature	524.5 K	Steam mass flow rate of HP steam turbine extraction
HP feed water heater inlet temperature	489.5 K	Steam mass flow rate of IP steam turbine first extraction
Deaerator subcooling degrees	0.001 K	Steam mass flow rate of IP steam turbine second extraction
Deaerator inlet LP feed water temperature	413.5 K	CO_2 compressor heat recovery feed water heater outlet temperature
Stripper reboiler inlet steam temperature	408.0 K	Back pressure steam turbine steam mass flow rate
COAL PULVERISERS		
Design variable	**Target**	**Manipulated variable**
Pulveriser outlet air & coal temperature	353.1 K	Primary airheater outlet air temperature
SECONDARY AIR HEATER		
Design variable	**Target**	**Manipulated variable**
Secondary airheater diluted gas temperature	427.0 K	Secondary air heater flue gas flow rate
NATURAL GAS COMBINED CYCLE		
Design variable	**Target**	**Manipulated variable**
Gas turbine outlet temperature	896.5 K	Gas turbine pressure ratio
NGCC net power output	150 MW	Natural gas mass flow rate
HRSG LP pinch temperature	10.0	HSRG LP water mass flow rate
CO_2 COMPRESSOR SYSTEM		
Design variable	**Target**	**Manipulated variable**
Turbine outlet C_3H_8 temperature	399.8 K	Refrigeration system C_3H_8 mass flow rate

Gas velocity calculator block

As fly-ash could cause erosion problems due to high gas velocities, the velocity of the gas has been computed in banks where its maximum value is reached, namely Reheater Bank2 and Primary Superheater Bank 2.

Combustion heat losses calculator block

In order to estimate the adiabatic flame temperature heat losses must be considered during the combustion process. These combustion heat losses are radiation losses and unburned carbon losses.

Steam turbines calculator block

This calculator block determines the stage swallowing capacity of each steam turbine by solving equation [4.1].This parameter is used to predict steam turbines behavior when they are retrofitted for carbon capture.

Heat exchanger calculator block

Aspen Plus heat exchangers evaluate overall heat transfer coefficient by only taking into account the convection heat transfer coefficient of the cold and hot stream. In pulverised coal boilers, the high temperature of the gas flowing around the tubes makes inter-tube radiation relevant. This heat transfer mechanism, together with steam and gas convection, have to be taken into account when the overall heat transfer rate is being evaluated. Consequently, the overall heat transfer coefficient is computed using either equation **[3.19]** or **[3.20]**, depending on the heat exchanger configuration, instead of the calculation proposed by Aspen Plus.

The heat exchanger calculator block also computes the total heat transfer surface area of each heat exchanger. This is determined by assuming an initial arrangement and then confirming the desired thermal performance.

Aspen Plus offers a wide variety of shell and tube heat exchanger types. However, in PC boilers, heat exchangers do not have a shell enclosing the tubes; they basically consist of tube bundles located in a large open volume where flue gas flows around them. In order to determine the surface arrangement of the heat exchangers the methodology proposed in **section 4.1.1** has been implemented.

The heat exchangers are first performed in rating mode, where Aspen Plus program determines if units are over/under surfaced. Then, the cleanliness factor of each heat exchanger is determined in order to meet the heat transfer area calculated by Aspen Plus program. The cleanliness factor must be close to 1; otherwise dimensional parameters (number of runs and the number of tubes per run) are wrongly assumed, and have to be re-estimated and calculations have to be repeated.

Once the surface arrangement is known, heat exchanger calculations are performed in simulation mode and the software determines outlet conditions. The simulation mode is used to evaluate the heat exchanger outlet temperatures when the PC Power Plant is retrofitted as GT flue gas windbox carbon capture retrofit.

A3.3.- Excel Unit Operation Model

Some calculations have been performed by using Aspen Plus operation blocks with an Excel spreadsheet. The coal pulveriser, furnace and cavities units have been computed with this tool.

This section explains how to create a simulation that uses Excel Microsoft Software to determine product stream properties.

<u>Set up the Aspen Plus model</u>

The first step is to build the process flow sheet. Select the User2 model icon, create feed and product streams and specify feed characteristics.

The icon selected for the coal pulveriser is a filter and for the furnace and cavities is a heat exchanger.

The order in which streams are created is relevant as Excel data will be passed to an Aspen Plus array, the first stream created corresponds to the first one in the data array.

The second step consists of specifying the location of the Excel file and entering user array data. These parameters will be used as input data in the calculations of the Excel spreadsheet. Excel results not related to stream properties could also be held in this array.

Table A3.3 reveals the array data of the operation blocks.

In the stream Flash tab, select the Temperature & Pressure option in the Flash type field. Excel will calculate the temperature and pressure of the product stream and Aspen Plus will evaluate the stream properties based on that temperature and pressure.

Table A3.3- Operating blocks array data.

LOWER & UPPER FURNACE PARAMETERS		
Integer	***Real***	***Description***
1	7.6	Top Level A (m)
	0	Bottom Level A (m)
	25.7	Top Level B - burner zone (m)
	34.5	Top Level C - furnace nose level (m)
	16.9	Width below furnace nose (m)
	11.4	Depth Furnace (m)
	0.99	Water Wall effectiveness factor
	0.5	Low furnace exit plane effectiveness factor
	0.4	Thermal efficiency of water walls
	11666	Coal high heat value (Btu/lb)
	$5.68 \cdot 10^{-8}$	Stefan Boltzmann Constant ($W/m^2/K^4$)
UPPER FURNACE ADDITOINAL PARAMETERS		
	Calculator block result	*Adiabatic flame temperature (K)*
	47.4	Level Zone D – Furnace exit (m)
	21.3	Width above furnace nose (m)
	12	Height exit (m)
	0.99	Platen superheater effectiveness factor
	0.6	Upper furnace exit plane effectiveness factor
CAVITY 1 & 2 PARAMETERS		
1	8.2	Height / Length of Boundary 1
	8.2	Height / Length of Boundary 3
	4.6	Height / Length of Boundary 4
	4.6	Height / Length of Boundary 2
	21.4	Furnace width
	Calculator block results	*Steam temperature – Boundary 3*
	Calculator block results	*Steam temperature – Boundary 4*
	Calculator block results	*Steam temperature – Boundary 1*
	Calculator block results	*Steam temperature – Boundary 2*
	11666.0	Coal High Heat Value (Btu / lb)

Set up the Excel model

The Excel template available in Aspen Plus software has been used and Excel security setting has been lowered to allow the macros to run. The Excel template has been modified to reflect the input and output parameters of each case.

Aspen Plus transfers input data from MSIN array to Excel and transfers results from Excel to SOUT array. Be aware that all Excel data have to be expressed in the International System (IS) of Units.

All the model equations and parameters have been introduced in Excel Worksheet Sheet1. This sheet calculates the product stream properties using input data from the other worksheets.

The Sheet1 of the Coal Pulveriser calculates the temperature at the exit of the Mill. The hot primary air will transport and dry the coal and, thus, the surface moisture of the coal will be transferred to the air. It has been assumed coal inherent moisture of 2%. A design specification will modify the temperature of the hot air in order to reach 80ºC at the exit of the Coal Pulveriser.

Two different Excel Unit Operation Models have been developed for the furnace. The Lower furnace model will calculate the gas temperature at the furnace nose level and the upper furnace model will compute it at the exit plane by applying equation [3.24]. The heat absorbed by the each section of the furnace is computed by means of equation [3.30].

The heat absorbed by the water walls, platen superheaters and exit plane is determined based on the ratio of the effective areas of each type of surface to the total furnace area. The effective areas ratios are used to simulate the energy fractions of the 'Furnace Splitter'.

Furthermore, due to the wide spacing between tubes the heat radiated to the exit plane reaches the final superheater, the screens and the outlet leg of the reheater. The direct view factor, equation [3.33], is used to simulate the energy fractions of the 'exit plane splitter'.

Figure 3.2 shows the Aspen Plus process flow sheet of the boiler furnace.

During design calculations, the furnace size and the effectiveness factors (user array data shown in Table A3.3) will be adjusted correctly when the gas temperature at the upper furnace exit reaches its design value and when the heat released in the furnace is equal to the heat absorbed by the water/steam in the water walls and platen superheater; otherwise, the dimensional parameters have to be re-estimated

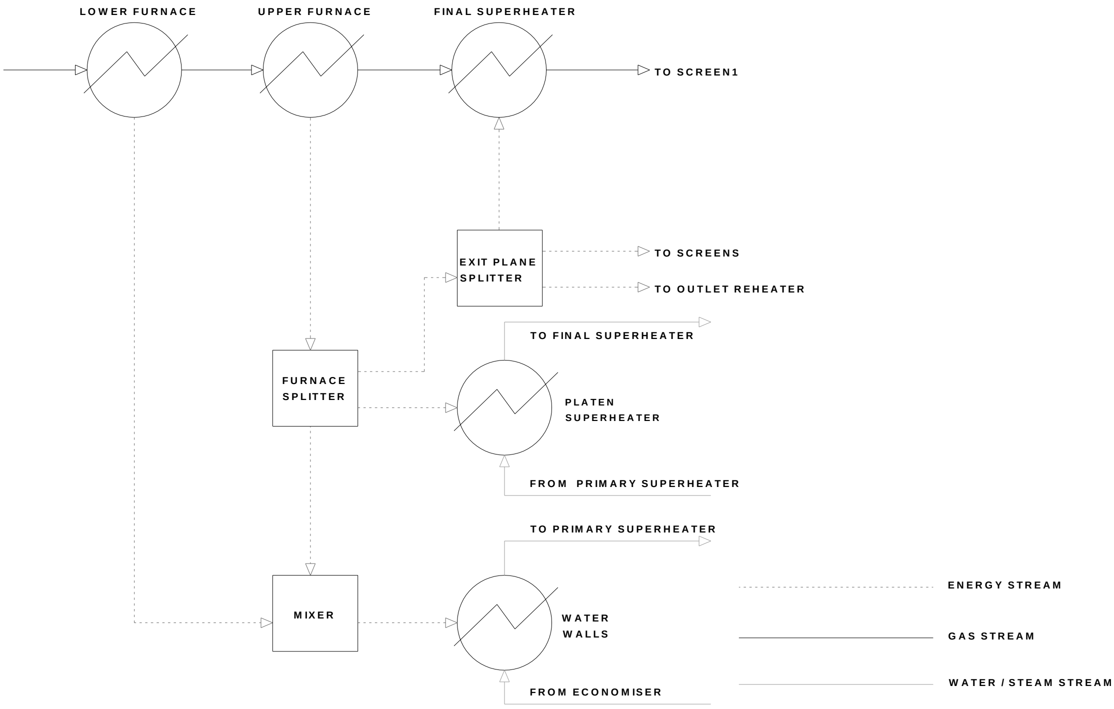

Figure A3.1. - Aspen Plus process flow sheet of the boiler furnace

Another two Models are developed to calculate the drop in gas temperature in the boiler cavities, CAV1 and CAV2 of ***Figure 3.***. The equations introduced in the model are the ones explained in Chapter 3 and Chapter 4.

Examining simulation Results

To check the results of the simulations, Aspen Plus data and Excel data have to be the same. It has been verified that Excel reads the real and integer parameters data from Aspen Plus regardless to units.

LIST OF PUBLICATIONS

Conference papers:

Sanchez del Rio, M.; Lucquiaud, M.; Gibbins, J. 2014, 'Maintaining the power output of an existing coal plant with the addition of CO_2 capture: Retrofits options with gas turbine combined cycle plants', Energy Procedia 63 (2014) 2530-2541.

Lucquiaud, M.; Sanchez del Rio, M.; Gibbins, J.2013, 'Carbon capture retrofit options with th on-site additon of gas turbine combined heat and power cycle', Energy Procedia 37 (2013) 2369 – 2376.

Oral presentations:

Sanchez del Rio, M.; Lucquiaud, M.; Chalmers, H.; Gibbins, J. 2015, 'Gas Turbine Repowering options for carbon capture retrofit', 8th Annual Conference on Trondheim CO_2 Capture Transport and Storage, Trondheim, Norway.

Sanchez del Rio, M.; Lucquiaud, M.; Chalmers, H.; Gibbins, J. 2015, 'A techno-economic assessment of integrated retrofits with sequential combustión of gas turbine flue gas', 14th Annual Conference on Carbon Capture Utilization and Storage, Pittsburgh, Pensylvania, U.S.A.

Sanchez del Rio, M.; Lucquiaud, M.; Gibbins, J. 2014, 'CO_2 capture retrofit to existing coal plants with supplementary gas firing', The second University of Texas Conference on carbon capture and Storage: UTCCS2, The University of Texas, Austin.

Sanchez del Rio, M.; Lucquiaud, M.; Gibbins, J. 2012, 'Combining post-combustion CO_2 Capture Retrofit to existing coal plants with a natural gas combined heat and cycle', 9th European Conference in Coal Research and Its Applications: ECCRIA9, University of Nottingham.

Sanchez del Rio, M.; Lucquiaud, M.; Gibbins, J. 2013, 'Sequential combustion in a post-combustion CO_2 capture retrofit of a coal boiler with added gas turbine', sixth international conference on Clean Coal Technology: CCT2013, Thessaloniki, Greece.

Posters:

Sanchez del Rio, M.; Lucquiaud, M.; Gibbins, J. 2014, 'Maintaining the power output of an existing coal plant with the addition of CO_2 capture. Retrofits options with CCGT plants'. International Conference Green House Gas Technologies: GHGT12, The University of Texas, Austin.

Sanchez del Rio, M.; Lucquiaud, M.; Gibbins, J. 2013, 'Boiler arrangement for sequential combustion in a post-combustion CO2 capture retrofit of a coal boiler wiht added gas turbine', Early Carreer Researchers Annual Meeting, UKCCSRC, Newcastle University